WANCHENG SITTIKIJYOTHIN

Rheological and Microstructural Properties of β-Lactoglobulin / Galactomannan Aqueous Systems

Universidade do Porto
FEUP Faculdade de Engenharia

Departamento de Engenharia Química

August 2006

WANCHENG SITTIKIJYOTHIN

Rheological and Microstructural Properties of β-Lactoglobulin / Galactomannan Aqueous Systems

A Thesis Presented to the Faculty of Engineering of the University of Porto

In partial fulfillment of requirements for the degree of

Doctor of Philosophy in Chemical Engineering

A thesis prepared under the orientation of Dr. Maria do Pilar Figueroa Gonçalves,

Associate Professor of the Department of Chemical Engineering at

the University of Porto

Universidade do Porto

FEUP Faculdade de Engenharia

Departamento de Engenharia Química

August 2006

This thesis was accomplished with the financial support

By the Fundação para a Ciência e a Tecnologia

(Ph.D. Grant SFRH/BD/6041/2001)

เพื่อ พ่อและแม่

For My parents

ฝูงชนกำเนิดคล้าย *คลึงกัน*

ใหญ่ย่อมเพศผิวพรรณ *แผกบ้าง*

ความรู้อาจเรียนทัน *กันหมด*

ยกแต่ชั่วดีกระด้าง *ห่อนแก้ ฤาไหว*

พระราชนิพนธ์ พระบาทสมเด็จพระจุลจอมเกล้าเจ้าอยู่หัว รัชกาลที่ ๕

Born men are we all *and one,*

Brown, black by the sun *cultured.*

Knowledge can be won *alike.*

Only the heart differs *from man to man.*

King Rama V of Siam

(English version by M.R. Seni Pramoj)

ABSTRACT

In this work, the rheological properties of heat-induced β-lactoglobulin gels, and of aqueous solutions of two galactomannans, locust bean gum and tara gum, were studied, in a first step. The rheological behaviour and the microstructure of β-lactoglobulin / galactomannan mixed aqueous systems were studied in a second step. The experiments were conducted at pH 7.0, when the protein bears a net negative charge, and at pH 4.6, near the isoelectric point of the protein. Rheological techniques (steady shear measurements, dynamic oscillatory shear and static tests) and confocal laser scanning microscopy (CLSM) were used for performing the experiments.

It was shown that the thermal gelation (80^{o}C) and the rheology of the pure β-lactoglobulin gels, obtained after quenching to 20^{o}C, depend on the protein concentration, the pH and the processing conditions. For similar concentrations, gels form at lower temperature and sooner at pH 4.6 than at pH 7.0; the final gels are stronger than those formed at pH 7.0 but show higher sensitivity to strain. Shearing during gelation proved to affect the rheological properties of the resulting gels, at both pH values. The effects depended on pH, temperature, duration and rate of shear and were more pronounced when shear was applied for a short period at 80^{o}C.

Regarding the galactomannans, the results obtained show that locust bean gum and tara gum exhibit quite similar rheological properties, in the range of concentrations and shear rates/frequencies studied. Experimental data were correlated with the Cross and Carreau models, in steady shear, and with the generalized Maxwell model with four elements and the Friedrich-Braun model, in oscillatory shear (mechanical spectra). Also, time-concentration superposition holds for their solutions, allowing master curves to be found for both the viscous and the linear viscoelastic response in shear flow. The similar profile observed probably reflects the existence of non-specific physical entanglements in these galactomannan solutions.

In the case of β-lactoglobulin / galactomannan mixed systems, phase separation was observed, in the sol and gel states, for all the concentrations/mixing ratios studied, at pH 7.0 and pH 4.6. This phenomenon is a key factor for the structure development and the rheological properties of

mixed systems. For liquid systems, at 20°C, CLSM images show that phase inversion occurs in the systems, when the concentration of galactomannan is increased. The change in the microstructure affects the rheological properties of the systems. For systems in which the continuous phase is enriched in β-lactoglobulin, a Newtonian behaviour is observed, as for pure β-lactoglobulin solutions. For systems in which the continuous phase is enriched in galactomannan, the behaviour is typical of a suspension, probably due to the flocculation of the disperse protein-rich phase; for these systems, flow curves, described by the modified Cross model, show apparent yield stresses. In the case of the gelled systems, the addition of the galactomannan affects the heat-set gelation behaviour of β-lactoglobulin solutions, the viscoelasticity and the microstructure of final gels. CLSM images reveal that stranded gels are obtained at pH 7.0 while less homogeneous, coarser, particulate gels are formed at pH 4.6, meaning that different aggregation/gelation processes took place at each pH. The rheological behaviour of mixed gels remains qualitatively similar to that of the pure protein gel and its quantitative modifications remain limited within the experimental window explored. These effects are more pronounced for locust bean gum, the less substituted of the two galactomannans studied, which points to a possible effect of the chemical structure on the rheology of the mixed systems. In large oscillatory shear experiments (strain sweeps), differences between the shapes of the curves at pH 7.0 and pH 4.6 were, however, observed in the non-linear region which probably reflects the very different microstructures of both type of gels.

The results obtained show that the structural and rheological properties of the mixed β-lactoglobulin / galactomannan aqueous systems, in the sol and gel states, are sensibly altered by modification of the concentration/mixing ratio of the two biopolymers, the pH of the medium and the processing conditions.

Keywords: Rheological properties; Microstructure; Phase separation; Gelation; β-lactoglobulin; Locust bean gum; Tara gum; Mixed protein / polysaccharide systems

RESUMO

Neste trabalho, foram estudadas, numa primeira fase, as propriedades reológicas, em meio aquoso, duma proteína globular, β-lactoglobulina, e de dois galactomananos (polissacarídeos neutros), gomas de tara e de alfarroba. Numa segunda fase, estudou-se o comportamento reológico e a microestrutura de sistemas aquosos mistos β-lactoglobulina /galactomanano. Os ensaios foram realizados a pH 7.0, quando a proteína está carregada negativamente, e a pH 4.6, valor próximo do ponto isoeléctrico da proteína. Os métodos utilizados foram ensaios reológicos (ensaios em regime estacionário, testes oscilatórios e testes estáticos) e ensaios de microscopia confocal por varrimento laser.

O estudo realizado com a proteína sózinha mostrou que a sua gelificação térmica (80ºC) e a reologia dos géis finais, obtidos após arrefecimento a 20ºC, dependem da concentração da proteína bem como do pH do meio e das condições de processamento. Para concentrações semelhantes, verificou-se que, a pH 4.6, os géis se formavam a temperatura mais baixa e mais rapidamente, e eram mais fortes, embora mais sensíveis à deformação, do que os géis formados a pH 7.0. Verificou-se, ainda, que a aplicação de tensões/velocidades de corte durante o processo de formação do gel, alterava a força e a deformação na fractura dos géis obtidos; essas variações dependiam do pH, da temperatura, da duração e da velocidade de corte.

No caso dos galactomananos, verificou-se que ambos exibiam propriedades reológicas semelhantes, em solução aquosa, a 20ºC. Na gama de concentrações estudada, as soluções apresentavam um comportamento reofluidificante descrito pelos modelos de Cross e Carreau. Os dados dos espectros mecânicos foram ajustados aos modelos de Friedrich-Braun e de Maxwell com quatro elementos. Curvas mestras foram, ainda, obtidas para os dois galactomananos, em regime estacionário e em regime dinâmico.

No caso dos sistemas mistos β-lactoglobulina/ galactomanano, verificou-se separação de fases, quer em solução, a 20ºC, quer nos sistemas gelificados, em toda a gama de concentrações/razões de mistura estudadas, a pH 7.0 e a pH 4.6. Este fenómeno é determinante no desenvolvimento da estrutura e das propriedades reológicas dos sistemas mistos. No caso de

sistemas líquidos, a 20ºC, as imagens obtidas por microscopia confocal mostram uma transição de sistemas com a fase contínua enriquecida em β-lactoglobulina para sistemas com a fase contínua enriquecida em galactomanano, à medida que a concentração do galactomanano aumenta. Essa inversão é acompanhada de alteração das propriedades reológicas. No caso da fase contínua estar enriquecida em proteína, o comportamento é Newtoniano, como para soluções puras de β-lactoglobulina. No caso da fase contínua estar enriquecida em galactomanano, o comportamento é típico de uma suspensão, provavelmente devido à floculação da fase dispersa enriquecida em proteína; para estes sistemas, as curvas de escoamento, descritas pelo modelo de Cross modificado, apresentam aparentes tensões de cedência. No caso dos sistemas gelificados, a presença do galactomanano influencia o comportamento do sistema durante a gelificação, a viscoelasticidade e a microestrutura dos géis finais. A pH 4.6, observaram-se, por microscopia confocal, géis particulados, heterogéneos e mais grosseiros que os géis filamentosos obtidos a pH 7.0 implicando diferentes processos de agregação/gelificação para cada pH. O comportamento reológico dos géis mistos é qualitativamente semelhante ao dos géis de proteína pura e as modificações quantitativas são limitadas na gama de concentrações estudadas, a cada pH. Os efeitos observados são mais pronunciados para a goma de alfarroba o que indica uma possível efeito da estrutura química do galactomanano na reologia dos géis mistos. Ensaios oscilatórios de varrimento em deformação, a pH 7.0 e pH 4.6, mostraram diferentes comportamentos dos géis a elevadas deformações, o que provavelmente reflecte as diferenças observadas nas respectivas microestruturas.

Os resultados obtidos permitiram concluir que as propriedades estruturais e reológicas dos sistemas mistos β-lactoglobulina / galactomanano, em meio aquoso, são sensivelmente modificadas por alteração da concentração/razão de mistura dos dois biopolímeros, do pH do meio e das condições de processamento utilizadas.

Palavras chave: Propriedades reológicas; Microestrutura; Separação de fases; Gelificação; β-lactoglobulina; Goma de alfarroba; Goma tara; Sistemas mistos proteína / polissacarídeo.

RÉSUMÉ

Dans ce travail, on a étudié, premièrement, les propriétés rhéologiques, en milieu aqueux, d'une protéine globulaire, la β-lactoglobuline, et de deux galactomannanes (polyosides neutres), la gomme de caroube et la gomme tara. Deuxièmement, le comportement rhéologique et la microstructure de systèmes mixtes β-lactoglobuline / galactomannane ont été étudiés. Les essais ont étés réalisés à pH 7.0, quand la protéine est chargée négativement, et à pH 4.6, près du point isoélectrique da la protéine. Les méthodes utilisées furent des essais rhéologiques (en régime stationnaire et en régime dynamique), et des essais de microscopie confocale à balayage laser.

L'étude réalisée avec la protéine seule a montré que sa gélification thermique (80ºC) et la rhéologie des gels obtenus après refroidissement à 20ºC dépendent de la concentration de la protéine, du pH du milieu et des procédés de traitement. Pour des concentrations semblables, on a observé qu'à pH 4.6, les gels se forment à des températures plus faibles et plus rapidement, et sont plus fort et plus sensibles à la déformation, que les gels formés à pH 7.0. Pour des gels subissant un cisaillement pendant leur formation, des changements de force et de déformation à la rupture ont étés observés, lesquels dépendaient du pH, de la température, de la durée et de la vitesse de cisaillement.

Dans le cas des galactomannanes, il a été observé que leurs propriétés rhéologiques, en solution aqueuse à 20ºC, étaient semblables. Pour la gamme de concentrations étudiées, les solutions présentaient un comportement rhéofluidifiant décrit par les modèles de Cross et Carreau. Les données des spectres mécaniques ont étés ajustés aux modèles de Friedrich-Braun et de Maxwell à quatre éléments. Des courbes maîtresses ont été obtenues pour les deux galactomannanes, en régime stationnaire et en régime dynamique.

Pour les systèmes mixtes β-lactoglobuline / galactomannane, une séparation de phases a été observée soit en solution, à 20ºC, soit en gel, pour toute la gamme de concentrations/ rapports de mélange, à pH 7.0 et à pH 4.6. Ce phénomène est le facteur déterminant le développement de la structure et les propriétés rhéologiques des systèmes mixtes. Dans le cas de systèmes liquides, à 20ºC, les images obtenues par microscopie confocale montrent une transition de

systèmes où la phase continue est enrichie en β-lactoglobuline pour des systèmes où la phase continue est enrichie en galactomannane, à mesure que la concentration de galactomannane augmente. A cette inversion correspond un changement des propriétés rhéologiques. Dans le cas où la phase continue est enrichie en β-lactoglobuline, le comportement est Newtonien, comme pour les solutions de β-lactoglobuline seule. Dans le cas où la phase continue est enrichie en galactomannane, le comportement est typique d'une suspension, probablement dû à la floculation de la phase dispersée, riche en protéine ; pour ces systèmes, les courbes d'écoulement, décrites par le modèle de Cross modifié, présentent des seuils d'écoulement apparents. Dans le cas des systèmes gélifiés, la présence du galactomannane modifie le comportement du système pendant la gélification, la viscoélasticité et la microstructure des gels obtenus. A pH 4.6, des gels particulaires, hétérogènes et plus grossiers que les gels filamenteux obtenus à pH 7.0, ont été observés par microscopie confocale ; ce fait montrent que les processus d'agrégation/gélification sont différents a chaque pH. Le comportement rhéologique des gels mixtes est qualitativement semblable à celui des gels de protéine pure et les modifications quantitatives sont limitées, dans la gamme de concentrations étudiées, à chaque pH. Les effets observés sont plus prononcés pour la gomme de caroube ce qu'indique un possible effet de la structure chimique du galactomannane dans la rhéologie des gels. Essais oscillatoires de balayage en déformation, à pH 7.0 et à pH 4.6, ont montré différents comportements des gels aux déformations élevées, ce que probablement est un reflet des différences observées dans leurs microstructures.

Les résultats obtenus ont permis de conclure que les propriétés structurales et rhéologiques des systèmes mixtes β-lactoglobuline / galactomannane, en milieu aqueux, sont sensiblement modifiés par altération de la concentration/ rapport de mélange des deux biopolymères, du pH et des procédés de traitement utilisés.

Mots clés: Propriétés rhéologiques; Microstructure; Séparation de phases; Gélification; β-lactoglobuline; Gomme de caroube; Gomme tara; Systèmes mixtes protéine / polyoside.

Acknowledgments

I would like to express my sincere thanks to my supervisor, Professor Dr. Maria do Pilar Figueroa Gonçalves, who so patiently offered her time, kindhearted, enthusiastic attitude, guidance, and encouragement throughout this research during my Ph.D. program, including her family for warmest welcome to their home many times during the time I spent in Portugal.

I owe thanks to the Department of Chemical Engineering, University of Porto, Portugal, where my work was carried out and granted me a scholarship fund during June till August of 2006. Also, I am grateful to Fundação Oriente and Fundação para a Ciência e a Technologia for the financial support during the past few months of 2001 and during 2002 - 2005, respectively.

A word of gratitude also goes to Professor Dr. Anake Kijjoa from Instituto de Ciências Biomédicas de Abel Salazar (ICBAS), University of Porto for his provided help, suggestions and criticism during my time in Portugal. Also, I would like to thank and respect to Professor Dr. Pichan Sawangwong, Professor Dr. Wirogana Ruengphrathuengsuka from Burapha University, Thailand and Professor Dr. Anake Kijjoa (again) for making my Ph.D. study possible.

I would like to thank Professor Dr. Isabel Ferreira from Faculty of Pharmacy, University of Porto for her kind guidance in HPLC part. Also, I am grateful to Professor Dr. Paula Sampaio from Instituto de Biologia Molecular e Celular (IBMC), University of Porto for the use of facilities and for her willingness to provide

assistance in microstructure part. Also, I express my special thanks and respect to Professor Dr. Jacques Lefebvre from Centre de Recherches de Nantes (INRA), France for his kind assistance in some parts of my work and his warmest relationship. Also, my sincere thanks are offered to Professor Dr. Manuel António Coimbra from Department of Chemistry, University of Aveiro for his assistance in the part of characteristic polysaccharide analysis.

I would like to give a big special thank to Américo Dimande who always cheers me up with love and understanding. Also, I am thankful to all my colleagues in the Laboratory of Food Engineering and Rheology, Dr. Marta Vázquez da Silva, Duarte Torres, Fabio Larotonda, Dr. Loic Hilliou, and Luis Mayor López for their pleasant company, help and unforgotten friendship. I also wish to thank all Thais in Porto, who I considered to be my sisters (P´Duang and Noot) and brothers (P´Ake and P´John) for their sense of humor, help, and share both sadness and happiness with me during my time in Porto.

And most of all, my most sincere appreciation from the depths of my heart goes to my mother, my father, my sisters and my brother, who always support me with their love and prayers from my home country, Thailand. Finally, I would like to say that the time I spent in Portugal so far has given me great experiences and opportunities to achieve a meaningful life. I love all the memories that I have had in Porto, Portugal.

Muito Obrigada

Table of Contents

List of Tables

List of Figures

List of Abbreviations

Latin capital letters

A	Power-law exponent ……	dimensionless
B	Power-law exponent ……	dimensionless
$C[\eta]$	Coil overlap parameter ……	dimensionless
C	Concentration of the solution ……..	(%, w/w)
C^*	Limit concentration for the dilute regime ……..…….	(%, w/w)
C^{**}	Limit concentration for the semi-dilute regime ……...	(%, w/w)
C_g	Critical gelation concentration ……	(%, w/w)
$C[\eta]$	Coil overlap parameter …….....	dimensionless
E	Strain hardening ……..	dimensionless
G	Relaxation modulus …….	(Pa)
G'	Storage modulus ……..	(Pa)
G''	Loss modulus ……...	(Pa)
G^*	Complex modulus ……...	(Pa)
G_e	Equilibrium modulus when the frequency tends to zero based on the Friedrich-Braun model ……...…….	(Pa)
G_i	Elastic modulus based on the generalized Maxwell model …….	(Pa)
G'_{max}	Maximum storage modulus during strain hardening ……..	(Pa)
G'_0	Constant storage modulus at strain sweep ……...	(Pa)
G''_0	Constant loss modulus at strain sweep ……	(Pa)
G_N^0	Plateau modulus based on the Cole-Cole model …….	(Pa)
ΔG	Parameter base on the Friedrich-Braun model ……...…….	(Pa)

J	Compliance in creep ……...……..	(Pa^{-1})
J_e	Equilibrium compliance of the solid …….	(Pa^{-1})
J_g	Glassy compliance ……	(Pa^{-1})
J_i	Compliance based on the generalized Kelvin-Voigt model ……..	(Pa^{-1})
J_r	Elastic (recoverable) contribution …….	(Pa^{-1})
J_v	Contribution of flow ……..	(Pa^{-1})
J_0	Elastic compliance …….	(Pa^{-1})
J'	Storage compliance ……..….	(Pa^{-1})
J''	Loss compliance ……..…..	(Pa^{-1})
J^*	Complex compliance ……..…....	(Pa^{-1})
J_e^0	Steady state compliance based on the retardation test ……..	(Pa^{-1})
J_N^0	Plateau compliance based on the Cole-Cole model ……...	(Pa^{-1})
J'_i	Storage compliance based on the generalized Kelvin-Voigt model ….	(Pa^{-1})
J''_i	Loss compliance based on the generalized Kelvin-Voigt model ……..	(Pa^{-1})
J''_r	Recoverable loss compliance in creep recovery ……...	(Pa^{-1})
K	Compliance in creep recovery ……...……	(Pa^{-1})
K_∞	Limited compliance in creep recovery ……..	(Pa^{-1})
L	Constant parameter ……..	(Pa)
M	Torque …….....	(N.m)
$\overline{M}_v$	Viscosity average molecular weight ……...	(Da)
N	Power law exponent of Carreau model ……..…….	dimensionless
P	Number of terms based on the generalized Kelvin-Voigt model	dimensionless
R	Angle of geometry ……	(rad)

S	Time at which applied stress is suppressed based on the retardation test …….	(h, min, s)
T	Temperature ……	(^oC)
T_g	Sol-gel transition (gelation) temperature …….	(^oC)
W	Number of terms based on the generalized Maxwell model ...	dimensionless

Latin small letters

a	Parameter based on the method of Kaschta and co-worker (1994) ……..	dimensionless
b	Parameter based on the method of Kaschta and co-worker (1994) ……..	dimensionless
c	Derivation orders of the differential operator of the Friedrich-Braun model ……..……..	dimensionless
d	Euclidean dimension ……...	dimensionless
d_f	Fractal dimension of the flocs …….	dimensionless
e	Derivation orders of the differential operator of the Friedrich-Braun model ……..……..	dimensionless
g	Gap width between plates ……...	(m)
k	Constant number of ideal solid material …….	dimensionless
k'	Huggins' coefficient ……..……..	dimensionless
k''	Kraemer's coefficient ……..……	dimensionless
l	Power-law exponent ……	dimensionless
m	Power law exponent of Cross and modified Cross models ….	dimensionless
n	Power-law exponent ……	dimensionless
o	Power-law exponent ……	dimensionless

p	Spread parameter related to the width of the peak based on the Cole-Cole model …….....	dimensionless
r	Upper plate radius ……...	(m)
s	Slope value of G' versus ω …….....	($Pa.s.rad^{-1}$)
t	Time/efflux time of the solution ……	(h, min, s)
t_M	Longest time based on the method of Kaschta and co-worker (1994) ……	(h, min, s)
t_s	Efflux time of the solvent …….	(h, min, s)
t_1	Shortest time based on the method of Kaschta and co-worker (1994) ……	(h, min, s)
x	Fractal dimension of the floc backbone ……..	dimensionless

Greek letters

α	Appropriate effective microscopic elastic constant ……	dimensionless
β	Parameter based on the model of Wu and co-worker (2001) ..	dimensionless
χ	Parameter based on the Mark-Howink relationship ……	dimensionless
δ	Phase angle between stress and strain ……...	degrees
ϕ	Particle volume fraction for a colloidal gel …….	dimensionless
γ	Shear strain …….....	(%)
$\dot{\gamma}$	Shear rate …….	(s^{-1})
γ^*	Complex shear strain ……...	(%)
γ_c	Critical strain or the limit of linearity ……..……	(%)
γ_r	Strain value at fracture ……..……..	(%)
γ_0	Maximum strain amplitude …….	(%)

η	Viscosity of the solution ……	(Pa.s)
$[\eta]$	Intrinsic viscosity ……	($dl.g^{-1}$)
η'	Dynamic viscosity ……	(Pa.s)
η''	Out of phase component of the complex viscosity ……	(Pa.s)
η^*	Complex viscosity ……	(Pa.s)
η_a	Apparent viscosity ……	(Pa.s)
$\eta_{cal,\ i}$	Viscosity value from fitting by model …….....	(Pa.s)
$\eta_{exp,\ i}$	Viscosity value from experimental data ……	(Pa.s)
η_p	Plateau Newtonian viscosity at intermediate shear rates ……..	(Pa.s)
η_{rel}	Relative viscosity …….……..	dimensionless
η_s	Viscosity of the solvent ……	(Pa.s)
η_{sp}	Specific viscosity ……...……..	dimensionless
η_{sp0}	Specific viscosity at zero-shear rate ……	dimensionless
η_0	Zero-shear rate apparent viscosity ……..……...	(Pa.s)
η_∞	Infinite shear rate viscosity or limiting Newtonian viscosity at high shear rates ……...……	(Pa.s)
λ	Time constants of Carreau model …….….	(s)
λ_F	Characteristic time of Friedrich-Braun model ……..……	(s)
λ_i	Parameter based on the generalized Maxwell model ……	(s)
θ_i	Terminal relaxation time of generalized Maxwell model ……..…	(s)
ρ	Density of the solution ……..	($kg.m^{-3}$)
ρ_s	Density of the solvent ……	($kg.m^{-3}$)
σ	Shear stress ……..	(Pa)

σ^*	Complex shear stress ……..	(Pa)
σ_a	Apparent yield stress ……..	(Pa)
σ_c	Critical stress ……..	(Pa)
σ_i	Applied stress based on the retardation test ……..…….	(Pa)
σ_0	Maximum stress amplitude …….	(Pa)
τ	Time constants of Cross and modified Cross models …….....	(s)
τ_i	Parameter based on the generalized Kelvin-Voigt model ……	(s)
τ_1	Shortest retardation time …….....	(s)
Ω	Angular velocity ……	($rad.s^{-1}$)
ω	Oscillatory frequency ……	($rad.s^{-1}$)
ω_0	Central frequency of the loss peak based on the Cole-Cole model ..	($rad.s^{-1}$)

Abbreviations

AR2000	Controlled stress rheometer
β-Lg	β-lactoglobulin
CLSM	Confocal laser scanning microscopy
GC-FID	Gas-liquid chromatography-flame ionization detector
FTIR	Fourier transform infrared
HPLC	High-performance liquid chromatography
LAOS	Large amplitude oscillatory shear
LBG	Locust bean gum
M/G	The mannose to galactose raito
NF	Nitrogen factor based on the Kjeldahl method
NMR	Nuclear magnetic resonance

pI	Isoelectric point
RE	Relative deviation error
RF	Relative response factors for each monosaccharide
RITC	Rheodamine isothiocyanate
RP-HPLC	Reversed-phase high-performance liquid chromatography
SEM	Scanning electron microscope
TG	Tara gum

General Introduction

Polysaccharides and proteins are two types of biopolymers present together in many kinds of food systems, contributing to the structure, texture and stability of these systems through their thickening or gelling behaviour and surface properties.

Presently, much is known at the molecular level about the functional properties of the individual biopolymers but the knowledge of the role of protein-polysaccharide interactions, in relation to their functionality in complex multiphasic systems, is still rather limited. However, this knowledge is relevant not only from a fundamental point of view but also for practical applications, to optimize product formulations and generate innovative textures.

In recent years, protein-polysaccharide systems are in high demand in the food industry because they offer the possibility to improve food texture and to develop new products.

In this study, particular attention will be given to the mixed systems of β-lactoglobulin and galactomannans (locust bean gum and tara gum).

β-lactoglobulin is the major protein in whey (a by-product of cheese manufacturing) and is used as ingredient in many food products. Galactomannans are neutral polysaccharides used in the food industry as thickening/stabilizing agents; in particular, locust bean gum, obtained from carob seeds, is produced in Portugal (in Algarve region). Mixed systems consisting of one gel forming globular protein (as β-lactoglobulin) and a neutral polysaccharide have been much less investigated than systems containing anionic polysaccharides, although their study constitutes *a*

priori a more direct approach to the basic phenomena since they are simpler, inter-species electrostatic interactions being excluded.

Thus, the study of the chosen systems seems relevant and may contribute to the valorisation of a national product (locust bean gum). The main goal of the study is, from a fundamental point of view, to get a better insight into the relationship between structure, rheological properties and composition of the β-lactoglobulin / galactomannan systems. It is expected that the obtained results will be useful for the development of new textures in media association globular proteins and polysaccharides in the formulation of food, cosmetic or pharmaceutical products.

At this point, a brief summary of the main content of the thesis is provided.

In Chapter 1, it is reviewed the existing body of information dealing with structure and properties in aqueous medium of β-lactoglobulin and galactomannans. Subsequently, interactions in mixed protein-polysaccharide systems and structure/properties relationships in these systems are also reviewed.

Chapter 2 deals with a detailed rheological investigation on heat-induced β-lactoglobulin gelation and on the properties of the final gels at two pH conditions: 7.0, where the protein bears a net negative charge, and 4.6, near the isoelectric point of the protein.

In the Chapter 3, the rheological behaviour of galactomannan (locust bean gum and tara gum) solutions was studied at 20^{o}C.

β-lactoglobulin / galactomannan mixed systems were studied afterwards. In Chapters 4 and 5, the study of the evolution of the microstructure and of the rheology of β-lactoglobulin systems, when different concentrations of galactomannan were added, was done in the liquid (Chapter 4) and gel (Chapter 5) states, at pH 7.0 and pH 4.6. The objective was to investigate possible correlations between microstructure and rheological properties of the mixed systems in the sol and gel states.

At the end of the thesis, the main conclusions arising from this work are given, and some topics for future research projects were recommended.

Chapter 1

Literature review

1.1 β-lactoglobulin

β-lactoglobulin is a globular protein with a molecular weight of 18,363 Da corresponding to a monomeric unit of around 162 amino acid residues (Bottomley, Evans, and Parkinson, 1990). It belongs to the lipocalin family, a class of small globular proteins that interact with hydrophobic molecules (Flower, 1996; Hoedemaeker, Visschers, Alting, de Kruif, Kuil, and Abrahams, 2002). Its isoelectric point (pI) is $\approx$5.1, as mentioned in many works (for example, Mulvihill and Donovan (1987); Olsson, Stading, and Hermansson (2000).

β-lactoglobulin is of direct interest to the food industry since its functional characteristics and properties, such as its gel-forming and surface-active properties, can be either advantageous or disadvantageous in dairy products and processing (Jost, 1993). Furthermore, β-lactoglobulin is a good model system for irreversible aggregation, gelation and phase separation and may therefore be investigated by various techniques at different stages of the process (Verheul, Roefs, and de Kruif, 1998; Olsson, Langton, and Hermansson, 2002).

1.1.1 Origin

1.1.1.1 Sources

β-lactoglobulin is the major protein constituent of whey in the milk of ruminants and many other mammals, but is absent from human milk and the milks of some other monogastrics (Mulvihill et al., 1987). It composes up to 50% of the total whey protein in bovine milk (CLA, 2002) as shown in Table 1.1.

Table 1.1 Composition of the proteins in bovine milk (CLA, 2002)

Component	**% Total**	**% Casein**	**% Whey**
Caseins	*83*		
α s1-Casein	36	44	
α s2-Casein	9	11	
β-Casein	21	25	
κ-Casein	12	14	
γ-Casein	4	5	
Whey	*17*		
β-lactoglobulin	10		58
α-lactalbumin	2		13
Immunoglobulins	2		12
Serum Albumin	1		6
Minor proteins	2		12

1.1.1.2 Structure

In its native state, β-lactoglobulin exists as a globular protein folded into a compact three-dimensional structure. Its structure, properties and biological role have been reviewed many times (see, for instance, Sawyer and Kontopidis, 2000; Kontopidis, Holt, and Sawyer, 2004). Recently, its structure has been determined by various techniques such as X-ray crystallography (Sawyer, Brownlow, Polikarpov, and Wu, 1998), Synchrotron X-ray scattering, circular dichroism, absorption and fluorescence spectroscopy (Arai, Ikura, Semisotnov, Kihara, Amemiya, and Kuwajima, 1998) and FTIR spectroscopy (Lefèvre and Subirade, 1999).

Several isoforms (genetic variants) of β-lactoglobulin are known (Mulvihill et al., 1987; Botelho, Valente-Mesquita, Oliveira, Polikarpov, and Ferreira, 2000). Isoforms A and B, which are prevalent in bovine milk, differ by only two amino-acid substitutions: Asp 64 and Val 118

in isoform A are replaced by glycine and alanine in isoform B, respectively (Botelho et al., 2000; Strzalkowska, Krzyzewski, Zwierzchowski, and Ryniewicz, 2002; Croguennec, O'Kennedy, and Mehra, 2004), as shown in Figure 1.1. For this reason the isoform B is slightly less hydrophobic and has one less positive charge at acidic pH. The molecule contains two disulfide bridges and one free sulfhydryl group. One of the disulfide bridges is between Cys 66 and Cys 160. The other seems to be a dynamic one that involves Cys 106 and is sometimes found with Cys 121 and sometimes with Cys 119. Thus, there is a 50:50 distribution of the bond between positions 119 and 121, which means that ½ of the Cys 119 and ½ of the Cys 121 exist as free sulfhydryl groups (Mulvihill et al., 1987; CLA, 2002).

Figure1.1 Primary structure of bovine β-lactoglobulin A. The locations of the amino acid substitutions in the isoforms are indicated.

The secondary structure of β-lactoglobulin contains about 20 – 30% β-sheet, with 50 – 60% unordered plus turn, and the remaining is α-helix. The antiparallel β-sheet is formed by nine strands wrapped round to form a flattened cone. The core of the molecule is an eight-stranded, antiparallel β-barrel. The center of the barrel is hydrophobic and can be involved in the binding of hydrophobic molecules (Bottomley et al., 1990). The lone α-helix is located on the surface of the molecule. The three dimensional structure of β-lactoglobulin is presented in Figure 1.2. (MLI, 2005).

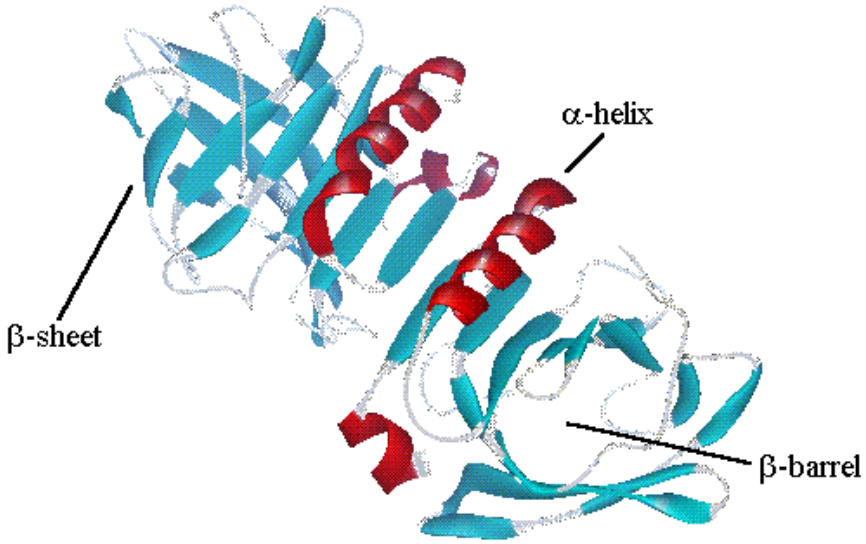

Figure 1.2 Three-dimensional representation of secondary structure of bovine β-lactoglobulin (MLI, 2005).

β-lactoglobulin exhibits many multimeric structures depending on the temperature, pH and protein concentration (McKenzie and Sawyer, 1967): at room temperature, β-lactoglobulin is predominantly a dimmer, in aqueous solutions at pH values between 5.5 and 7.5. Below pH 3.5 and above pH 7.5, the dimmer dissociates into the monomeric subunits while at pH 3.7–5.1 it

forms an octamer, especially at temperatures below 20ºC (Verheul, Pederson, Roefs, and de Kruif, 1999). The octomer is a compact cyclic structure and conformational changes accompany these association reactions. In the alkaline region, the protein undergoes a conformational change at pH 7.5, accompanied by a molecular expansion. Above pH 7.0, there is a rapid increase in the reactivity of the free thiol group; dissociation of the dimer also occurs in this region. At pH 8.0 and above, the protein can be regarded as unstable, since it will form aggregates of denatured protein. Nevertheless, its native state remains fairly intact at lower pH values, as determined using NMR spectroscopy (Uhrinova, Smith, Jameson, Uhrin, Sawyer, and Barlow, 2000). Besides, the concentration is a parameter which governs the quaternary structure of the protein. McKenzie et al., 1967 reported that the equilibrium is shifted towards the monomeric form at low concentration of β-lactoglobulin.

1.1.2 Globular protein gelation

Gelation of globular proteins has been extensively investigated (Doi, 1993; Gosal and Ross-Murphy, 2000; Clark, Kavanagh, and Ross-Murphy, 2001) and can be induced by both physical and chemical ways (Totosaus, Montejano, Salazar, and Guerrero, 2002). Physical techniques involve heat (Croguennec et al., 2004) and pressure (Zasypkin, Dumay, and Cheftel, 1996; Botelho et al., 2000) induced gelation. Chemical ways are acidification, salt (Ju and Kilara, 1998) or enzymatic hydrolysis (Doucet, Gauthier, and Foegeding, 2001).

Here, the review will be limited to heat-induced gelation.

1.1.3 Heat-induced gelation of β-lactoglobulin

Heat-induced gelation of whey proteins or β-lactoglobulin has been studied various investigators (see, for instance, Stading and Hermansson, 1990; McSwiney, Singh, and Campanella, 1994; Croguennec et al., 2004), since it is very important for commercial production of foods and pharmaceuticals, being responsible for the structure present in the products. Also, heat-induced gelation is significant in manufacturing lines because it can cause problems such as the fouling of pipes (Ghashghaei, 2003); hence, for controlling the processes, it is necessary to understand the fundamentals of heat-induced gelation.

Heat-induced gelation of globular proteins results from an aggregation process which is generally triggered by a conformational change of the protein induced by a modification of solvent conditions. The heat induced aggregation of β-lactoglobulin can be interpreted as proceeding in two steps: a denaturation equilibrium (with a first-order unfolding reaction) followed by second-order aggregation reactions (Verheul et al, 1998). Upon unfolding, the thiol group is exposed and becomes reactive. In the aggregation reactions either or both covalent (inter- and intramolecular disulphide bonds) and non covalent bonds (hydrophobic, hydrogen and ionic interactions) are involved (Mulvihill et al., 1987). The experimental conditions (pH, ionic strength, heating temperature) determine the rate and nature of the reactions occurring (Galani and Apenten, 1999; Havea, Carr, and Creamer, 2004). β-lactoglobulin gels may be of two types depending on the pH and ionic strength. Transparent gels, composed of more or less flexible linear strands ("fine-stranded gels"), are formed, at low ionic strength, above pH 6 and below pH 4. Opaque gels, characterized by a random association into large and almost spherical aggregates linked together to constitute the threads of the network ("particulate gels"), are

formed between pH 4 and 6 (Stading et al., 1990; Stading and Hermansson, 1991), close to the pI or at high ionic strength (Doi, 1993).

For fine-stranded gels, the heating process induces the dissociation of the dimmers into monomers and, then, the proteins undergo extensive denaturation before aggregation and formation of a three dimensional network (Figure 1.4). Langton and Hermansson (1992) and Stading, Langton, and Hermansson (1995) showed that different strands were obtained at low and high pH values; at pH 3.5 the distance between cross-links was short and the strands were straight and stiff while at pH 7 the strands were slightly thicker and more flexible, and the distance between cross-links was longer.

In another study, Baussay, Le Bon, Nicolai, Durand, and Busnel (2004) observed that the initial step of heat-induced denaturation of β-lactoglobulin, at pH 7, was the formation of primary aggregates containing clusters of about 100 monomers, which formed only above a critical association concentration, and then self semi-flexible aggregates with a large scale structure were formed by association of the primary aggregates. In this aggregation step, the onset time is related to a critical concentration of primary particles (Verheul et al., 1998).

Figure 1.3 shows a schematic drawing of the aggregation process, at pH 7 and 0.1M salt. In order to form a gel, the protein aggregates have to grow sufficiently large to fill up the whole space. Gelation may be delayed if the growth stagnation occurs when the aggregates are already close to space filling conditions. However, if the growth stagnation occurs when aggregates are still small, the gel is not formed (Durand, Gimel, and Nicolai, 2002).

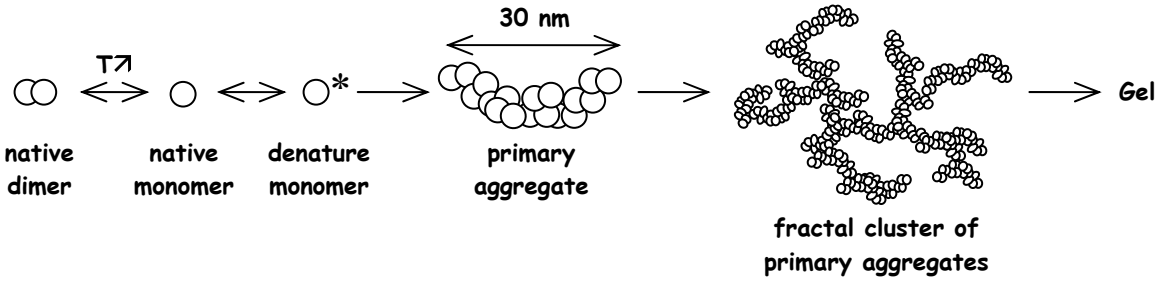

Figure 1.3 Schematic representation of aggregation process of β-lactoglobulin at pH 7 and 0.1 M salt (Durand, Le Bon, Croguennoc, Nicolai, and Clark, 2002).

For the particulate gels, β-lactoglobulin keeps the dimeric form; the gelation process starts directly by the aggregation of proteins in the dimeric form accompanied by partial protein unfolding. Aggregation continues further leading to the formation of the gel (Lefèvre and Subirade, 2000) (Figure 1.4).

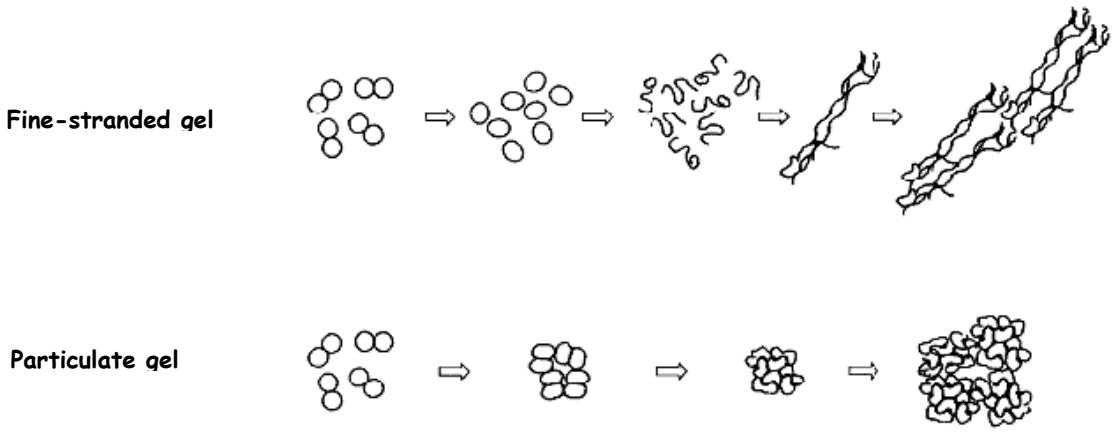

Figure 1.4 Mechanisms of denaturation and aggregation of β-lactoglobulin for fine-stranded and particulate gels (Lefèvre et al., 2000).

1.1.4 Factors influencing gel properties

β-lactoglobulin gels properties are strongly affected by the protein concentration, processing conditions (heating and cooling rates, shear) and environmental factors (pH, ionic strength) (Mulvihill et al., 1987; Doi, 1993; Roefs and De Kruif, 1994; Verheul et al., 1998).

1.1.4.1 Protein concentration

In favorable conditions, the protein aggregates have to grow sufficiently large in order to form a gel. In general, higher protein concentration leads to more and larger aggregates (Mleko, 1999). If the protein concentration is too low, a protein network is difficult to establish (Durand et al., 2002).

Thus, many earlier works have concentrated on the critical gelation concentration, C_g; for example, Le Bon, Nicolai, and Durand (1999) observed that β-lactoglobulin gels could not be formed at concentrations as low as 10 $g.L^{-1}$. Besides, they also found that the protein concentration influenced the gel time: decreasing of protein concentration increased the gel time. In turn, Stading and co-worker (1990) noted that the critical concentration for β-lactoglobulin gelation depended on the pH range: the critical gelation concentration, at pH 4.5-5.5, was lower than the one observed below pH 4.5 or above pH 5.5.

1.1.4.2 Temperature and heating time

Temperature and heating time, including heating rate, are the prior factors that influence globular protein gelation and have been extensively studied over many years (for instance,

Stading, Langton, and Hermansson, 1993; McSwiney et al., 1994; Verheul et al., 1998; Galani et al., 1999; Bryant and McClements, 2000). Most previous studies have looked at denaturation and aggregation of protein, for example: the protein denaturation becomes rate limiting at high temperature heating (Verheul et al., 1998). Besides, the temperature can affect globular protein aggregation mechanism, almost certainly the non-covalent interaction (Galani et al., 1999), and the size of protein aggregates is also increased with increasing heating time (Durand et al., 2002).

Considering the heating rate, Stading and co-workers (1993) showed that, at a fast heating rate (5-10^{o}C/min), gels formed homogeneous networks with pore size of 20-30 μm while, at a slow heating rate (0.1-1^{o}C/min), gels showed inhomogeneous networks with lager pores (~100-500 μm). In addition, the gels formed at a slow heating rate had a higher G' which was explained by the microstructure of the strands (Langton et al., 1992; Stading et al., 1993).

1.1.4.3 pH and ionic strength

The effects of pH and ionic strength have been already described in section 1.1.3. Here, the focus will be on the different types of intermolecular interactions that control hear-induced aggregation and gelation of globular proteins. During thermal denaturation, the macromolecular structure uncoils and exposes previously hidden non-polar amino acid side-chains, which can give rise to intermolecular hydrophobic interactions. This type of interaction was reported to be involved in the formation of primary aggregates at pH values between 6 and 9 (McSwiney et al., 1994). At acid pHs, hydrogen bonds, resulting from the interaction of polar amino acid side-chains, are responsible for the network formation (Shimada and Cheftel, 1988). At pH values far from the isoelectric point of the protein, repulsive electrostatic interactions play an

important role and lead to the formation of the so-called fine-stranded network structures (Renard, Lefebvre, Griffin, and Griffin, 1998; Aymard, Nicolai, Durand, and Clark, 1999). Also, intermolecular covalent bonds result from reactions of sulfhydryl groups, which can form intermolecular disulphide linkages with other reactive sulfhydryl groups or through sulfhydryl-disulphide interchange reactions. These covalent cross-links are, together with hydrophobic interactions, the main determinants of the network of whey proteins gels at neutral and alkaline pHs (Shimada et al., 1998).

Stading and co-workers (1991; 1995) verified that fine-stranded and particulate β-lactoglobulin gels had totally different mechanical properties. Lower values for G' and higher strain at fracture were found for gels obtained at pH 7.0, when compared to gels formed at intermediate pH values. These authors were able to show that the strand structure influenced both the modulus as well as the fracture properties of both type of gels. Homogeneous gels obtained at pH 7.0 consisted of thin strands (<5 nm), curled and not very stiff, with short distances between cross-links while particulate gels, formed at pH 5.3, had flexible strands of uniform, spherical particles arranged like beads on a string, and pores of ~20 – 50 μm. In large deformation measurements, the structure was broken; the weaker areas were broken before the stronger ones. For particulate gels, the pores were probably the weakest element of the network and were responsible for the fracture (Standing et al., 1995). Microstructural analysis showed differences in the regularity and particle size of particulate network structures: regular structures, composed of particles with a narrow size distribution, were observed between pH 5 and 6, while irregular structures (coarse, uneven aggregation) formed at pH 4.5 (Langton et al., 1992).

In another study, Baussay and co-workers (2004) observed that the critical gel concentration, C_g, for β-lactoglobulin, at pH 7.0, decreased with increasing ionic strength. For $C > C_g$, gels formed, except at high ionic strength where C_g was so small that the gel was very fragile, collapsed under gravity and a precipitate was formed.

1.1.4.4 Shear

The network structure and the rheological properties of protein gels can be strongly influenced by exposing the suspensions to shear during heat-induced aggregation. As most of the products on the market have a process history (flow through pipes, heat exchanger, filters, etc.), it is important to be aware of the relationships between product quality and process conditions. Thereby, the effects of shear on biopolymer gel properties have interested many investigators (for example, Taylor and Fryer, 1994; Walkenström, Panighetti, Windhab, and Hermansson, 1998; Altmann, Cooper-White, Dunstan, and Stokes, 2004).

For pH 7.0 solutions of whey protein concentrate, Taylor and co-worker (1994) found that the final gel strength of sheared gels was a complex function of the time of shear, the final gel strength decreasing with increasing time of shear, suggesting the disruption of protein aggregates by shear. The same authors found that, at pH 5.2, shear during the initial stages of heating, at 85^{o}C, increased the gel strength, probably due to shear preventing rapid aggregation into weak network, but longer periods of shear lead to a decrease in gel strength as protein aggregates were disrupted by shear.

Walkenström, Windhab, and Hermansson (1998) also reported changes in the microstructure and the rheology of sheared particulate whey protein gels, at pH 5.4. These changes depended

on the temperature range of exposure to shear ($T < T_g$ or $T > T_g$) and on the shear rate applied. Gels sheared at continuous shear rates less than ~6 s^{-1}, till $T < T_g$, had similar microstructures but lower G', less frequency dependence and higher stress at fracture than unsheared gels. In contrast, if shearing was done till $T > T_g$, two different types of microstructure were observed: one open and loose, having similar particle and pore size to those in the unsheared network; the other was dense and compact with smaller particles and pores. In this case, the gels had lower stress at fracture than the unsheared ones. For short periods of shear treatment in the vicinity of the gel point, gels showed more inhomogeneous network structures and a G' value twice as high as that for the unsheared gel (Walkenström et al., 1998). When the study was done with whey protein gels formed at pH values far from pI (fine stranded gels), the effect of short periods of shear treatment in the vicinity of the gel point proved to be minor (Walkenström and Hermansson, 1996).

1.2 Galactomannans

Galactomannans are heteropolysaccharides whose structural components are two monosaccharides: D-mannose and D-galactose (McCleary, Clark, Dea, and Rees, 1985; LSB, 2005). They are plant carbohydrates that occur in large amounts in the endosperm of the seeds of many plants of the legume family such as carob (*Ceretonia siliqua* L.), guar (*Cyamopsis tetragonolobus*), fenugreek (*Trigonella foenum-graecum* L.) and tara (*Caesalpinia spinosa*) (Rol, 1973; Dea and Morrison, 1975).

1.2.1 Origin

Locust bean gum:

Locust bean gum or carob gum is extracted by grinding the endosperm portions of the seeds of carob tree (*Ceretonia siliqua*), a very ancient leguminous plant (Rol, 1973; Batlle and Tous, 1997). Its origins lie in the Middle East; then, carob tree was moved along the North African coast and into Spain and Portugal by Arabs (CYB, 2005). The carob tree is important in the Mediterranean basin as a crop that can be grown on marginal lands where few other crops can be grown economically (Batlle et al, 1997).

The carob seed has a very uniform size, about 200 mg and was used as a standard weight in medieval times by jewelers (Rol, 1973; CYB, 2005). It has been perpetuated until this day as the weight unit of diamonds, the "carat", which is derived from the name "carob," in reference to carob seeds. Pods of the carob tree often grow directly from the main branches of the tree dark brown carob pods are represented in Figure 1.5.

Tara gum:

Tara gum is a new hydrocolloid thickener and gelling agent recently introduced. It is the refined endosperm of the seed of *Caesalpinia spinosa* or *Caesalpinia tinctoria*, a shrub tree indigenous of Peru and Bolivia (EXP, 2004). Tara tree, an uncultivated plant, grows in tropical and subtropical climates along Peruvian coastline, as well as on the western slopes and in the valleys of the Andes Mountains. Tara gum has an immense medical, nutritional and industrial potential (FAO, 2003; EXP, 2004). The tara fruits are show in Figure 1.5: they are orange-colored, when immature, and of a dull blackish color, when mature.

Figure 1.5 Fruits, trees and pod split open of locust bean gum and tara gum (CDM, 2005; BOT, 2005; MEM, 2005).

1.2.2 General applications

The great advantage of galactomannans is their ability, at relatively low concentrations, to form very viscous solutions which are only slightly affected by pH, added ions, and heat processing. For this reason, galactomannans are used as thickening agent, emulsifiers, and stabilizers in a wide range of food industrial applications (Rol, 1973; FAO, 2003).

Some of the many foods containing galactomannans are ice cream, other milk-based products, baking and desserts, mayonnaises, dressings, meat products and deep-frozen foods (Rol, 1973; Batlle et al., 1997). In ice cream, the galactomannans impart excellent meltdown resistance and improve storage properties (FAO, 2003; CYB, 2005). In cream cheese, they are used to bind water and produce a spreadable texture without imparting sliminess (CYB, 2005). For sausage products, they function as a binder and lubricant (FAO, 2003). However, galactomannans are used not only in foodstuffs - produced for humans and animals - but also in cosmetics, textiles and pharmaceutical products (Rol, 1973; Dea et al., 1975).

1.2.3 Chemical structure

The galactomannans are neutral (nonionic) polysaccharides. They are linear polysaccharides having a backbone of β-1→4 linked D-mannose residues. To this chain, single α-D-galactose residues are linked by C-1 through a glycosidic bond to C-6 of mannose (Dea et al., 1975; CYB, 2005) (Figure 1.6).

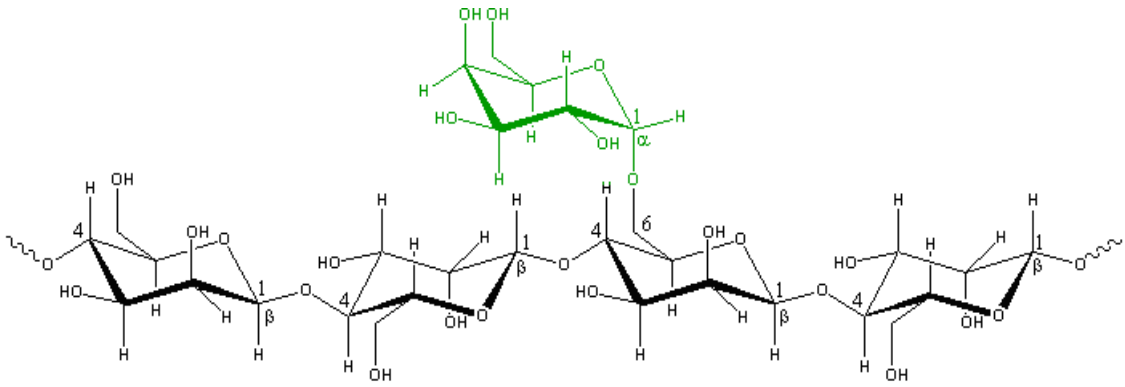

Figure 1.6 Representative structure of a typical galactomannan (locust bean gum); D-mannose: in black; D-galactose: in green (LSB, 2005).

Galactomannans differ in the ratio of mannose to galactose units, M/G, which is one of their main biochemical characteristics. The more substituted of the commercial galactomannans is guar gum (M/G ~2:1); in tara gum, the M/G is ~ 3:1 while in locust bean gum is ~ 4:1 (McCleary and Neukom, 1982; Alais and Linden, 1991; Batlle et al., 1997; Ruiz-Ángel, Simó-Alfonso, Mongay-Fernández, and Ramis-Ramos, 2002) (see Table 1.2).

The structural characteristics of galactomannans, especially guar gum and locust bean gum, have been extensively studied by several researchers (for example, Courtois and Le Dizet, 1966; McCleary et al., 1985).

Table 1.2 Galactomannan substitution levels (FAO, 2003)

Galactomannans	**D-mannose to D-galactose ratio (M/G)**
Fenugreek gum	1:1
Guar gum	2:1
Tara gum	3:1
Locust bean gum	4:1

The distribution of the galactosyl residues has been investigated by various techniques such as computer analysis (Clark, Dea, and Rees, 1985) and enzymatic determination (Courtois et al., 1966; Dass, Schols, and de Jongh, 2000). It was possible to conclude that the galactose units were not regularly distributed along the mannan backbone but, for the less substituted galactomannans like locust bean gum, there were bare zones, with no galactose side chains, and hairy zones with branched galactose units. The functional properties are related to both the structural features and the molecular masses (Batlle et al., 1997; Ruiz-Ángel et al., 2002). For similar M/G ratios, differences in the interaction properties have been detected between galactomannans of different sources, which were attributed to differences in their fine structures

(Dea, Clark, and McCleary, 1986). For similar molecular masses, locust bean gum and guar gum give solutions of similar viscosity but with quite different synergistic interactions; the M/G ratio seems to be the main factor for these different behaviours (Dea, Morris, Rees, Welsh, Barnes, and Price, 1977; Fernandes, Gonçalves, and Doublier, 1991).

1.2.4 Rheological properties of galactomannan solutions

1.2.4.1 Concentration dependence of viscosity

On dissolving, the galactomannans lose their ordered structure and go into solution as conformationally-disordered "random coils". Depending on concentration, different types of solution behaviour are observed: dilute, semi-dilute and concentrated regimes (Castelain, Doublier, and Lefebvre, 1987; da Silva and Rao, 1992) (see in Figure 1.7).

In dilute solution, the polysaccharides act as isolated "particles", too dilute to interact with each other. At a critical concentration C^*, defined as the limit for the dilute regime, there is a change in the concentration dependence of solution viscosity; the "particles" start to interact significantly because their total excluded volume approaches close packing, moving coils to an entangled network (Morris, 1995), as illustrated in Figure 1.7. Further increase in concentration leads to much greater overlap of biopolymer coils and rapid increase in viscosity. A second critical concentration, C^{**}, the concentration beyond which the chain dimensions become independent of concentration (Castelain et al., 1987), defines the limit of the semi-dilute regime. For higher concentration ($C > C^{**}$), in the concentrated regime, the individual polymer molecules are no longer readily distinguishable and overlap in a tangled mass, the viscosity increases much more steeply with increasing concentration (Morris, 1995), and the solution starts to show some solid-like behaviour.

The onset of coil overlap and entanglement depends both on the number of coils present (proportional to concentration) and on the volume that each occupies (proportionally to intrinsic viscosity, $[\eta]$) and can therefore be characterized by the (dimensionless) "coil overlap parameter", $C[\eta]$. For most random-coil polysaccharides, Morris, Cutler, Ross-Murphy, Rees, and Price (1981) showed that plots of viscosity against $C[\eta]$ were closely superimposable, irrespective of polymer type, molecular weight or solvent conditions, and the C^* transition occurred at a value of $C[\eta] \sim 4.0$. For the galactomannans locust bean gum and guar gum, the same authors observed that the C^* transition occurred at a lower value of $C[\eta]$ (~ 2.5) and the subsequent concentration dependence of viscosity was greater (about $C^{4.0}$, instead of $C^{3.3}$ as for the other random-coil polysaccharides). This has been attributed to the presence of more specific interactions between the macromolecules ("hyperentanglements"), in addition to the non-specific physical entanglements.

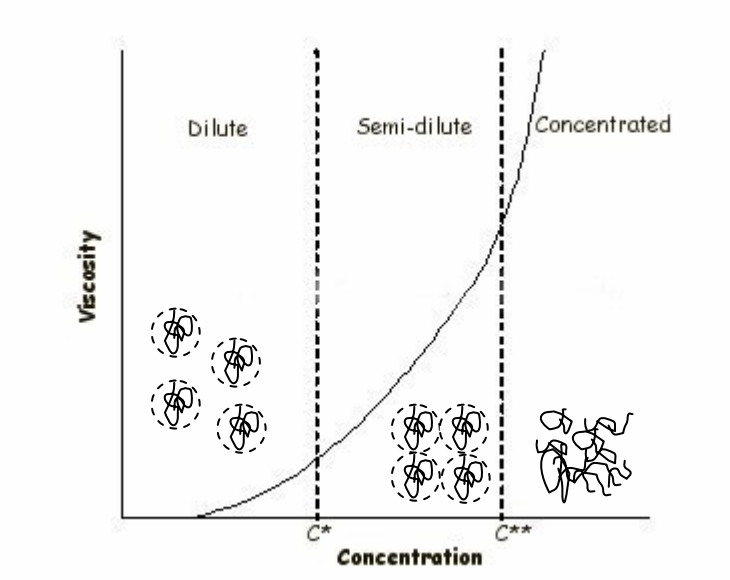

Figure 1.7 Diagram illustrating three concentration regions of biopolymer solutions.

1.2.4.2 Shear-rate dependence of viscosity

The apparent viscosity of galactomannans solutions, like for other random-coil polysaccharide solutions, is strongly dependent on shear rate, $\dot{\gamma}$, for $C > C^*$ (Figure 1.8). At low shear rates, viscosity remains constant at the "zero-shear" value, η_0. With increasing shear rate, however, viscosity falls (shear thinning behaviour). The shear-thinning behaviour may be regarded as arising from modifications in macromolecular organization in the solution as the shear rate changes. At low shear rates, the disruption of entanglements by the imposed shear is balanced by the formation of new ones, so that no net change in entanglements occurs; it is the Newtonian plateau region, where the viscosity has a constant value, the zero-shear rate apparent viscosity, η_0. For higher shear rates, disruption predominates over formation of new entanglements, molecules align in the direction of flow and the apparent viscosity decreases with increasing shear rate. As a consequence, the shear rate corresponding to the transition from Newtonian to shear-thinning behaviour moves to lower values as the concentration increases.

Morris and co-workers (1981) observed the same shear thinning profile for different polysaccharides irrespective of chemical type, concentration or molecular weight. This has been interpreted as reflecting the existence of non-specific physical entanglements in the polysaccharide solutions. Flow master curves could be obtained by shifting along the two axes the flow curves obtained at different concentrations of the polysaccharides solutions. By using a similar reduced variables procedure, other authors obtained master flow curves for sodium alginate, λ-carrageenan (Gonçalves, 1984) and cellulose derivatives (Castelain et al., 1987). Many equations have been proposed to describe the shear thinning behaviour of solutions of coil-type macromolecules, like galactomannans; those of Cross (1965) and Carreau (1972) were successfully used by da Silva and co-worker (1992) and Alves, Garnier, Lefebvre, and

Gonçalves (2001) to study the flow behaviour of locust bean gum alone and in mixtures with pectins or gelatin; more recently, Oblonsek, Sostar-Turk, and Lapasin (2003) used the Cross model to describe the flow properties of concentrated guar gum solutions. These models will be discussed in Chapters 3 and 4 of the present thesis.

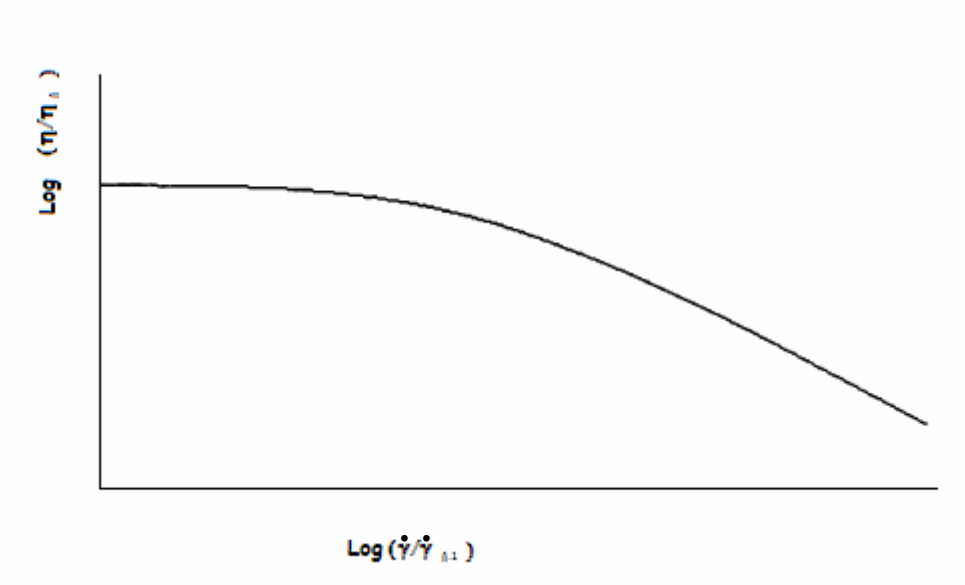

Figure 1.8 Generalized shear rate dependence of viscosity for concentrated solutions of random-coil polysaccharides (adapted from da Silva et al., 1992).

1.2.4.3 Viscoelastic properties

Dynamic measurements have been extensively used to study viscoelasticity of polysaccharide solutions. For several galactomannans and other random-coil polysaccharides, at relatively high concentrations, a liquid-like behaviour ($G'' > G'$) was observed at low frequencies; at higher frequencies, the magnitude of G' increased due to macromolecular distortion, and approached that of G'' when the time of one oscillation period was low enough to prevent entanglement disruption. When the frequency was high enough that translational movements were no longer possible within the period of oscillation, the system behaved like a solid, with $G' > G''$, and

both moduli showed little change with frequency. The "cross-over frequency" (where $G' = G''$, which corresponds to the beginning of the elastic plateau) typically moved towards lower frequency values when the concentration increased (Figure 1.9), that is as the degree of entanglement increased (Robinson, Ross-Murphy, and Morris, 1982; da Silva, Gonçalves, and Rao, 1993; Andrade, Azero, Luciano, and Gonçalves, 1999; Oblonsek et al., 2003).

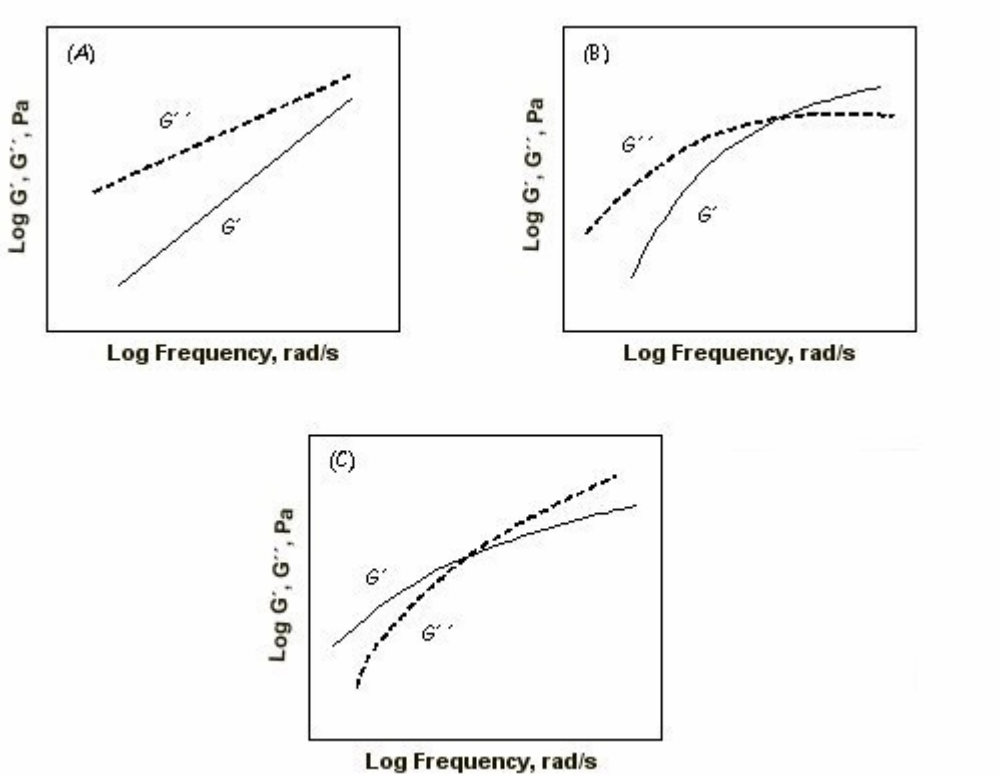

Figure 1.9 Typical mechanical spectra for: a dilute solution (A), a concentrated solution (B), and a weak gelled system (C) (adapted from Morris, 1995; Steffe, 1996).

As for flow curves, master curves can be obtained for G' and G'' by superimposing curves obtained at different concentrations. The approaches to model the viscoelastic behaviour fall into two main categories: the molecular and the phenomenological approaches. The former is based on the definition of rheological properties starting from molecular or microscopic

parameters which identify the components of the system. The latter deals with the development and definition of the model according to the principles of continuum mechanics; it is based upon achieving the maximum agreement between predicted and experimental data. Using this last approach, the dynamic response of viscoelastic materials can be described using a generalized Maxwell model or the Friedrich–Braun model (1992), which belongs to the class of the fractional derivative models. These two models were used to describe the frequency dependence of G' and G'', in the linear viscoelastic regime, for different polysaccharides such as guar gum (Oblonsek et al., 2003), welan, gellan and carboxymethylcellulose (Zupancic and Zumer, 2001; Manca, Lapasin, Partal, and Gallegos, 2001) and will be discussed further in Chapter 3 of this thesis.

1.3 Mixed protein-polysaccharide system

1.3.1 Type of interactions

The structural functions of proteins and polysaccharides are greatly affected by their interactions with each other and with other components of food systems. When mixing a protein and a polysaccharide in solution, it may be observed one of the following possibilities: i) miscibility or co-solubility, ii) complex coacervation or complexation (biopolymers associate, excluding solvent from their vicinity; two distinct immiscible aqueous phases are formed and one of them is loaded with both polymer species, whereas the other one is depleted of polymer. This situation is typical of solutions of oppositely charged polyelectrolytes) or iii) thermodynamic incompatibility (biopolymers being mutually segregating one from the other; two distinct aqueous phases are formed but, this time, each of them is mainly loaded with one biopolymer species) (Syrbe, Bauer, and Klostermeyer, 1998; de Kruif and Tuinier, 2001), as depicted in Figure 1.10. The main difference between the two phase separation mechanisms is

that thermodynamic incompatibility is predominantly entropically driven, whereas complex coacervation is both entropically and enthallpically driven (de Kruif et al., 2001).

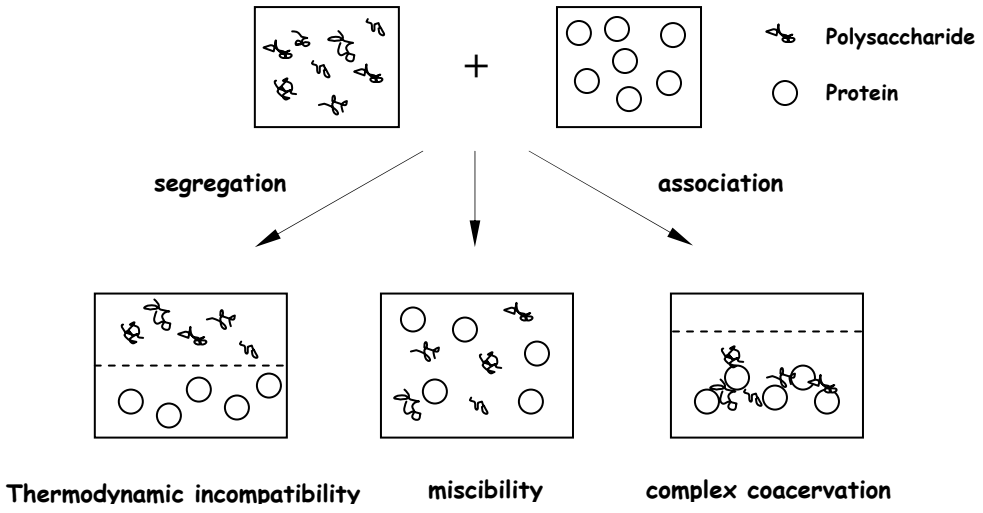

Figure 1.10 Schematic representation of the equilibrium phases possible for mixed protein and polysaccharide solutions (adapted from de Kruif et al. (2001)).

During the last decades, scientists have approached these systems using polymer concepts. They built phase diagrams and investigated the influence of various physicochemical parameters on protein-polysaccharide interactions. The main limitations of their approach were its lack of time resolution and mechanistic understanding (Turgeon et al., 2003).

Nevertheless, experimental evidence shows that incompatibility is a very general phenomenon in aqueous protein-polysaccharide solutions (Tolstoguzov, 1991, 1992; Durrani, Prystupa, Donald, and Clark, 1993; Grinberg and Tolstoguzov, 1997; Antonov and Gonçalves, 1999; Alves, Antonov, and Gonçalves, 1999). Only few examples of complete miscibility are

reported, such as serum albumin / pectin systems (Semenova, Bolotina, Dmitrochenko, Leontiev, Polyakov, Braudo, and Tolstoguzov, 1991).

1.3.2 Mixed β-lactoglobulin / polysaccharide mixtures

In the case of globular proteins, as β-lactoglobulin, the addition of a polysaccharide induces depletion interactions which lead to an effective mutual attraction between the proteins and accelerates phase separation effects (Tuiner, Dhont, and de Kruif, 2000). Depletion interactions theories have been used to analyze the phase behaviour of colloid-biopolymer mixtures (Tuinier, Rieger, and de Kruif, 2003) and, in particular, of proteins and polysaccharides (de Kruif et al., 2001; Wang, van Dijk, Odijk, and Smit, 2001). The mechanism behind phase separation of β-lactoglobulin and pullulan was explained in terms of the depletion interactions in a suspension of small spheres (proteins) in a semi-dilute solution of coils (polysaccharides) forming an entangled network (Wang et al., 2001). Several other authors have recently studied phase separation in milk protein (colloidal casein) and polysaccharide mixtures (see, for instance, Bourriot, Garnier, and Doublier, 1999; Schorsch, Jones, and Norton, 1999; Tuinier and de Kruif, 1999; de Bont, van Kempen, and Vreeker, 2002; de Bont, Hendriks, van Kempen, and Vreeker, 2004).

In general, results obtained support the idea that depletion interactions are the driving force for phase separation in milk protein / polysaccharide mixtures. In some of these studies, where galactomannans were used, emulsion-link microstructures have been observed with milk proteins concentrated in spherical droplets (Bourriot et al., 1999; Schorsch et al., 1999), while in others (where amylopectin was used) CLSM revealed the appearance of aggregate structures when phase separation occurred (de Bont et al., 2002; 2004). The observed microstructural

difference was ascribed to a low value of the biopolymer-colloid size ratio for milk protein / amylopectin systems.

When globular protein / polysaccharide mixtures are heated, competition between phase separation and gelling can lead to many different gel microstructures depending on the interplay of the kinetics of the two processes, resulting in a wide range of properties (Doublier, Garnier, Renard, and Sanchez, 2000; Turgeon, Beaulieu, Schmitt, and Sanchez., 2003).

In recent literature, the behaviour of mixed β-lactoglobulin (whey proteins) / anionic polysaccharides (κ-carrageenan, xanthan) was described as governed by segregative phase separation phenomena. Capron, Nicolai, and Durand (1999) and Capron, Nicolai, and Smith (1999) showed that the presence of κ-carrageenan did not alter the kinetics of the early stage of the aggregation process but accelerated the large scale aggregation leading to gel formation and that the structure of the resulting gel and its properties depended upon the size of aggregates just after the gel point. Synergistic interaction in β-lactoglobulin / κ-carrageenan was exhibited in conditions where the two biopolymers gelled close to neutrality; this synergy was taken as a consequence of segregative phase separation (Ould, Eleya, and Turgeon, 2000a, 2000b). The same phenomenon appears to govern the rheological behaviour of mixed whey proteins / xanthan gels. Synergistic effects were observed at low xanthan concentrations while antagonistic effects prevailed for higher xanthan concentrations (Bryant et al., 2000). SEM observations showed that the size of the protein aggregates was increased in the presence of xanthan (Zasypkin et al., 1996). It was also reported that the presence of xanthan, under static conditions, resulted in a more homogeneous whey protein network. Applying shear to mixed suspensions generally increased the inhomogeneity of the network structure. Under low

stresses, a shear treatment during heating lead to gels with increased G', while the opposite was observed when shearing at higher stresses (Walkenström and Hermansson, 1998).

Mixed systems consisting of one gel-forming globular protein and a neutral polysaccharide have been much less investigated although their study constitutes *a priori* a more direct approach to the basic phenomena since they are simpler, inter-species electrostatic interactions being excluded. Segregative phase separation is mentioned to occur in the case of whey protein / methylcellulose (Syrbe, Fernandes, Dannenberg, Bauer, and Klostermeyer, 1995), β-lactoglobulin / non-gelling potato amylopectin (Olsson et al., 2000) and whey protein / galactomannan (Monteiro, Tavares, Evtuguin, Moreno, and da Silva, 2005; Tavares, Monteiro, Moreno, and da Silva, 2005) mixed gels. In the former case, gels contained liquid inclusions of methylcellulose and a slight reinforcement effect on the modulus was seen with increasing methylcellulose concentration. For β-lactoglobulin / non-gelling potato amylopectin systems, the state of aggregation of β-lactoglobulin was influenced both by concentration and properties of potato amylopectin; the higher the potato amylopectin concentration the larger the pores in the β-lactoglobulin gel. In the later case, it was concluded that galactomannan molecular weight was a limiting factor for phase separation to occur and the resulting microstructures depended on both galactomannan molecular weight and protein-to-polysaccharide ratio (Monteiro et al., 2005). The branching degree of galactomannan had an effect on the microstructure and viscoelasticity of the whey protein gels but the effect was limited to a short range of mannose-to-galactose ratios (Tavares et al., 2005).

Chapter 2

Rheological behaviour of heat-induced β-lactoglobulin gels

2.1 Introduction

A large amount of work on heat-induced gelation of globular proteins has been published for the past years, as referred in Chapter 1. The aggregation of globular proteins is regulated by many factors such as covalent bonding, electrostatic interactions, hydrogen bonding, hydrophobic interactions and van der Waals forces, and a gel is often formed at sufficiently high protein concentration (Roefs et al, 1994; Verheul et al, 1998; Totosaus et al., 2002). To systematically understand the behaviour of the macroscopic physical properties of protein gels, the relationship between the structure of the aggregates and these properties are currently being investigated. However, the mechanisms creating network structures of protein gels are yet unclear.

In this chapter, the heat-induced gelation of β-lactoglobulin solutions was studied at two pH conditions: 7.0, where the protein bears a net negative charge, and 4.6, near the isoelectric point of the protein. Although it is not the purpose of this work to explore the rheological behaviour of β-lactoglobulin gels (already studied by other authors), its study under experimental conditions similar to those used for mixed systems is essential for the understanding of the properties of these systems.

In the first series of experiments, in section 2.3.3, β-lactoglobulin solutions were gelled in test tube, in order to select the concentration range to be studied at each pH, and to assess visually possible differences between the formed gels.

In section 2.3.4, the heat-induced gelation and the viscoelastic properties of the final β-lactoglobulin gels were studied at pH 7.0, using rheological measurements described in section 2.2.6.

The structures of protein gels formed at pH 7.0 were analyzed in section 2.3.5, using fractal models previously applied on globular protein by many authors (for instance, Hagiwara, Kumagai, and Matsunaga, 1997; Hagiwara, Kumagai, and Nakamura, 1998; Wu and Morbidelli, 2001).

In section 2.3.6, the heat-induced gelation and the viscoelastic properties of the final β-lactoglobulin gels were studied at pH 4.6 and compared to the properties of gels formed at pH 7.0.

In the section 2.3.7, the effect of a shear treatment on the rheology of some of heat-induced protein gels was studied at pH 7.0 and pH 4.6, in order to assess the influence of processing conditions on the properties of studied gels.

Finally, in section 2.4, the main conclusions were described.

2.2 Materials and methods

2.2.1 Materials

The commercial sample of β-lactoglobulin (PSDI-2400) was kindly supplied by Arla Foods Ingredients amba, Videbaek, Denmark.

2.2.2 Characterization of β-lactoglobulin

2.2.2.1 Moisture, ash and protein content measurements

The moisture content of the protein samples was determined by drying the sample at 105^{o}C for 5 h, following the weight loss on drying test described by the Food Chemicals Codex (FCC III, page 518, 1981).

Total ash content was determined at 550^{o}C, by ignition of the sample in a muffle furnace, following the general method as described in the Food Chemicals Codex (FCC III, page 466, 1981).

Protein content was obtained from the total nitrogen content of the sample, using a nitrogen factor (NF) of 6.38 (DGHS, page 38, 2005). The total nitrogen content was determined by the Kjeldahl method, as described in the Official Methods of Analysis (AOAC, page 15, 1975).

2.2.2.2 Chromatographic analysis

Reversed-phase high-performance liquid chromatography (RP-HPLC) was used for protein analysis, at the Faculty of Pharmacy of the University of Porto.

An analytical HPLC unit (Jasco) equipped with two type PU-980 pumps, a type UV-970 detector and a type 7125 Rheodyne Injector with a 20 μl loop was used. The column was a reversed-phase column *Chrompack* P 300 RP that contains a polystyrene-divinylbenzene copolymer-based packing (8 μm, 300 Å, 150 × 4.6mm i.d.). A *Chrompack* P RP (24×4.6 mm i.d.) was used as a pre-column.

Gradient elution was carried out with a mixture of two solvents. Solvent A: 0.1% trifluoroacetic acid (TFA) in water and solvent B: 0.1% TFA in 80% aqueous acetonitrile, (v/v), as described by Mota, Ferreira, Oliveira, Rocha, Teixeira, Torres, and Gonçalves (2004, 2006). Proteins were eluted as follows: 0 to 1 min, 90% A; 1 to 10 min, 90 to 80% A; 10 to 15 min, 80 to75% A; 15 to 20 min, 75 to 60% A; 20 to 30 min, 60 to 50% A; 30 to 33 min, 50 to 40% A; 33 to 36 min, 40 to 30% A; 36 to 39 min, 30 to 20% A; 39 to 41 min, 20 to 0% A. Returning to initial conditions in 9 minutes. The flow-rate was 0.5 $ml.min^{-1}$. The column was used at ambient temperature and detection was done at 215 nm. Total run time was 50 min. Purified bovine standards of β-lactoglobulin and α-lactalbumin were supplied by Sigma Chemical Co and dissolved in ultra purified water.

2.2.3 Turbidity measurement

The turbidity of β-lactoglobulin dispersions was measured on an UV-Visible Spectrometer (Unicam Ltd., Cambridge, UK) at room temperature, as the absorbance at a wavelength of 420 nm (Stading et al., 1990). The sample concentrations were used 0.05 and 0.1 wt%, and distilled water was used as the reference. Measurements were carried out in triplicate.

2.2.4 Preparation of β-lactoglobulin solutions

2.2.4.1 Stock solutions preparation

β-lactoglobulin stock solutions (23 wt%) were prepared by dispersing a known amount of the powder in distilled water under gentle stirring at room temperature, for 18 h. Sodium azide was added (5ppm) to avoid bacterial growth.

The pH of β-lactoglobulin stock solution (6.8 - 6.9, at natural pH) was then adjusted to the required value (7.0 or 4.6) by careful addition of KOH or HCl solutions. After pH adjustment, the stock solutions were centrifuged for 2 h at 35,000 g at 20^{o}C to remove insoluble matter. Then, protein concentration was determined by the Bradford (Bio-Rad) Protein Assay (Bradford 1976).

2.2.4.2 Bradford (Bio-Rad) protein assay

The assay is based on the observation that the absorbance maximum for an acidic solution of Coomassie Brilliant Blue G-250 shifts from 465 nm to 595 nm when binding to protein occurs

(Sedmak and Grossberg, 1977; Zor and Selinger, 1996). The extinction coefficient of a dye-all complex solution is constant over a 10-fold concentration range (Spector, 1978).

The microprotein assay was chosen: 1 mL of 5000- to 7000-fold diluted protein sample was mixed with 5 mL of assay reagent (1:4, Bio-Rad assay reagent:distilled water) using a vortex. After at least five minutes incubation at room temperature, the absorbance of the solution was measured at 595 nm. A standard curve of β-lactoglobulin (concentrations ranging from 0.0005 to 0.005 wt%) was established, following the same procedure. The protein concentration was determined from this curve, taking into account the initial dilution of the sample.

2.2.5 Heat-induced gelation of β-lactoglobulin solutions

This test was performed in capped test tubes each containing ~1.7 g of β-lactoglobulin solution. The tubes were placed in a water bath, heated from 20 to 80^{o}C (~2^{o}C/min), held at 80^{o}C for 20 min and then cooled down to 20ºC. Gelation of the solutions was assessed visually.

2.2.6 Rheological measurements

2.2.6.1 Instrumentation

Rheological characterization of our systems was done using the controlled stress rheometer AR2000 (TA Instruments, Leatherhead, UK, see in Figure 2.1). A Peltier system in the bottom plate provided fast temperature control and a very quick response time to sudden changes in sample temperature.

Two different measuring devices were used: cone-and-plate (Figure 2.2) and parallel plate (Figure 2.3) geometries.

Figure 2.1 The controlled stress rheometer (TA instrument AR2000) fitted with the cone-and-plate geometry.

The cone-and-plate measuring system is very useful in liquid homogeneous systems and in systems containing particles smaller than 1 μm. When compared with other measuring geometries, this one ensures uniform shear in the sample, small inertia, small sample volume and easy handling. Cone-and-plate geometrics are normally referred by their diameter and cone angle (usually less than 6^{o}). The cone is often truncated by a small amount. An accurate gap setting mechanism is then employed to ensure that the "virtual" tip is in contact with the lower plate when running samples (Figure 2.2).

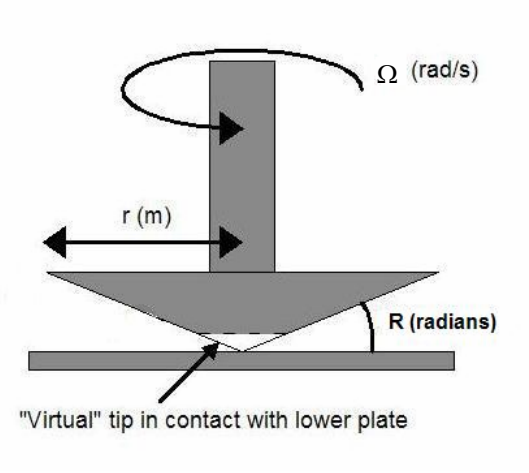

Figure 2.2 Schematic representation of the cone-and-plate measuring systems.

The parallel plate geometry allows measurements in samples containing micro metric particles. In this measuring system, the distance between the plates (the "gap") can be adjusted; in general, the magnitude of this parameter must be at least three to five times higher than the size of the bigger particles in the samples. The parallel plate geometry is used as an alternative to the cone and plate geometry for the study of the effect of changing temperature in the sample. Plates with radial grooves to avoid slippage during measurements are used. The main disadvantage of this measuring system is the non uniformity of the shear stress applied to the sample. However this effect is minimized by the software of the apparatus.

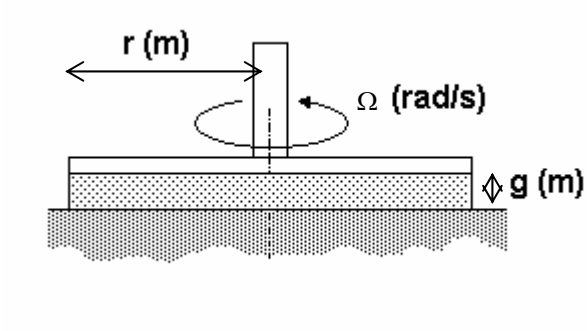

Figure 2.3 A parallel plate system.

2.2.6.2 Fundamentals of the rheological methods

2.2.6.2.1 Steady shear measurements

The rheological parameters shear rate ($\dot{\gamma}$) and shear stress (σ), in the cone-and-plate geometry, can be calculated from the values of angular velocity (Ω) and torque (M) using the following equations:

$$\dot{\gamma} = \frac{\Omega}{R} \qquad \text{(Eq. 2.1)}$$

$$\sigma = \frac{3M}{2\pi r^3} \qquad \text{(Eq. 2.2)}$$

In fact, flow in this geometry can be very complex requiring a laborious solution of the fundamental equations of motion (Walters, 1975). When using a cone with a small angle R (less than 4^o) and sufficiently low rotational speeds, the shear rate is very nearly the same everywhere in the sample and can be calculated from Eq. 2.1.

In the parallel plate geometry, the shear rate and shear stress are functions of the plate radius. They can be calculated at the edge of the plate using the following equations (Walters, 1975):

$$\dot{\gamma} = \frac{\Omega r}{g} \qquad \text{(Eq. 2.3)}$$

$$\sigma = \left(\frac{M}{2\pi r^3}\right)\left(3 + \frac{d \ln M}{d \ln \dot{\gamma}}\right) \qquad \text{(Eq. 2.4)}$$

Where g is the gap width between plates and r is the upper plate radius.

2.2.6.2.2 Dynamic oscillatory shear testing

In a dynamic oscillatory test, the material is exposed to a sinusoidally varying shear strain (γ) or stress (σ), depending on the type of rheometer. For example, if a small harmonically varying strain is applied to the material according to (Eqs. 2.5).

$$\gamma = \gamma_0 \sin(\omega t) \qquad \text{(Eq. 2.5)}$$

and if the material behaves linearly, i.e., if the ratio of stress to strain at any particular time or frequency is independent of the magnitude of the applied stress or strain, the resulting shear stress will also oscillate sinusoidally at the same oscillation frequency but will be out of phase with the strain

$$\sigma = \sigma_0 \sin(\omega t + \delta) \qquad \text{(Eq. 2.6)}$$

Where γ_0 and σ_0 are the maximum strain amplitude and the maximum stress amplitude, respectively, ω is the oscillatory frequency (rad.s^{-1}), t is time (seconds) and δ is the phase angle between stress and strain.

The phase angle is dependent on the viscoelastic nature of the material. For an ideal solid material, stress is directly proportional to strain while, for a Newtonian fluid, stress exhibits a direct proportionality to shear rate (Eqs. 2.7 and 2.8).

Shear stress:

Ideal solid material: $$\sigma = k\gamma = k\gamma_0 \sin(\omega t) \qquad \text{(Eq. 2.7)}$$

Newtonian fluid:

$$\sigma = \eta \dot{\gamma} = \eta \omega \gamma_0 \cos(\omega t) \qquad \text{(Eq. 2.8)}$$

This means that the shear stress wave for an ideal solid is in phase with the shear strain wave ($\delta = 0$), whereas the shear stress wave for Newtonian fluid as ideal viscous material is 90^o out of phase ($\delta = 90^o$). A viscoelastic material will have a phase angle between 0^o and 90^o. The sinusoidal time variations in the stress and strain are as shown in Figure 2.4.

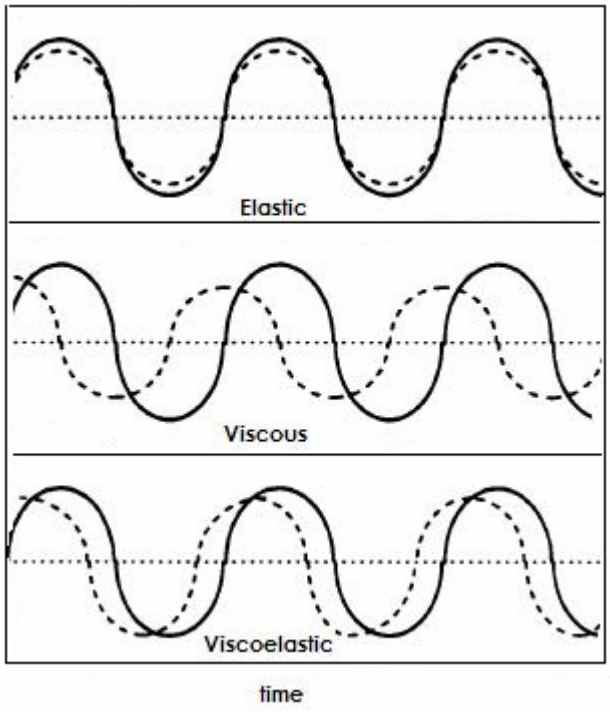

Figure 2.4 Idealized dynamic response of elastic (solid), viscous (fluid), and viscoelastic systems to sinusoidal oscillatory shear. Shear strain (solid curves) and shear stress (dashed curves).

By decomposing the stress wave into two waves of the same frequency, two dynamic moduli, the storage modulus, G', and the loss modulus, G'', are introduced:

$$\sigma = \gamma_0 G' \sin(\omega t) + \gamma_0 G'' \cos(\omega t) \qquad \text{(Eq. 2.9)}$$

The storage modulus, G', and the loss modulus, G'', are the real and the imaginary components of the complex modulus, G^*, respectively:

$$G^* = \frac{\sigma^*}{\gamma^*} = G' + iG'' \qquad \text{(Eq. 2.10)}$$

G^* includes the complete information of the viscoelastic properties of the material. G' is defined as the ratio of the stress in phase with the strain to the strain and G'' is defined as the ratio of the stress 90^o out of phase with the strain to the strain. The absolute value of G^* is given as

$$G^* = |G^*| \frac{\sigma_0}{\gamma_0} = \sqrt{G'^2 + G''^2} \qquad \text{(Eq. 2.11)}$$

The magnitudes of G' and G'' are influenced by temperature, frequency and strain applied to the material. However, for strain values within the linear domain, G' and G'' are independent of strain. Their dependence on frequency can be expressed in terms of the stress and strain amplitudes ratio and the phase angle:

$$G' = (\frac{\sigma_0}{\gamma_0}) \cos \delta \qquad \text{(Eq. 2.12)}$$

$$G'' = (\frac{\sigma_0}{\gamma_0}) \sin \delta \qquad \text{(Eq. 2.13)}$$

The data from sinusoidal experiments can also be expressed in terms of a complex compliance

$$J^* = \frac{\gamma^*}{\sigma^*} = \frac{1}{G^*} = J' - iJ'' \qquad \text{(Eq. 2.14)}$$

The storage compliance J' is the ratio of the strain in phase with the stress to the stress whereas the loss compliance J'' is the ratio of the strain 90^o out of phase with the stress to the stress. G' and J' are directly proportional to the average energy storage in a cycle of deformation. G'' and J'' are directly proportional to the average dissipation or loss of energy as heat in a cycle of deformation (Ferry, 1980)

$$J' = \frac{G'}{\left(G'^2 + G''^2\right)} \qquad \text{(Eq. 2.15)}$$

$$J'' = \frac{G''}{\left(G'^2 + G''^2\right)} \qquad \text{(Eq. 2.16)}$$

The phase relationships can equally well be expressed by a complex viscosity,

$$\eta^* = \frac{G^*}{\omega} = \eta' - i\eta'' \qquad \text{(Eq. 2.17)}$$

The individual components are given by

the dynamic viscosity: $\eta' = G'' / \omega$ (Eq. 2.18)

The out of phase component
of the complex viscosity: $\eta'' = G' / \omega$ (Eq. 2.19)

Additionally, the loss tangent defined as:

$$\tan\delta = G'' / G' = J' / J'' = \eta' / \eta'' \qquad \text{(Eq. 2.20)}$$

measures the ratio of the dissipation and storage energies in a cycle of deformation.

2.2.6.3 Experimental procedures

Samples of protein solutions were placed into the measuring device of the rheometer, at 20°C. The air exposed surface was covered with a layer of paraffin oil to prevent evaporation during the experiments.

Dynamic small-strain rheological measurements were used to follow the heat-induced gelation of the samples, at 80°C, and the properties of the resulting gels after quenching to 20°C. A rough acrylic plate (40 mm diameter, 800 μm gap) was used in these experiments. The following sequence of measurements was done:

- Temperature sweep from 20 to 80°C, at a constant heating rate of 2°C/min. Gelation was monitored by measuring G' and G'' at 6.28 rad.s^{-1}. The sol-gel transition temperature (T_g) was defined as the temperature at which cross-over of the moduli occurred ($G' = G''$) in the conditions of the experiment.
- Time sweep at 80°C: the evolution of G' and G'' was measured at a fixed frequency of 6.28 rad.s^{-1}, during 6 hours.
- Frequency sweep (mechanical spectrum) at 80°C: the evolution of the moduli (G' and G'') was measured for a frequency range of 0.06 – 125 rad.s^{-1}.
- Temperature sweep from 80 to 20°C at a constant cooling rate of 2°C/min.
- Time sweep at 20°C: the evolution of G' and G'' was measured at a fixed frequency of 6.28 rad.s^{-1}, during 1.5 hours.

- Frequency sweep at 20°C: the evolution of the moduli was measured for a frequency range of of 0.06 – 125 rad.s^{-1}.
- Strain sweep: the evolution of the moduli was measured at 6.28 rad.s^{-1} up to fracture of the gel.

For temperature, time and frequency sweeps, the values used for the strain amplitude depended on the concentration / pH of the samples. Values of 0.0007 – 0.01, for samples at pH 7.0, and 0.0005 – 0.001, for samples at pH 4.6, were used which was within the linear viscoelastic region, determined by preliminary experiments.

The effect of a steady shear treatment, before gelation, on the rheological properties of the final gels, was studied on some protein systems, using the same rheometer fitted with a cone-and-plate geometry (stainless steel cone with 4° angle, 40 mm diameter and 109 μm truncation).

The sequence of procedures described above was maintained in these experiments. However, some changes were introduced, especially in the first step (20 to 80°C heating step), during which shear was applied to the system. Also, time sweeps were shorter: one hour, at 80°C, and 20 min, at 20°C. The short time at 20°C was enough to equilibrate the final gels, as tested in preliminary experiments. Also, as the purpose of these experiments was to study the final gels, the mechanical spectrum was recorded only at this temperature. The strain amplitudes were fixed at 0.05 (for samples at pH 7.0) and 0.001 (for samples at pH 4.6), which was within the linear viscoelastic region.

Different shear treatments were applied to the studied samples:

- During heating from 20 to 75°C or 77°C, the samples were exposed to steady shear, at constant rates between 40 and 120 s^{-1}.
- At the end of the heating step (80°C), the systems were sheared, for 3 min, at constant rates between 60 and 360 s^{-1}.

2.3 Results and discussion

2.3.1 Characterization of β-lactoglobulin

The moisture, ash and protein contents of β-lactoglobulin sample are presented in Table 2.1. Analytical reverse-phase HPLC showed that the commercial β-lactoglobulin sample contained only traces of α-lactalbumin (Figure 2.5).

Table 2.1 Chemical composition of β-lactoglobulin sample

	β-lactoglobulin
Moisture	6.88 ± 0.10
Ash	6.52 ± 0.14
Protein (NF is 6.38)	91.91± 0.10

All values (%) on a dry matter basis (except for moisture) are mean ± standard deviation of three determinations.

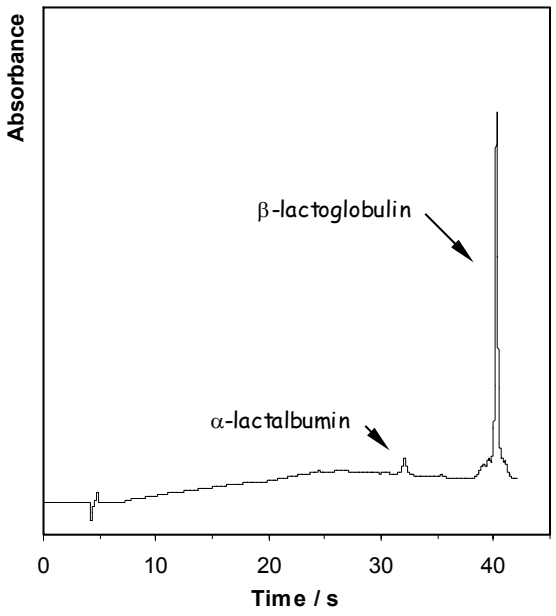

Figure 2.5 HPLC chromatogram of commercial β-lactoglobulin.

2.3.2 Turbidity of β-lactoglobulin solutions

The turbidity differences of 0.05 and 0.1 wt% β-lactoglobulin solutions were observed at a wavelength of 420 nm in function of the pH. As can be seen in Figure 2.6, at both concentrations small absorbance values were observed at pH < 3.5 or pH > 6.0 whereas there was a high absorbance at intermediate pH values (3.0 – 6.0). The maximum was observed at pH 4.6, which is close to the reported isoelectric point (pI) of β-lactoglobulin. This behaviour near the pI indicates that some kind of aggregates has formed in the solution, increasing the number and size of the protein particles (Stading et al., 1990; Schmitt, Sanchez, Thomas, and Hardy 1999).

At other pH values (higher than 6.0 or lower than 3.5), the protein bears a net (negative or positive) charge and no aggregates are formed, due to electrostatic repulsions.

These results were consistent with the observations on turbidity of β-lactoglobulin solutions by Stading and co-worker (1990). These authors also found a large increase of the absorbance at 420 nm at intermediate pH 4 – 6. Schmitt and co-workers (1999) obtained the maximum of the absorbance (measured at 650 nm) at pH 4.8 for β-lactoglobulin solutions.

The turbidity curve can be considered as the inverse of the solubility curve of β-lactoglobulin in distilled water (Stading et al., 1990). The increase in solution´s turbidity, as said before, is caused by the formation of aggregates due to the protein net charge close to zero, implying an absence of repulsion. This feature, may lead to protein precipitation with the consequent decrease of protein solubility. In a previous work, Schmitt, Sanchez, Despond, Renard,

Thomas, and Hardy (2000) observed that the solubility curve of the 1.0 wt% of β-lactoglobulin dispersions exhibited a minimum at pH 4.75, which is consistent with our results.

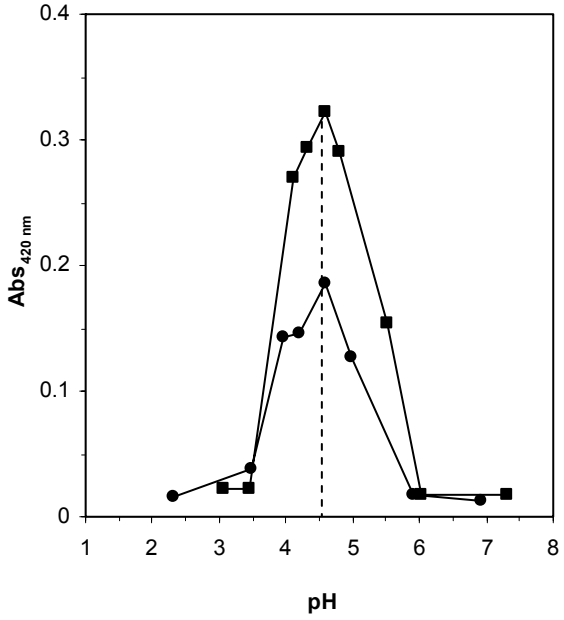

Figure 2.6 Absorbance at 420 nm of β-lactoglobulin solutions in function of pH at room temperature. β-lactoglobulin concentrations: 0.05% (●) and 0.10% (■).

2.3.3 Heat-induced gelation of β-lactoglobulin solutions

This test was performed as described in section 2.2.5, at two pH values: 7.0 and 4.6 (near the pI of β-lactoglobulin). As can be seen in Figure 2.7, β-lactoglobulin forms gels at different concentrations, depending on pH. In the conditions of the experiments, gels were obtained only for concentration ≥ 6.5 wt%, at pH 7.0, (Figure 2.7C) while, at pH 4.6, gels were obtained for all the concentrations tested (Figure 2.7D). Visual inspection showed that, at pH 7.0, gels were translucent, without visible syneresis, whereas, at pH 4.6, gels were opaque, whitish, exhibiting syneresis for the lower concentrations (2.3 and 2.7 wt%). These findings are in accordance with previous results of other authors (see, for instance, Stading et al., 1990; Langton et al., 1992; Ju

et al., 1998). Stading and co-worker (1990) observed that the critical concentration for gel formation was much lower (~1%) for β-lactoglobulin gels formed in the pH range 4.5-5.5 than for gels formed at higher pH which, in their opinion, was indicative of a very open structure. i.e. the network of a fine-stranded gel was much denser than that of an aggregate gel.

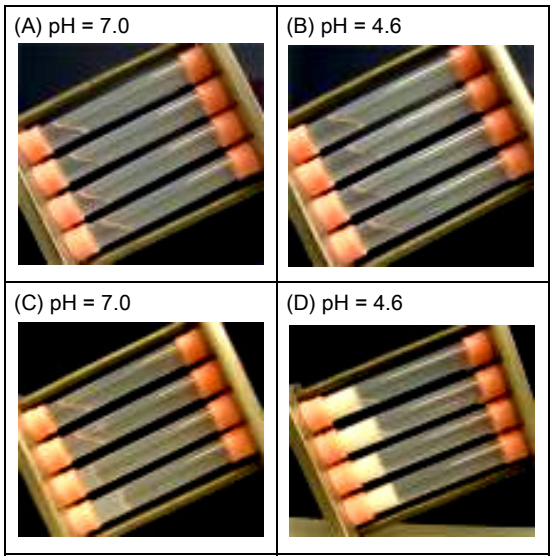

Figure 2.7 β-lactoglobulin aqueous solutions at different concentrations before heating (A and B) and gelled samples after heating at 80°C for 20min (C and D). Concentrations, from left to right, in the capped test tubes: 4.7, 5.7, 6.5 and 7.8 wt% at pH 7.0; 2.3, 2.7, 4.6 and 6.5 wt% at pH 4.6.

2.3.4 Rheological behaviour of heat-induced β-lactoglobulin gels

Dynamic small-strain rheological measurements were used to follow the heat-induced gelation, at 80°C, of β-lactoglobulin solutions with concentrations ranging from 6.0 to 13 wt%, at pH 7.0, and the properties of the resulting gels after quenching to 20°C. The experimental procedures were described in section 2.2.6.3.

2.3.4.1 Gel formation and quenching

The evolution of the systems during thermal history was monitored as the variation of G', measured at 6.28 rad.s^{-1}, with time, as shown in Figure 2.8 for two protein concentrations. For all systems studied, the curves had similar shapes. During the ascending temperature ramp step, G' remained extremely small up to 70 to 80°C (depending on protein concentration), and so remained G'' (results not shown for the sake of clarity), the values of both moduli being in the limit of what can be measured with the rheometer. It is difficult to determine the time after which the gel formed on the basis of this type of experiments at a fixed frequency. Thermal gelation of globular proteins solutions results from an aggregation process, triggered by the heat-induced molecular conformation change of the protein. The formation of aggregates increasing in number and/or in size suffices to cause a large increase in G', without the necessity for them to entangle or connect to form a tri-dimensional network pervading the sample volume. For the sake of simplicity, we take the criterion of $G' = G''$ (or $\tan \delta = 1$) for defining the "gel point" (Tung and Dynes, 1982). Other definitions of the gel point are also used by different authors: (1) the event when G' becomes greater than the noise level and (2) the point where G'' has a maximum. The three definitions have some flaws and there is no perfect practical definition of the gel point. So, in all the work reported in these thesis, the $G'= G''$ criterion was adopted.

Gelation occurred during the 20 to 80°C heating step, for the higher protein concentrations (> 9 wt%); for the lower concentrations (6 – 8 wt%), gelation occurred during the time sweep at 80°C.

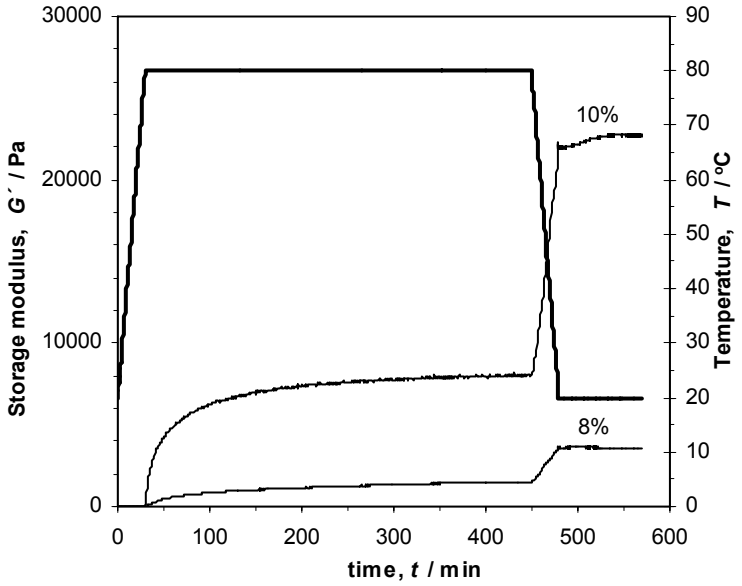

Figure 2.8 Thermal gelation of β-lactoglobulin solutions (8 and 10 wt%) at 6.28 rad.s^{-1} and pH 7.0. The thick line represents the temperature profile.

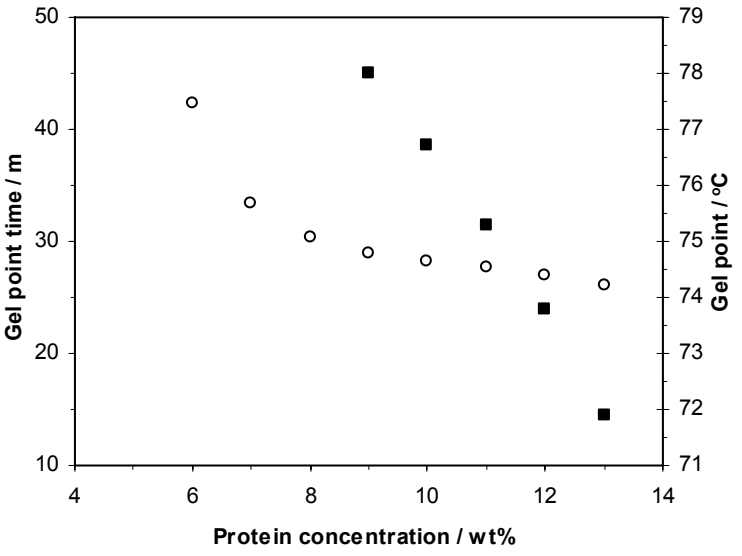

Figure 2.9 Effect of β-lactoglobulin concentrations (pH 7.0) on time (O) and temperature (■) of protein gelation.

Figure 2.9 shows the effect of concentration on time and temperature of gelation, for the former solutions. Both of them decreased when the protein concentration increased which is in

accordance with previous works (Le Bon et al., 1999; Pouzot, Nicolai, Durand, and Benyahia, 2004).

At the beginning of the time sweep at 80°C and above the gel point, *G′* increased rapidly, then slowed down till a plateau was approached after 7 h at 80°C (Figure 2.10). *G′′* followed a similar course but kept much lower values than *G′* (~100 × less) for all the concentrations studied (not shown). Analysis of the values of the moduli, at the end of this step, showed that an increase of the protein concentration led to an increase of the strength (*G′* increased) and of the elasticity (tan δ decreased) of the gels at 80°C.

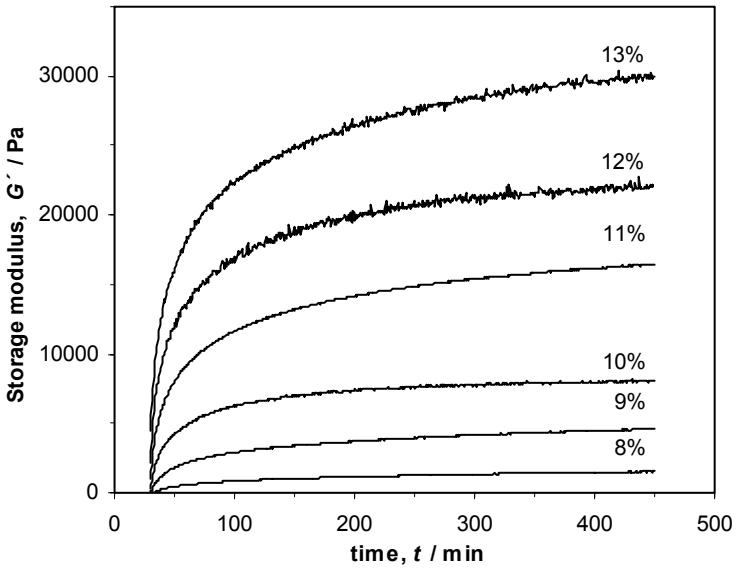

Figure 2.10 Evolution of the storage modulus at 6.28 rad.s^{-1} in the time sweep at 80°C for β-lactoglobulin solutions (pH 7.0) at different concentrations.

In addition, an attempt was made to analyse the evolution of *G′*, during this step, through its time derivative considered as indicative of the gelation rate. Figure 2.11 shows that, at lower protein concentrations, four zones could be defined in the d*G′*/dt *versus* time curve: an initial steep increase (*phase a*), followed by a steep decrease (*phase b*), a less pronounced decrease

(*phase c*), and a plateau (*phase d*) where d*G´*/dt reached a constant value. At higher concentration (≥ 10 wt%), *phase a* was not observed (not shown), because the gels were already formed during the 20 to 80°C heating step.

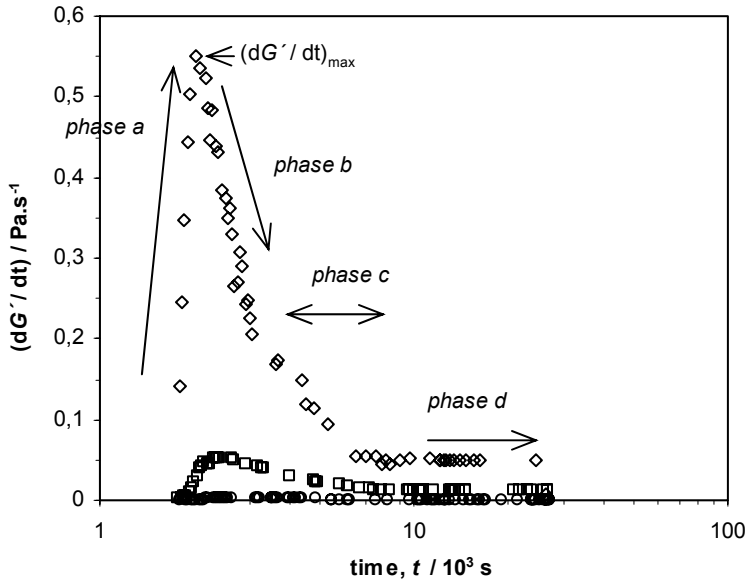

Figure 2.11 Evolution of the storage modulus rate of change during time sweep at 80°C for some β-lactoglobulin solutions: 6 wt% (O), 7 wt% (□), and 8 wt% (◇) at pH 7.0.

Considering a linear variation of d*G´*/dt with time in the two first phases, the corresponding slopes were obtained and a maximum "gelation rate", $(dG'/dt)_{max}$, was determined for each system. The values of these parameters, together with the plateau values of d*G´*/dt in *phase d* were collected in Table 2.2. The slope values (positive in *phase a* and negative in *phase b*) increased (in absolute value) as well as the plateau value (*phase d*), with increasing protein concentration. The maximum "gelation rate" was also significantly affected by the protein concentration.

Table 2.2 Empirical parameters of β-lactoglobulin gelation kinetics and gel quenching, at pH 7.0

Protein concentration (%)	$(dG'/dt)_{max}$ (Pa/s)	Slope of dG'/dt in *phase a* $\times 10^3$ (Pa/s^2)	Slope of dG'/dt in *phase b* $\times 10^3$ (Pa/s^2)	dG'/dt in *phase d* (Pa/s)	Cooling step (80 to 20°C) dG'/dT (Pa/°C)
6	0.0029	0.0025	-0.0007	0.0007	-0.97
7	0.0521	0.0989	-0.0170	0.0123	-11
8	0.5497	1.8206	-0.3679	0.0500	-36
9	2.6412	4.8023	-2.9404	0.0846	-123
10	-	-	-10.7760	0.2993	-239
11	-	-	-25.9600	0.5000	-427
12	-	-	-40.1710	1.0000	-600
13	-	-	-60.6250	1.1098	-816

After the heating step at 80ºC, mechanical spectrum was recorded at 80°C (see, for example in Figure 2.13A) then gels were quenched to 20ºC. The moderate cooling rate chosen (2°C/min) ensured that the temperature within the sample was close to that measured by the sensor at any moment during this step. G' increased as temperature decreased. The curves obtained for different protein concentrations could be approximated by straight lines, at least in the temperature interval 70 to 20°C (Figure 2.12). The slopes of these lines (dG'/dT) are given in Table 2.2: the variation of G' increased steeply with protein concentration. This increase in G' has been previously observed for other globular protein gels (see, for instance, Tavares and da Silva, 2003; Ould Eleya, Ko, and Gunasekaran, 2004) and has been attributed to an increase of

attractive forces (van der Waals interactions and hydrogen bonding) within the gel network, during cooling of the systems.

After the cooling step, gels were left to equilibrate for 1.5 h. No further evolution of G' and G'' was observed (results not shown). It was then possible to characterize the rheological behaviour of the final gels.

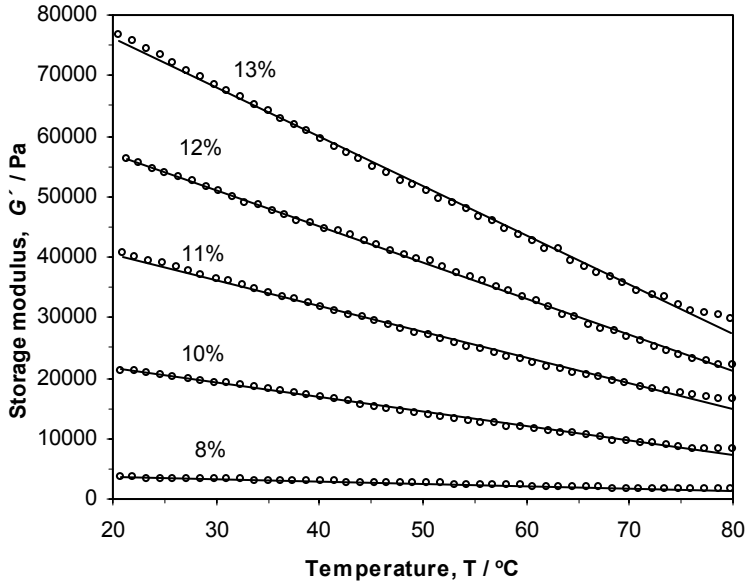

Figure 2.12 Changes in the storage modulus with the temperature during the cooling (80 to 20°C) step for different concentrations of β-lactoglobulin gels at pH 7.0. The lines represent the linear fits of the data (see text).

2.3.4.2 Viscoelastic properties

Mechanical spectra were recorded at 20°C. Quenching the gel at 20°C increased G' and G'' as compared to the spectra at 80°C (Figure 2.13). As expected, the moduli increased with increasing protein concentration. However, the shapes of the moduli at both temperatures were similar with almost flat curve over the frequency range studied.

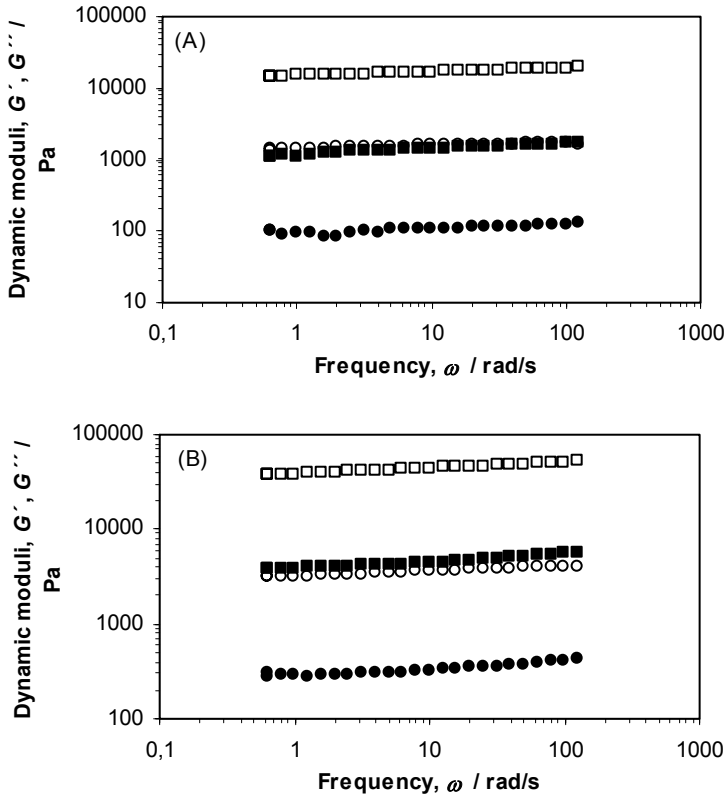

Figure 2.13 Mechanical spectra at 80°C (A) and 20°C (B) of β-lactoglobulin gels at pH 7.0 with different concentrations: 8% (O) and 11% (□). G' (open symbols) and loss modulus G'' (full symbols).

G' values at 6.28 rad.s^{-1} were taken from the frequency sweeps at 80°C and at 20°C and plotted as a function of protein concentration (Figure 2.14). This figure shows that, at both temperatures, G' exhibited a power-law behaviour that could be fitted to the form $G' \sim G^n$, where n is the power-law exponent. In fact, two sets of points were defined, one for the lower protein concentrations (6 - 8 wt%), and the other for the higher ones (9 - 13 wt%). As expected, the values of the exponent were positive for all gels.

For $C \geq 9$ wt%, the exponent n of G' versus C at 80°C (n = 5.23) was almost the same as that of G' versus C at 20°C (n = 5.28), indicating that cooling samples from 80 to 20°C did not induce

significant structural changes in the gel network. A similar behaviour was found (Ould Eleya et al., 2004) for heat-induced gels of egg white proteins.

In the zone of lower protein concentrations (6 - 8 wt%), the concentration dependence at 80°C (n = 14.8) was stronger than at 20°C (n = 13.6), suggesting that the structure of the protein network differed from that at higher concentrations. Probably, at these lower concentrations, a longer heating time of the system at 80°C was needed to obtain a stronger gel.

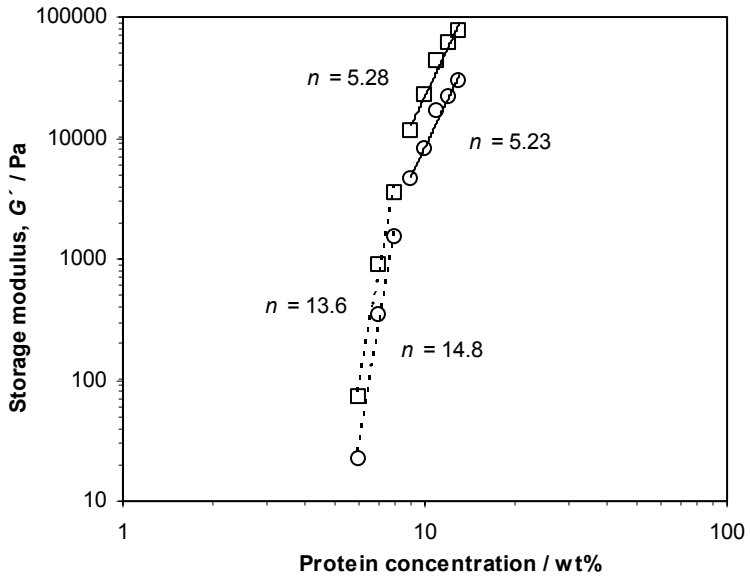

Figure 2.14 The storage modulus, G' of β-lactoglobulin gels as a function of protein concentration at 20°C (□) and 80°C (O), at pH 7.0. The continuous and dotted lines represent fits to the concentration dependence: $G' \sim C^n$, where n is the power-law exponent.

In fact, the heating conditions influence the characteristics of the final gels. Pouzot and co-workers (2004) measured the concentration dependence of G' for β-lactoglobulin solutions in 0.1 M NaCl, at pH 7.0, after heating at 80°C for 24 h. They obtained a value of n = 4.5 in the range from 2 - 10 wt%. Verheul and Roefs (1998) obtained an exponent value of 4.5 for a whey

protein isolate containing 70%β-lactoglobulin in the concentration range 3.5 - 8 wt% after heating at 68.5°C for 20 h. In our β-lactoglobulin systems, the exponent *n* was about 5.2 in the concentration range from 9 - 13 wt% after heating at 80°C for 6 h. Probably, the higher exponent is due to the different experimental conditions used.

Gels were submitted to a range of increasing stresses (dynamic stress sweeps) till they ruptured. The dependence of G' on strain (γ), at 6.28 rad.s^{-1}, was determined. The results are shown in Figure 2.15.

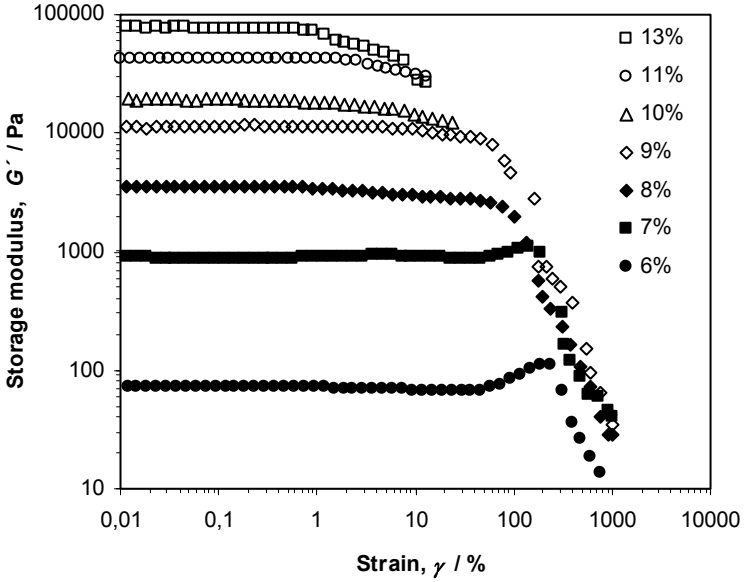

Figure 2.15 Strain dependence of the storage modulus, at 6.28 rad.s^{-1}, of heat-induced β-lactoglobulin gels (pH 7.0 and 20°C) with different concentrations (wt%).

As the strain amplitude increased, G' remained almost constant (G'_0), up to a critical strain amplitude, after which it deviated. Depending on the protein concentration, (1) G' decreased as strain increased (for 9 - 13 wt% gels) or (2) an increase of G' followed by a dramatic decay (for 6 - 8 wt% gels) was observed. Moreover, the higher the concentration of the gel the lower the

strain at which G' started to deviate. Evolution of G'' was similar but it kept much lower values for all strains before rupture.

This evolution of the moduli indicates a transition from a linear to a non-linear behaviour. The region below the critical strain amplitude is defined as the linear region, and the region above the critical strain amplitude is called nonlinear. The measured moduli in the nonlinear region lose their physical meaning as defined in the linear region due to the higher harmonic contributions, and must be analyzed cautiously. This does not necessarily mean that the measured properties are meaningless. For more precise analysis, Fourier transformation of the stress signal is necessary. However, the behaviour can be treated in a less precise way, neglecting the higher order contributions, as was done by Sim, Ahn, and Lee (2003), and still provide information on the microstructure of the systems.

If G' and G'' data obtained for each gel were normalized by G'_0 and G''_0, curves superposed at low strains and deviated at higher strains (Figure 2.16). The shape of the curves was different for the low (6 to 8 wt%) and high (9 to 13 wt%) concentration ranges, in the nonlinear region: at lower protein concentrations, both G' and G'' showed strain hardening behaviour (both moduli increased) followed by strain thinning (Figure 2.16A) whereas, at higher concentration, only G'' showed strain hardening followed by strain thinning (Figure 2.16B). This type of behaviour was observed in many complex polymeric systems and was used by Hyun, Kim, Ahn, and Lee (2002) to classify them. According to these authors, the large amplitude oscillatory shear (LAOS) behaviour of complex systems can be classified into four types: type I, strain thinning (G' and G'' decreasing); type II, strain hardening (G' and G'' increasing); type III, weak strain overshoot (G' decreasing, G'' increasing following by decreasing); type IV, strong strain overshoot (G' and G'' increasing followed by decreasing). Our systems fall

into type III, weak strain overshoot, (systems with higher protein concentration) and type IV, strong strain overshoot, (systems with lower protein concentration).

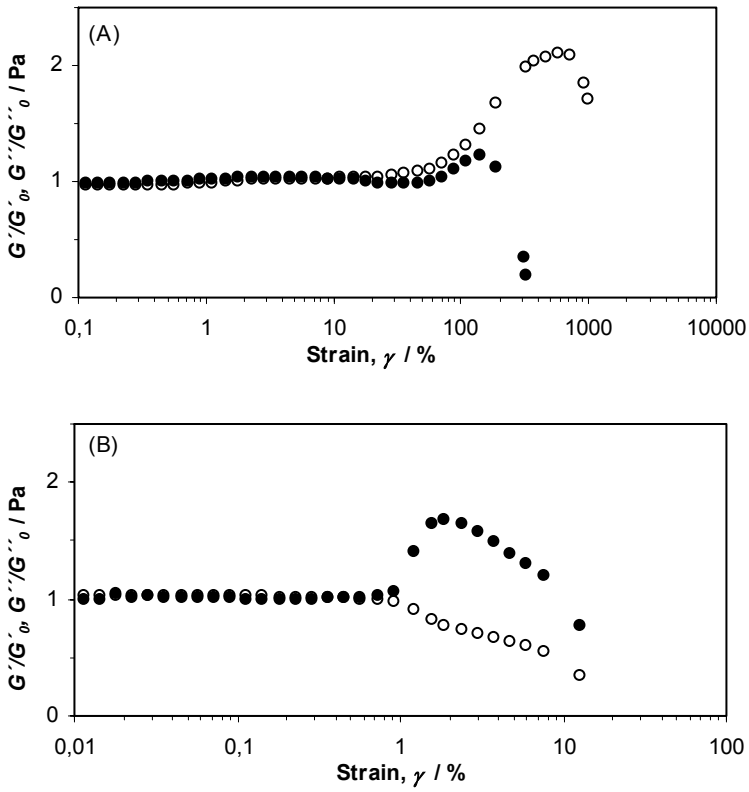

Figure 2.16 Reduced moduli (G'/G'_0: O) and (G''/G''_0: ●) versus strain, where G'_0 and G''_0 are the values of the moduli in the linear viscoelastic region. Two types of LAOS behaviour: strong strain overshoot type of 7%β-lactoglobulin (A) and weak strain overshoot type of 13%β-lactoglobulin (B).

To explain such complex behaviour, Sim and co-workers (2003) developed a network model. By adjusting the model parameters that defined the formation and destruction rates of network junctions, they were able to reproduce the four types of behaviour observed in the experiments. For our systems, both the formation and destruction rates of network junctions increased with the strain amplitude, but the speed of formation was a little larger than that of destruction for

gels in type IV (strong strain overshoot), while the destruction rate was faster than that of formation for gels in type III (weak strain overshoot). The overshoot may be regarded as coming from the balance between the formation and the destruction of the network junctions. Thus, it can be said that the interaction to form a network or a microstructure in type IV systems (lower protein concentration gels, in our case) is stronger than that of type III (Sim et al., 2003).

2.3.5 Fractal analysis

Various scaling models, relating the structure of the gels to their rheological properties, have been developed and applied to several protein and colloidal gel systems in the past decades (Brown and Ball, 1985; Bremer, Vliet, and Walstra, 1989; Shih, Shih, Kim, Liu, and Aksay, 1990; Wu et al., 2001). In our case, the data from oscillatory frequency and strain sweep tests were analyzed by the fractal models of Shih and co-workers (1990) and Wu and co-worker (2001).

i) Model of Shin and co-workers (1990)

Shin and co-workers (1990) developed a scaling model for colloidal gels far from their gelation threshold by defining two separate regimes: strong-link regime, at low particle concentrations, and the weak-link regime, at high particle concentrations. In this model, it is assumed that the structure of gels is constituted by fractal flocs, which during gelation aggregate with each other. The elastic properties of a floc are dominated by its effective backbone, which can be approximated as a linear chain of springs.

In the strong-link regime where the inter-floc links are stronger than that the intra-floc links, the macroscopic elasticity of the gel is given by that of intralinks. It is then possible to derive the

following expressions relating the fractal dimension of the flocs (d_f) and the fractal dimension of the floc backbones (x) to the storage modulus (G') and the limit of linearity (γ_c):

$$G' \sim \phi^{(d+x)/(d-d_f)} \sim \phi^A \quad \text{(Eq. 2.21)}$$

$$\gamma_c \sim \phi^{-(1+x)/(d-d_f)} \sim \phi^B \quad \text{(Eq. 2.22)}$$

Where ϕ is the particle volume fraction, d is the Euclidean dimension of the system (3 for our case) and $1 \leq x < d_f$.

In the weak-link regime, where the inter-floc links are weaker than the intra-floc links, the elasticity of the inter-flock links determines the elasticity of the gel. In this case, the expressions for G' and γ_c are, respectively:

$$G' \sim \phi^{1/(d-d_f)} \quad \text{(Eq. 2.23)}$$

$$\gamma_c \sim \phi^{1/(d-d_f)} \quad \text{(Eq. 2.24)}$$

Thus, from experimentally measured values of G' and γ_c as a function of ϕ, it is possible to estimate A and B and then, from the above equations, the values of both d_f and x.

ii) Model of Wu and co-worker (2001)

The strong- and weak-link regimes described by Shin and co-workers (1990) represent two extreme situations. The transition from one to the other with the particle concentration must be continuous, leading to intermediate situations where inter- and intra-floc links contribute to gel´s overall elasticity.

Based on the previous model, Wu and co-worker (2001) developed a new scaling model that relates the structural parameters of the gel to its elastic properties and is valid not only for the strong- and weak-link regimes but also for the intermediate regimes.

An appropriate effective microscopic elastic constant α was introduced to account for the mutual elastic contributions of both inter- and intra-floc links. This leads to a new parameter $\alpha \in [0,1]$, which indicates the relative importance of these two contributions. This parameter can be estimated from the rheological data and its value determines the prevailing gel regime. The following equations were obtained:

$$G' \sim \phi^{\beta/(d-d_f)} \sim \phi^A \qquad \text{(Eq. 2.25)}$$

$$\gamma_c \sim \phi^{(d-\beta-1)/(d-d_f)} \sim \phi^B \qquad \text{(Eq. 2.26)}$$

$$\beta = (d-2) + (2+x)(1-\alpha) \qquad \text{(Eq. 2.27)}$$

Thus, from the experimental values of G' and γ_c as a function of the particle volume fraction, ϕ, the exponents A and B can be estimated, which allows the determination of both β and d_f using the above equations.

This model correctly reproduces the results from the model developed by Shin and co-workers (1990), for the strong-ling ($\alpha = 0$) and weak-link ($\alpha = 1$) regimes.

The two models above were used with the rheological data obtained for the 9 to 13%β-lactoglobulin gels. Firstly, the variation of the maximum linear strain (critical strain, γ_c) of the gels with the protein concentration was evaluated, at 20°C. The values of γ_c were difficult to

determine accurately; however, they were estimated from the stress-strain curve (Hagiwara et al., 1997) as shown in Figure 2.17 for the 13 wt% gel. The critical strain showed a power-law relationship with protein concentration, i.e. $\gamma_c \sim C^l$ with l the power-law exponent. A negative value (l = -2.9) was obtained. Wu and co-worker (2001) reported that l values covered a wide range of both negative and positive values, between – 3.4 and 5.3, depending on the nature of protein gels and how they were prepared. So, our l value agrees with this report.

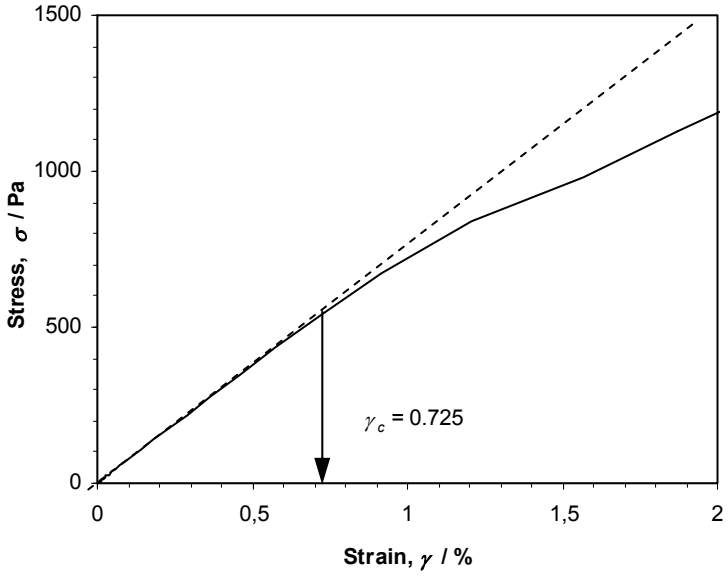

Figure 2.17 An example of estimation of the limit of linearity γ_c from stress-strain curve of 13%β-lactoglobulin gels.

The fractal dimension d_f of protein aggregates in β-lactoglobulin gels at 20°C were estimated from power-law exponents n (obtained from $G' \sim C^n$, in section 2.3.4.2) and l, using scaling models of Shin and co-workers (1990) and Wu and co-worker (2001).

The slope of the log-log plot of elasticity versus protein concentration (n = 5.28, obtained in sections 2.3.4.2), that is, the value of parameter A, and the slope of the log-log plot of the

maximum linear strain versus protein concentration (l = -2.9, obtained in Figure 2.18), that is the value of parameter B, were used to estimate the fractal dimension, d_f. As the estimated l value was negative, the gel system was classified as being in the strong-link regime, according to the model of Shin and co-workers (1990). Using equations 2.21 and 2.22, the values of d_f and x were easily estimated (Table 2.3).

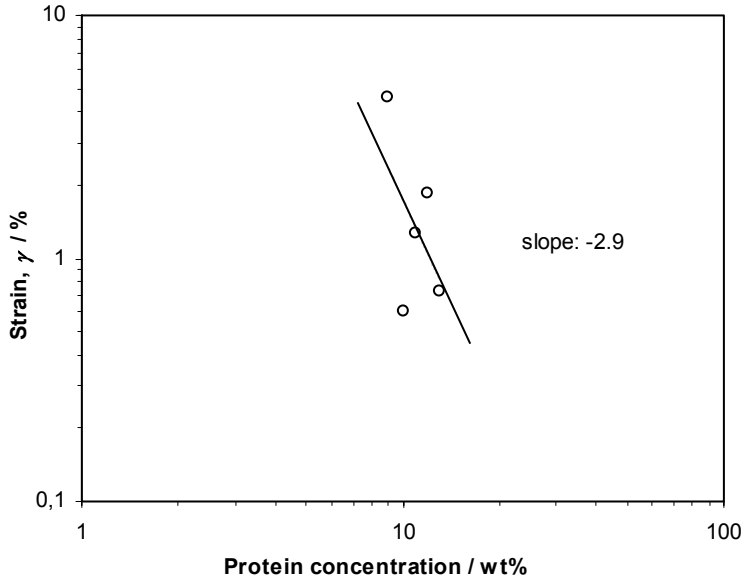

Figure 2.18 Critical strain, γ_c, of β-lactoglobulin as function of protein concentration at pH 7.0 and 20°C.

Table 2.3 Rheological data and evaluated structural parameters of heat-induced β-lactoglobulin gels at pH 7.0

Power-law exponents		Model of Shin and co-workers (1990)		Model of Wu and co-worker (2001)				Regime
A^a	B^b	d_f	x	d_f	β	α at x = 1.0	α at x = 1.3	
5.28	-2.9	2.16	1.44	2.16	4.44	-0.15	-0.04	strong-link gel

[a] Power-law exponent relating G' to concentration: $G' \sim C^A$.
[b] Power-law exponent relating γ_c to concentration: $\gamma_c \sim C^B$.

The value d_f = 2.16 is in accordance with values of fractal dimension obtained for other protein system which was between 1.5 and 2.8 (Hagiwara et al., 1997, 1998; Wu et al, 2001; Ould Eleya et al., 2004; Zhong, Daubert, and Velev, 2004). The value of x = 1.44, comprised between 1 and d_f, is a reasonable one.

Using the model of Wu and co-worker (2001), the d_f value obtained was identical to that estimated using the strong-link model of Shin and co-workers (1990) (Table 2.3). The model allowed the derivation of two additional parameters, α and β (Table 2.3). Parameter α values were estimated for two x values, 1 and 1.3, which are commonly considered to be a good approximation of the fractal dimension of the backbone of colloidal aggregates (Ould Eleya et al., 2004). In both cases, the values were close to zero, which confirmed that the gels were in the strong-link regime as found using the model of Shin et al. (1990).

Values of d_f close to the one obtained here were reported by Stading and co-worker (1993) for fine-stranded gels (d_f ~2.5) and particulate (d_f ~2.9) β-lactoglobulin gels, and by Pouzot, Nicolai, Benyahia, and Durand (2006) for β-lactoglobulin gels at pH 7.0 and 0.1M NaCl (d_f = 2).

The d_f value also agreed with that reported in literature for reaction-limited cluster-cluster aggregation processes (Meakin, 1987). In these processes, aggregation is slow due to the presence of a repulsive (electrostatic) barrier between approaching particles. Usually, numerous encounters must occur between two particles or clusters before a binding event takes place. The results of computer simulations and experiments revealed that aggregates grown under these conditions are characterized by fractal dimensions of 2.0 – 2.2 (Meakin, 1987; Ikeda, Foegeding, and Hagiwara, 1999).

2.3.6 Effect of pH

In this section, gel formation and the viscoelastic properties of the final gels were studied at pH 4.6, a value close to the pI of the protein. This pH value corresponded to the maximum turbidity of β-lactoglobulin solutions, as experimentally determined in section 2.3.2, indicating the existence of some aggregation in the solution. The solubility of β-lactoglobulin was considerably less than at pH 7.0, which brought some experimental constrains for solutions preparation and limited the range of available concentrations. So, the study was done using low concentrations (6 - 7 wt%) and the results were compared to those obtained at pH 7.0, for gels of the same protein concentration. The experimental procedure was the same as for pH 7.0, as described in section 2.2.6.3.

2.3.6.1 Gel formation and quenching

The aggregation/gelation process started during the heating (20 to 80ºC) step: values of tan δ << 1 were observed at the beginning of the 80ºC heating step. For samples at pH 7.0, it started later during the time sweep at 80ºC: values of tan δ < 1 were obtained only after 12 min of the time sweep at 80ºC, in the case of the 6%β-lactoglobulin solution, taken as an example (Figure 2.19).

During the isothermal heating step and for both pHs, tan δ decreased, rapidly at first, attaining a plateau value at the end of the step (Figure 2.19). The plateau value was lower for systems at pH 4.6, indicating a higher elasticity of the gels. Also, G' values, at the end of this step, were higher at pH 4.6 (results not shown), indicating that the resulting gels were stronger than at pH 7.0

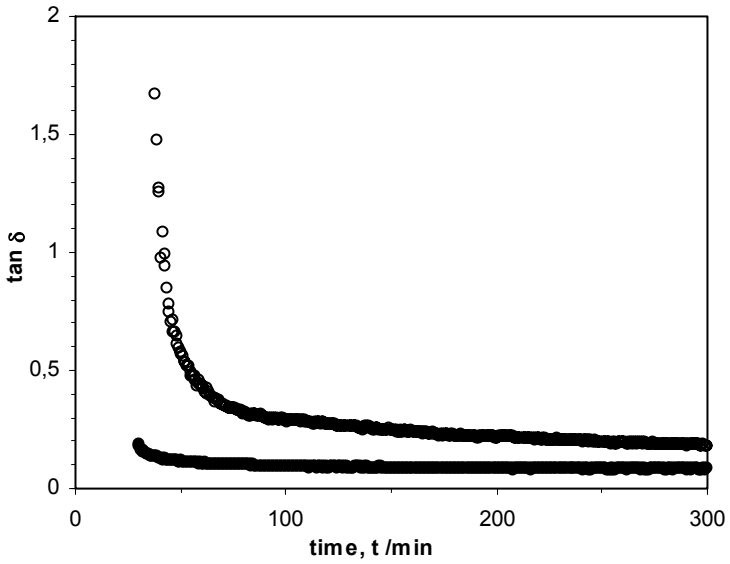

Figure 2.19 Evolution of tan δ with the time during time sweep at 80ºC, for 6%β-lactoglobulin samples at pH 7.0 (O) and pH 4.6 (●).

Clearly, the aggregation/gelation process for the systems was different at both pHs. As mentioned by Lefèvre and co-worker (2000), at pH 4.6, the heat-induced gelation process might have started directly by the aggregation of proteins in the dimeric form accompanied by a partial protein unfolding; aggregation continued further leading to the formation of the gel. So, aggregation preceded denaturation, in this case. At pH 7.0, gelling of the protein was preceded by denaturation and aggregation of partially unfolded protein molecules; as a result of primary aggregates interactions, a network was formed (Hoffmann and van Mill, 1997; Verheul et al., 1998; Lefèvre et al., 2000).

Subsequently, gels were quenched to 20^{o}C and hold at this temperature for 1.5 h. As for pH 7.0, cooling the gels resulted in an increase of gel strength. No further evolution of the gels was detected after the holding period at 20^{o}C, which permitted to characterize the rheological behaviour of the final gels.

2.3.6.2 Viscoelastic properties

After equilibration of the gels, frequency sweeps were performed at 20ºC. The spectra obtained framed a section of the viscoelastic plateau, with $G' > G''$ for the range of frequencies studied. G' and G'' increased monotonously over the range of frequencies studied as shown, in Figure 2.20. Viscoelastic measurement showed once more that the gels formed at pH 4.6 were stronger (higher G') than the gels formed at pH 7.0.

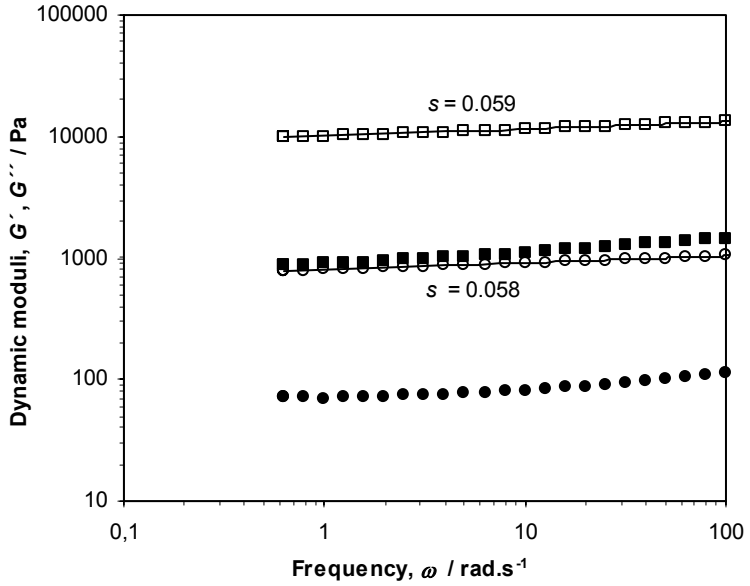

Figure 2.20 Storage modulus G' (open symbols) and loss modulus G'' (full symbols) vs oscillation frequency for 7%β-lactoglobulin gels, at 6.28 rad.s^{-1} and 20ºC, at pH 7.0 (O) and pH 4.6 (□). The lines represent the linear fit of G' and s is their slope.

In addition, mechanical spectra can provide information about the resemblance between the sample gel and a strong, covalent gel. A covalent gel is frequency independent, while a physical gel is slightly frequency dependent. The degree of frequency dependence can be quantitatively expressed by the constant s as followed:

$$\log G' = s \log \omega + L \qquad \text{(Eq. 2.28)}$$

Where G' is the storage modulus, ω is the oscillation frequency and L is a constant. The constant s is the slope in a log-log plot of G' versus ω; the covalent gels have $s = 0$, while the physical gels have $s > 0$. In the present study, all sample gels, both at pH 4.6 and pH 7.0, had $s > 0$, as exemplified in Figure 2.20 for 7 wt% gels, suggesting that they were physical gels, according to the definition of Clark and Ross-Murphy(1987). In a study of Stading et al. (1990) values of s were similar, at intermediate pHs, to those obtained here but decreased to ~0.04 at low and high pH, which provided a way to distinguish between aggregate gels (higher s values) and fine stranded gels (lower s values). Here, values of s were similar, not allowing distinguishing between the two gel types.

Finally, protein gels were submitted to a range of increasing stresses (dynamic stress sweep test) till they ruptured. No strain hardening was observed, as was the case at pH 7.0. Instead, G' and G'' remained almost constant and then suddenly decreased with increasing strain (Figure 2.21). This type of behaviour is often seen in polymer solutions and melts. We have not seen it described for aggregated gels; probably, as the strain sweep test is normally used for confirming whether the measurement is within the linear viscoelastic range, an analysis of the strain sweep spectrum has not yet been done in that case. If the classification of Hyun and co-workers (2002) is adopted, these gels would be of type I (strain thinning). The network model of Sim and co-workers (2003) specify that the formation rate is decreased while the destruction rate is increased as the strain amplitude increased. When the strain is large, the networks junctions are easily lost and G' and G'' decrease. Using the same model, gels at pH 7.0 were classified in type IV (strong strain overshoot), as described in section 2.3.4.2.

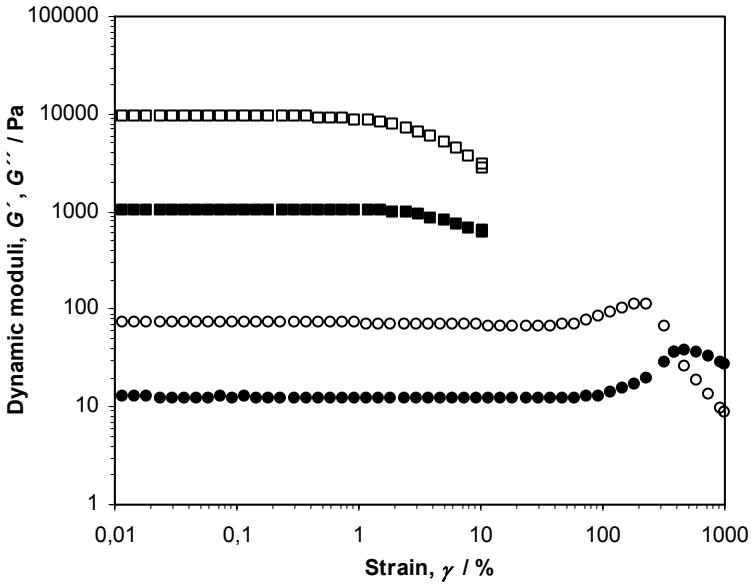

Figure 2.21 Strain dependence of the storage (*G´*: open symbols) and loss (*G´´*: full symbols) moduli at 6.28 rad.s^{-1} for 6%β-lactoglobulin gels, at pH 7.0 (O) and pH 4.6 (□).

Compared to similar gels, at pH 4.6, these gels were stronger (higher *G´* values) and showed higher sensitivity to strain (lower critical strain), as shown in Figure 2.21 for 6 wt% gels. These differences in the rheological properties reflect differences in the microstructures. In fact, Standing and co-workers (1991, 1995) verified that fine-stranded and particulate β-lactoglobulin gel had totally different mechanical properties. Lower values for *G´* and higher strain at fracture were found, as in the present study, for gels obtained at pH 7.0, when compared to gels formed at intermediate pH values. These authors were able to show that the strand structure influenced both the modulus as well as the fracture properties of both type of gels. Homogeneous gels obtained at pH 7.0 consisted of thin strands (< 5 nm), curled and not very stiff, with short distances between cross-links while particulate gels, formed at pH 5.3, had flexible strands of uniform, spherical particles arranged like beads on a string, and pores of ~20 - 50 μm. In large deformation measurements, the structure was broken; the weaker areas were

broken before the stronger ones. For particulate gels, the pores were probably the weakest element of the network and were responsible for the fracture (Standing et al., 1995).

2.3.7 Effect of shear treatment

In this section, the effects of steady shear on the rheological behaviour of β-lactoglobulin gels was investigated using the procedures described in section 2.2.6.3.

In the first set of experiments, 10%β-lactoglobulin samples, at pH 7.0, were used. The steady shear was performed during heating from 20 to 75°C or 77°C, at constant rates between 40 and 120 s^{-1} (Figure 2.22).

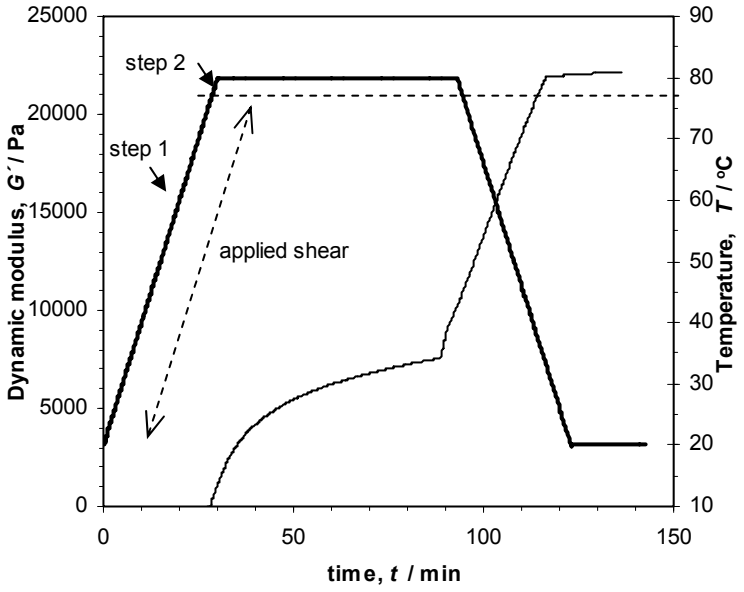

Figure 2.22 Thermal gelation of 10%β-lactoglobulin sample at pH 7.0 with steady shear applied (120 s^{-1}) during heating step 1 (20 to 77°C) at 2°C/min. The heating step 2 is from 77 to 80°C without shearing at the same heating rate. The thick line represents the temperature profile.

The gelation temperature, T_g, of unsheared gels submitted to the same thermal treatment was around 77°C, as determined in a previous experiment (see Figure 2.9). So, when shearing was performed up to 75°C ($T<T_g$), the stage of aggregation of the protein was different from that at 77°C ($T\sim T_g$). As could be expected, the effect of shear was different in each case. For $T<T_g$, shear did not induce significant changes in the gelation temperature for the different shear rates used. In fact, sheared and unsheared gels presented the same T_g (77°C, $G' = G''$), independently of the applied shear rate (Figure 2.23). For $T\sim T_g$, however, shear induced changes in the gel point; for all shear rates applied, the gel point was observed at lower temperature (< 77°C) than for the unsheared gel (not shown).

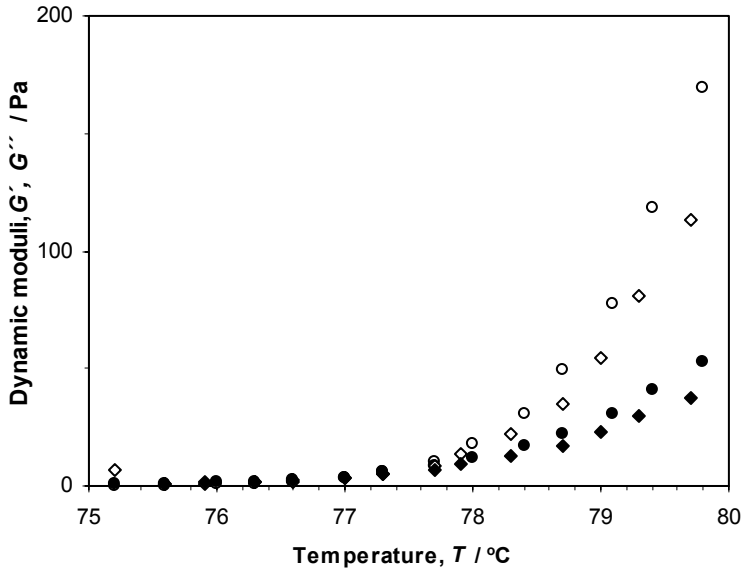

Figure 2.23 Temperature of gelation of 10%β-lactoglobulin samples at pH 7.0 in heating step 2 (75 to 80°C) at 6.28 rad.s^{-1} with and without shear during heating step 1 (20 to 75°C). Storage modulus G´: open symbols; loss modulus G´´: full symbols; unsheared: O; sheared at 40 s^{-1}: ◇.

Also, changes in viscosity of the samples during the heating step were observed for the shear treated gels (Figure 2.24). The viscosity of the samples decrease until the temperature reached a value around 71°C and lower viscosity values were obtained for the sample sheared at a higher

shear rate. Then, a steady increase in viscosity was observed which must be due to the denaturation of the protein (Hegg, 1980). Tang, Munro, and McCarthy (1993) studied viscosity changes in whey protein suspensions at pH 7.0, during temperature increase. At a constant rate of 291 s^{-1}, they observed a steady increase in viscosity starting at 60°C. This result was interpreted in terms of structure formation in the suspensions. In the present study, the viscosity increase was steeper, though starting at a higher temperature, for the sample sheared at higher shear rate. These features may reflect differences in structure formation depending on the shear rate applied.

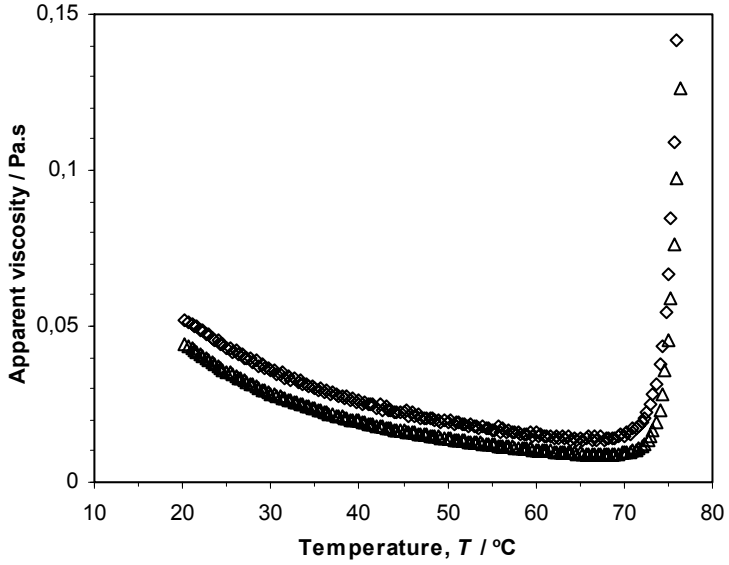

Figure 2.24 Apparent viscosity versus temperature increase from 20 to 77°C, at two shear rates: 40 s^{-1} (◇) and 120 s^{-1} (Δ) for 10%β-lactoglobulin sample at pH 7.0.

After cooling to 20°C, gels were left to equilibrate during 1 h, *G´* reached a constant value which permitted to characterize the rheological behaviour of the final gels. Mechanical spectra were recorded as shown in Figure 2.25. Frequency sweeps did not reveal important differences in the viscoelastic properties of shear-treated and unsheared gels. A small decreased of *G´* was observed for the shear-treated gels; however, the shape to the *G´* and *G´´* curves was the same

for all gels (Figure 2.25). In small deformation measurements, the whole structure contributes equally since no parts of the structure are broken. However, in large deformation measurements, the structure is broken starting by the weaker areas. So, some information about differences in the structure of the gels would be expected from stress sweep experiments performed up to rupture. But, only minor differences were observed between shear-treated and unsheared gels (Figure 2.26). According to the classification of Hyun and co-workers (2002), all gels fall into type III, weak strain over shoot (*G´* decreasing, *G´´* increasing following by decreasing) (Figure 2.26).

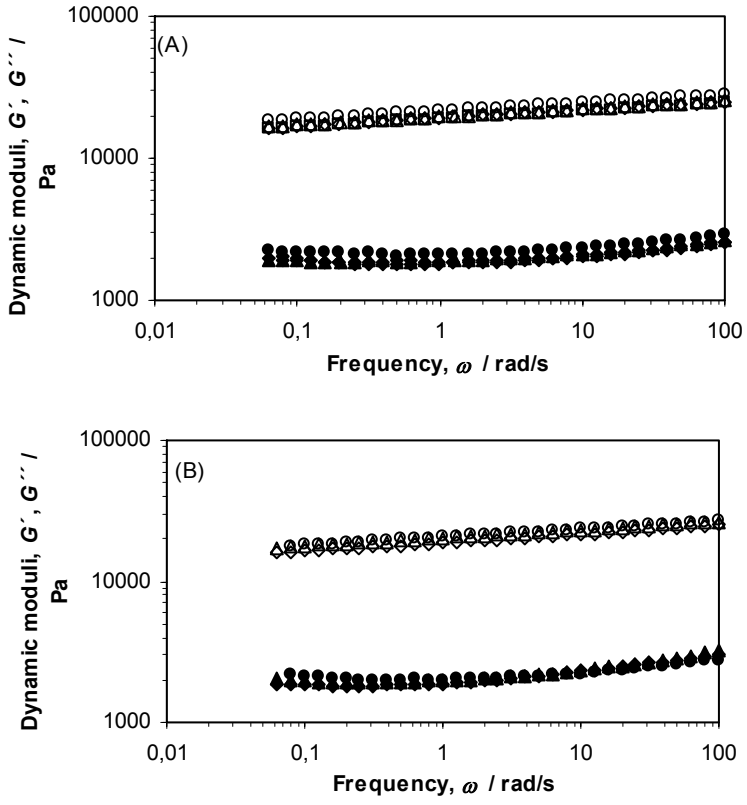

Figure 2.25 Storage modulus *G´* (open symbols) and loss modulus *G´´* (full symbols) vs oscillation frequency at 6.28 rad.s^{-1} and 20°C of 10%β-lactoglobulin gels at pH 7.0 with different shear applied: unsheared (O), 40 s^{-1} (◇), 70 s^{-1} (□), and 120 s^{-1} (Δ) during heating step from 20 to 75°C (A) and to 77°C (B).

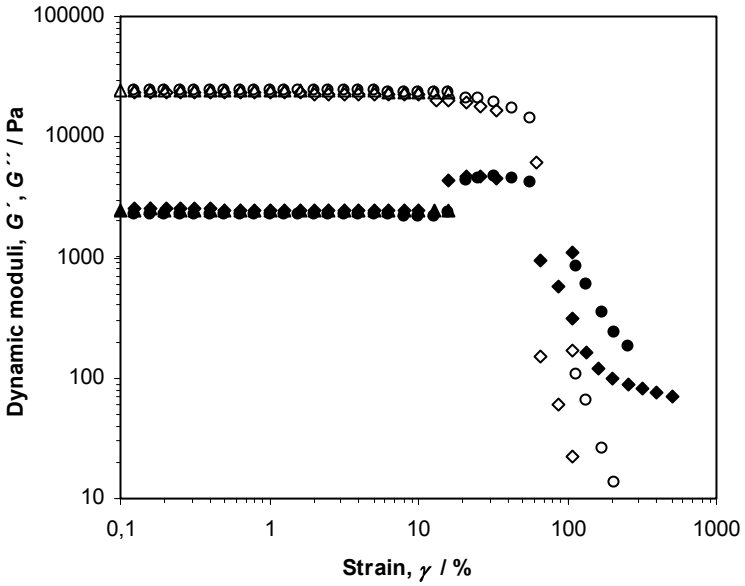

Figure 2.26 Strain sweeps for 10%β-lactoglobulin gels at 6.28 rad.s^{-1}, at 20^{o}C and pH 7.0. Shear treatments were performed during heating step from 20 to 77^{o}C. Symbols: unsheared (O), 40 s^{-1} (◇), 120 s^{-1} (Δ), (*G´*: open symbols) and (*G´´*: full symbols).

In the second set of experiments, 6.5%β-lactoglobulin samples, at pH 7.0, were heated till 80^{o}C (2^{o}C/min) and then were sheared, for 3 min, at constant rates between 60 and 360s^{-1}, as shown in Figure 2.27. Gelation occurred during the isothermal heating at 80^{o}C at this protein concentration. For an unsheared gel submitted to the same thermal treatment the gel point (*G´* = *G´´*) was attained after ~6.5 min at 80^{o}C while, for the sheared gels, the gel point was attained earlier (see Table 2.4).

In these experiments, where shear was applied for a short period near T_g, the shear-treated gels had quite different mechanical properties form the previous ones. Frequency sweep tests, performed at 20^{o}C, showed an increase of moduli with increasing shear rate (Figure 2.28). Apparently, shearing of the systems favored aggregation of the protein.

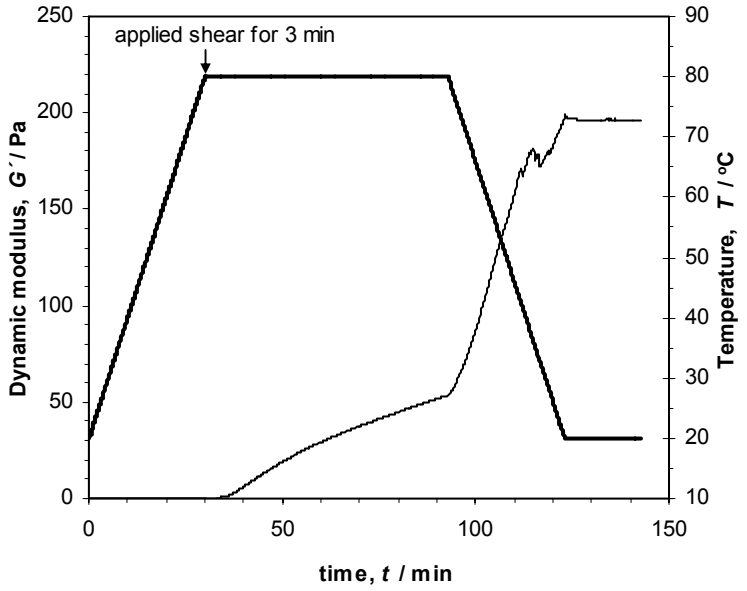

Figure 2.27 Thermal gelation of 6.5%β-lactoglobulin sample at pH 7.0 with steady shear applied ($60s^{-1}$) after heating step (20 to 80°C) for 3 min. The thick line represents the temperature profile.

Table 2.4 Gel time of 6.5%β-lactoglobulin sample at pH 7.0 without and with shear treatment, for 3 min, after heating from 20 to 80°C

Shear applied (s^{-1})	Gel time at 80°C (at $G' = G''$) (min)
0	6.5
60	2.1
120	2.0
360	1.4

Stress sweeps, performed for all gels, showed that they fall into type IV, strong strain overshoot (G', G'' increasing following by decreasing) (Hyun et al., 2002). The shear-treated gels showed

a narrower linear viscoelastic region and fracture at lower strains than the unsheared gels independently of the shear rate (Figure 2.29).

The same set of experiments was also performed for 6.5 wt% gels prepared at pH 4.6. This time samples were sheared at $120s^{-1}$. In this case, as gelation occurred during the 20 to 80°C heating step (results not shown), shearing was applied after gelation occurred, though still in incipient gels.

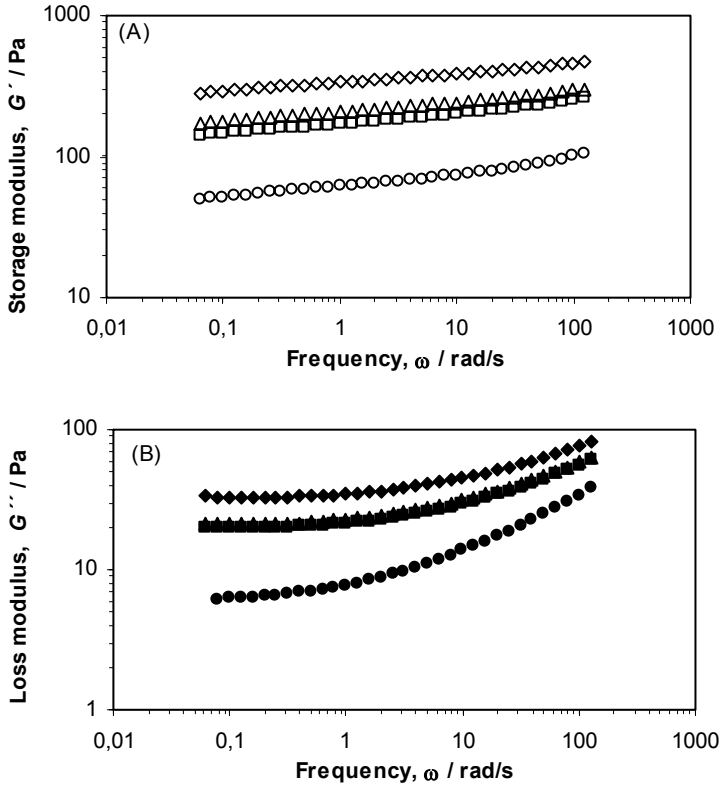

Figure 2.28 Effect of shear at different rates on moduli of 6.5%β-lactoglobulin gels at 20°C and pH 7.0 when shear was applied for 3 min after the heating step (20 to 80°C): 0 s^{-1} (O), 60 s^{-1} (□), 120 s^{-1}(Δ) and 360 s^{-1} (◇).

Unlike the data of 6.5%β-lactoglobulin gels at pH 7.0, which showed increasing gel strength with shear, the gel strength of sheared gels at pH 4.6 was much smaller than for the unsheared one (Figure 2.30). Stress sweeps performed for all gels showed that they fall into type I, strain thinning (Hyun et al., 2002). The shear-treated gel showed weaker G' and higher strain fracture than the unsheared gel (Figure 2.31).

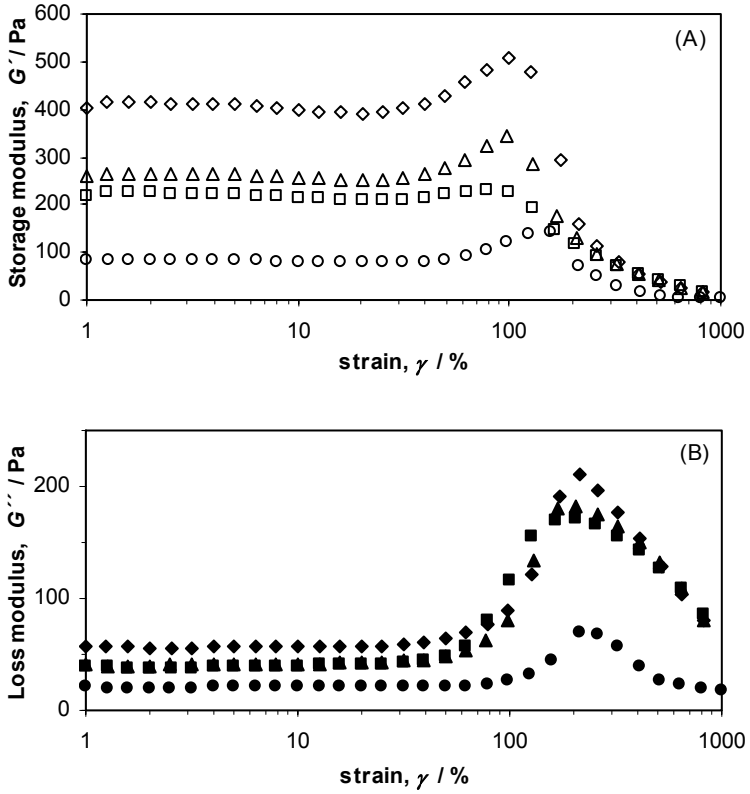

Figure 2.29 Strain dependence of the storage modulus, G' (A) and loss modulus, G'' (B) at 6.28 rad.s^{-1} for 6.5%β-lactoglobulin gels at 20°C and pH 7.0 with different shearing after heating step (20 to 80°C) for 3 min: 0 s^{-1} (O), 60s^{-1} (□), 120 s^{-1}(Δ) and 360 s^{-1} (◇).

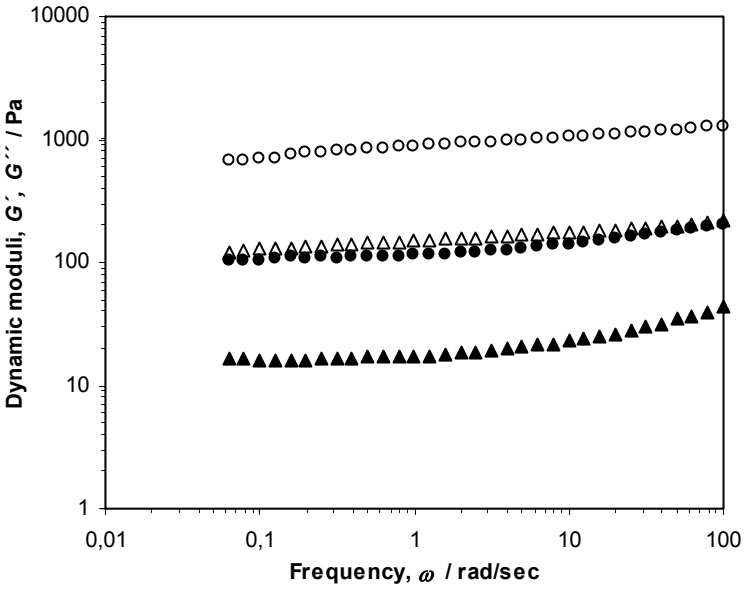

Figure 2.30 Storage modulus G' (open symbols) and loss modulus G'' (full symbols) vs oscillation frequency at 6.28 rad.s^{-1} of 6.5%β-lactoglobulin gels at 20°C and pH 4.6: unsheared (O) and 120 s^{-1} (Δ) after heating from 20 to 80°C step for 3 min.

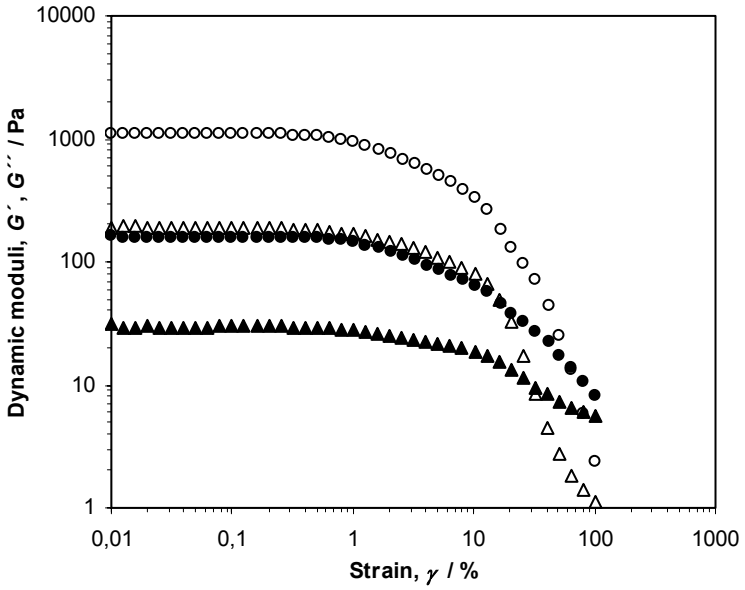

Figure 2.31 Strain dependence of the storage modulus, G' and loss modulus, G'' at 6.28 rad.s^{-1} for 6.5%β-lactoglobulin gels at 20°C and pH 4.6: unsheared (O) and 120 s^{-1} (Δ) after heating from 20 to 80°C step for 3 min.

The above results show that different shear conditions result in different rheological properties. The differences are most likely caused by the various shear conditions in relation to the aggregation states of the protein. Shearing during the heating step, at pH 7.0, did not induce important changes in the rheology and, probably, in the microstructure of the final gels. Shearing for a short period (> 60 s^{-1}) at 80°C brought some changes to the gel behaviour. For pH 7.0 solutions of whey protein concentrate, Taylor and co-worker (1994) found that the final gel strength of sheared gels was a complex function of the time of shear, the final gel strength decreasing with increasing time of shear, suggesting the disruption of protein aggregates by shear. The same authors found that, at pH 5.2, shear during the initial stages of heating, at 85°C, increased the gel strength, probably due to shear preventing rapid aggregation into weak networks, but longer periods of shear (> 60 s^{-1}) lead to a decrease in gel strength as protein aggregates were disrupted by shear. Walkenström and co-workers (1998) also reported changes in the microstructure and the rheology of sheared particulate whey protein gels, at pH 5.4. These changes depended on the temperature range of exposure to shear ($T < T_g$ or $T > T_g$) and on the shear rate applied. The effects of short periods of shear treatment in the vicinity of the gel point have been investigated in particulate whey protein suspensions by Walkenström and co-workers (1998). The gels showed a G' value twice as high as that for the unsheared gel. The shear-treated gels were found to be more inhomogeneous than the unsheared ones. This contrasts with the results in the present study where sheared gels were weaker. But their protein system and the experimental conditions were different which may be the reason for the observed differences.

2.4 Conclusions

The results in this chapter confirm that the heat-set gelation and the rheology of the final β-lactoglobulin gels depend on the concentration of the protein as well as on the pH of the medium and the processing conditions.

For each pH, increasing the protein concentration decreased the time and temperature of gelation and increased the strength (higher G' values) of the final gels. When comparing gels of similar concentration obtained at different pHs, it was verified that, at pH 4.6, gels formed at lower temperature and sooner than at pH 7.0. Moreover, the former gels were stronger (higher G' values) and showed higher sensitivity to strain (lower critical strain) than gels formed at pH 7.0.

These findings are consistent with the microstructures expected for the two types of gels (extensively reported in the literature), which is a consequence of the balance between repulsive and attractive forces among protein molecules. For gels of the same concentration but formed at different pHs, differences in G' are considered mainly due to the changes in the size of flocs building the protein network and in the thickness of the strands in the flocs (strands become thicker, at pH 4.6, due to reducing repulsive forces and thus increasing attractive forces among protein molecules). Also, as the number of flocs in gels increases with decreasing floc size, it is reasonable to conclude that fine-stranded gels with smaller flocs are more strain resistant than particulate gels, as was observed experimentally.

The rheological analysis proved to be a useful method to analyze the structure of concentrated β-lactoglobulin gels (C > 9 wt%), at pH 7.0. All gels showed power law relationships between

G' or γ_c (the limit of linearity) and protein concentration, consistent with previous results for globular protein gels having fractal structures. The value of the fractal dimension evaluated using scaling relationship agreed with that reported in literature for reaction-limited cluster-cluster aggregation processes, suggesting that, because of electrostatic repulsions, many collisions must occur before the protein molecules stick together forming aggregates.

Finally, shearing during gelation proved to affect the rheological properties of the resulting gels, at both pH values. The effects on gels strength and strain at fracture depended on pH, on the duration, temperature and rate of shear and were more pronounced when shear was applied for a short period at 80^{o}C. It is concluded that the differences are most likely caused by the various shear conditions in relation to the aggregation state of β-lactoglobulin. Shear may prevent rapid aggregation into weak networks causing an increase in gel strength, or it may disrupt β-lactoglobulin aggregates causing a decrease in gel strength, these effects being a complex function of the above variables.

Chapter 3

Rheological behaviour of galactomannan solutions

3.1 Introduction

The structural characteristics of galactomannans, especially guar gum and locust bean gum, have been extensively studied by several researchers (for example, Courtois et al., 1966; McCleary et al., 1985). Their functional properties are related to both the structural features and the molecular masses (Dea et al., 1986; Dea et al., 1977; Fernandes et al., 1991). In literature, the rheological behaviour, in steady and dynamic shear conditions, of aqueous solutions of several random-coil polysaccharides, like galactomannans, are well documented, as described in Chapter 1.

Here, and as was the case in Chapter 2 for β-lactoglobulin, the study of the rheological properties of galactomannan solutions was done under the same experimental conditions as those used in Chapter 4, for the mixed liquid systems. Two galactomannans were studied: locust bean gum (LBG) and tara gum (TG). Both are neutral, non-gelling galactomannans, differing in the mannose to galactose ratio, M/G (see Chapter 1, section 1.2). Tara gum, contrarily to locust bean gum, is a less studied galactomannan. In this chapter, its rheological behaviour was investigated, at 20^{o}C, and compared to that of LBG in order to see if a generalized behaviour could be established for the two galactomannans.

Locust bean gum and tara gum samples were characterized in section 3.3.1 using the methods described in section 3.2.2. The flow and the viscoelastic properties of galactomannan solutions were studied in section 3.3.2. For each polysaccharide, analysis of flow data was done using the Cross and Carreau flow models. The viscoelastic data were fitted with the generalized Maxwell model with four elements and the Friedrich-Braun model. Then, the relation between the steady

shear and dynamic rheological properties was studied. Finally, in section 3.4, the main conclusions were described.

3.2 Materials and methods

3.2.1 Materials

Commercial samples of locust bean gum (Ref. H01091-990) and tara gum (Ref. 1760), were kindly supplied by Degussa Texturant Systems (France) and Carob S.A. (Spain), respectively. The tara gum sample was used after purification, as described in section 3.2.2.1.

3.2.2 Characterization of the samples

3.2.2.1 Purification of the gum

Crude tara gum was purified by precipitation with isopropanol as previously described by da Silva and Gonçalves (1990).

An aqueous dispersion of the crude gum (~1 wt%) was prepared as described in section 3.2.3.1. After cooling, the non-dissolved material was removed by centrifugation at 19,000 g for 1 h, at 20^{o}C. The solubilized galactomannan was precipitated from the solution by pouring into a two-volume excess of isopropanol, and allowing the mixture to stand for 30 min. The white fibrous precipitate formed was collected by filtration under vacuum, on a porous glass filter (G2), and washed twice with isopropanol and then with acetone. After drying under vacuum at 30^{o}C for 27 h, the precipitate was ground to a fine powder.

3.2.2.2 Measurement of moisture and ash contents

The moisture and ash contents of the galactomannan samples were measured following the general method as previously described in section 2.2.2.1.

3.2.2.3 Measurement of the mannose-galactose ratio

The determination of the D-mannose to D-galactose ratio (M/G) of each galactomannans was performed by gas-liquid chromatography (GC-FID) after hydrolysis of the polysaccharides and conversion of the obtained monosaccharides into alditol-acetates.

The procedure used, based on that described by Blakeney, Harris, Henry, and Stone (1983), was the following (Coimbra, Delgadillo, Waldron, and Selvendran, 1996):

- Weight (2-3 mg) of the sample in a capped glass tube.
- Add 200 μL of 72% (w/w) H_2SO_4, and incubate for 3 h at ambient temperature.
- Add 2.2 mL of distilled water and hydrolyze for 2.5 h at 100°C.
- Cool the tubes in an ice bath and add 200 μL of internal standard (2-deoxiglucose 1 mg/mL) solution.
- Transfer 1 mL of sample to a test tube and neutralize with 200 μL of 25% NH_3. Reduce the samples with 100 μL of $NaBH_4$ 15% (w/v) in 3 M NH_3, for 1 h at 30°C. Note that the $NaBH_4$ solution must be freshly prepared just before addition (150 mg in 1 mL).
- Cool in an ice bath and end the reduction reaction by 2 additions of 50 μL glacial acetic acid.
- Transfer a 300 μL of aliquot to a SOVIREL test tube (important to avoid interference peaks from the caps of the other tubes) put the tubes in the ice bath and add 450 μL of 1-methylimidazole and 3 mL of acetic anhydride. Mix well in a vortex mixer and incubate at 30°C for 30 min.

- Add 4 mL of water (to destroy the remaining acetic anhydride) and 2.5 mL of dichloromethane, screw on caps and mix well (20 times by hand) to extract the alditol acetates. Leave for 15 min then put in the centrifuge (3000 rpm, Kubota 2010) for 30 s.
- Remove the upper aqueous phase.
- Add 3 mL of water and 2.5 mL of dichloromethane and mix thoroughly, centrifuge and remove aqueous phase as above.
- Wash the organic phase twice with 3 mL of water. Mix, centrifuge and remove aqueous phase as above. Make sure that there is no aqueous phase left after the last wash.
- Transfer the dichloromethane phase to a new test tube and evaporate the solvent under a stream of nitrogen at 40°C (Techne Dri-block DB3B).
- Remove the remaining water by adding 1 mL of anhydrous acetone and evaporate to dryness as above (2 times). (The acetylated sugar can be kept dry in the tube in a desiccator).

For the chromatographic analysis, the alditol acetates were dissolved in 50 μL anhydrous acetone. The analysis was performed in a gas chromatograph (HP 5890), with a flame ionization detector, equipped with a DB-225 capillary column (30 m length, 0.25 mm internal diameter and 0.15 μm film thickness). The operating conditions were:

Carrier gas: helium

$V_{injection}$ = 2 μL,

$T_{injector}$ = 220°C, $T_{detector}$ = 230°C and T_{oven} = 220-230°C.

Time program: 4 min at 220°C for; 25°C/min until 230°C; 6.5 min at 230°C. Total run time: 11 min.

The M/G ratios were determined on the basis of the peak areas and of the relative response factors (RF) for each monosaccharide, using 2-deoxiglucose 1 mg.mL^{-1} as the internal standard.

$$\text{RF} = \frac{\text{Peak area of alditol acetate / Peak area of the internal standard}}{\text{Weight of the alditol acetate / Weight of the internal standard}} \qquad \text{(Eq. 3.1)}$$

$$\text{Ratio M/G} = \frac{\text{Peak area of the mannitol acetate} \times \text{RF of galactitol acetate}}{\text{Peak area of the galactitol acetate} \times \text{RF of mannitol acetate}} \qquad \text{(Eq. 3.2)}$$

3.2.2.4 Determination of limiting viscosity number

The limiting viscosity number or intrinsic viscosity, $[\eta]$, is defined as the limiting value of the reduced viscosity (specific viscosity/concentration) at infinite dilution (Eq. 3.3):

$$[\eta] = \lim_{c \to 0} \left(\frac{\eta_{sp}}{C} \right) \qquad \text{(Eq. 3.3)}$$

Where $\eta_{sp} = \left[\frac{(\eta - \eta_s)}{\eta_s} \right] = \eta_{rel} - 1$ is the (dimensionless) specific viscosity, $\eta_{rel} = \frac{\eta}{\eta_s}$ is the (dimensionless) relative viscosity, η and η_s are the viscosity of the solution and of the solvent, respectively, and C the concentration of the solution.

The two equations commonly employed for determining the $[\eta]$ value were proposed by Huggins' (1942) (Eq. 3.4) and Kraemer (1938) (Eq. 3.5):

$$\frac{\eta_{sp}}{C} = [\eta] + k'[\eta]^2 C \qquad \text{(Eq. 3.4)}$$

$$\frac{(\ln \eta_{rel})}{C} = [\eta] + k'[\eta]^2 C \qquad \text{(Eq. 3.5)}$$

where k' and k'' are the Huggins' and Kraemer's coefficients, respectively.

It thus becomes necessary to find the reduced and the relative viscosities of solutions, at different concentrations, and then extrapolate to zero concentration.

Galactomannan solutions were prepared to give relative viscosities from about 1.2 to 2.0, to assure good accuracy and linearity of extrapolation to zero concentration (Morris and Ross-Murphy, 1981).

Viscosities of the solutions were measured at 20.0 ± 0.1ºC with a capillary Cannon Fenske viscometer (ASTM-D2515, ISO 3105, Series 100), using exactly 10 mL of solution sample. From the equation of Hagen-Poiseuille and as measurement of relative viscisities is our goal, then:

$$\frac{\eta}{\eta_s} = (\frac{\rho}{\rho_s})(\frac{t}{t_s}) \qquad \text{(Eq. 3.6)}$$

Where ρ and ρ_s are the densities of the solution and of the solvent, respectively, and t and t_s are the efflux times of the solution and of the solvent, respectively.

After determination of η_r, η_{sp} and η_{rel} could be calculated. Then, the limiting viscosity number was obtained by extrapolation to zero concentration of Huggins and Kraemer equations (Eqs. 3.4 and 3.5).

3.2.2.5 Viscosity average molecular weight determination

The viscosity average molecular weight ($\overline{M}_v$), for each galactomannan sample, was estimated by using the Mark-Howink relationship (Eq. 3.7) given by Doublier and Launay (1981) for guar gum modified by Gaisford, Harding, Mitchell, and Bradley (1986) to take into account the different mannose to galactose ratios (M/G) of the galactomannans:

$$[\eta] = 11.55 \times 10^{-6} \left((1 - \chi) \overline{M}_v \right)^{0.98} \qquad \text{(Eq.3.7)}$$

where $\chi = 1/[(M/G) + 1]$ and $[\eta]$ is expressed in $dL.g^{-1}$.

3.2.3 Rheological measurements

3.2.3.1 Preparation of solutions

The required amount of the powdered gum was gradually added to the appropriate amount of distilled water in the presence of sodium azide (5 ppm) in order to prevent bacterial degradation. The dispersion was moderately stirred for 1 h, at room temperature, and then heated at 80ºC in a water bath for 30 min, under continuous stirring. After cooling, a clear solution was, normally, obtained. Eventually, a centrifugation (35,000 g for 1 h, at 20ºC), to separate insoluble matter, was needed. The concentration of the final solutions was determined from their dry matter contents.

3.2.3.2 Rheological procedures

The controlled stress rheometer AR2000, described in section 2.2.6, was used in the experiments, fitted with a cone and plate geometry (2^o cone angle, 40 mm diameter, 54 μm

truncation). The samples were covered with a thin layer of paraffin oil to prevent evaporation. Measurements were performed at 20^{o}C.

For each sample studied and due to the non-destructive character of low amplitude oscillatory experiments, a frequency sweep (mechanical spectrum) test followed by the determination of the flow curve was done.

Frequency sweeps were performed in the 0.1 to 100 rad.s^{-1} range, with strain amplitude of 5%, which was within the linear viscoelastic strain region, determined by preliminary experiments. Steady shear experiments were performed first in increasing order of applied torque followed by decreasing order, in a continuous manner, so that shear rates varied from 0.01 to 1000 s^{-1} (up and down). The torque amplitude was imposed using a logarithm ramp, in order to decrease the initial acceleration and the effects due to instrument inertia.

3.3 Results and discussion

3.3.1 Characterisation of galactomannan samples

3.3.1.1 Moisture content, ash content and M/G ratio

In Table 3.1, the main characteristics of the galactomannan samples are presented. With the purification process used for tara gum (TG), the ash content was drastically reduced and the M/G ratio increased. This increase of M/G may be due to the elimination of small and highly substituted molecules, with low M/G, which are more soluble and, consequently, are not precipitated by isopropanol during the purification step. The obtained values ($\cong 3$) are in good agreement with those reported by Morris (1990) (M/G $\cong$ 2.7-3.0) and Fernandes and co-workers (1991) (M/G = 3.1). The M/G ratio for locust bean gum (LBG) is close to values in the literature: $\cong$ 3.5 (Morris, 1990), 3.85 (Alves et al., 1999) and 3.30 (Andrade et al., 1999).

Table 3.1 Chemical composition of LBG and TG samples

	LBG	TG	
		Crude	Purified
Moisture	6.41 ± 0.07	11.22 ± 0.01	7.81± 0.44
Ash	0.80 ± 0.03	0.77 ± 0.02	0.07 ± 0.02
M/G	3.63 ± 0.09	2.95 ± 0.04	3.03 ± 0.07

All values (%) are mean ± standard deviation of three determinations.

3.3.1.2 Intrinsic viscosity and molecular weight

Intrinsic viscosity and molecular weight of the galactomannan samples were estimated, at 20°C. Values of these parameters obtained for purified TG, were higher than for LBG, while the value of the Huggins' coefficient, k', was lower, as shown in Table 3.2. Values for k' depend on solute-solvent interactions and on the state of aggregation of macromolecules; in theory, values are independent of molecular masses. In a good solvent and for flexible macromolecules, $k' \sim 0.35$ (Wang, Ellis, and Ross-Murphy, 2000); but, it can be higher than 1.0 in case of aggregation. Values of 0.64 - 0.82, in Table 3.2, may reflect some intermolecular aggregation in our samples.

Table 3.2 Physical-chemical parameters of LBG and TG samples, at 20°C

	LBG	Purified TG
Intrinsic viscosity ($dl.g^{-1}$), $[\eta]$	11.76	16.94
Huggins' coefficient, k'	0.82	0.64
Viscosity average molecular mass, $\overline{M}_v$ (Da x 10^{-6})	1.72	2.61

Figure 3.1 displays the determination of $[\eta]$, by extrapolation to zero concentration of Huggins' (Eq. 3.4) and Kraemer (Eq. 3.5) plots. In general, our results for k' and $[\eta]$ are quite consistent with others previously reported (da Silva et al., 1990; da Silva, Gonçalves, and Rao, 1992; Alves et al., 1999).

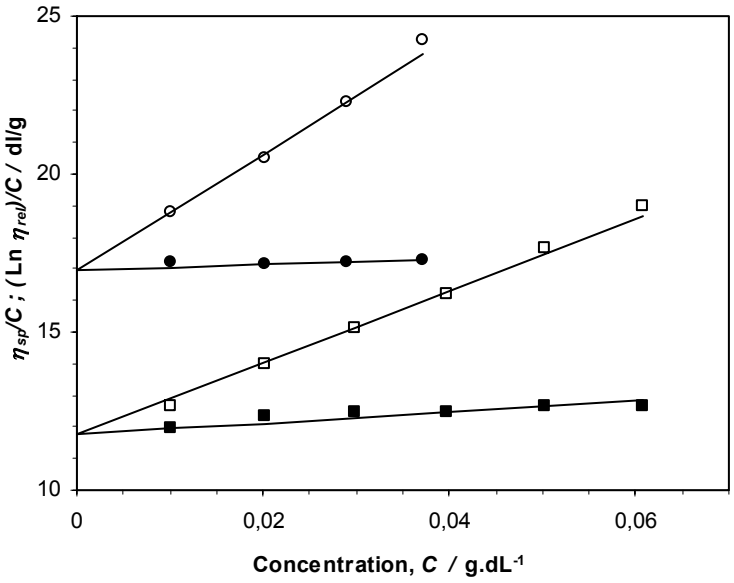

Figure 3.1 Determination of intrinsic viscosity from Huggins and Kraemer plots, η_{sp}/C (open symbols) and $(ln\ \eta_{sp})/C$ (full symbols) against concentration (C) for LBG (□) and TG (O) at 20°C.

3.3.2 Rheological behaviour of galactomannan solutions

3.3.2.1 Steady shear properties

The rheological behaviour of LBG and TG solutions was investigated at 20°C and pH 7.0, in a concentration range between 0.15 and 1.30 wt%, using the controlled stress rheometer AR2000. The galactomannan solutions were prepared as descried in section 3.2.3.1 and the rheological experiments were carried out according to the protocol defined in section 3.2.3.2.

Flow curves for TG and LBG solutions, at different concentrations, are shown in Figure 3.2. In all cases, the flow behaviour was typically shear-thinning, that is the viscosity decreased with increasing shear rate, with a Newtonian region in the low shear rate range. However, for similar concentrations, LBG solutions were less viscous than TG solutions, which reflected the

differences in intrinsic viscosity of the samples; also, the shear-thinning behaviour appeared at a higher shear rate for LBG. The shear-thinning behaviour may be regarded as arising from modifications in macromolecular organization in the solution as the shear rate changes.

At low shear rates, the disruption of entanglements by the imposed shear is balanced by the formation of new ones, so that no net change in entanglements occurs; it is the Newtonian plateau region, where the viscosity has a constant value, the zero-shear rate apparent viscosity, η_0 (Morris, 1995). For higher shear rates, disruption predominates over formation of new entanglements, molecules align in the direction of flow and the apparent viscosity decreases with increasing shear rate. As a consequence, the shear rate corresponding to the transition from Newtonian to shear-thinning behaviour moves to lower values as the concentration increases.

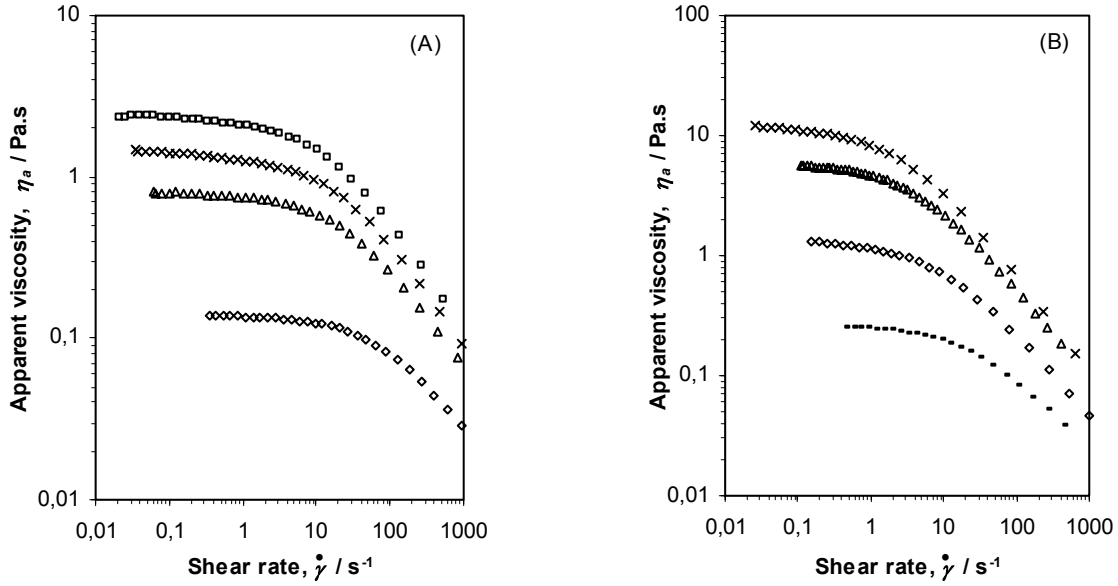

Figure 3.2 Flow curves of galactomannan solutions at different concentrations, at 20°C. (A) LBG, 0.44% (◇), 0.63% (Δ), 0.72% (X) and 0.82% (□); (B) TG at 20°C, 0.31% (–), 0.44% (◇), 0.65% (Δ) and 0.71% (X).

The Cross (1965, Eq. 3.8) and the Carreau (1972, Eq. 3.9) flow models have been used to describe the shear-thinning behaviour of the TG and LBG solutions:

$$\eta_a = \eta_\infty + \frac{(\eta_o - \eta_\infty)}{\left[1 + (\tau \dot{\gamma})^m\right]} \qquad \text{(Eq. 3.8)}$$

$$\eta_a = \eta_\infty + \frac{(\eta_o - \eta_\infty)}{\left[1 + (\lambda \dot{\gamma})^2\right]^N} \qquad \text{(Eq. 3.9)}$$

where $\dot{\gamma}$ is the shear rate (s^{-1}), η_a is the apparent viscosity (Pa.s), η_0 is the zero-shear rate apparent viscosity (Pa.s), η_∞ is the infinite shear rate viscosity (Pa.s), τ (s) and λ (s) are time constants, and m and N are dimensionless constants related to the power law exponent o by m = 1-o and N = (1-o)/2 ($0 \leq N < 0.5$), for the case $\eta_\infty << \eta_a << \eta_0$. Since the high shear rate Newtonian viscosity was never approached in our study, the above equations were simplified (only three adjustable parameters), assuming $\eta_0 >> \eta_\infty$. Both models have been used successfully to describe the behaviour of aqueous galactomannan solutions (see, for instance, da Silva et al., 1992; da Silva, Gonçalves, and Rao, 1994).

As shown (Figure 3.3, Tables 3.3 and 3.4) both models described the apparent viscosity shear rate data well, especially when there were experimental data in the plateau region, at low shear rates. A comparison with experimental data demonstrates very good agreement with model predictions, as illustrated by magnitudes of RE (relative deviation error) (Tables 3.3 and 3.4).

In general, the Cross model provided a slightly better fit. The Carreau model predicted zero shear rate viscosity values lower than the experimental ones; also, for this model, deviations between predicted and experimental values were observed at high shear rates (Figure 3.3). As

expected, due to the increase in shear-thinning behaviour with concentration, the values of η_0, m and N increased with increasing concentration.

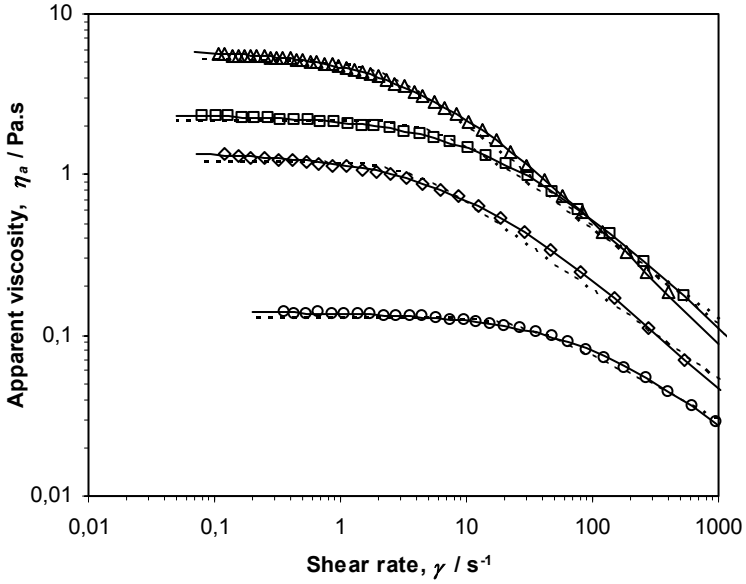

Figure 3.3 Flow curves for galactomannan samples, at 20°C. Symbols: 0.44%LBG (O), 0.44%TG (◇), 0.82%LBG (□) and 0.65%TG (Δ). Full line represents predictions of the Cross model and dotted lines those of the Carreau model.

As said above, shear-thinning appeared at lower shear rates when concentration increased; this means that the rate of formation of new entanglements diminished as concentration increased; so, as can be seen in Tables 3.3 and 3.4, the time constants increased with concentration. The dependence of the Cross parameters η_0 and τ on galactomannan concentration was described by similar scaling laws for LBG and TG systems (Figure 3.4).

Table 3.3 Magnitudes of the Cross model parameters for steady simple shearing, obtained for LBG and TG samples, at 20°C

Samples	Conc.(wt%)	η_0 (Pa.s)	τ (s)	m	RE*
LBG	0.15	0.0073	0.0002	0.499	0.0017
	0.25	0.0198	0.0009	0.637	0.0033
	0.35	0.0882	0.0048	0.663	0.0029
	0.49	0.279	0.0083	0.693	0.0091
	0.68	0.971	0.0242	0.747	0.0074
	0.79	1.84	0.0421	0.740	0.0089
	0.82	2.34	0.0520	0.756	0.0092
	1.3	14.8	0.201	0.760	0.0224
TG	0.16	0.0237	0.0023	0.701	0.0131
	0.23	0.0576	0.0058	0.763	0.0102
	0.31	0.206	0.0208	0.738	0.0122
	0.44	1.37	0.0997	0.727	0.0171
	0.50	1.90	0.112	0.776	0.0045
	0.65	5.96	0.200	0.791	0.0084
	0.71	11.9	0.349	0.796	0.0163
	0.82	18.9	0.421	0.830	0.0034
	1.0	26.7	0.512	0.835	0.0060

*RE, relative deviation error = $\sum_{i=1}^{n} \left| \frac{\eta_{\exp,i} - \eta_{cal,i}}{\eta_{\exp,i}} \right| \Big/ n$

Table 3.4 Magnitudes of the Carreau model parameters for steady simple shearing, obtained for LBG and TG samples, at 20°C

Samples	Conc.(wt%)	η_0 (Pa.s)	λ (s)	N	RE*
LBG	0.15	0.0069	0.0165	0.0469	0.0068
	0.25	0.0189	0.0311	0.0681	0.0123
	0.35	0.0790	0.0320	0.159	0.0231
	0.49	0.261	0.0484	0.193	0.0300
	0.68	0.924	0.0998	0.241	0.0425
	0.79	1.73	0.179	0.231	0.0496
	0.82	2.21	0.166	0.276	0.0629
	1.3	13.6	0.519	0.299	0.0861
TG	0.16	0.0226	0.0217	0.150	0.0124
	0.23	0.0753	0.0535	0.186	0.0215
	0.31	0.241	0.108	0.224	0.0335
	0.44	1.23	0.274	0.277	0.0754
	0.50	1.79	0.322	0.286	0.0557
	0.65	5.25	0.451	0.308	0.0494
	0.71	11.3	0.739	0.348	0.0957
	0.82	18.1	0.901	0.358	0.0636
	1.0	25.8	1.09	0.363	0.0640

*RE, relative deviation error = $\sum_{i=1}^{n} \left| \frac{\eta_{\exp,i} - \eta_{cal,i}}{\eta_{\exp,i}} \right| \Big/ n$

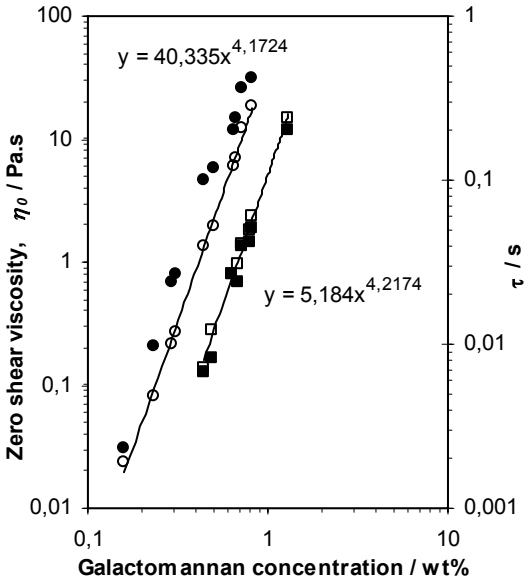

Figure 3.4 Concentration dependence of zero-shear rate apparent viscosity, η_0 (full symbols) and time constant, τ (open symbols) for galactomannan samples: LBG (□) and TG (O), at 20°C.

Although the absolute values of η_0 and the shear rates at which shear thinning begun differed for the two galactomannans, the pattern of their shear thinning was similar. For this concentrated regime, it was possible to obtain a viscosity (flow) master curve, after performing a concentration-dependent shift using the 0.82%LBG solution as the reference (Figure 3.5). It can be seen that this time-concentration superposition principle is valid for these galactomannans in this concentration range (within the accessible range of shear rates).

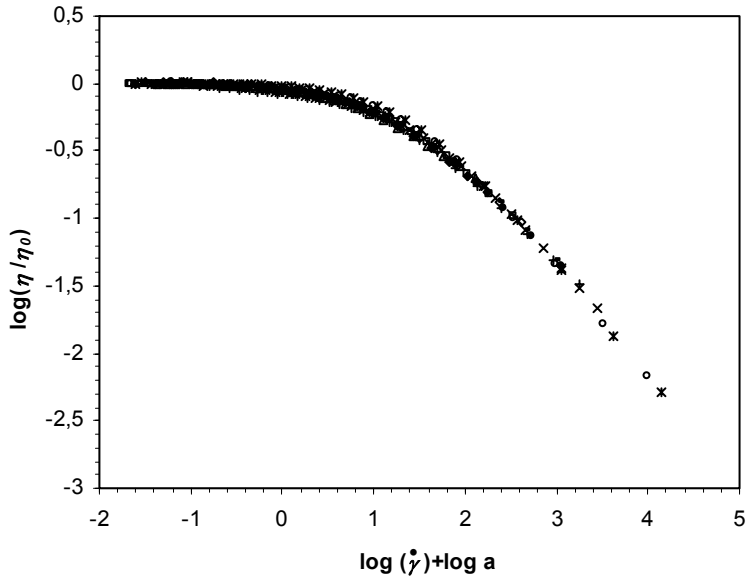

Figure 3.5 Shear rate/concentration superposition for galactomannan solutions, at 20°C. Master curve at the reference concentration of 0.82%LBG. Symbols: 0.49%LBG (Δ), 0.68%LBG (◇), 0.79%LBG (□), 0.82%LBG (●), 1.3%LBG (×), 0.31%TG (♦), 0.44%TG (+), 0.50%TG (–), 0.82%TG (O), and 1.0%TG (∗).

It was necessary to use both vertical and horizontal shifts to obtain the superposition of the different flow curves. The values of these shifts are presented in Figure 3.6. Both the vertical shift, which is given by the ratio of the zero-shear rate apparent viscosities of the solution under consideration and the reference solution, and the horizontal shift (which represents the concentration shift factor) increased with concentration, for each galactomannan; this is consistent with the increasing degree of entanglement of the systems.

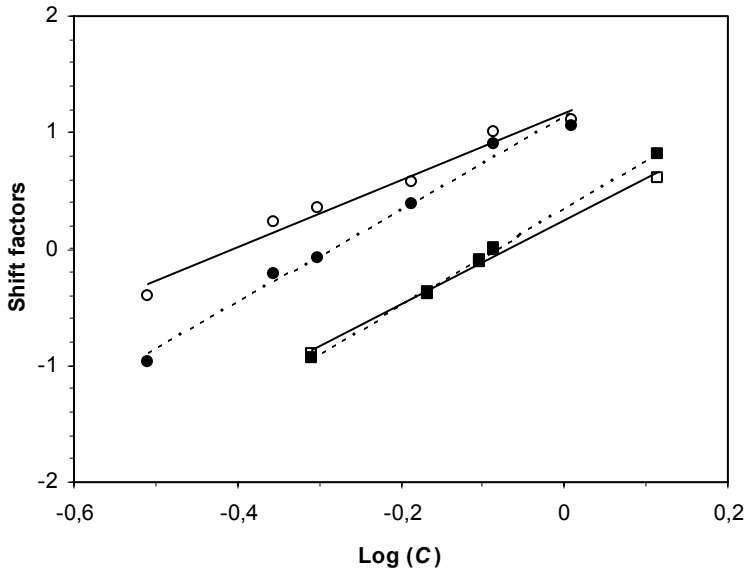

Figure 3.6 Shift factors (horizontal: open symbols; vertical: full symbols) used for the concentration superposition of the flow data obtained for galactomannan solutions at the reference concentration of 0.82%LBG, at 20°C: LBG (□) and TG (○).

The dependence of the specific viscosity at zero-shear rate, η_{sp0}, of galactomannan solutions on the coil overlap parameter, $C[\eta]$, is shown in Figure 3.7. It is interesting to note that, by this reduction process, a similar behaviour for the two polymers is put in evidence. This was expected since both are galactomannans with similar chemical structures and conformations.

If we assume, as described in literature for different polysaccharides (Cuvelier and Launay, 1986; Castelain et al., 1987), the existence of three different concentration regimes, dilute, semi-dilute and concentrated as mentioned in Chapter 1, it is possible, in principle, to define two critical concentrations, C^* and C^{**}, delimiting these regimes. From our data in Figure 3.7, it is not possible to determine C^* but we can make an estimation of C^{**}; this would be about $6.92/[\eta]$ giving $C^{**} \sim 0.59\%$ for LBG and $C^{**} \sim 0.41\%$ for TG.

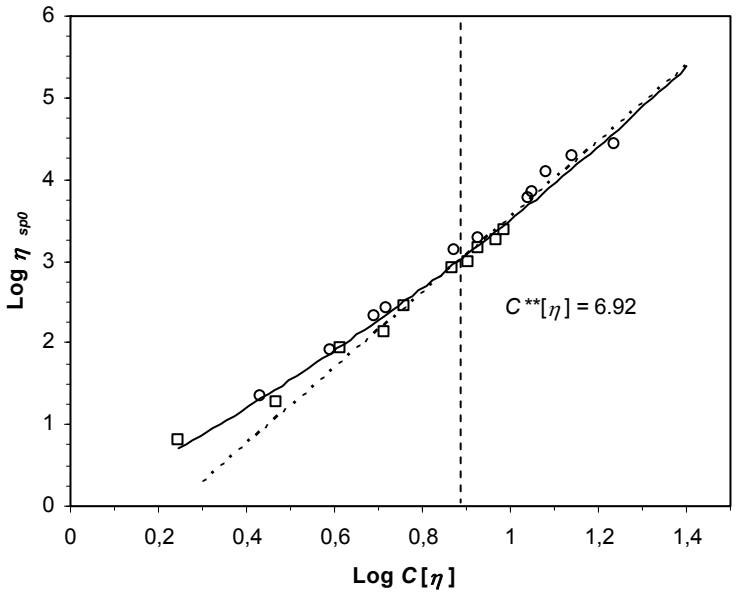

Figure 3.7 Specific viscosity at zero shear rate (η_{sp0}) as a function of $C[\eta]$ in a log-log plot for galactomannans solutions: LBG (□) and TG (O), measured at 20°C.

The concentrated domain ($C > C^{**}$) is characterized, as expected, by a power law dependence of viscosity on concentration. For typical polymers, the exponent is usually found to be in the range 3 – 4. In our case, a significant higher value (4.25) was found; perhaps this is related to a relatively high rigidity of LBG and TG backbones as compared to typical polymers. This value is in good agreement with previous results obtained for galactomannans (da Silva et al., 1992; Andrade et al., 1999). A value of ~ 3.4 was obtained by Morris and co-workers (1981) for several random coil polysaccharides. However, they observed a greater concentration dependence of viscosity for guar gum and locust bean gum (~ 4). Their interpretation of this behaviour was that, for both galactomannans in this concentration range, normal polymer entanglement was augmented by chain-chain association, as in solid state.

3.3.2.2 Viscoelastic properties

The frequency sweeps ("mechanical spectra") for both galactomannan solutions showed the typical shape for macromolecular solutions (Figure 3.8): at low frequencies (terminal zone), the loss modulus, G'', is higher than the storage one (G') whereas, at higher frequencies, G' is predominant. This kind of behaviour was found for several galactomannan solutions and other disordered random-coil polysaccharides (Oblonsek et al., 2003). Both curves tend asymptotically to the characteristic slopes of 1 and 2 for G'' and G', respectively. The first G' - G'' crossover, marking the low-frequency limit of the elastic plateau is visible for the higher concentrations and it typically moved to lower frequency value, when the concentration increased (Figure 3.8). This cross-over frequency decreased as concentration increased as a consequence of increasing relaxation times.

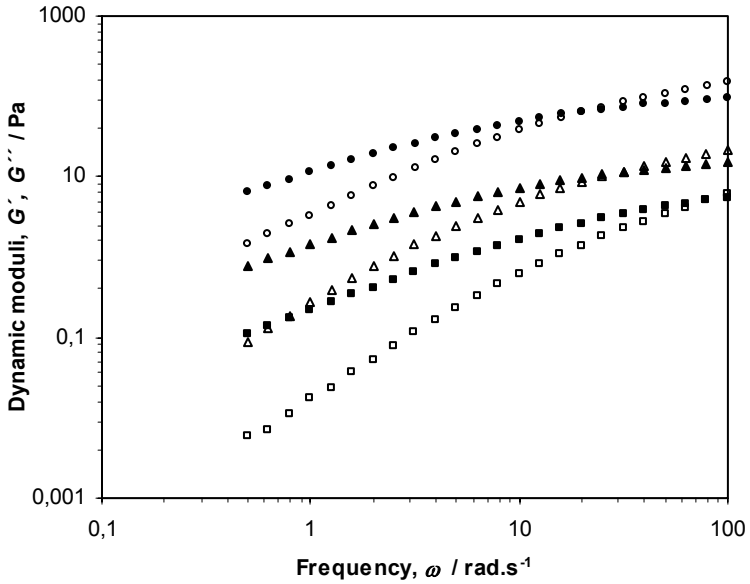

Figure 3.8 Mechanical spectra at 20°C of galactomannan solutions: 0.31%TG (□), 0.50%TG (Δ) and 1.3%LBG (O). G': open symbols and G'': full symbols.

As we did for flow curves, it was possible to superpose all curves (of LBG and TG at different concentrations) by shifting along the two axes and obtain master curves for G' and G''. Figure 3.9 shows the master curves from recorded data at 20°C obtained by this procedure with the 0.82%LBG solution as reference. The vertical and horizontal shift factors were the same for both G' and G'' curves. Horizontal shifts were equal to those in Figure 3.6 for flow while vertical shifts decreased with concentration for each galactomannan (not shown). From the master curves in Figure 3.9, we can see that the characteristic slopes would be only approached at frequencies < 0.3 rad.s^{-1}, in the case of the 0.82%LBG solution.

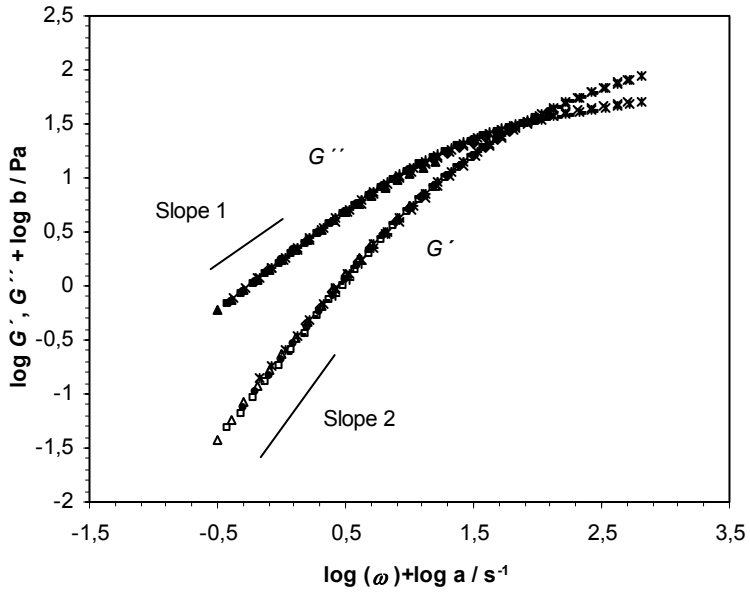

Figure 3.9 Frequency/concentration superposition of the dynamic moduli (G' and G'') of galactomannan solutions for a concentration reference of 0.82%LBG, measured at 20°C. Symbols: 0.49%LBG (Δ), 0.68%LBG (◇), 0.79%LBG (□), 0.82%LBG (O), 1.3%LBG (×), 0.44%TG (+), 0.50%TG (–), and 0.65%TG (∗).

3.3.2.3 Modelling the rheological behaviour under dynamic shear

Two mechanical models were used to fit the experimental viscoelastic data: the generalized Maxwell model with four elements (Eqs. 3.10 and 3.11) and the Friedrich–Braun model (Eqs. 3.12 and 3.13) (Friedrich et al., 1992). Both models have been already successfully used by other authors for describing the rheological behaviour of guar gum galactomannan (Oblonsek et al., 2003), and other polysaccharide systems (Zupancic et al., 2001; Manca et al., 2001).

In the generalized Maxwell model, the values of the overall G' and G'', at any frequency, are given by the sum of 4 contributions from 4 Maxwell elements in parallel:

$$G'(\omega) = \frac{G_1(\omega\theta_1)^2}{1+(\omega\theta_1)^2} + \frac{G_2(\omega\theta_2)^2}{1+(\omega\theta_2)^2} + \frac{G_3(\omega\theta_3)^2}{1+(\omega\theta_3)^2} + \frac{G_4(\omega\theta_4)^2}{1+(\omega\theta_4)^2} \qquad \text{(Eq. 3.10)}$$

$$G''(\omega) = \frac{G_1\omega\theta_1}{1+(\omega\theta_1)^2} + \frac{G_2\omega\theta_2}{1+(\omega\theta_2)^2} + \frac{G_3\omega\theta_3}{1+(\omega\theta_3)^2} + \frac{G_4\omega\theta_4}{1+(\omega\theta_4)^2} \qquad \text{(Eq. 3.11)}$$

where G_i is the elastic modulus, ω is the oscillatory frequency and θ_i is the terminal relaxation time. The dynamic response of a viscoelastic liquid over a range of frequencies can be modelled by choosing a range of Maxwell elements with appropriate values of G and θ chosen to cover the range used in the experiment for which G' and G'' values are available.

Alternatively, the Friedrich-Braun model, which is based on fractional derivatives, can be used to achieve a satisfactory data correlation. In oscillatory shear conditions, G' and G'' can be expressed as:

$$G'(\omega) = G_e + \Delta G \frac{(\lambda_F\omega)^e\left[\cos(\frac{\pi}{2}e) + (\lambda_F\omega)^c\cos(\frac{\pi}{2}(e-c))\right]}{1+2(\lambda_F\omega)^c\cos(\frac{\pi}{2}c) + (\lambda_F\omega)^{2c}} \qquad \text{(Eq. 3.12)}$$

$$G''(\omega) = \Delta G \frac{(\lambda_F \omega)^e \left[\sin(\frac{\pi}{2} e) + (\lambda_F \omega)^c \sin(\frac{\pi}{2}(e-c)) \right]}{1 + 2(\lambda_F \omega)^c \cos(\frac{\pi}{2} c) + (\lambda_F \omega)^{2c}} \qquad \text{(Eq. 3.13)}$$

where G_e is the equilibrium modulus when the frequency tends to zero, ΔG is a parameter that rules the magnitude of the viscoelastic response, λ_F is a characteristic time and the exponents c and e are derivation orders of the differential operators. The model describes liquid like response if $G_e = 0$. When $c = e = 1$ and $G_e = 0$, this model coincides with the Maxwell model and, then, λ_F becomes the relaxation time of the fluid.

In Figure 3.10, the results of the fitting of the two models to some experimental data for LBG and TG at 20°C are shown. The full and dotted lines represent the best fits to both models on recorded data at both temperature conditions. Similar high fitting quality of the dynamic moduli was found in the case of other samples (not shown).

As a result of the fitting with the Maxwell model, relaxation spectra of each galactomannan sample can be evaluated (Figure 3.11). At low concentrations, the elastic modulus, G_i, continuously decreased with increasing relaxation time θ_i. The increase of galactomannan concentrations leads to a gradual shifting of the relaxation spectrum to higher values. The typical profiles for polysaccharide solutions were obtained, with increasing contribution of higher relaxation times for increasing polymer concentration.

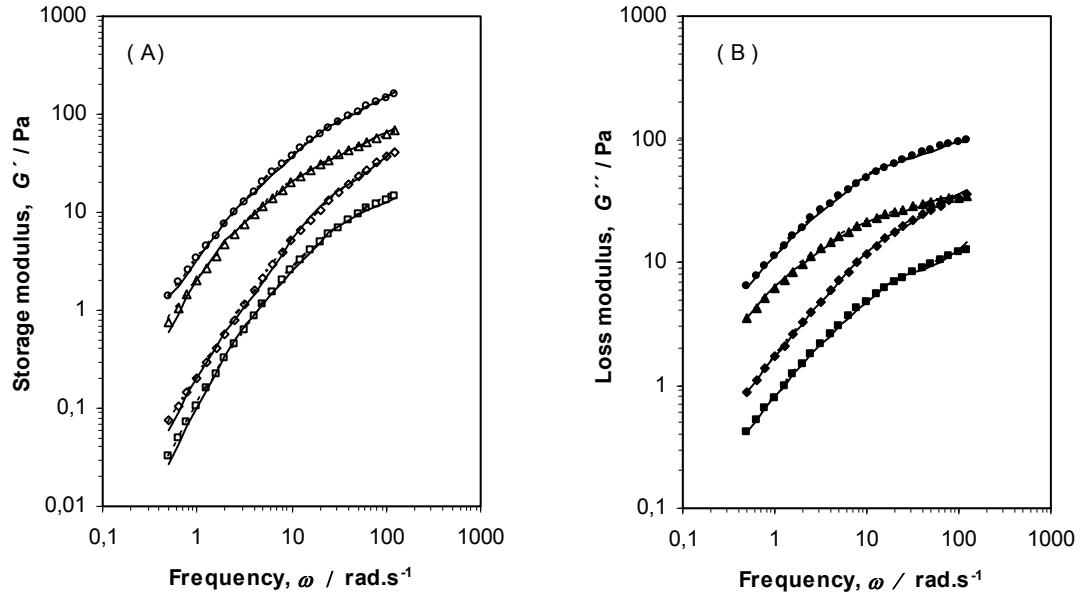

Figure 3.10 Storage modulus G' (A) and loss modulus G'' (B) vs oscillation frequency for galactomannans at different concentrations and 20°C: 0.82%LBG (◇), 1.3%LBG (○), 0.44%TG (□), and 0.71%TG (Δ). Continuous lines represent predictions of the generalized Maxwell model (Eqs. 3.10 and 3.11) and dotted lines those of the Friedrich–Braun model (Eqs. 3.12 and 3.13).

In the Friedrich–Braun model, G_e was set equal to zero, so reducing the number of adjustable parameters. These were determined by applying the fitting procedure simultaneously to $G'(\omega)$ and $G''(\omega)$. The parameters of the Friedrich-Braun model are presented in Figure 3.12. The variation of model parameters exhibited similar trends for both galactomannan samples, ΔG and λ_F gradually increasing with concentration.

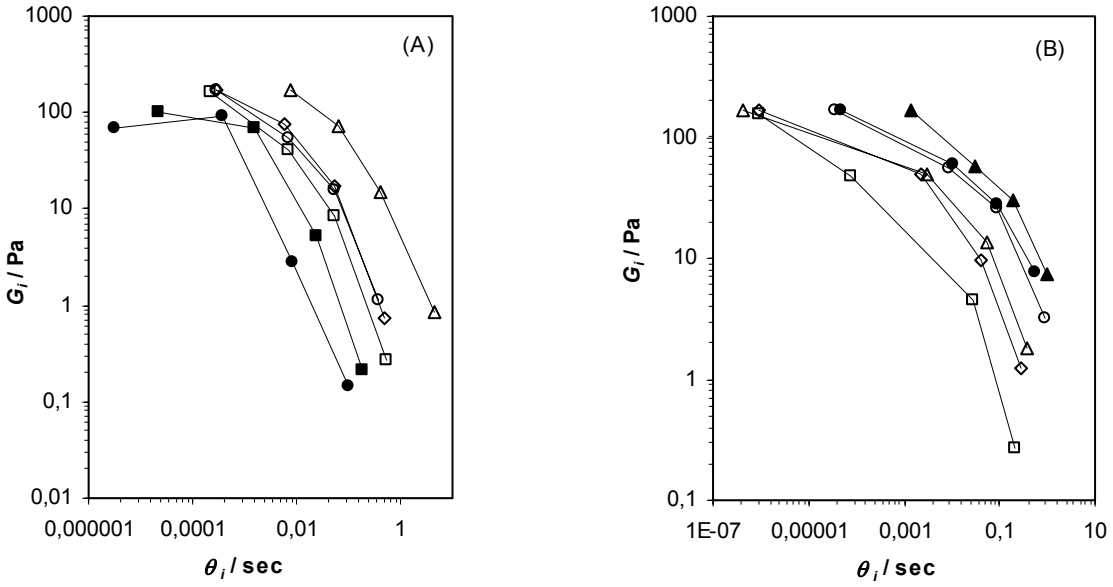

Figure 3.11 The relaxation spectra of galactomannan systems, at 20°C. (A) LBG: 0.35% (●), 0.49% (■), 0.68% (□), 0.79% (O), 0.82% (◇), and 1.3% (Δ); (B) TG: 0.31%(□), 0.44% (◇), 0.50%TG (Δ), 0.65% (O), 0.71%TG (●), and 0.82%LBG (▲).

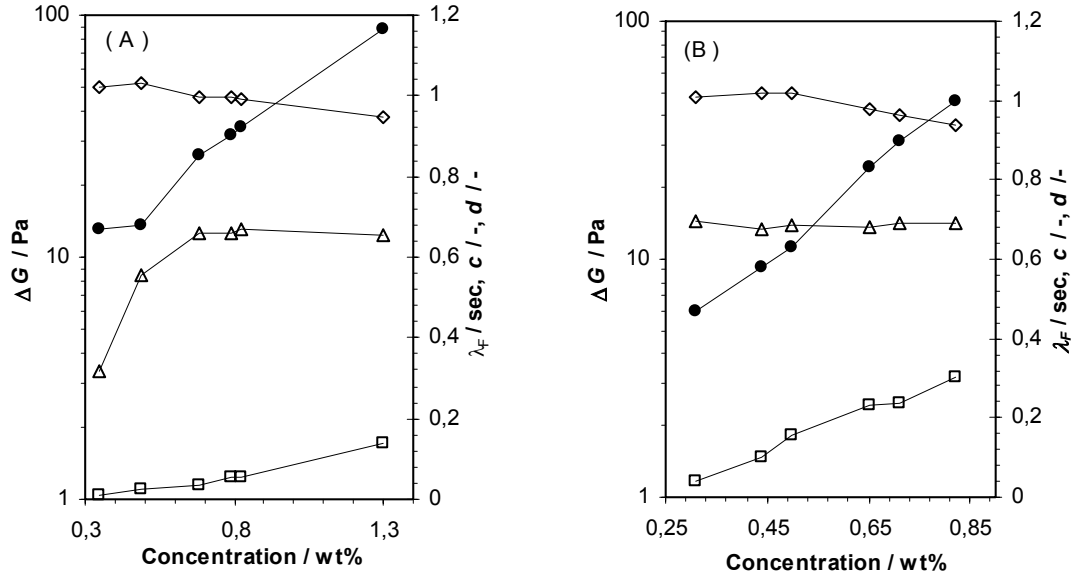

Figure 3.12 Parameters of Friedrich-Braun models (Eqs. 3.12 and 3.13) for galactomannan systems, at 20°C. (A) LBG and (B) TG: ΔG (●), λ_F (□), c (Δ), and e (◇).

3.3.2.4 Correlation between steady shear and dynamic rheological properties

The magnitude of the apparent viscosity in steady shear (η) and the magnitude of the complex viscosity in oscillatory shear (η^*) were compared at equal values of shear rate and frequency, as represented for LBG in Figure 3.13. For other LBG and TG solutions, similar results were obtained. As can be seen, these solutions followed satisfactorily the correlation of Cox-Merz (1958) which proposes that, for flexible chain polymers, the steady shear viscosity computed at $\dot{\gamma}$ coincides with the value of the modulus of the complex viscosity computed at $\omega = \dot{\gamma}$:

$$\eta(\dot{\gamma}) = \left|\eta^*(\omega)\right| \quad where \quad \left|\eta^*\right| = \sqrt{\left(\eta'^2 + \eta''^2\right)} \qquad \text{(Eq. 3.14)}$$

In fact, $\left|\eta^*\right|(\omega)$ and $\eta(\dot{\gamma})$ almost superimposed, leading to the conclusion that both galactomannans behaved like ordinary polysaccharides. Similar results were obtained by da Silva and co-workers (1993), Ross-Murphy (1995) and Andrade and co-workers (1999) with several galactomannan dispersions.

A common feature observed in these results was that the dynamic viscosity (η') approached the zero shear rate viscosity at low frequency and shear rate. With increasing frequency and shear rate, apparent viscosity in steady shear and dynamic viscosity began to diverge gradually, with the expected more rapid decrease of dynamic viscosity with frequency than apparent viscosity with shear rate; this can be attributed to the very different molecular motions involved in the dynamic and steady shears at high frequency and shear rate (Ferry, 1980). With increasing concentration of galactomannan, the dynamic viscosity becomes more divergent as shown in Figure 3.13.

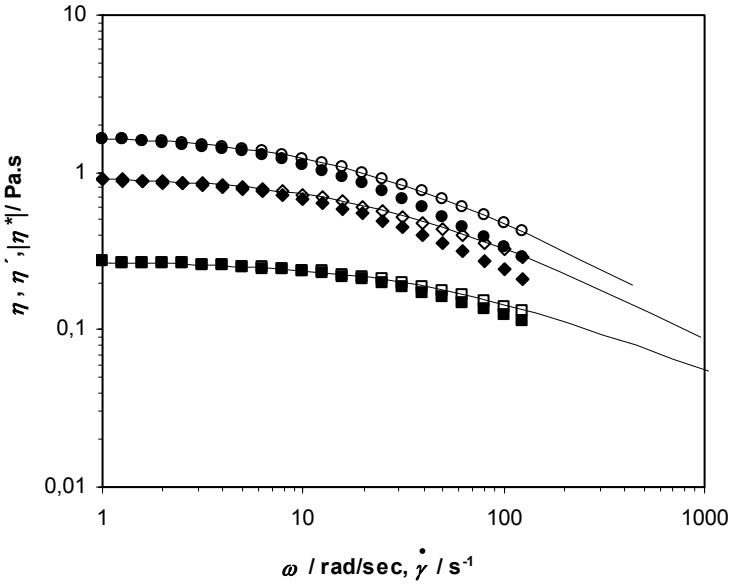

Figure 3.13 Cox-Merz plot for LBG solutions at different concentrations, at 20°C: 0.49% (O), 0.68% (◇), 0.79% (□). η (continuous line), η' (full symbols) and $|\eta^*|$ (open symbols).

3.4 Conclusions

The results obtained showed that both galactomannans exhibited quite similar rheological properties, in the range of concentrations and shear rates/frequencies studied. The dependence of the specific viscosity at zero shear rate, η_{sp0}, on the coil overlap parameter, $C[\eta]$, put in evidence a similar behaviour for the two polysaccharides; results supported the random coil type behaviour for both galactomannans. Flow curves exhibited shear-thinning behaviour, with a Newtonian region in the low shear rate range. The similar concentrations, LBG solutions were less viscous than TG solutions, which reflected the differences in the intrinsic viscosities of the samples.

Experimental data were correlated with the Cross and Carreau models. Both models described the apparent viscosity shear rate data well. In general, the Cross model provided a slightly better fit. The dependence of the Cross parameters η_0 and τ on galactomannan concentration is described by similar scaling laws for LBG and TG systems. Two mechanical models were used for fitting the experimental data in oscillatory shear (mechanical spectra): the generalized Maxwell model with four elements and the Friedrich-Braun model. Both models correlate the experimental data very well. The correlation between dynamic and steady shear properties (Cox-Merz rule) was satisfactory for the two galactomannans.

Also, time-concentration superposition holds for their solutions, allowing master curves to be found for both the viscous and the linear viscoelastic response in shear flow. The similar profile observed probably reflects the existence of non-specific physical entanglements in TG and LBG solutions.

Chapter 4

Rheology and microstructure of β-lactoglobulin / galactomannan aqueous mixtures

4.1 Introduction

Protein-polysaccharide mixed systems have been extensively studied in the last decades, because the interactions between the two types of biopolymers are of great importance to understand and develop novel food products (Tolstoguzov, 1991). Presently, it is generally accepted that the phase state of such systems determines to a large extent their functional properties (Turgeon et al., 2003). When the possibility of intermolecular complexes formation is excluded, the most common behaviour is thermodynamic incompatibility, inducing phase separation, except in dilute solutions (Grinberg et al., 1997; Doublier et al., 2000). Globular protein / neutral polysaccharide aqueous mixed systems generally undergo segregation and phase separation of the biopolymers above a certain concentration threshold (Syrbe et al., 1995; Wang et al., 2001). The rheological behaviour of such systems depends on the phase state and on the rheology and microstructure of the phases. However, few studies dealt with the rheology of β-lactoglobulin / neutral polysaccharide mixtures in the liquid state (Syrbe et al., 1995).

In this chapter, the rheological and microstructural properties of β-lactoglobulin aqueous solutions, in presence of galactomannan (locust bean gum or tara gum), were investigated at 20°C and at two pH values: 7.0, where the protein bears a net negative charge, and 4.6, near the isoelectric point the protein.

In a first series of experiments, an attempt has been made to establish phase diagrams for the mixed systems, at each pH, spanning a wide range of concentrations and mixing ratios.

Experimental constraints (high viscosity of galactomannan solutions, moderate solubility, especially at pH 4.6, of the protein), restricted the range of accessible concentrations / mixing

ratios of the two biopolymers. For the limited number of solutions where some incipient phase separation could be detected visually, it was found actually the two phases to be difficult to separate by centrifugation and to characterise. Protein and polysaccharide determination indicated that, after centrifugation, the upper phase was very slightly enriched in LBG and very slightly less concentrated in protein, whereas the lower one was moderately enriched in protein; the results were actually questionable and the idea to establish phase diagrams was discarded.

Instead, a fixed β-lactoglobulin concentration was chosen and a study of the evolution of the microstructure and of the rheology of the system when different concentrations of galactomannan (locust bean gum or tara gum) were added, was done. The objective was to investigate possible correlations between microstructure and rheological properties of the mixed systems.

In section 4.3.1, the microstructures of the pure β-lactoglobulin and mixed β-lactoglobulin / galactomannan systems were studied at pH 4.6 and pH 7.0. In section 4.3.2, the flow and viscoelastic properties of the same systems were described and correlated with the microstructure. Finally, in section 4.4, the main conclusions were described.

4.2 Materials and methods

4.2.1 Materials

Studies in this chapter were conducted using the β-lactoglobulin (β-Lg) sample characterized in section 2.2.2, and the galactomannan samples (locust bean gum, LBG, and purified tara gum, TG) characterized in section 3.2.2.

4.2.2 Preparation of sample solutions

β-lactoglobulin stock solutions (23 wt%) were prepared as described in section 2.2.4.1. Galactomannan stock solutions (1.3 wt%) were prepared as described in section 3.2.3.1.

Stock solutions of β-lactoglobulin and galactomannan were mixed at different ratios, keeping a constant 6.5%β-lactoglobulin concentration and varying the galactomannan concentration: 0 to 0.82 wt% for LBG and 0 to 0.71 wt% for TG. The solutions were mixed for 18 h, under moderate stirring, at room temperature and the pH (4.6 or 7.0) of the mixtures was rechecked.

It is to be noted here that the 6.5%β-lactoglobulin concentration was chosen taking into account the subsequent experimental study on heat-set gelation of mixed systems (see Chapter 5): as described in section 2.3.3, this was the lowest concentration for which a β-lactoglobulin gel with no visible syneresis formed at both pH values, in the conditions of the experiments. Also, for higher concentrations of the protein and due to the experimental constraints referred in the introduction (section 4.1), a narrower range of concentrations/mixing ratios would be accessible.

4.2.3 Confocal Laser Scanning Microscopy (CLSM)

4.2.3.1 Equipment

The samples were examined by using a confocal laser scanning microscope Leica TCS SP2 AOBS (Leica Ltd, Heidelberg, Germany, see in Figure 4.1), with an oil immersion ×20 objective.

4.2.3.2 Principle

Confocal Laser Scanning Microscopy was used in the fluorescence mode, based on the property of some atoms and molecules to absorb light at a particular wavelength and to subsequently emit light of longer wavelength after a brief interval, termed the fluorescence lifetime.

A beam of gas laser light is focused into a small point at the focal plane of the specimen. A computer controlled scanning mirror can move or scan this beam in the x-y direction at the focal plane. The florescent emission created by the point as it scans in the focal plane is detected by a photon multiplier tube. This detection input is reconstructed by computer hardware into an image (Dürrenberger, Handschin, Conde-Petit, and Escher, 2001). This method acts as an optical scanner, being able to focus on only one plane, located at a well defined depth in the sample, which means that the emission of fluorescence of the rest of the sample does not interfere with the structural information coming from the focal plane. Information can be collected from different focal planes by raising or lowering the microscope stage. The computer can generate a three-dimensional picture of a specimen by assembling a stack of these two-dimensional images from successive focal planes.

As laser scanning confocal microscopy depends on fluorescence, a sample usually needs to be treated with fluorescent dyes to make things visible. However, the actual dye concentration can be very low so that the disturbance of the systems is kept to a minimum.

4.2.3.3 Experiment

β-lactoglobulin was stained with the fluorescent dye Rhodamine Isothiocyanate (RITC) through covalent linking of the RITC groups to the amino ($-NH_2$) groups of the protein molecules. Mixtures with galactomannan were prepared as described above (section 4.2.2), placed between a slide and a concave slip and hermetically sealed to prevent evaporation. RITC was excited at 543 nm with a HeNe laser and the emission fluorescence was recorded between 548 and 631 nm.

Figure 4.1 Leica TCS SP2 AOBS laser scanning confocal microscope (CLSM).

4.2.4 Rheological measurements

All rheological measurements were performed at 20°C using a controlled stress rheometer AR2000 (TA Instruments), described in section 4.2.6.1, fitted with a cone-and-plate geometry (stainless steel cone with 2° angle, 40 mm diameter, 54 μm truncation). The following sequence of measurements was done:

- Frequency sweeps were performed for a frequency range of 0.1 - 100 rad.s^{-1}. The values used for the strain amplitude depended on the concentration / pH of the systems. Values of 0.001–0.1, for samples at pH 7.0, and 0.1, for samples at pH 4.6, were used which was within the linear viscoelastic region, determined by preliminary experiments.
- Flow curves were recorded by using a steady state flow ramp in the 0.01 to 1000 s^{-1} range of shear rate. The shear rate was recorded point by point with consecutive 3 min steps of constant shear rate. This time allowed obtaining constant shear rates for each point. The viscosity could then be determined for each point and the flow curve could be built.

Some sets of the experiment were duplicated in order to verify the reproducibility of the results.

4.3 Results and discussion

4.3.1 Microstructure of mixtures

Micrographs of the systems were obtained using CLSM, in the fluorescence mode (×20 objective) as described in section 4.2.3.3. Clear areas in the micrographs correspond to the fluorescence of the label (RITC) bound to the protein while the dark areas correspond to zones devoid of protein, thus containing mostly galactomannans.

At both pH values (7.0 and 4.6), the results show that 6.5 wt% β-lactoglobulin solutions looked homogeneous at the scale of CLSM observations (Figures 4.2A and 4.3A) while the mixed systems were two-phase. It is to be said here that by nature, phase separation in protein-polysaccharide systems is a kinetic process that arises from local fluctuations of the biopolymer concentration within the entire volume of the mixture. So, the microstructure of the systems evolutes with time and, depending on the time-scale of phase separation, eventually two layers will be formed. We followed the evolution of the microstructure of two systems - 6.5%β-Lg+0.31%LBG and 6.5%β-Lg+0.72%LBG - in a first experiment, for at least five hours (results not shown). No striking modifications could be seen in the micrographs. Additionally, for the same mixtures, no significant changes in the viscoelastic moduli, G' and G'', were detected during the same time. Then, for all the systems described below, the micrographs were obtained within 1-4 hours after preparation of the samples.

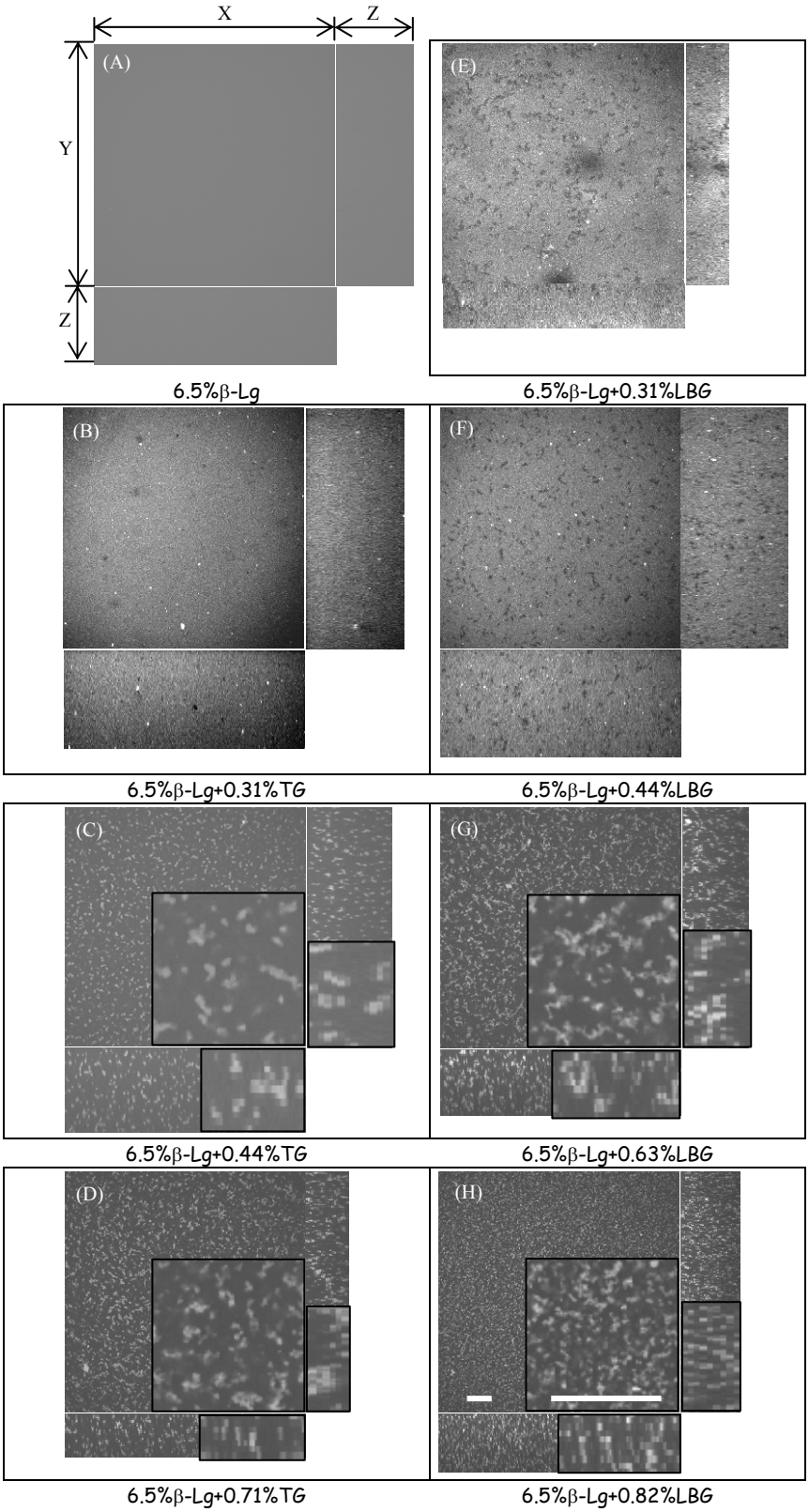

Figure 4.2 CLSM micrographs for samples at 20°C and pH 7.0. The images were obtained in the planes XY, XZ and YZ of the sample, at ×20 magnification. Scale bar = 80 μm.

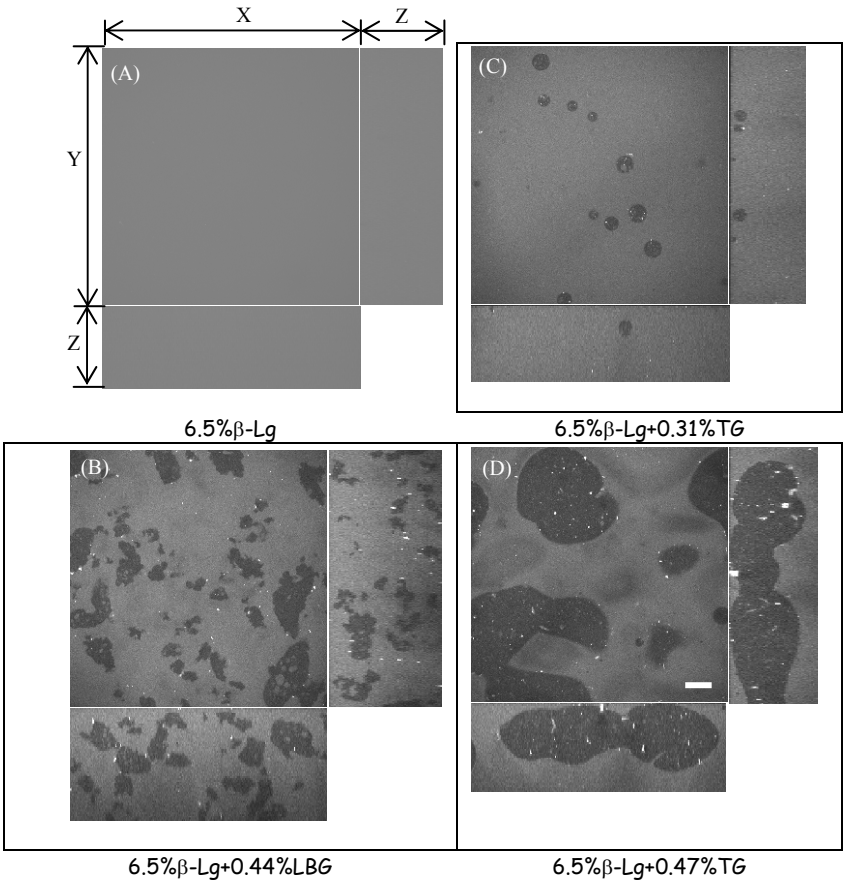

Figure 4.3 CLSM micrographs for mixture solutions at 20°C and pH 4.6. For each case, are shown images obtained in the planes XY, XZ and YZ of the sample, at ×20 magnification. Scale bar = 80 μm.

Clearly, the concentration of the galactomannans in the mixtures and the pH affected the microstructure of the systems. At pH 4.6, mixtures with 0.44%LBG and 0.31%TG showed a β-lactoglobulin continuous phase containing galactomannan inclusions, some amount of the continuous phase seems to be entrapped inside the inclusions (Figures 4.3B and C). Such a structure was already reported in gelatin / locust bean gum (Alves et al., 2001) and dextran / locust bean gum (Garnier, Schorsch, and Doublier, 1995) systems. The inclusions were round shaped in the case of TG whereas they were irregular for LBG; these different shapes must result from differences in the interfacial tensions of the systems. Another possibility is that in

the concentrated LBG domain there are intermolecular interactions that create "gel" structures; then, the domain does not have the mobility to rearrange into a sphere even though this is the most stable configuration as a result of interfacial energy considerations.

Increasing the concentration of the galactomannan led to significant changes in the microstructure: the system 6.5%β-Lg+0.47%TG seems to be a bi-continuous one, with large inclusions of TG enriched phase extended through the β-lactoglobulin enriched phase (Figure 4.3D).

At pH 7.0, a rather different picture was observed. In Figure 4.2B, E and F, systems 6.5%β-Lg+0.31%TG, 6.5%β-Lg+0.31%LBG, and 6.5%β-Lg+0.44%LBG showed a β-lactoglobulin continuous phase, like at pH 4.6; but, in this case, smaller inclusions of the galactomannan, apparently devoid of continuous phase entrapped, were observed.

In addition, increasing the galactomannan concentration led to substantial change of the microstructure. For concentrations of TG ≥ 0.44 wt% or LBG ≥ 0.63 wt%, the systems evolved from a structure where a continuous matrix of β-lactoglobulin contained some inclusions of the galactomannan, to a structure where, apparently, the galactomannan phase constitutes the continuous phase containing dispersed aggregates of the protein phase (Figures 4.2C-D and G-H). The size of the aggregates seems to decrease with increasing galactomannan content in the mixed system.

Depletion interactions theories have been used to analyse the phase behaviour of colloid-biopolymer mixtures (Tuinier et al., 2003) and, in particular, of proteins and polysaccharides

(de Kruif et al., 2001; Wang et al., 2001). The mechanism behind phase separation of β-lactoglobulin and pullulan was explained in terms of the depletion interactions in a suspension of small spheres (proteins) in a semi-dilute solution of coils (polysaccharides) forming an entangled network (Wang et al., 2001).Several other authors have recently studied phase separation in milk protein (colloidal casein) and polysaccharide mixtures (see for instance Bourriot et al., 1999; Schorsch et al., 1999; Tuinier et al., 1999; de Bont et al., 2002, 2004).

In general, results obtained support the idea that depletion interactions are the driving force for phase separation in milk protein-polysaccharide mixtures. In some of these studies, where galactomannans were used, emulsion-like microstructures have been observed with milk proteins concentrated in spherical droplets (Bourriot et al., 1999; Schorsch et al., 1999), while in others (where amylopectin was used) CLSM revealed the appearance of aggregate structures when phase separation occurred (de Bont et al., 2002, 2004). The observed microstructural difference was ascribed to a low value of the biopolymer-colloid size ratio for milk protein-amylopectin systems.

In our case, aggregate structures were also observed at pH 7.0, for mixed systems with concentrations of LBG $\geq$ 0.63wt% or TG $\geq$ 0.44wt%. Also, like in milk protein / amylopectin systems, the sizes of the protein-rich areas appear to depend on the composition of the mixture and decrease with increasing polysaccharide concentration. A scan performed into the z-direction of the sample did not reveal interconnection of the aggregated protein areas for the concentrations studied.

However, in our case, contrarily to the milk protein / amylopectin mixtures, a low biopolymer-colloid size ratio should not be expected since β-lactoglobulin is a small protein and the galactomannans used are long polysaccharide chains. The theories were developed for hard colloidal spheres and non-adsorbing biopolymers (Gast, Russel, and Hall, 1986; Lekkerkerker, Poon, Pusey, Stroobants, and Warren, 1992). Our systems are not expected to behave like such an ideal system. Galactomannans are polydisperse and the protein is negatively charged at pH 7.0. These factors may shift to higher values the size ratio above which the transitions are predicted to occur.

4.3.2 Rheological behaviour

4.3.2.1 Flow behaviour

Figure 4.4 displays some flow curves obtained at 20ºC and at both pHs for water and aqueous solutions of the biopolymers alone: 6.5%β-lactoglobulin and, as an example, 0.31%TG and 0.44%LBG.

The flow curve corresponding to water clearly showed that there were some experimental limitations, especially for the rheological characterization of solutions of low viscosity. A Newtonian behaviour was expected for water. Instead, we saw an initial wavering regime of the viscosity that could be related to limitations in torque sensitivity of the rheometer. Then a second regime was defined, for shear rates between ~100 and 500 s^{-1}, where the expected Newtonian plateau was measured; finally, a third zone where the viscosity rose with the shear rate, which might be related to the apparatus inertia.

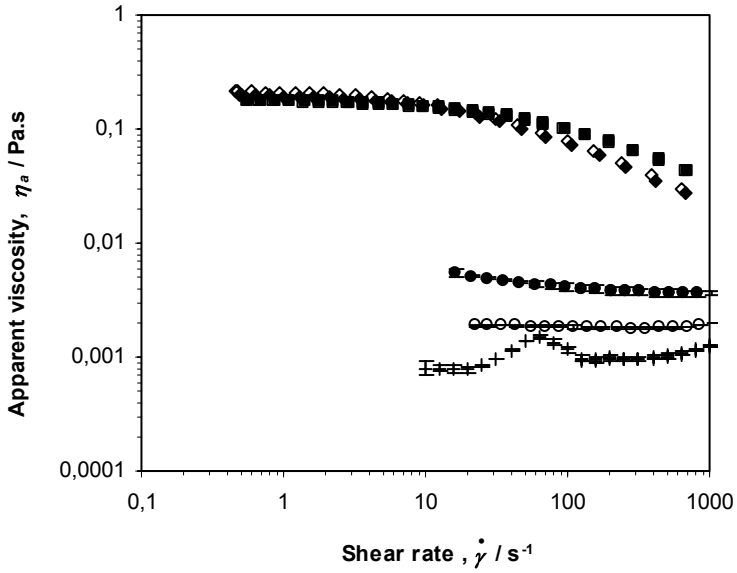

Figure 4.4 Flow curves for biopolymers alone, at 20°C, at pH 4.6 (open symbols) and pH 7.0 (full symbols): 0.31%TG (◇), 0.44%LBG (□), 6.5%β-Lg (O), and water (+).

Alternatively, data associated with more viscous samples, as was the case for galactomannan samples, appeared free of experimental artefacts.

It is clearly seen in the figure that the behaviour of the protein depended on pH while, apparently, this was not the case for the galactomannans. At both pHs, and taking into account the experimental limitations referred above, the β-lactoglobulin solution exhibited a Newtonian behaviour. However, the viscosity was higher at pH 7.0 (see Table 4.3). At this pH, the protein bears a net negative charge while at pH 4.6, near its isoelectric point, it has almost a zero net charge; protein self-association is then enhanced. As previous observed (see in section 2.3.2), turbidity differences were visible in β-lactoglobulin solutions at these pHs. A high absorbance (at 420 mm) was measured at pH 4.6 which indicates the presence of some kind of aggregates (less solubility of β-lactoglobulin) at this pH. This difference in the aggregation state of the

protein must be responsible for the observed difference in viscosity of its solutions of similar concentration and different pH.

For the galactomannans, as expected for neutral polysaccharides, the change of pH did not affect the flow behaviour: for all concentrations studied, a shear thinning behaviour was observed.

Mixed systems behaved differently of the individual components: in the shear rate range studied, the viscosity of these systems laid between those of the protein and of the galactomannan alone, at the same concentration as in the mixture. This is illustrated in Figure 4.5 for two β-lactoglobulin / TG mixtures, at pH 7.0, taken as an example. Results of the experiments carried out at pH 4.6, for similar concentrations of the biopolymers, were qualitatively similar but the magnitude of the apparent viscosity was lower than at pH 7.0 (see Figure 4.7).

As depicted in Figure 4.5, for lower concentrations of the galactomannan in mixture (0.31%TG), the flow behaviour approached that of the pure β-lactoglobulin solution: a Newtonian behaviour was observed though the viscosity (η_a = 0.0224 Pa.s) was higher than for the pure protein solution of the same concentration as in the mixture. The same behaviour was also found for mixed β-lactoglobulin / LBG systems; but, in this case, the flow behaviour of the mixtures approached that of the pure β-lactoglobulin for LBG concentrations ≤ 0.44 wt% (results not shown).

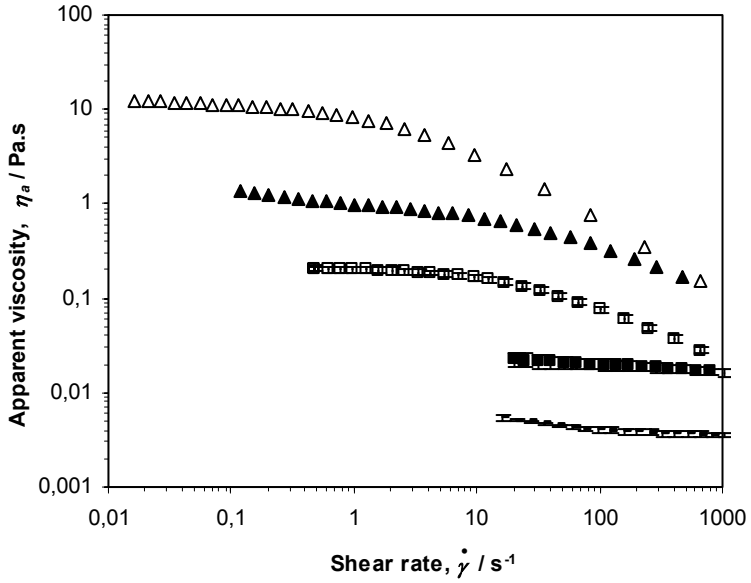

Figure 4.5 Flow curves for pure β-Lg, pure TG and β-Lg / TG mixtures at 20°C and pH 7.0.: 6.5%β-Lg (–), 6.5%β-Lg+0.31%TG (■), 6.5%β-Lg+0.71%TG (▲), 0.31%TG (□), 0.71%TG (Δ).

Confocal microscopy observations have shown that these mixed systems were two-phase (see Figure 4.2B, E and F) with a β-lactoglobulin enriched continuous phase; it was, then, expected that the behaviour was dominated by the rheology of the continuous phase. The main effect of the galactomannan was an increase of the apparent viscosity of the system, at least in the shear rate range their low viscosities allowed to explore. This increase in viscosity can be ascribed to a concentration of the protein in the continuous phase due to phase separation. However, the apparent Newtonian behaviour is not intuitive because the volume fraction of the polysaccharide will be significant for these mixtures.

In contrast, at increased galactomannan concentration, the flow behaviour was closer to that of the pure galactomannan solution; but, in this case, an apparent yield stress appeared at low shear rates (see also Figure 4.7).

Apparent yield stresses at low shear rates were also observed for guar gum solutions with added rice starch acting as filler (Rayment, Ross-Murphy, and Ellis, 1995) and for BSA / hydroxyethylcellulose mixed systems (Castelain, Lefebvre, and Doublier, 1986). In this case, the yield stress was seen as a consequence of the flocculation of the BSA enriched disperse phase, at low shear rates.

In our case, confocal microscopy revealed that these systems were two-phase with a galactomannan enriched continuous phase (see Figure 4.2C, D, G and H) and a protein enriched disperse phase, which may explain the observed flow behaviour.

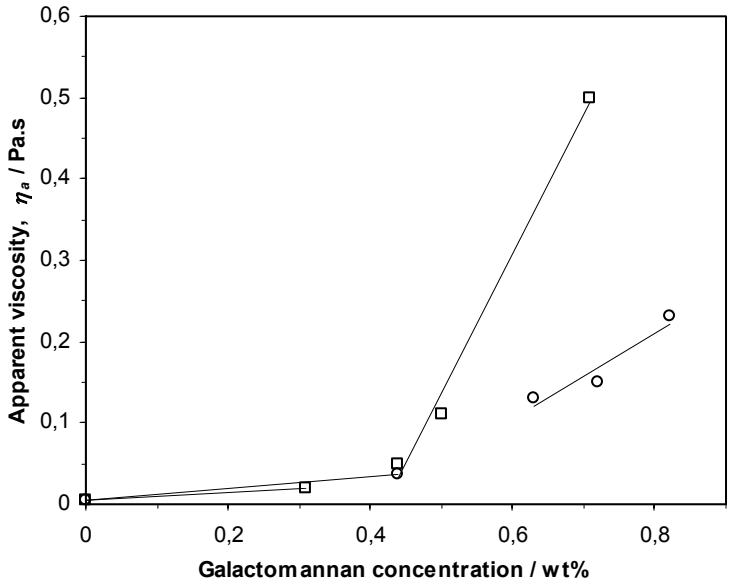

Figure 4.6 Apparent viscosity, at 27 s^{-1}, of the mixtures as a function of galactomannan concentration at 20°C and pH 7.0. Symbols: LBG (O) and TG (□).

In Figure 4.6, the viscosity of the mixtures at shear rate = 27 s^{-1} is plotted against the galactomannan concentration: two regions can be clearly seen, one with a small slope, for the lower galactomannan concentrations (corresponding to the mixtures with a β-lactoglobulin enriched continuous phase), and another with high slope, for the higher galactomannan

concentrations (corresponding to the mixtures with a galactomannan enriched continuous phase).

The flow curves for the mixed systems with higher galactomannan concentrations, at pH 7.0, were tentatively fitted by the modified Cross model (Eq. 4.1):

$$\eta_a = \eta_\infty + \left(\frac{\sigma_a}{\dot{\gamma}} \right) + \frac{(\eta_p - \eta_\infty)}{\left[1 + (\tau \dot{\gamma})^m \right]} \qquad \text{(Eq. 4.1)}$$

Where η_a is the apparent viscosity of the system measured at the shear rate ($\dot{\gamma}$), η_p the plateau Newtonian viscosity at intermediate shear rates, η_∞ the limiting Newtonian viscosity at high shear rates or infinite shear rate viscosity ($\eta_\infty << \eta_0$ or η_p; we took $\eta_\infty = 0$), τ the characteristic time related to the longest relaxation time of the system, m a dimensionless exponent and σ_a the apparent yield stress. The fitting results show that the modified Cross model described the apparent viscosity shear rate reasonably well, especially when there were enough experimental data in the shear thinning region, at higher shear rates (Figure 4.7 and Table 4.1).

In all cases, values of the parameters, as compared to those corresponding to galactomannan solutions of the same concentration as in the mixture (determined as referred in section.3.3.2.1) were different: η_0 (when compared with η_p) and m were decreased while τ seems to be of the same order of magnitude for LBG mixtures and to decreased for TG mixtures (Tables 4.1 and 4.2). Also, values of m were roughly constant for mixtures of β-lactoglobulin with each galactomannan: ~0.4 for LBG and ~0.5 for TG. The higher value for TG mixtures might

indicate a slightly higher elasticity for these mixtures. Values of σ_a were always low but seemed to increase with galactomannan concentration in the mixtures.

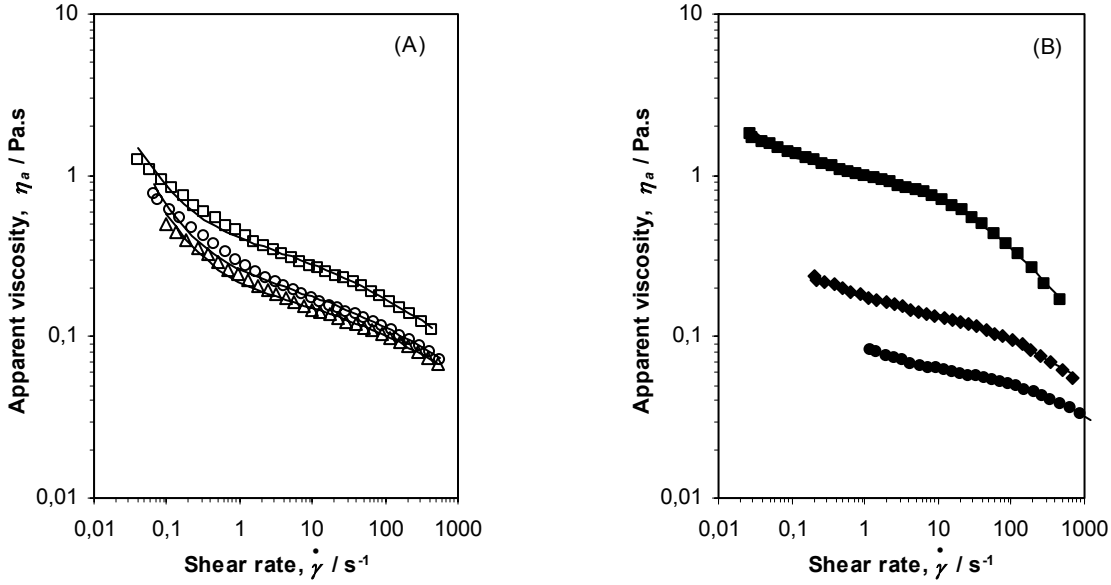

Figure 4.7 Flow curves for mixed solutions with LBG (A) and TG (B), at 20°C and pH 7.0. Symbols: 6.5%β-Lg+0.63%LBG (Δ), 6.5%β-Lg+0.72%LBG (O), 6.5%β-Lg+0.82%LBG (□),6.5%β-Lg+0.44%TG (●), 6.5%β-Lg+0.50%TG (♦), and 6.5%β-Lg+0.71%TG (■); lines represent predictions of the modified Cross model.

A noticeable decrease of viscosity was also observed for the two-phase gelatin-locust bean gum system (Alves et al., 2001) and for the casein guar gum system (Lefebvre, Doublier, and Antonov, 1996), when the galactomannan enriched phase was the continuous one. In the latter case, the decrease in viscosity was attributed to a possible elongation of the droplets of the disperse phase due to shear deformation.

Table 4.1 Magnitudes of the modified Cross model parameters for steady simple shearing, obtained for mixtures at 20°C and pH 7.0

Samples	σ_a	η_p (Pa.s)	τ (s)	m	RE*
6.5%β-Lg+0.63%LBG	0.0371	0.221	0.0164	0.374	0.0340
6.5%β-Lg+0.72%LBG	0.0404	0.279	0.0273	0.375	0.0450
6.5%β-Lg+0.82%LBG	0.0423	0.487	0.0501	0.383	0.0398
6.5%β-Lg+0.44%TG	0.0260	0.0657	0.0011	0.530	0.0047
6.5%β-Lg+0.50%TG	0.0142	0.182	0.0087	0.425	0.0140
6.5%β-Lg+0.71%TG	0.0235	1.13	0.0393	0.592	0.0233

*RE : relative deviation error = $\sum_{i=1}^{n} \left| \frac{\eta_{\exp,i} - \eta_{cal,i}}{\eta_{\exp,i}} \right| \Big/ n$

Table 4.2 Magnitudes of the Cross model parameters for steady simple shearing, obtained for LBG and TG samples at 20°C with $[\eta]$ values 11.76 and 16.94 dl.g^{-1}, respectively

Samples	Conc.(wt%)	η_0 (Pa.s)	τ (s)	m	RE*
LBG	0.44	0.182	0.0075	0.716	0.0065
	0.63	0.805	0.0269	0.734	0.0063
	0.72	1.41	0.0397	0.738	0.0131
	0.82	2.34	0.0520	0.756	0.0092
TG	0.31	0.206	0.0208	0.738	0.0122
	0.44	1.37	0.0997	0.727	0.0171
	0.50	1.90	0.112	0.776	0.0045
	0.71	11.9	0.350	0.796	0.0163

*RE : relative deviation error = $\sum_{i=1}^{n} \left| \frac{\eta_{\exp,i} - \eta_{cal,i}}{\eta_{\exp,i}} \right| \Big/ n$

For mixtures with low galactomannan concentration, at pH 7.0, a Newtonian behaviour, in the experimental shear rate range available, was observed. Viscosity values are presented in Table 4.3. At pH 4.6 and due to experimental constraints, the range of concentrations was more limited than at pH 7.0; as observed by confocal microscopy, all the mixtures were of the same type, with a protein enriched continuous phase (Figure 4.3). The rheological behaviour was Newtonian, at least for the lower galactomannan concentrations (Figure.4.8). The viscosity of the mixtures increased with galactomannan concentration (Table 4.3).

At both pH values, the viscosity of mixtures with similar β-lactoglobulin / galactomannan concentrations was higher when the galactomannan was TG (see Figure 4.7 for 0.71%TG and 0.72%LBG, for example); this was expected since the TG sample used was of higher intrinsic viscosity than the LBG sample. This difference in viscosity was considerably reduced when the comparison was done for mixtures with similar "reduced concentration", $C[\eta]$, of the galactomannan, especially at pH 4.6 (mixtures 6.5%β-Lg+0.23%TG and 6.5%β-Lg+0.33%LBG and mixtures 6.5%β-Lg+0.31%TG and 6.5%β-Lg+0.44%LBG, Figure 4.8).

As was seen in section.3.3.2.1 for solutions of the pure galactomannans of the same reduced concentration, values of η_0 were similar and a viscosity (flow) master curve could be obtained after performing a concentration-dependent shift using a 0.82%LBG solution as the reference. For the mixed systems, no master curves could be obtained.

Table 4.3 Apparent viscosity of pure β-lactoglobulin and mixed solutions, at 20°C, at pH 4.6 and pH 7.0

pH	Samples	η_a (Pa.s)
7.0	6.5%β-Lg	0.0039
	6.5%β-Lg+0.44%LBG	0.0420
	6.5%β-Lg+0.31%TG	0.0224
4.6	6.5%β-Lg	0.0019
	6.5%β-Lg+0.33%LBG	0.0059
	6.5%β-Lg+0.44%LBG	0.0107
	6.5%β-Lg+0.23%TG	0.0065
	6.5%β-Lg+0.31%TG	0.0130

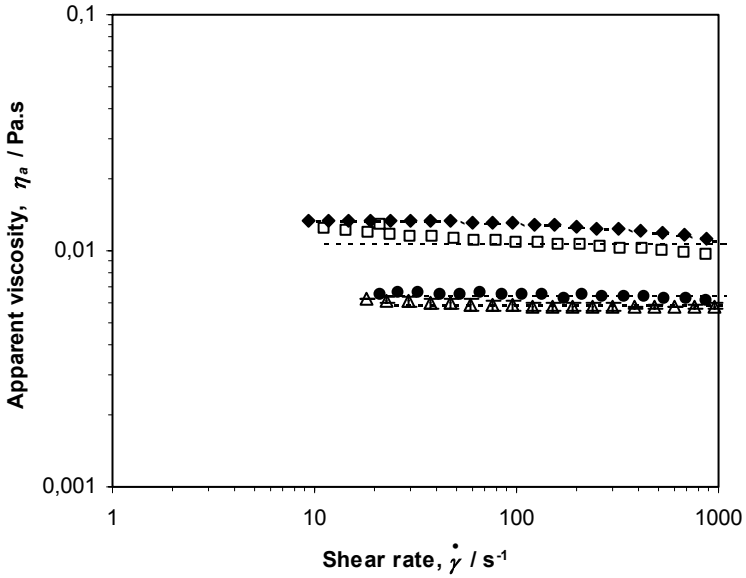

Figure 4.8 Flow curves for mixed solutions at 20°C and pH 4.6. Symbols: 6.5%β-Lg+0.33%LBG (Δ), 6.5%β-Lg+0.44%LBG (□), 6.5%β-Lg+0.23%TG (●) and 6.5%β-Lg+0.31%TG (♦); dotted lines represent values of η_a.

4.3.2.2 Viscoelastic properties

The effect of pH on the viscoelastic behaviour of pure β-lactoglobulin and pure galactomannan solutions is shown in Figure 4.9. As expected, no significant differences were found in the mechanical spectra of the polysaccharides while this was not the case for the protein solutions: values of G' and G'' were higher at pH 7.0; at pH 4.6, when the viscosity of the β-lactoglobulin solution was low (see Figure 4.4), G' values were below the noise level and could not be recorded.

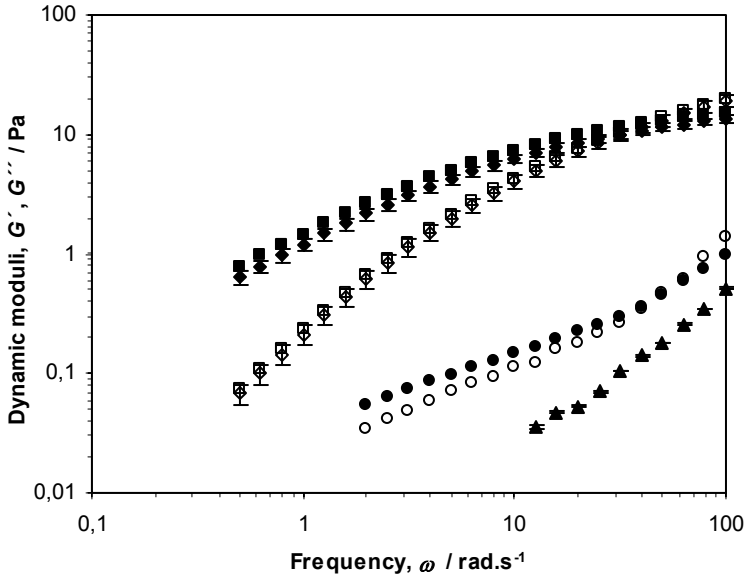

Figure 4.9 Effect of pH on dynamic moduli as a function of frequency of pure biopolymers at 20°C. G': open symbols; G'': full symbols; 0.50%TG at pH 4.6: ◇; 0.50%TG at pH 7.0: □; 6.5%β-Lg at pH 4.6: Δ; 6.5%β-Lg at pH 7.0: O.

At both pH values, the mechanical spectra of the mixed systems exhibited an intermediate behaviour, the magnitudes of both moduli lying between those obtained for pure biopolymer solutions. In Figure 4.10, mixtures of β-lactoglobulin with LBG and with TG, at pH 4.6, are

presented as an example. At this pH, due to experimental constraints, the concentration of the polysaccharide in the mixtures was low and the spectra recorded were in the lower limit of apparatus detection. At pH 7.0, however, a wider range of mixing ratios could be tested; results for β-lactoglobulin / TG mixtures are presented in Figure 4.11. At this pH and for similar concentrations of the galactomannan, values of the moduli were higher than at pH 4.6, as was the case for pure β-lactoglobulin solutions. When increasing TG concentration in the mixture, both moduli increased (Figure 4.11) and the shape of the spectra approached that of the pure galactomannan (Figure 4.11C). For β-lactoglobulin / LBG mixtures, a similar evolution of the moduli was observed (not shown). For similar concentration of the galactomannan (LBG or TG), mixtures with TG had higher moduli values than mixtures with LBG. Much closer values of the moduli were found when comparing mixtures with similar "reduced concentration" of the galactomannans (mixtures 6.5%β-Lg+0.50%TG and 6.5%β-Lg+0.72%LBG, Figure 4.12).

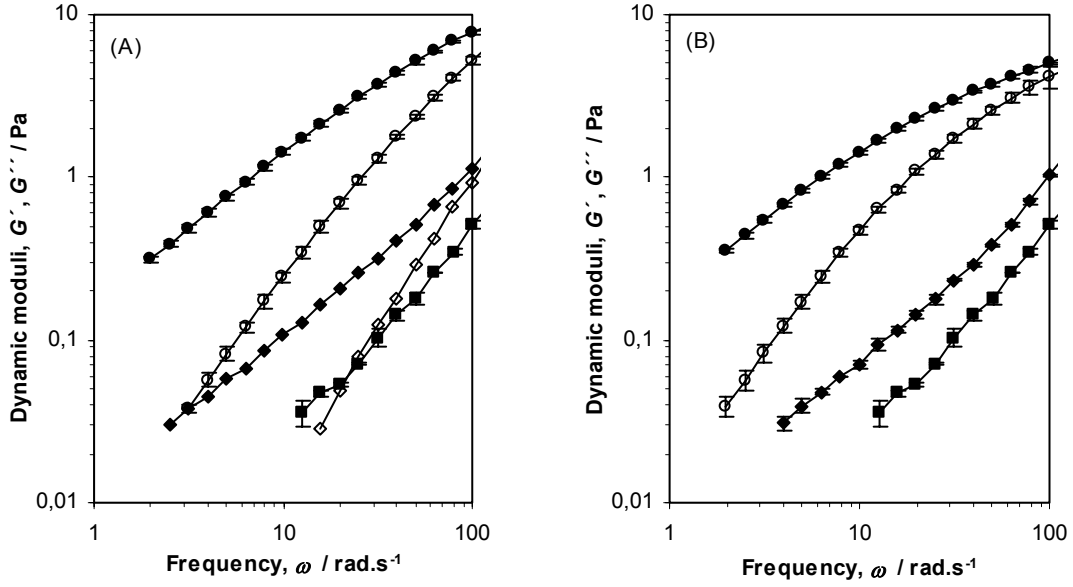

Figure 4.10 Mechanical spectra, recorded at 20°C, of pure 6.5%β-Lg (□), pure galactomannans (O) and their mixture (◇) at pH 4.6 (*G´*: open symbols, *G´´*: full symbols; A and B represent the systems of 0.44%LBG and 0.31%TG, respectively).

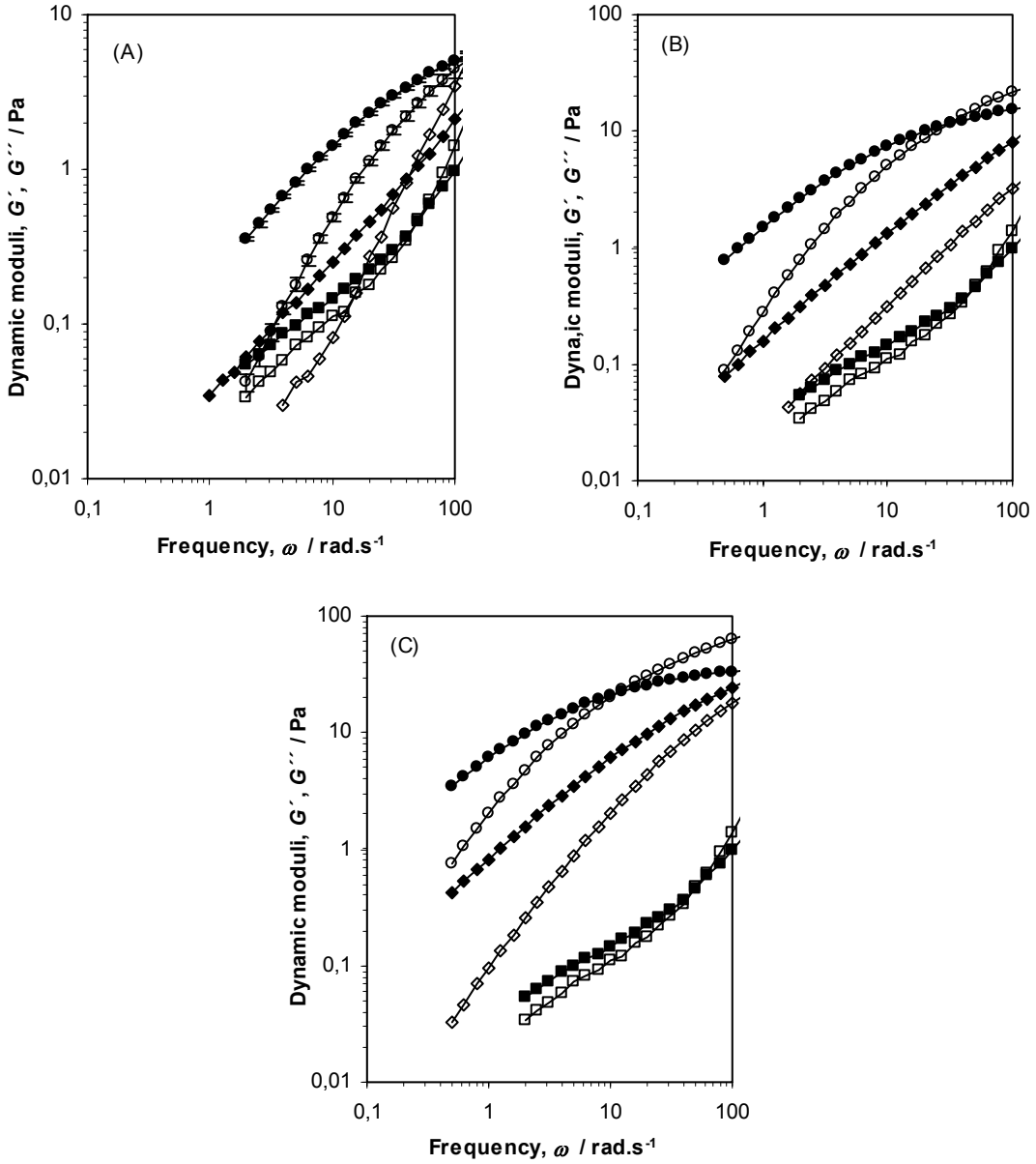

Figure 4.11 Mechanical spectra, recorded at 20°C, of pure 6.5%β-Lg (□), pure TG (O) and their mixture (◇) at pH 7.0 (*G´*: open symbols, *G´´*: full symbols; A, B and C represent the systems of 0.31%TG, 0.50%TG and 0.71%TG, respectively).

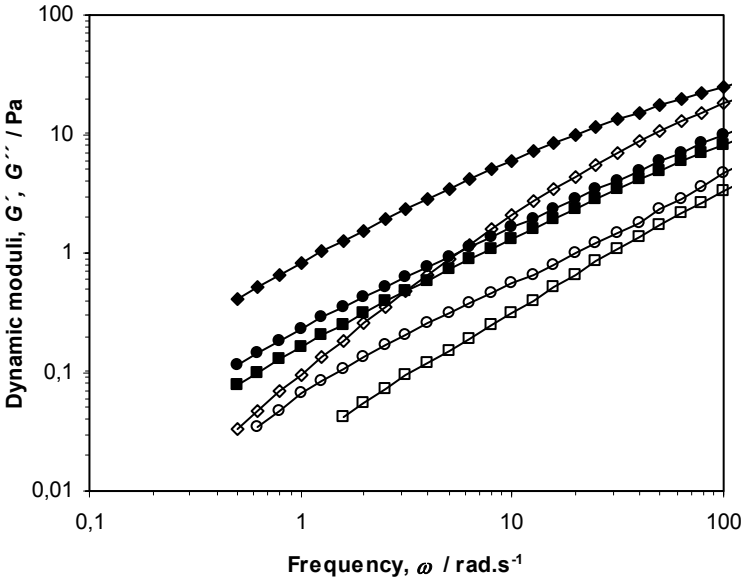

Figure 4.12 Mechanical spectra, recorded at 20°C, of mixtures at pH 7.0 (G´: open symbols, G´´: full symbols): 6.5%β-Lg+0.72%LBG (O), 6.5%β-Lg+0.50%TG (□) and 6.5%β-Lg+0.71%TG (◇).

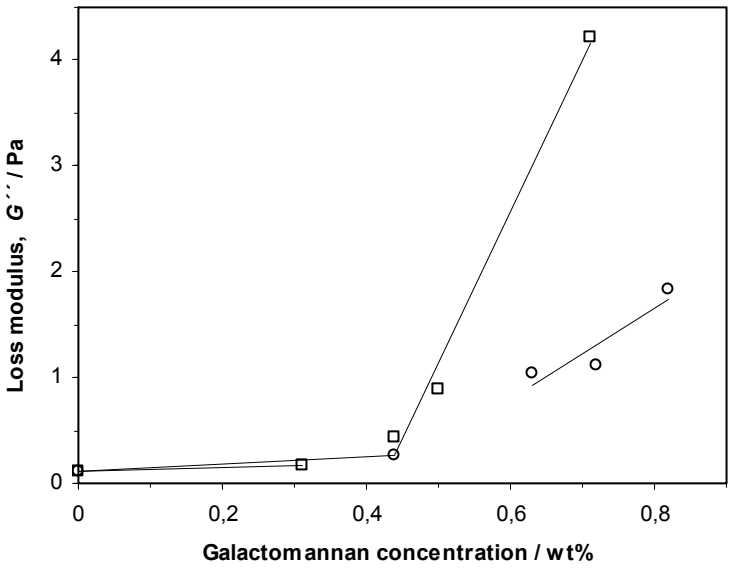

Figure 4.13 The loss modulus, *G´´* of mixed systems as a function of galactomannan concentration at 20°C and 6.28 rad.s^{-1}. Symbols: LBG (O) and TG (□).

In Figure 4.13, G'', at 6.28 rad.s^{-1}, (obtained from mechanical spectra of the mixtures), is represented versus galactomannan concentration in the mixtures, at pH 7.0. Similarly to what was observed with apparent viscosity (Figure 4.6), the phase inversion depicted in the micrographs (Figure 4.2) could be detected by rheology, as a change in the slope of the G'' versus galactomannan concentration curve.

4.4 Conclusions

In this chapter, the flow behaviour and the viscoelastic properties at 20°C of protein / galactomannan mixtures were examined at pH 7.0 and pH 4.6. For the mixtures, different rheological responses were achieved by varying biopolymer concentration in the mixtures and pH condition. These systems were better understood when rheological behaviour was correlated with information from microstructure.

CLSM images revealed that phase separation occurred for all mixed systems, in the liquid state, in the concentration range studied, at pH 7.0 and pH 4.6. The observed microstructure depended on the pH and on the composition of the mixed systems. At pH 4.6, in the concentration range studied, the microstructure corresponded to systems in the region of the phase diagram where β-lactoglobulin was the enriched continuous phase. The flow curves, like β-lactoglobulin alone, showed practically a Newtonian behaviour.

At pH 7.0, a wider range of concentrations could be tested and different types of structure could be visualized. Increasing the galactomannan concentration, the microstructure of the systems evolved from a continuous matrix of β-lactoglobulin enriched continuous phase containing some small inclusions of the galactomannan, to a matrix of galactomannan enriched continuous phase containing aggregates of β-lactoglobulin. The size of the aggregates decreased with increasing concentration of the galactomannan in the system. The microstructures of the mixed systems with TG and LBG were similar when comparing systems with similar reduced concentration of the two galactomannans.

In the region where the continuous phase was enriched in β-lactoglobulin, the flow behaviour of the mixtures was Newtonian, like that of the pure protein. However, the viscosity was higher (increasing with the galactomannan concentration in the mixture), probably due to the concentration of the protein in the continuous phase as a result of phase separation, induced by the presence of the polysaccharide.

In the region where the continuous phase was enriched in galactomannan, the flow behaviour was typical of a suspension, probably as a result of the flocculation of the β-lactoglobulin enriched disperse phase. The flow curves, with an apparent yield stress, could be described by the modified Cross model. For all mixtures, the plateau viscosity was lower than the η_0 for the galactomannan solution of the same concentration as in the mixture.

From the results obtained, we can conclude that it is possible to modify the structural and rheological properties of the mixed β-lactoglobulin / galactomannan aqueous systems, in the sol state, by changing the mixing ratio of the two biopolymers and the pH of the medium.

Chapter 5

Rheology and microstructure of β-lactoglobulin / galactomannan mixed gels

5.1 Introduction

The addition of a polysaccharide to a protein solution may bring important modifications of the gelation process. It is well known that when a mixed globular protein / polysaccharide solution is heated above the gel temperature of one of the components or of both of them, phase separation and gelation become competing processes and several alternative gel microstructures are possible (Grinberg et al., 1997). The resulting structure depends not only on the characteristics of the individual macromolecules themselves but also on the degree of their miscibility in solution, the relative time scales of phase separation and gelation, and the thermal history to which the mixture is subjected. These complex phenomena have attracted much attention because, besides being intrinsically interesting, they can be exploited to create or to modify food textures (Doublier et al., 2000; Turgeon et al., 2003).

In this chapter, the effect of galactomannans (locust bean gum and tara gum) on the thermal gelation of β-lactoglobulin, at 80^{o}C and pH 7.0 or pH 4.6, and on the gel properties after quenching to 20^{o}C was studied.

Rheological experiments – dynamic and retardation (creep and creep recovery) tests – and confocal laser scanning microscopy were used in this study.

As mentioned before in Chapter 4, experimental constraints restricted the range of accessible concentrations/mixing ratios of the two biopolymers. So, a fixed β-lactoglobulin concentration was chosen and a study of the evolution of the microstructure and of the rheology of the final gels, when different concentrations of galactomannan (locust bean gum or tara gum) were added, was done.

In section 5.3.1, the heat-induced gelation and the viscoelastic properties of the final mixed gels were studied at pH 7.0 and pH 4.6 and correlated with the observed microstructures. Particular attention was given to the effects of pH and of the type of galactomannan in the observed properties.

In section 5.3.2, the effect of a shear treatment on the rheology of some of the mixed gels was investigated in order to assess the influence of processing conditions on the properties of the studied gels.

In section 5.3.3, by combination of transient and dynamic measurements, a wider frequency (time) window was obtained which enabled a better characterization of the viscoelasticity of the mixed gels.

Finally, in section 5.4, the main conclusions obtained throughout this chapter were described.

5.2 Materials and methods

5.2.1 Materials

Studies in this chapter were done with the β-lactoglobulin and the galactomannan (locust bean gum and tara gum) samples used in the previous chapter, where the behaviour of mixed systems, in the sol state, was described.

5.2.2 Preparation of mixtures

Mixtures were prepared as described in Chapter 4 (see in section 4.2).

5.2.3 Rheological measurements

The rheological measurements were performed with the controlled stress rheometer AR2000 (TA Instruments), described in section 2.2.6.1, using the rough acrylic plate geometry (40 mm diameter, 800 μm gap).

5.2.3.1 Steady shear and dynamic oscillatory shear experiments

The fundamentals of these two types of experiments were previously described in Chapter 2, sections 2.2.6.2.1 (steady shear) and 2.2.6.2.2 (oscillatory shear).

5.2.3.2 Creep and recovery (static test)

5.2.3.2.1 General introduction to the technique

In addition to dynamic tests, static tests are also useful non-destructive techniques to analyze the viscoelastic behaviour of materials; they can be used to elucidate mechanisms that occur over relatively long time periods.

In a creep – recovery experiment, sometimes called the retardation test, a fixed stress σ_i is applied to the sample "instantaneously", for a given time, during which the deformation of the sample is monitored (creep curve). Then, the stress is "instantaneously" removed and the evolution of the deformation is measured (recovery curve). Results are usually expressed in terms of compliance, *J*, which is the quotient of the resulting strain to the constant stress applied to the sample:

$$J(t,\sigma) = \frac{\gamma(t,\sigma_i)}{\sigma_i} \qquad \text{(Eq. 5.1)}$$

Where $\gamma(t, \sigma_i)$ is the strain, at time, *t*, and σ_i is the applied stress.

When the rheological behaviour is linear, i.e. when effects of sequential changes in strain are additive (Boltzmann superposition principle), which is generally the case for macromolecular systems provided the strain remains small enough, the compliance is independent of the value of the applied stress and a function of time only.

Idealized creep and recovery curves are illustrated in Figure 5.1.

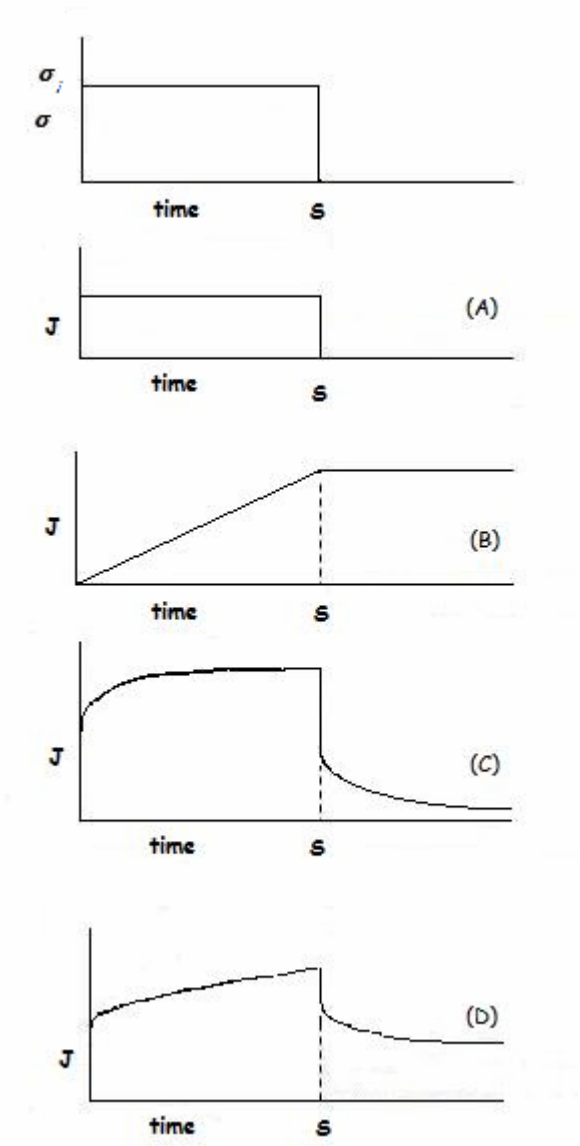

Figure 5.1 Typical creep and creep recovery curves, determined at applied constant stress. A: ideal elastic material; B: ideal viscous material; C: viscoelastic solid material; D: Viscoelastic liquid material (adapted from Steffe (1996)).

In an ideal elastic material subjected to a constant stress, σ_i , strain/compliance would be constant due to lack of flow, and the material would return to the original shape upon removal of the stress (Figure 5.1A).

An ideal viscous material would show steady flow, producing a linear response to stress with the inability to recover any of the imposed deformation (Figure 5.1B).

Viscoelastic materials would exhibit a nonlinear response. In a viscoelastic solid, an initial sharp increase of the compliance, followed by a progressive increase till its final value, is observed. When the stress is removed, a sharp decrease of the compliance, followed by a progressive decrease till a final value of zero, is observed (Figure 5.1C), since the strain is completely reversible (no flow). For a viscoelastic liquid, and initial instantaneous increase of the compliance, followed by a progressive increase is observed till the removal of the stress; then, an instantaneous decrease of the compliance, followed by a progressive decrease till a final finite value, is observed, which reflects the irreversible flow in the recovery curve (Figure 5.1D).

The analysis of the creep and the recovery curves for a viscoelastic liquid is represented schematically on Figure 5.2 (thick solid line), in terms of the flow contribution (curve 1) and the elastic contribution (curve 2). For the sake of clarity, the compliance function is represented by *J* in creep and by *K* in creep recovery (Lefebvre, 1996). If the stress is maintained for a time long enough, the creep compliance reaches a permanent regime corresponding to the linear terminal region of the creep curve; this means that the behaviour is dominated by flow at long observation times. The slope of the terminal region gives therefore the Newtonian viscosity η_0 of the material in permanent flow regime while the intersection with compliance-axis is the steady state compliance J_e^0 of the viscoelastic liquid. The contribution of flow, $J_v(t)$, to the total creep response, represented by curve 1 in the Figure 5.2, will be

$$J_v(t) = t / \eta_0 \qquad \text{(Eq. 5.2)}$$

and the elastic contribution $J_r(t)$, represented by curve 2, is obtained readily by subtracting $J_v(t)$ from the total creep compliance $J(t)$,

$$J(t) = J_v(t) + J_r(t) \qquad \text{(Eq. 5.3)}$$

The elastic contribution $J_r(t)$ is indeed identical to the response of a viscoelastic solid and the steady state compliance J_e^0 of the viscoelastic liquid analogous to the equilibrium compliance J_e of the solid.

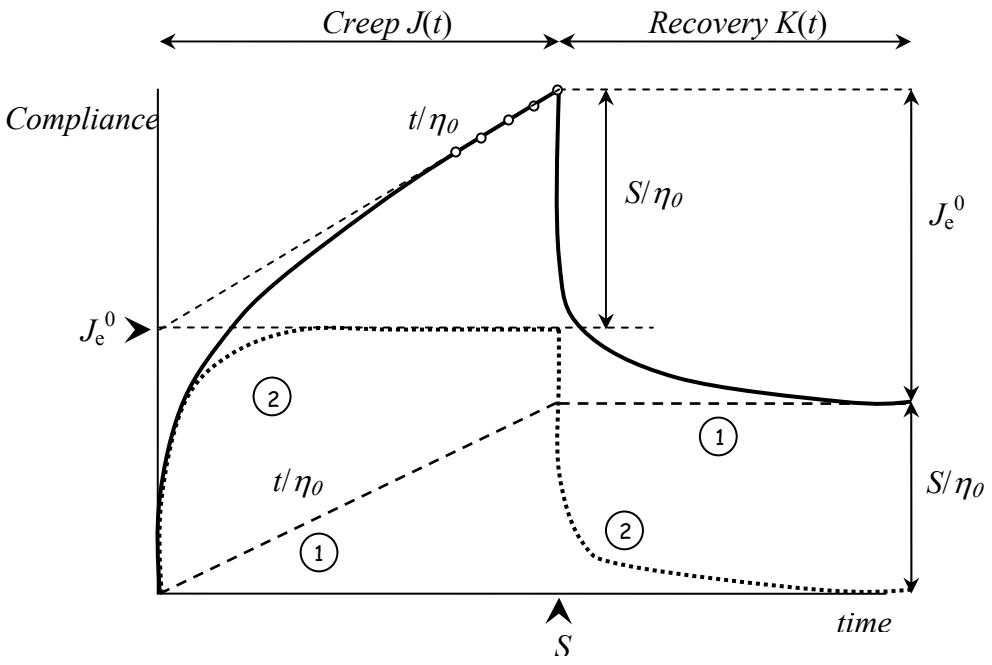

Figure 5.2 Schematic representation of the creep and creep recovery curves (on linear scales) of the model linear viscoelastic liquid, and its analysis in terms of the flow and recoverable contributions to the total compliance $J(t)$. Curve 1 represents the contribution of flow, $J_v(t)$, and curve 2 the elastic (recoverable) contribution, $J_r(t)$ (adapted from Lefebvre (1996)).

A similar analysis of the creep recovery curve, $K(t)$, of a viscoelastic liquid can be carried out. At long enough recovery times (t-S), $K(t)$ approaches a limit K_∞ which measures the irrecoverable part of the total strain reached at the end of the creep period:

$$K_\infty = S / \eta_0 \qquad \text{(Eq. 5.4)}$$

The recoverable part (elastic contribution) of the total strain will be obviously $J(S)$-K_∞, so that

$$J_e^0 = J(S) - K_\infty \qquad \text{(Eq. 5.5)}$$

Eqs. 5.4 and 5.5 can allow to check the results obtained for η_0 and J_e^0 from the creep part of the test. At each time t during recovery, the recovered strain will be $J(S)$-$K(t)$. When the behaviour is linear, the relation in Eq. 5.6 should be verified.

$$J_r(t - S) = J(S) - K(t) \qquad \text{(Eq. 5.6)}$$

5.2.3.2.2 Determination of dynamic storage and loss compliances from creep data

The calculation of the real and imaginary components of the complex compliance and of the complex modulus was done through the determination of the discrete retardation spectrum from creep recovery results.

The procedure comprised two steps:

- The determination of the discrete retardation spectrum using Kaschta´s method (Kaschta and Schwarzl, 1994).
- The calculation of $J'(\omega)$ and $J''(\omega)$ (and then $G'(\omega)$ and $G''(\omega)$).

Determination of the discrete retardation spectrum

As the relaxation modulus $G(t)$ of a viscoelastic liquid can be represented as the sum of P+1 exponential terms (generalized Maxwell model)

$$G(t) = \sum_{1}^{W} G_i \exp(-\frac{t}{\lambda_i}) \qquad \text{(Eq. 5.7)}$$

So its recoverable compliance can be represented by a Prony-Dirichlet series of P terms (generalized Kelvin-Voigt model):

$$J_r(t) = \sum_{1}^{P} J_i \left[1 - \exp(-\frac{t}{\tau_i}) \right] \qquad \text{(Eq. 5.8)}$$

However, in both cases, the problem is undetermined ("ill-posed") since there is not one and only one solution: if a series of P terms fits $J_r(t)$, then series with P+1, P+2, etc. terms will do as well. The question is to fit properly the data with a reasonable number of adjustable parameters giving physically possible (i.e. all positive) values for the parameters J_i, τ_i (or G_i and λ_i). Many "solutions" for this ill-posed problem has been, and are still, proposed.

Schematically, two approaches are possible:

a) very large P, with the J_i and the τ_i linked by some relations;

b) P limited in some physically reasonable way.

Approach b) is preferable. The method of Kaschta was chosen because is easy to handle. This method limits P by taking a specified number of equally logarithmically spaced spectral lines per decade of time. In practice, two retardation times per decade is a good choice: this

corresponds to b=5 in Kaschta´s paper (Kaschta et al., 1994). The number of terms in Eq. 5.8 is then obtained by dividing the logarithmic span of the experimental time window by the spacing:

$$P = \log(\frac{t_M}{t_1}) / \log(b) \qquad \text{(Eq. 5.9)}$$

Where t_M is the longest time and t_1 the shortest one taken into consideration. Normally, t_M should be on the recoverable compliance plateau J_e^0. The second logical step is to collocate the grid of retardation times on the time scale; this is achieved by just writing that the shortest retardation time τ_1 is $\tau_1 = a.t_1$ (a<1); so,

$$\tau_i = a.t_1.b^{i-1} \qquad \text{(Eq. 5.10)}$$

The procedure is then to fit (Eq. 5.8) to the data with the retardation times given by (Eq. 5.10); the P+1 adjustable parameters are the J_i and a. The rest resorts to fitting techniques.

Calculation of $J'(\omega)$ and $J''(\omega)$

Once J_i and τ_1 are obtained, $J'(\omega)$, $J''_r(\omega)$ (ω=1/t) are calculated readily as the sum of J'_i and J''_i of P Kelvin-Voigt elements.

$$J'(\omega) = J_0 + \sum_{i=1}^{P} J_i \frac{1}{1+\omega^2\tau_i^2} \qquad \text{(Eq. 5.11)}$$

$$J''(\omega) = \frac{1}{\omega\eta_0} + \sum_{i=1}^{P} J_i \frac{1}{1+\omega^2\tau_i^2} \qquad \text{(Eq. 5.12)}$$

J''_r is the recoverable loss compliance:

$$J''_r(\omega) = J''(\omega) - \frac{1}{\omega\eta_0} \qquad \text{(Eq. 5.13)}$$

Then, using for the viscosity the value determined from the terminal part of the creep curve, $J''(\omega)$ can be calculated. From the values of $J'(\omega)$ and $J''(\omega)$, the values of $G'(\omega)$ and $G''(\omega)$ can be obtained (see Chapter 2, Eqs. 2.15 and 2.16). Of course, this is valid only in the linear domain of the viscoelastic behaviour.

5.2.3.3 Experimental procedures

The samples were covered with a layer of paraffin oil to prevent evaporation, after having been placed into the measuring device.

In a first series of experiments, the following sequence of measurements was done:

- Temperature sweep from 20 to 80°C, at a constant heating rate of 2°C/min. Gelation was monitored by measuring G' and G'' at 6.28 rad.s^{-1}.
- Time sweep at 80°C: the evolution of G' and G'' was measured at a fixed frequency of 6.28 rad.s^{-1}, during 1 hour.
- Temperature sweep from 80 to 20°C at a constant cooling rate of 2°C/min.
- Time sweep at 20°C: the evolution of G' and G'' was measured at a fixed frequency of 6.28 rad.s^{-1}, during 20 min.
- Frequency sweep at 20°C: the evolution of the moduli was measured for a frequency range of 0.06 – 200 rad.s^{-1}.
- Strain sweep: the evolution of the moduli was measured, at 6.28 rad.s^{-1}, until fracture of the gel.

For temperature, time and frequency sweeps, the values used for the strain amplitude depended on the concentration/pH of the samples. Values of 0.05, for samples at pH 7.0, and 0.003, for samples at pH 4.6, were used which was within the linear viscoelastic region, determined by preliminary experiments.

To check that the data recorded during the frequency sweeps were obtained within the linearity domain of the systems, an approximation of the Kronig-Kramers relationship was used to calculate $G''(\omega)$ from $G'(\omega)$ data, and the calculated values were compared to the measured ones; the approximation was (Tschoegl, 1989):

$$G''(\omega) = \frac{\pi}{2}\frac{d(G'(\omega))}{d\ln(\omega)} \qquad \text{(Eq. 5.14)}$$

In a second series of experiments, the effect of a steady shear treatment, during gelation, on the rheological properties of the final gels, was studied on some of the mixed systems tested in the first series, using the same rheometer fitted with the cone-and-plate geometry (stainless steel cone with 4^o angle, 40 mm diameter and 109 μm truncation).

The sequence of procedures described above was maintained in these experiments. The only difference was that, at the end of the first step (20^oC – 80^oC heating step), shear was applied to the system, for 3 min, at a constant rates of 120 s^{-1}. The strain amplitude was fixed at 0.05, which was within the linear viscoelastic region.

In the third series of experiment, a new set of mixed systems (10%β-Lg+0 - 0.78%LBG) was studied, using the same rheometer fitted with the cone-and-plate geometry (stainless steel cone with 4^o angle, 40 mm diameter and 109 μm truncation). Gels were formed by submitting the

samples to a similar thermal cycle as in the first series, but time sweeps were longer (5 hours, at 80°C, and 1.5 hours, at 20°C). Immediately after the thermal cycle was completed, the mechanical spectrum of the quenched gel was recorded at 20°C over the frequency range 0.05–100 rad.s^{-1}, under strain amplitude of 0.01. Finally the gel was submitted to a retardation test, at 20°C: 1 hour 45 min for creep test, 5 hours 15 min for creep recovery test. The stress was comprised between 7 and 17 Pa, depending on galactomannan concentration; its value was chosen so as to keep the maximum creep strain below 0.01.

5.2.4 Confocal microscopy

The gel samples were examined by using a confocal laser scanning microscope described in Chapter 4, in the fluorescence mode. β-lactoglobulin and β-lactoglobulin / galactomannan mixtures were prepared as described in Chapter 4 (section 4.2.3), poured on a concave slide, covered with a glass cover and hermetically sealed to prevent evaporation. Then the systems were submitted to a heat treatment similar to that of the rheological measurements. The gels formed were examined under the microscope, as described in the previous chapter (section 4.2.3); $\times 20$ and $\times 63$ magnifications were used.

5.3 Results and discussion

5.3.1 Effect of galactomannan addition on the microstructure and rheology of heat-induced gels of β-lactoglobulin

In a first series of experiments, the effect of the addition of the galactomannans (locust bean gum, LBG, or tara gum, TG) on the heat-induced gelation of β-lactoglobulin and on the viscoelasticity and microstructure of the final gels was studied. The experiments were carried out at pH 7.0, where the protein bears a net negative charge, and at pH 4.6, near the isoelectric point of the protein. The two galactomannans had different M/G ratio and molecular weights, as shown before (see Tables 3.1 and 3.2). For these experiments and as pointed out before in Chapter 4 (see section 4.2.2), mixtures with a constant 6.5%β-lactoglobulin concentration and varying galactomannan concentrations (0 - 0.80 wt%, for LBG, and 0 - 0.56 wt%, for TG) were studied.

5.3.1.1 Gel formation and quenching

When the systems (β-lactoglobulin alone or β-lactoglobulin / galactomannan mixtures) were heated (20 - 80^{o}C), a gel formed at both pHs. In the case of β-lactoglobulin / galactomannan mixtures, since LBG and TG are non-gelling galactomannans, it was the gelation of β-lactoglobulin that was, actually, monitored when the mixed systems were heated.

Figure 5.3 shows the evolution of the 6.5%β-lactoglobulin pure and mixed systems with TG, during the thermal cycle. Similar evolution profile was observed for mixed systems with LBG (results not shown). All curves had similar shapes.

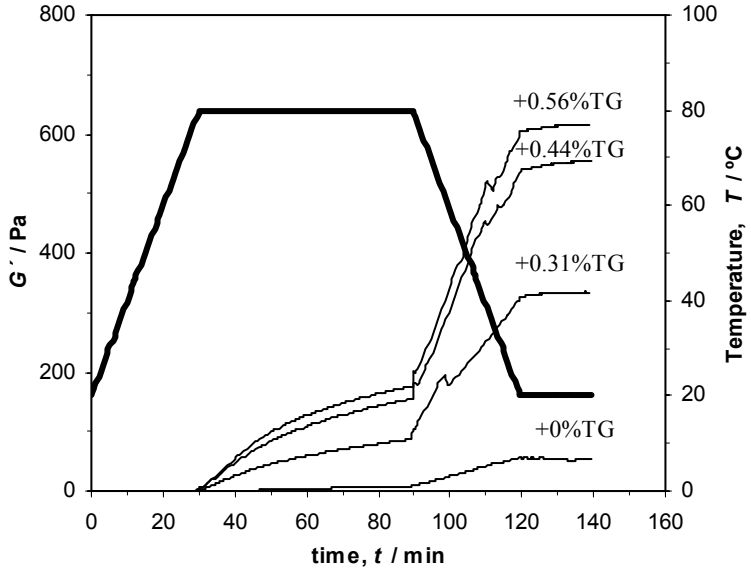

Figure 5.3 Effect of TG concentration on thermal gelation of the mixtures, at pH 7.0. The thick line represents the temperature profile.

The aggregation/gelation process for 6.5%β-lactoglobulin system, at pH 7.0, developed during the 80°C heating step while, for the mixed systems (with the exception of 6.5%β-Lg+0.44%LBG system), it started during the 20 - 80ºC heating ramp (Figure 5.4A). At pH 4.6, it started during the 20 - 80ºC heating ramp for all the studied systems (Figure 5.4B). In fact, using the criterion of G'/G'' cross-over (or tan δ = 1) for defining the gelling temperature, T_g, it can be seen in Figure 5.4 and Table.5.1 that T_g decreased with increasing galactomannan concentration.

The effect seems slightly more pronounced for TG than for LBG mixed gels (Table 5.1), which may be due to the higher molecular mass of TG. Similar effects were described by Tavares and co-workers (2005) for whey protein / galactomannan mixtures, at pH 7.0. However, in their case, they also found that, for low M/G ratios of the galactomannan (as in the case of guar

gum), the degree of branching had also an important role on the whey protein gelation behaviour.

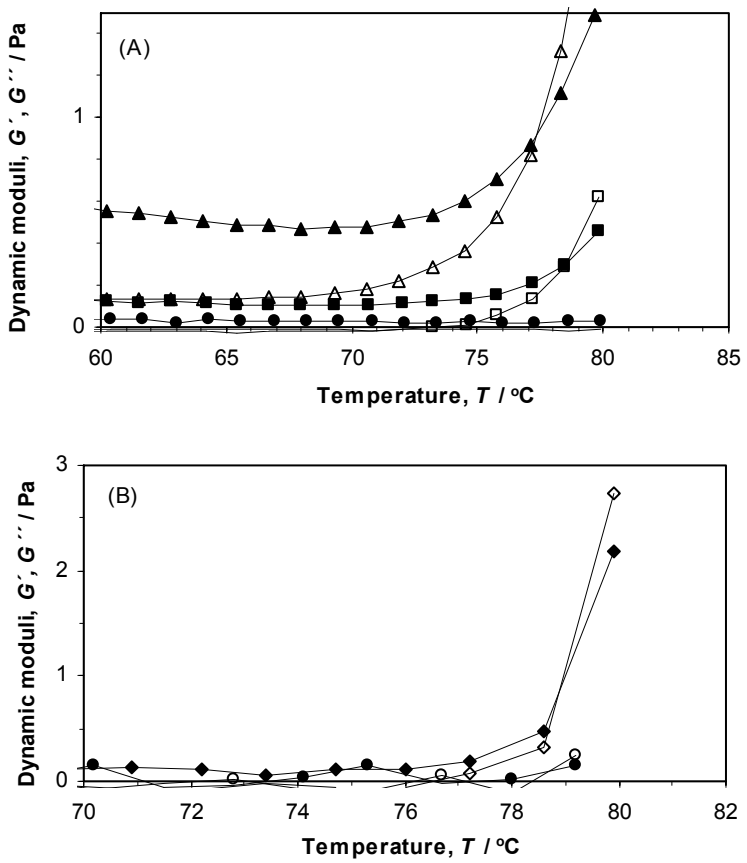

Figure 5.4. *G′* and *G′′* values during heating step (20 to 80°C), recorded at 6.28 rad/s, for mixed systems at pH 7.0 (A) and pH 4.6 (B). TG concentrations (A): 0% (O), 0.31% (□) and 0.56% (Δ); (B): 0% (O) and 0.63% (◇). Open symbols: *G′*; full symbols: *G′′*.

At the beginning of the 80°C isothermal heating step, the rate of the gelation process is high and then it slackens and tends towards a plateau. At the end of the step, *G′* ranges in the order of increasing galactomannan concentration.

Table 5.1 The gelation point for mixed systems

pH	Galactomannan concentration (wt%)		Gel temperature at heating step (20 to 80°C) (°C)	Gel time at time sweep at 80°C (min)
7.0		0	-	7.7
	LBG	0.44	-	0.3
		0.63	78.5	-
		0.80	79.8	-
	TG	0.31	78.5	-
		0.44	75.7	-
		0.56	77.1	-
4.6		0	78.7	-
	LBG	0.33	78.2	-
		0.50	76.0	-
		0.63	75.4	-
	TG	0.23	77.8	-
		0.44	75.7	-
		0.63	79.0	-

Analysis of such "kinetics" of gelation cannot convey information but empirical. During the 80°C heating step, temperature ramp and gelation "kinetics" are convoluted; moreover, moduli are below or close to the sensitivity threshold during most of this step; finally, there is a competition between the decreases of the moduli as temperature increases due to the contribution of the polysaccharide and its increase due to protein gelation. Therefore, although the presence of the polysaccharide could induce indeed a modification of protein denaturation

temperature, any attempt to interpret the differences of the temperature thresholds above which *G′* begins to increase in terms of a possible effect of the galactomannan on β-lactoglobulin denaturation temperature is precluded. On the other hand, the choice of the fixed frequency at which measurements are carried out is arbitrary, and the rheological behaviour of the system is likely to shift along the frequency axis as well as along the moduli axis during the thermal history. As a result, in principle, values of *G′* and *G′′* measured during the two first steps (i.e. before the system has actually reached, or, at least, is approaching a pseudo equilibrium) have actually no meaning as regards the state of the system. We have nevertheless, for comparative purpose, tentatively analysed the evolution of *G′* during the 80°C heating step through its time derivative considered as indicative of the gelation rate.

In Figure 5.5A, three zones could be defined in the d*G′*/dt *versus* time curve, at pH 7.0, for β-Lg / TG mixed systems: an initial steep increase (*phase a*), followed by a steep decrease (*phase b*) and, finally, a less pronounced decrease (*phase c*); no constant value of d*G′*/dt was attained. Similar behaviour was observed for mixed systems with LBG (results not shown). The slope values (positive in *phase a* and negative in *phase b*) showed a net increase (in absolute value) with increasing galactomannan concentration. This is indication of a change in the evolution of the gel with time. Also the maximum "gelation rate" (attained at the end of *phase a*) was considerably affected by the addition of galactomannan to β-lactoglobulin. Values of this maximum rate, when compared to that for the pure protein system, were 40 to 53 times larger, for the mixed systems with LBG, and 13 to 27 times larger, for mixed systems with TG.

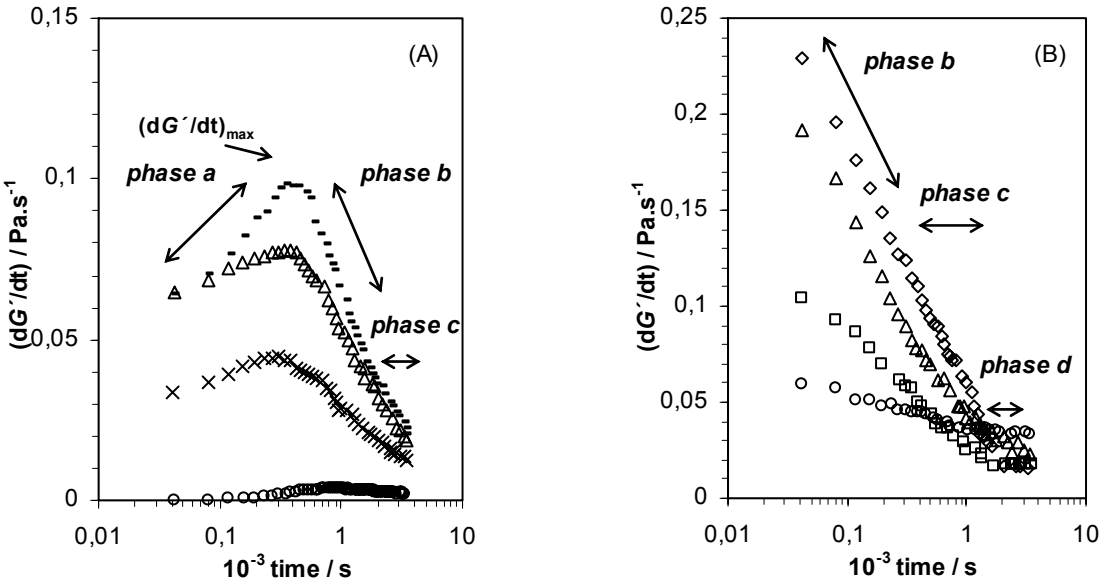

Figure 5.5 Evolution of the storage modulus rate of change during isothermal heating time at 80°C for mixed systems at pH 7.0 (A) and pH 4.6 (B). TG concentrations: 0% (O), 0.23% (□), 0.31% (×), 0.44% (Δ), 0.56% (–) and 0.63% (◇).

In contrast, the evolution of *G´*, at pH 4.6, was different (Figure 5.5B): the maximum of d*G´*/dt had been probably attained during the heating ramp because, at the beginning of the heating step, a steep decrease of the gelation rate was observed (*phase b*), followed by a plateau (*phase d*) where d*G´*/dt attained a constant value. The decrease was steeper for the mixed systems but the final gelation rate, in *phase d*, was higher for the pure β-lactoglobulin system. Clearly, the aggregation/gelation process for the systems was different at both pH values (4.6 and 7.0). However, in both cases, the presence of the galactomannan increased the gelation rate (gels formed more quickly) and the strength (*G´* increased) of the gels, at 80°C.

After the heating step at 80ºC, gels were quenched to 20ºC. As expected, an increase in *G´* values was observed during this step revealing a strengthening of the gel. Similar increase in *G´*

has been previously observed for other globular protein gels (see, for instance, Gonçalves, Torres, Andrade, Azero, and Lefevre, 2004; Ould Eleya et al., 2004) and has been attributed to an increase of attractive forces (van der Waals interactions and hydrogen bonding) within the gel network, during cooling of the systems.

Gels were left to equilibrate at 20ºC for 20 min; practically, no further evolution of moduli was detected during this period. It was then possible to characterize their rheological behaviour.

5.3.1.2 Viscoelastic properties

After equilibration of the gels, frequency sweeps were performed at 20ºC. The viscoelastic behaviour observed was similar for all the systems analysed. The spectra obtained framed a section of the viscoelastic plateau, with $G' > G''$ for the range of frequencies studied. G' increased monotonously while G'' showed a minimum towards the low frequencies as shown, for some of the studied systems, in Figure 5.6.

The good agreement between measured $G''(\omega)$ and its values calculated from $G'(\omega)$ using Eq. 5.14 showed that the frequency sweeps were actually recorded below the linearity limit of viscoelastic behaviour and confirmed that the gels had not undergone appreciable structural changes during this record (Figure 5.6).

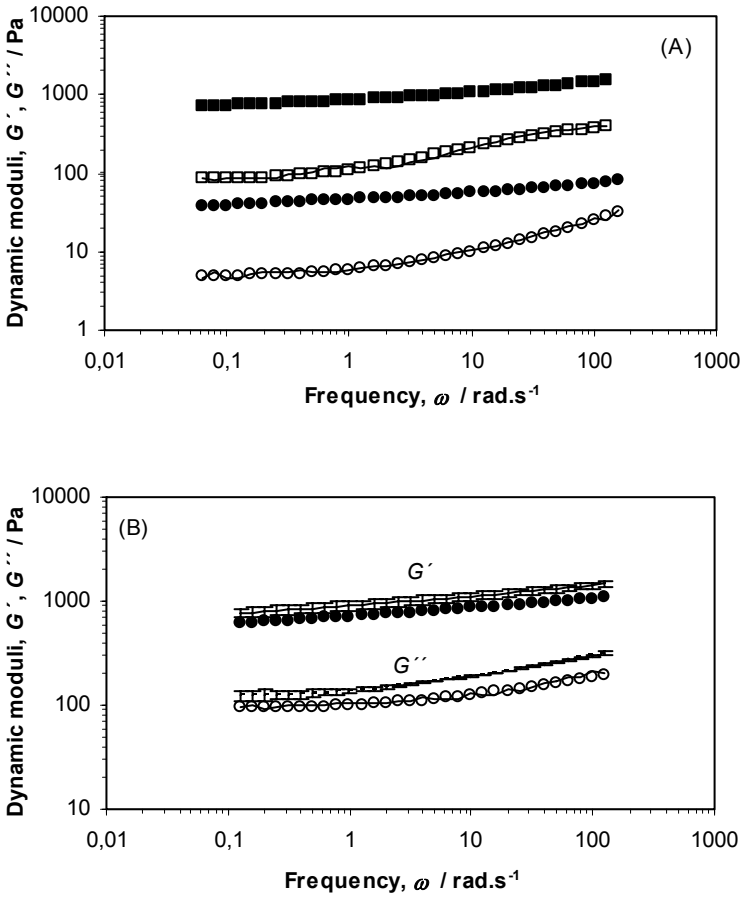

Figure 5.6 Mechanical spectra of gel systems, at 20°C, at pH 7.0 (A) and pH 4.6 (B). LBG concentrations: 0% (O) and 0.63% (□ for pH 7.0, lines for pH 4.6). Full symbols: experimental *G´* values; Open symbols: experimental *G´´* values; the lines: *G´´* recalculated values from *G´* experimental values using Eq. 5.14.

The general effect of the addition of galactomannan to β-lactoglobulin was the increase in gel rigidity (*G´* increased) and the decrease of gel elasticity (tan δ increased). The increase of tan δ with galactomannan concentration seems reasonable, due to the increased concentration of the viscous non-gelling polysaccharide in the mixed systems. At pH 7.0, mixed gels with LBG (the galactomannan with lower degree of branching and lower molecular weight) were more rigid and more elastic than mixed gels with TG (Table 5.2).

Table 5.2 Values of tan δ and G' for cured gels, at 20°C and 6.28 rad.s^{-1}

pH	Galactomannan concentration (wt%)		tan δ	G' (Pa)
7		0	1.66×10^{-1}	5.33×10
	LBG	0.44	1.36×10^{-1}	8.28×10^{2}
		0.63	1.84×10^{-1}	9.95×10^{2}
		0.80	1.96×10^{-1}	1.05×10^{3}
	TG	0.31	1.85×10^{-1}	3.30×10^{2}
		0.44	2.02×10^{-1}	5.50×10^{2}
		0.56	2.19×10^{-1}	6.10×10^{2}
4.6		0	1.43×10^{-1}	8.24×10^{2}
	LBG	0.33	1.66×10^{-1}	5.05×10^{2}
		0.50	1.63×10^{-1}	8.72×10^{2}
		0.63	1.60×10^{-1}	1.12×10^{3}
	TG	0.23	1.45×10^{-1}	5.85×10^{2}
		0.44	1.49×10^{-1}	1.11×10^{3}
		0.63	1.72×10^{-1}	1.13×10^{3}

Representation in terms of the components $J'(\omega)$ and $J''(\omega)$ of the complex compliance provided a better insight into the viscoelastic behaviour of the gels. In Figure 5.7, are represented, as an example, J' and J'' versus frequency (ω) for β-Lg / TG systems, at pH 7.0 (Figure 5.7A and C), and at pH 4.6 (Figure 5.7B and D). The experimental window framed the high frequency end of the viscoelastic plateau; $J'(\omega)$ began to slope down from its plateau value J_N^0, and the peak of $J''(\omega)$, which marks the beginning of the transition zone, appeared, as shown in Figure 5.7C. The maximum of this peak was higher than 200 rad.s^{-1}, the upper limit of

the frequency range studied, for the 6.5%β-lactoglobulin gel, but shifted to lower values in the case of the mixed systems. The data have been tentatively fitted with a Cole-Cole model:

$$J'(\omega) = J_g + \left(J_N^0 - J_g\right)\frac{\left((\omega_0/\omega)^p + \cos(\pi p/2)\right)}{\left((\omega/\omega_0)^p + 2\cos(\pi p/2) + (\omega_0/\omega)^p\right)} \qquad \text{(Eq. 5.15)}$$

$$J''(\omega) = \left(J_N^0 - J_g\right)\frac{\left(\sin(\pi p/2)\right)}{\left((\omega/\omega_0)^p + 2\cos(\pi p/2) + (\omega_0/\omega)^p\right)} \qquad \text{(Eq. 5.16)}$$

where $J_N^0 = 1/G_N^0$ is the plateau compliance, J_g the "glassy" compliance (the high frequency limit of $J'(\omega)$), ω_0 the central frequency of the loss peak, and the exponent p a spread parameter related to the width of the peak.

The fits were performed with $J_g = 0$ since $J_g << J_N^0$ in the plateau region. Figure 5.7 shows that they fit reasonably well the data in the high frequency region. Values obtained for the parameters are presented in Table 5.3.

At pH 7.0, values of G_N^0 obtained from the fitting increased with increasing galactomannan concentration. A striking decrease of ω_0 was observed when galactomannan was added to β-lactoglobulin gels. The spread coefficient, p, was lower for the mixed gels, probably reflecting a broader distribution of retardation times. However, in the case of pure β-lactoglobulin gel, the experimental frequency window framed only a small part of the high frequency loss peak; the results are to be taken only as indicative.

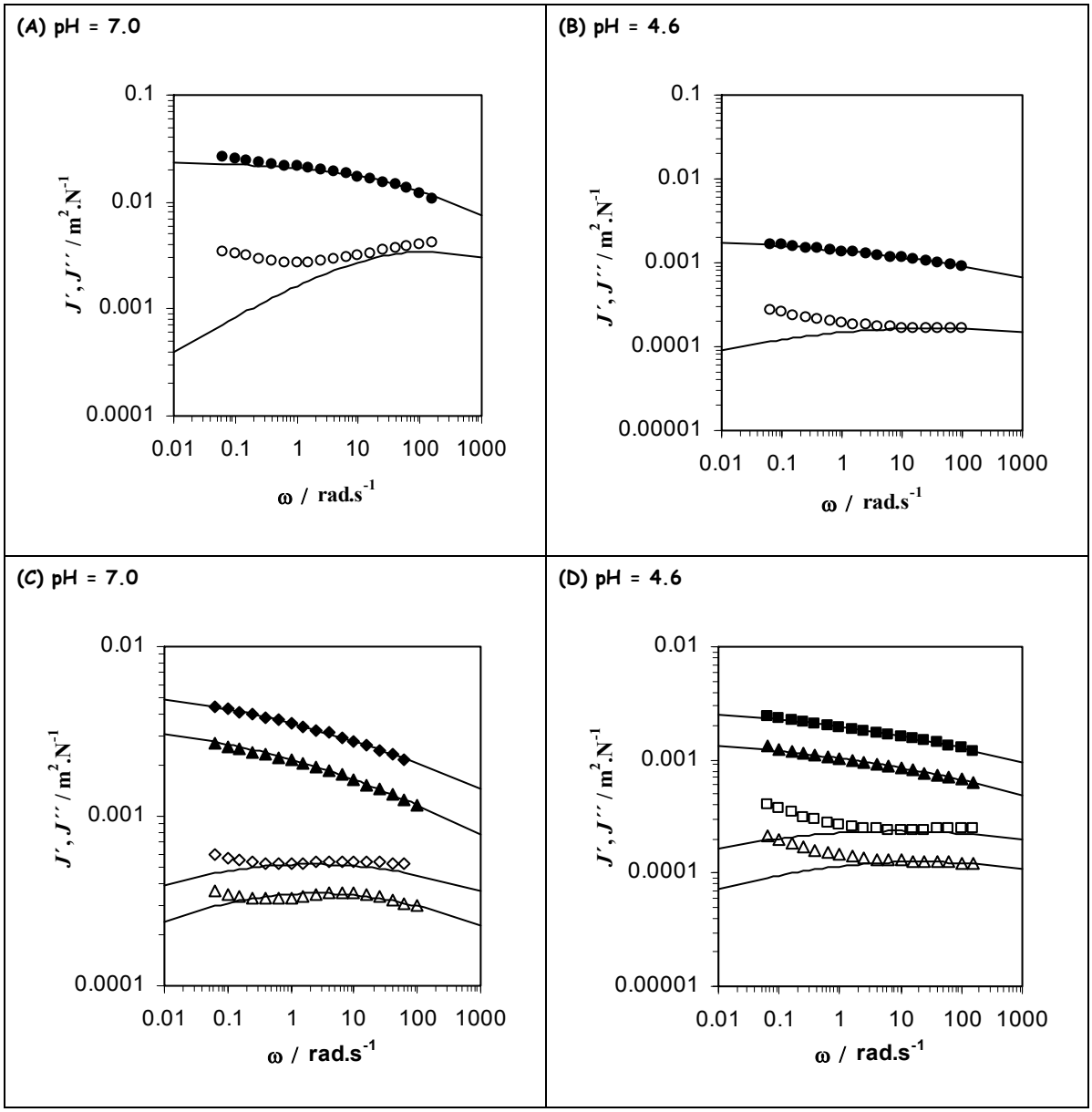

Figure 5.7 Storage and loss compliance vs frequency curves of gel systems, at 20°C, at pH 7.0 ((A) and (C)) and pH 4.6 ((B) and (D)). TG concentrations: 0% (O), 0.23% (□), 0.31% (◇) and 0.44% (Δ). Full symbols: storage compliance (J'); Open symbols: loss compliance (J''); the continuous and dotted lines represent the fits of Cole-Cole functions (Eqs. 5.15 and 5.16).

Table 5.3 Rheological parameters extracted from the analysis of the mechanical spectra of the gels, recorded at 20ºC. (Values obtained by fitting Eqs. 5.15 and 5.16 with $J_g = 0$)

pH	Galactomannan concentration (%)		$G_N^0 = 1/J_N^0$ (Pa)	ω_0 (rad.s^{-1})	p
7.0		0	42	140	0.36
	LBG	0.44	469	17	0.20
		0.63	555	10	0.25
		0.80	651	20	0.29
	TG	0.31	152	2.1	0.20
		0.44	256	2.5	0.23
		0.56	304	3.8	0.24
4.6		0	478	28	0.20
	LBG	0.33	308	35	0.25
		0.50	545	43	0.25
		0.63	679	75	0.27
	TG	0.23	303	8	0.18
		0.44	629	20	0.20
		0.63	715	55	0.23

For systems at pH 4.6, the values for G_N^0 ranged in the order: 0.23%TG < 0%TG < 0.44%TG < 0.63%TG and 0.33%LBG < 0%LBG < 0.50%LBG < 0.63%LBG, in accordance with the experimental results in Table 5.3. When TG was added to β-lactoglobulin gels, ω_0 changed: a pronounced decrease of this parameter was observed for the 0.23%TG mixed gel when compared to pure β-lactoglobulin gel; but it increased with increasing TG concentration for the other mixed gels studied. In mixed gels with LBG, ω_0 increased with LBG concentration.

However, values of ω_0 are affected by a large error; an enlargement of the frequency window would be necessary to better characterize the viscoelasticity of these gels.

Gels were submitted to a range of increasing stresses (dynamic stress sweep test) till they ruptured. The dependence of G' and G'' on strain (γ), at 6.28 rad.s^{-1}, was determined.

The general behaviour of the gels depended on pH. At pH 7.0, the results showed an initial constant value, G'_0; then, for γ values higher than 30-50% (depending on the sample composition), an increase of G' followed by a dramatic decay (for strains about 100-200% depending, again, on the sample) was observed. Evolution of G'' was similar to that of G' but it kept much lower values for all strains below rupture. If G' and G'' data obtained for each gel were normalized by G'_0 and G''_0 curves superimposed at low strains and deviated at higher strains. Both G' and G'' showed strain hardening behaviour (both moduli increased) followed by strain thinning (Figure 5.8A and B).

These non-linear properties of protein gels at large deformations were reported for different biopolymer systems (Michon, Chapuis, Langendorff, Boulenger, and Cuvelier, 2004; Pouzot et al., 2006) and colloidal particles (Gisler, Ball, and Weitz, 1999). During strain hardening, tan δ decreased for the mixed gels although both G' and G'' were increasing; for higher deformation, however, tan δ started to increase (Figure 5.9) which was probably caused by irreversible fracture (Pouzot et al., 2006).

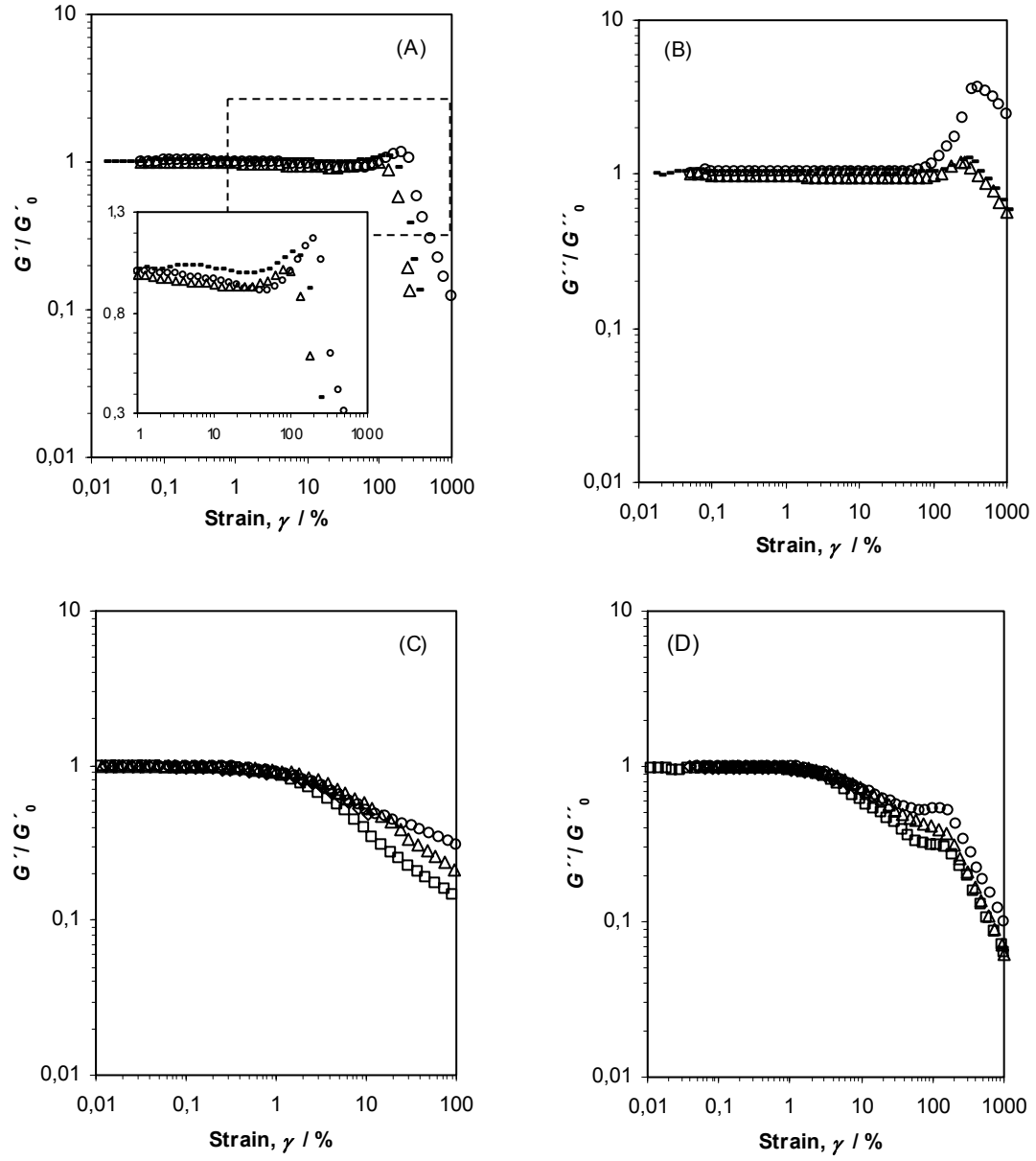

Figure 5.8 Strain dependence of reduced storage modulus (G'/G_0') and (G''/G_0'') for gel systems at pH 7.0 (A and B) and pH 4.6 (C and D), respectively. TG concentrations: 0% (O), 0.23% (□), 0.44% (Δ), 0.56% (–) and 0.63% (◇).

According to Hyun and co-workers (2002), the large amplitude oscillatory shear (LAOS) behaviour of our systems, at pH 7.0, falls into type IV, strong strain overshoot (G' and G'' increasing followed by decreasing). This behaviour was explained in terms of the formation and

destruction rates of network junctions by Sim and co-workers (2003): both the formation and destruction rates increased with the strain amplitude, but the speed of formation was a little larger than that of destruction leading to the strain hardening. The destruction term became dominant at larger strain amplitude leading to the strain thinning. The overshoot may be regarded as coming from the balance between the formation and the destruction of the network junctions.

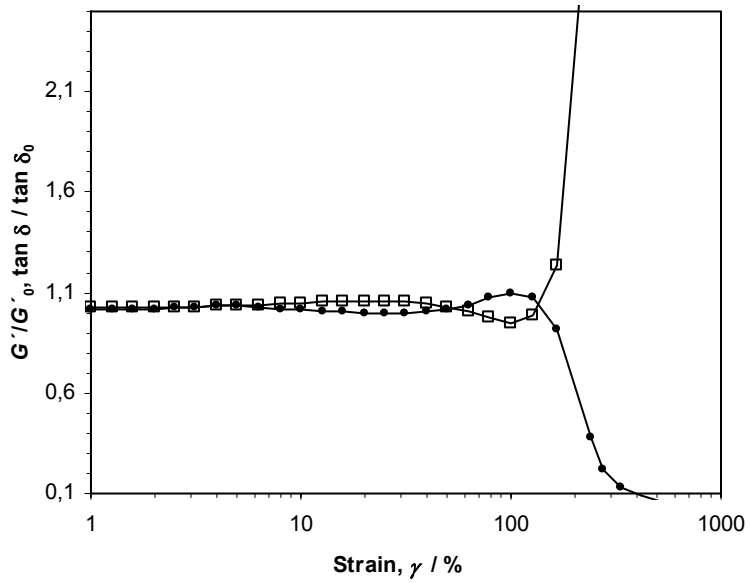

Figure 5.9 Comparison of the relative dependence of G' (O) and tan δ (□) on the strain for a 6.5%β-Lg+0.56%TG gel at pH 7.0.

Experimental values for G'_0, G'_{max} (maximum value of G' during strain hardening) and γ_r (the strain at fracture taken as the value of γ for G'_{max}) are given in Table 5.4. The relative increase of G' due to strain hardening, E, was higher for the pure β-lactoglobulin gel. This pure protein gel was, however, less rigid (lower G'_0), as referred before, and fractured at higher deformations than mixed gels.

Table 5.4 Values obtained from strain sweep tests for gel systems at 20°C

pH	Galactomannan	Galactomannan conc. (%)	G'_0 (Pa)	G'_{max} (Pa)	γ_r (%)	γ_c (%)	σ_c (Pa)	$E = G'_{max} / G'_0$
7.0	TG	0	56	66	198	-	-	1.18
		0.44	562	583	100	-	-	1.04
		0.56	602	649	99	-	-	1.08
4.6	LBG	0	870	-	-	0.63	5.27	-
		0.33	533	-	-	0.32	1.62	-
		0.50	941	-	-	0.80	7.20	-
		0.63	1112	-	-	1.27	13.56	-
	TG	0.23	583	-	-	0.46	2.62	-
		0.44	1124	-	-	0.73	4.01	-
		0.63	1225	-	-	1.00	11.02	-

At pH 4.6, no strain hardening was observed. Instead, G' and G'' remained almost constant and then suddenly decreased with increasing strain, indicating a transition from a linear to a non-linear behaviour (Figure 5.8C and D). This type of behaviour is often seen in polymer solutions and melts. However, in the present systems, the evolution of G'' seems more complex showing a two-step decrease with applied strain. If the classification of Hyun and co-workers (2002) is adopted, these gels could be a variation of type I (strain thinning) or a combination of type I (strain thinning) and type III (weak strain overshoot; G' decreasing and G'' increasing followed by decreasing). For both types; the network model of Sim and co-workers (2003) specifies that the destruction rate is increased as the strain amplitude is increased. When the strain is large, the networks junctions are lost and G' and G'' decrease.

The strain amplitude at which G' decreased 5 % from its maximum value was determined and taken as a measure of the critical strain γ_c of the gel (Rueb and Zukoski, 1997). Values of G'_0, γ_c and σ_c (the critical stress) are presented in Table 5.4: the variation in these parameters ranged in the order 0.23%TG < 0%TG < 0.44%TG < 0.63%TG and 0.33%LBG < 0%LBG < 0.50%LBG < 0.63%LBG. Compared to similar gels at pH 7.0, these gels were stronger (higher G'_0 values) and showed higher sensitivity to strain.

5.3.1.3 Microstructure of mixed gels

Some micrographs obtained for gels at pH 7.0 are presented in Figures 5.10 and 5.11; the protein is fluorescent and appeared bright in the micrographs. Within the resolution of the confocal microscope, the pure β-lactoglobulin gels looked homogeneous while mixed gels were two-phase: the protein enriched continuous phase appeared as a concentrated dispersion of globules forming an aggregated network (colloidal gel). When analysing the behaviour of mixed systems, it is clear that the presence of galactomannan influenced the microstructure of β-lactoglobulin gels: a more open and less homogeneous structure, with larger pores between the clusters, was observed when the galactomannan concentration increased.

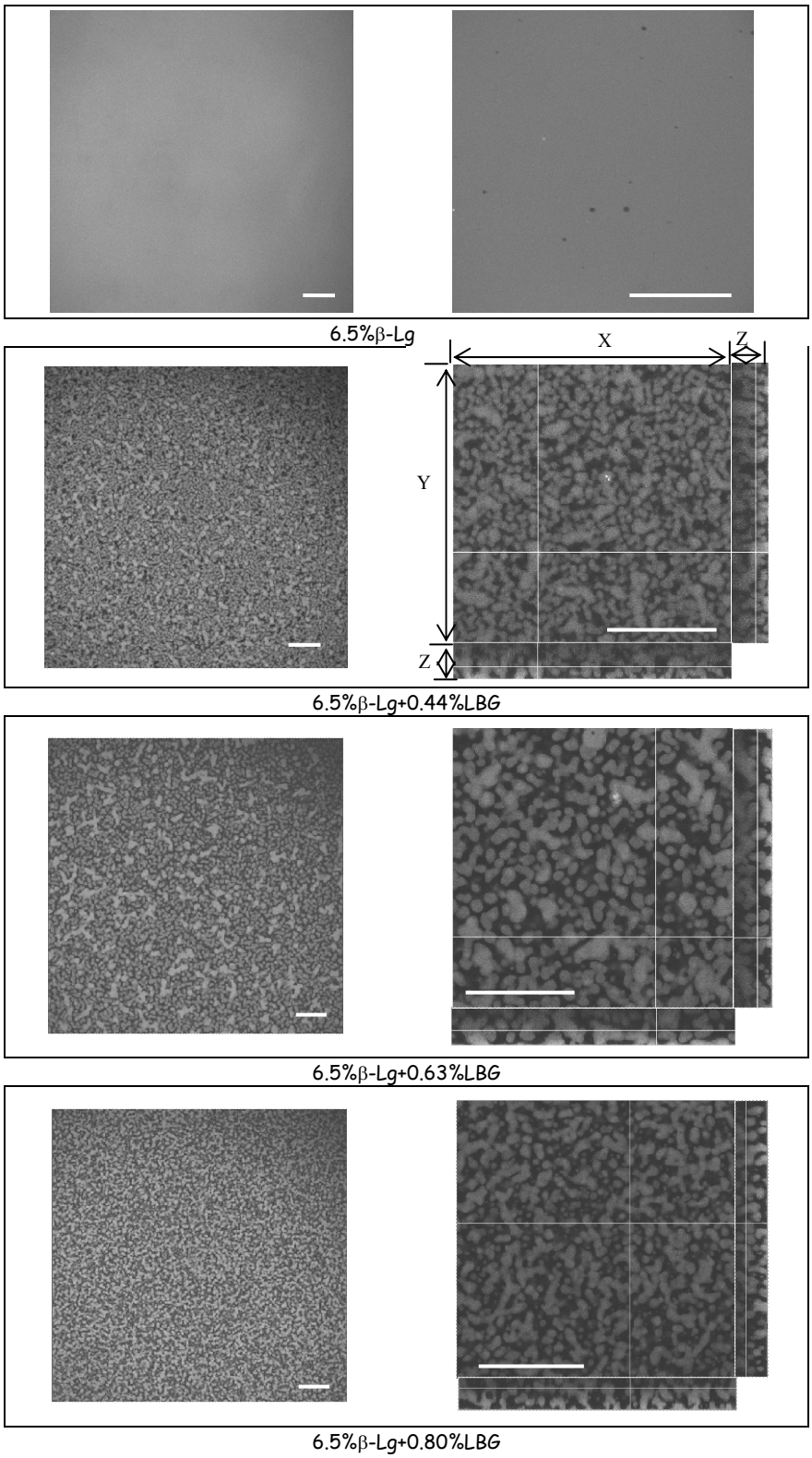

Figure 5.10 CLSM micrographs of β-Lg gels, pure or mixed with LBG, at 20°C and pH 7.0, at ×20 (left column) and ×63 magnification (right column). For mixed gels, are shown images obtained in the planes XY, XZ and YZ of the samples. Scale bar = 80 μm.

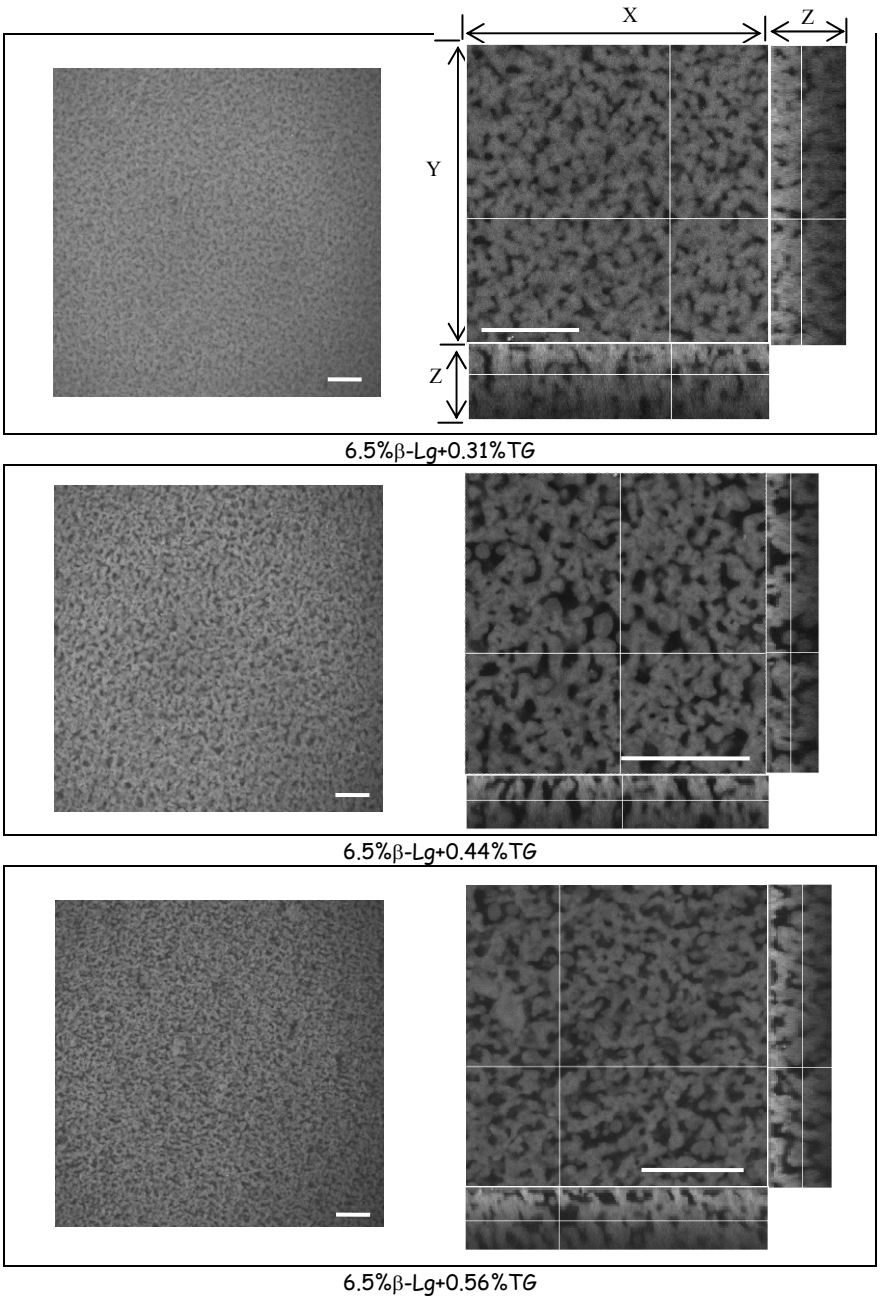

Figure 5.11 CLSM micrographs of β-Lg gels mixed with TG, at 20°C and pH 7.0, at ×20 (left column) and ×63 magnification (right column). For mixed gels, are shown images obtained in the planes XY, XZ and YZ of the samples. Scale bar = 80 μm.

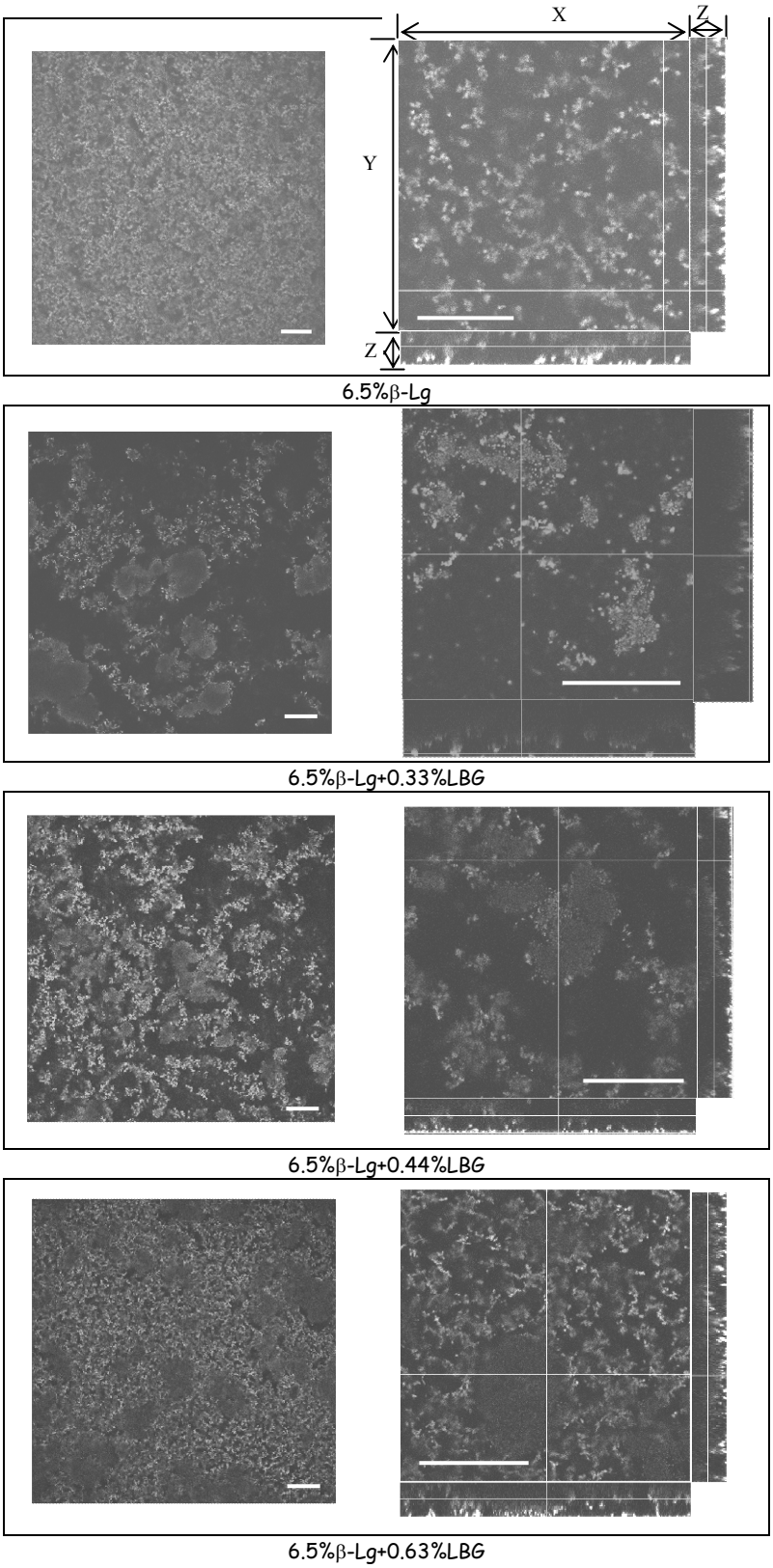

Figure 5.12 CLSM micrographs of β-LG gels, pure or mixed with LBG, at 20°C and pH 4.6, at ×20 (left column) and ×63 magnification (right column). For mixed gels, are shown images obtained in the planes XY, XZ and YZ of the samples. Scale bar = 80 μm.

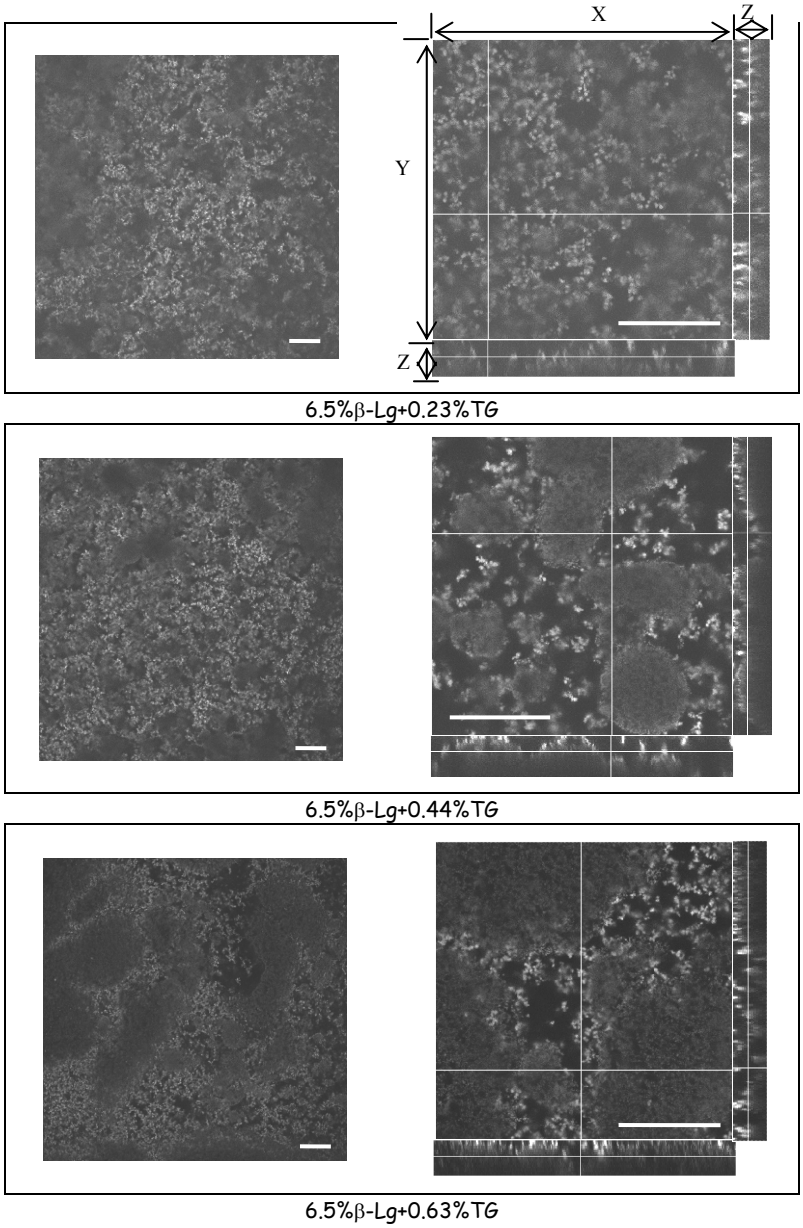

Figure 5.13 CLSM micrographs of β-LG gels mixed with TG, at 20°C and pH 4.6, at ×20 (left column) and ×63 magnification (right column). For mixed gels, are shown images obtained in the planes XY, XZ and YZ of the samples. Scale bar = 80 μm.

Figures 5.12 and 5.13 show some micrographs obtained for gels prepared at pH 4.6: less homogeneous, coarser, particulate gels are now observed, differing from the stranded gels obtained at pH 7.0. The pure β-lactoglobulin gel appeared like a homogeneous and dense

network with small pores between the strands of clusters, when the ×20 objective was used (Figure 5.12, left column). At higher magnification, the gel showed the same type of structure. When galactomannan was added, the microstructure was altered: it became less homogeneous and more open, with larger pores, the higher the galactomannan concentration (Figures 5.12 and 5.13, right columns). The clusters were largest for gels containing the highest concentration of galactomannan. It was also possible to see that the density of the protein phase depended on where in the gel we were looking. Gels with higher galactomannan concentrations had a more heterogeneous protein structure with small and large pores between the clusters of protein.

When analysing the above results on β-lactoglobulin / galactomannan mixed systems, it is clear that the presence of the galactomannan influenced the rheological properties and the microstructure of β-lactoglobulin gels, at both pHs. These observations may be explained by the phase separation occurring in the systems induced by the polysaccharide. A possible driving force for phase separation is depletion of polysaccharide chains at the surfaces of the protein aggregates (Croguennoc, Durand, Nicolai, and Clark, 2001).

During heating of the mixed systems, the protein aggregates grow in size; depletion-induced phase separation may occur as soon as the aggregates reach some critical size, which depends on the polysaccharide concentration. In the present study and as was seen in the previous chapter (section 4.3.1), mixed systems were already phase-separated at room temperature. Because of phase separation, protein concentration increased in the protein-rich phase which possibly explains the increased aggregation/gelation rate of the mixed systems. As the polysaccharide concentration increased, the microstructure coarsened. Probably, this may be explained by the formation of denser protein particle aggregates meaning that, for a given protein concentration, the volume fraction of the particle aggregates became smaller

(Croguennoc, Durand, Nicolai, and Clark, 2001). The coarsening of the structure was not enough to weaken the gels, in the present case, as was observed before in other protein / polysaccharide systems (Gonçalves et al., 2004; Capron et al., 1999). In fact, values of *G´* increased with galactomannan concentration. The only exceptions were the 0.23%TG and the 0.33%LBG mixed gels, at pH 4.6 (Table 5.4). A probable explanation for the decrease of *G´* and stress at fracture for these two mixed gels is that the connectivity of the protein network is less than for the pure β-lactoglobulin gel. However, from the micrographs in Figures 5.12 and 5.13, it is not obvious to confirm this assumption. As pointed out by Olsson and co-workers (2002), the connectivity of the protein network is a very dominant parameter and gels with similar cluster and pore sizes can show completely opposite rheological behaviour. There is probably interplay between the connectivity, the size of clusters and the size of pores between the clusters. For observing an increase in *G´*, the strands of clusters have to be connected to each other no matter how thick they are or how large the clusters are.

From the low oscillatory shear experiments, no marked differences could be seen between the pure and mixed gels, at each pH, although they presented different microstructures. The shape of the gelation curves and that of the mechanical spectra were little affected. Only an enhancement of the aggregation rate and of the strength of the final gel was observed. These effects were more pronounced for LBG, the less substituted of the two galactomannans studied. A similar behaviour was found by Tavares and co-workers (2005) for whey protein / galactomannan mixed gels, at pH 7.0. These authors considered that the dispersed polysaccharide-rich phase acted as active filler that reinforced the protein network and increased the moduli (Monteiro et al., 2005).

In large oscillatory shear experiments (strain sweeps), differences between the shapes of the curves at pH 7.0 and pH 4.6 were, however, observed in the non-linear region which probably reflected the very different microstructures of both type of gels.

5.3.2 Effect of shear treatment on the rheology of mixed gels

In a second series of experiments, the effects of steady shear treatment, during gelation on the rheological properties of the final gels was studied on some of the mixed systems tested in section 5.3.1, using the procedures describe in section 5.2.3.2. Shear was applied to the system, at the end of the first step (20 – 80°C heating step), for 3 min, at a constant rate of 120 s^{-1}. Results were compared with those obtained for unsheared systems, at similar concentrations.

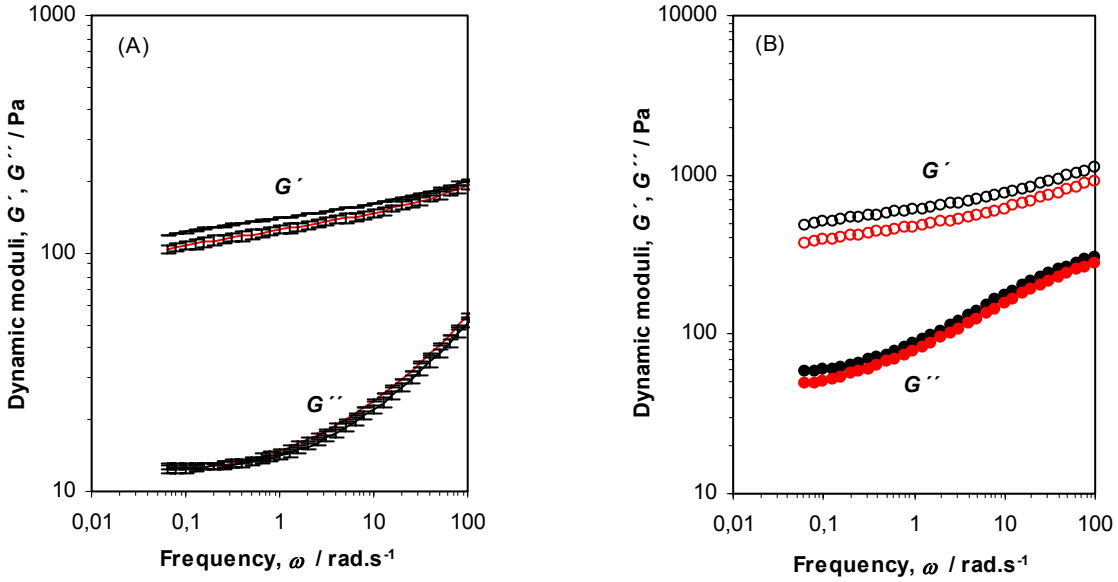

Figure 5.14 Effect of shear on the mechanical spectra for mixed gel systems, at 20°C and pH 7.0. A: 6.5%β-Lg+0.20%TG and B: 6.5%β-Lg+0.60%TG. Shear treatment: unsheared (black colour) and 120 s^{-1} (red colour).

Frequency sweeps did not reveal important differences in the viscoelastic properties of shear-treated and unsheared gels. A small decrease of G' was observed for the shear-treated gels; however, the shape of the G' and G'' curves was the same for all gels (Figure 5.14). The effect of applied shear was, then, a decrease of gel rigidity (G' decreased) and of gel elasticity (tan δ increased) (Table 5.5).

Table 5.5 Values of tan δ and G' for unsheared and sheared mixed gels, at 20°C and pH 7.0, at 6.28 rad.s^{-1}

TG concentration (wt%)	Shear applied (s^{-1})	tan δ	G' (Pa)
0.20	0	1.27×10^{-1}	1.57×10^{2}
	120	1.46×10^{-1}	1.46×10^{2}
0.44	0	2.15×10^{-1}	3.84×10^{2}
	120	2.26×10^{-1}	3.28×10^{2}
0.60	0	2.10×10^{-1}	7.20×10^{2}
	120	2.33×10^{-1}	5.76×10^{2}

Results obtained by fitting a Cole-Cole model to the compliance data, showed that the height of the viscoelastic plateau, G_N^0, and the position of the peak, ω_0, decreased while the spread coefficient, p, did not significantly change (Table 5.6).

Table 5.6 Rheological parameters extracted from the analysis of the mechanical spectra for unsheared and sheared mixed gels, recorded at 20ºC and pH 7.0. (Values obtained by fitting Eqs. 5.15 and 5.16 with $J_g = 0$)

TG concentration (%)	Shear rate (s^{-1})	$G_N^0 = 1/J_N^0$ (Pa)	ω_0 (rad.s^{-1})	p
0.20	0	132	270	0.41
	120	125	240	0.41
0.44	0	217	12	0.29
	120	179	8	0.29
0.60	0	417	12	0.29
	120	303	7	0.28

In small deformation measurements, the whole structure contributes equally since no parts of the structure are broken. However, in large deformation measurements, the structure is broken starting by the weaker areas. So, some information about differences in the structure of the gels would be expected from stress sweep experiments performed up to rupture. But, only minor differences were observed between shear-treated and unsheared gels (Figure 5.15), both exhibiting strain hardening.

Shear-treated gels showed lower G'_0 and E (G'_{max}/G'_0) values and fractured at lower strains than the unsheared gels (Table 5.7).

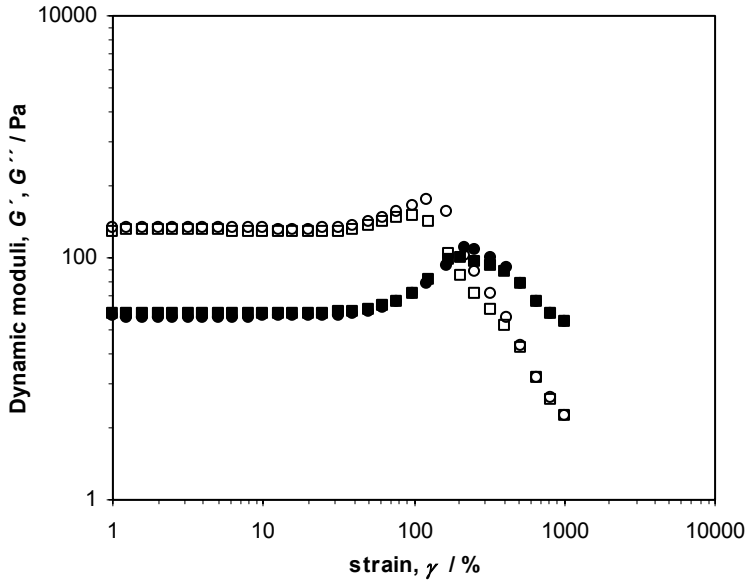

Figure 5.15 Strain dependence of storage modulus G' (open symbols) and loss modulus, G'' (full symbols) at 6.28 rad.s^{-1} for 6.5%β-Lg+0.20%TG gels. Unsheared gel: (O); sheared gel (120 s^{-1} for 3 min, at 80 ºC): (□).

Table 5.7 Values obtained from strain sweep tests for unsheared and sheared mixed gels, at 20^{o}C and pH 7.0

TG concentration (wt%)	Shear applied (s^{-1})	G'_0 (Pa)	G'_{max} (Pa)	γ_r (%)	$E = G'_{max} / G'_0$
0.20	0	175	299	123	1.71
	120	165	219	99	1.33
0.44	0	482	495	39.65	1.03
	120	422	431	39.61	1.02
0.60	0	896	963	79	1.07
	120	745	754	50	1.01

The above results show that the applied shear did not induce important changes in the rheology and, probably, in the microstructure of the final gels.

Other experiments, using different shear rates/time of shear, should be tested to obtain a wider range of data allowing a better characterization of the shear effects on the mixed gels.

5.3.3 Characterization of the viscoelasticity of mixed gels by combination of transient and dynamic measurements

In a third series of experiments, a new set of mixed systems (10%β-Lg+0 – 0.78%LBG) was studied, at pH 7.0. Heat-set gels were prepared according to the procedures described in section 5.2.3.2. Mechanical spectra were recorded at 20°C; then, gels were submitted to a retardation (creep and creep recovery) test (see section 5.2.3.2).

5.3.2.1 Analysis of creep and creep recovery curves

Figure 5.16 gives examples of creep and creep recovery curves, showing that the gels are viscoelastic liquids. The liquid character is unambiguously demonstrated by the fact that a substantial part of the final creep strain is not recovered after five hours recovery, while recovery strain is approaching or has reached a plateau value.

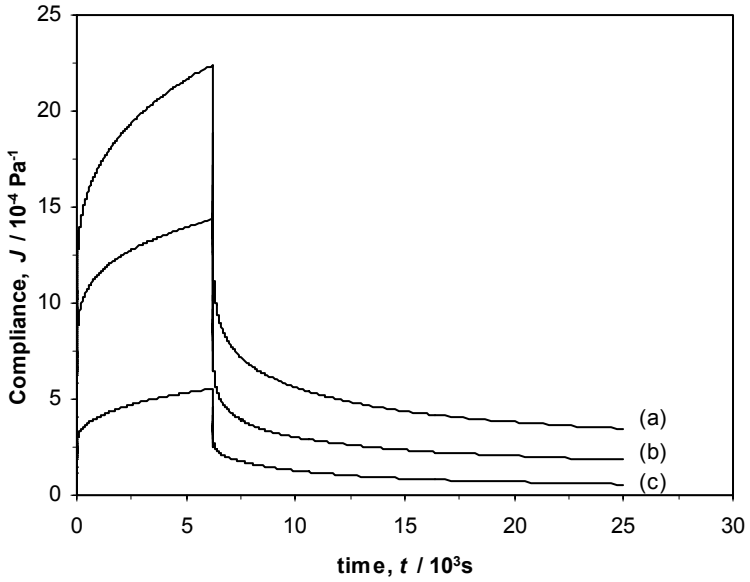

Figure 5.16 Creep and creep recovery curves for gels of 10%β-Lg (a), 10%β-Lg+0.35%LBG (b), and 10%β-Lg+0.55%LBG (c) at 20°C and pH 7.0.

From the terminal regions of the creep and of the recovery curves, the steady state recoverable compliance, J_e^0, and steady state viscosity, η_0, can be determined following the procedure as described in section 5.2.3.2.1.

Values of J_e^0 and η_0 obtained from creep curves were close to those obtained from recovery curves (Table 5.8), giving indication that the retardation tests were performed within the linear viscoelastic range of the gels. This is confirmed by the fact that the curves of the recoverable compliance $J_r(t) = J(t)-1/(\eta_0.\omega)$ obtained from creep data practically superimpose on those of $J_r(t)$ directly determined from recovery data (Figure 5.17). Figure 5.17 illustrates, moreover, that the viscoelastic response of the gels spans a very large time scale.

Table 5.8 Comparison of the values of steady state recoverable compliance, J_e^0, and steady state viscosity, η_0, determined from the creep part with those determined from the creep recovery part of retardation tests applied to gel systems, at 20°C

LBG Conc.	Creep		Creep recovery	
(wt%)	J_e^0 (1/Pa)	η_0 (Pa.s)	J_e^0 (1/Pa)	η_0 (Pa.s)
0	1.83×10^{-3}	1.51×10^{7}	1.75×10^{-3}	1.29×10^{7}
0.35	1.22×10^{-3}	2.86×10^{7}	1.18×10^{-3}	2.37×10^{7}
0.45	3.97×10^{-4}	6.61×10^{7}	3.97×10^{-4}	1.19×10^{8}
0.55	4.45×10^{-4}	5.66×10^{7}	4.50×10^{-4}	5.96×10^{7}
0.65	4.92×10^{-4}	5.67×10^{7}	4.91×10^{-4}	5.54×10^{7}
0.78	3.93×10^{-4}	7.71×10^{7}	4.02×10^{-4}	8.58×10^{7}

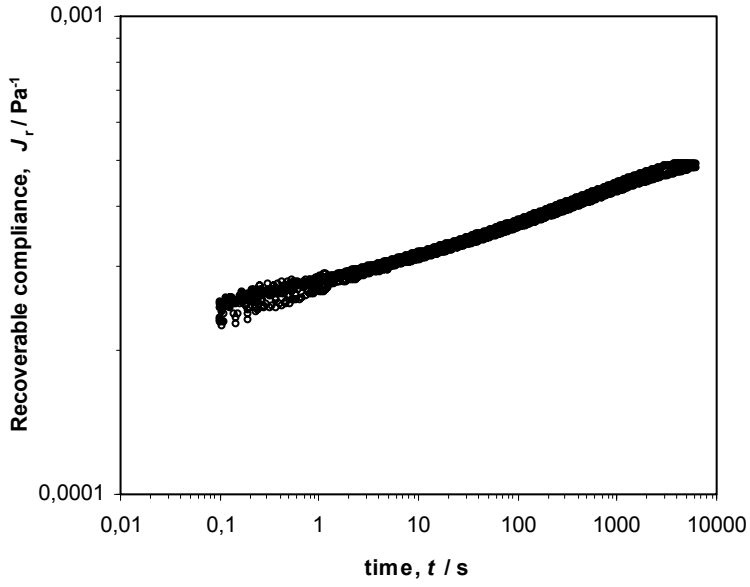

Figure 5.17 Recoverable compliance $J_r(t)$ from creep (full symbols) and from creep recovery (open symbols) data of 10%β-Lg+0.65%LBG gel at pH 7.0.

5.3.2.2 Combination of dynamic and creep recovery results

After equilibration of the gels at 20°C, mechanical spectra were recorded in dynamic mode Very similar shapes, characteristic of colloidal gels, were observed: rather flat G' and G'', but relatively high tan δ values (ca. 0.1) in all cases (results not shown). The data, represented in terms of the storage and loss compliance, were tentatively fitted with a Cole-Cole model (see section 5.3.1.2). Values obtained from the fitting are given in Table 5.9.

Table 5.9 Rheological parameters extracted from the analysis of the mechanical spectra of the gels, recorded at 20ºC and pH 7.0. (Values obtained by fitting Eqs. 5.15 and 5.16 with $J_g = 0$)

LBG concentration (%)	$J_N^0 = 1/G_N^0$ (Pa^{-1})	ω_0 ($rad.s^{-1}$)	p
0	1.13×10^{-3}	1160	0.23
0.35	8.45×10^{-4}	37	0.24
0.65	2.99×10^{-4}	630	0.32
0.78	2.55×10^{-4}	300	0.30

The ratio J_e^0 / J_N^0 is between 1.5 and 1.7, which seems a reasonable value. The dynamic measurements yield results of quite higher quality than do transient methods (creep and creep recovery) at short times (high frequencies). In compensation, transient methods are well suited for experiments carried over for long periods of time. In order to obtain a better characterization of the viscoelasticity of the gelled systems, an enlargement of the frequency (time) window is required. Such an enlargement is possible in the low frequency (large time) direction by combining the data of the retardation test with those of dynamic measurements. The discrete retardation spectra were obtained from the recoverable compliance $J_r(t)$ using the method of

Kaschta (Kaschta et al., 1994). To avoid the problem related with the delimitation of the creep terminal region, the creep recovery data were used (Table 5.10).

Table 5.10 Retardation spectra as calculated from the creep recovery data for gel systems at 20°C with a logarithmic equidistant spacing of retardation times

10%β-Lg		10%β-Lg+0.35%LBG		10%β-Lg+0.45%LBG	
$t_1 = 3.01\times10^{-1}$ s, $t_M = 1.88\times10^{4}$ s		$t_1 = 2.51\times10^{-1}$ s, $t_M = 1.88\times10^{4}$ s		$t_1 = 1.99\times10^{0}$ s, $t_M = 1.87\times10^{4}$ s	
$J_0 = 8.04\times10^{-4}$ Pa^{-1}		$J_0 = 5.43\times10^{-4}$ Pa^{-1}		$J_0 = 1.97\times10^{-4}$ Pa^{-1}	
τ_i (s)	J_i (Pa^{-1})	τ_i (s)	J_i (Pa^{-1})	τ_i (s)	J_i (Pa^{-1})
1.77×10^{-1}	1.57×10^{-7}	6.18×10^{-2}	1.24×10^{-7}	2.89×10^{-1}	1.65×10^{-8}
8.83×10^{-1}	8.80×10^{-5}	3.09×10^{-1}	5.63×10^{-5}	1.45×10^{0}	1.75×10^{-5}
4.42×10^{0}	8.25×10^{-5}	1.55×10^{0}	5.53×10^{-5}	7.23×10^{0}	1.80×10^{-5}
2.21×10^{1}	1.05×10^{-4}	7.73×10^{0}	6.38×10^{-5}	3.62×10^{1}	2.61×10^{-5}
1.10×10^{2}	1.60×10^{-4}	3.87×10^{1}	8.11×10^{-5}	1.81×10^{2}	3.31×10^{-5}
5.52×10^{2}	1.59×10^{-4}	1.93×10^{2}	1.13×10^{-4}	9.04×10^{2}	3.66×10^{-5}
2.76×10^{3}	3.48×10^{-4}	9.66×10^{2}	1.18×10^{-4}	4.52×10^{3}	7.16×10^{-5}
-	-	4.83×10^{3}	2.07×10^{-4}	-	-

10%β-Lg+0.55%LBG		10%β-Lg+0.65%LBG		10%β-Lg+0.78%LBG	
$t_1 = 3.01\times10^{-1}$ s, $t_M = 1.88\times10^{4}$ s		$t_1 = 1.61\times10^{0}$ s, $t_M = 1.88\times10^{4}$ s		$t_1 = 1.99\times10^{-1}$ s, $t_M = 1.88\times10^{4}$ s	
$J_0 = 6.81\times10^{-7}$ Pa^{-1}		$J_0 = 2.53\times10^{-4}$ Pa^{-1}		$J_0 = 1.77\times10^{-4}$ Pa^{-1}	
τ_i (s)	J_i (Pa^{-1})	τ_i (s)	J_i (Pa^{-1})	τ_i (s)	J_i (Pa^{-1})
4.24×10^{-2}	1.97×10^{-4}	2.41×10^{-1}	6.38×10^{-8}	1.96×10^{-1}	2.14×10^{-5}
2.12×10^{-1}	1.74×10^{-5}	1.21×10^{0}	2.67×10^{-5}	9.82×10^{-1}	1.85×10^{-5}
1.06×10^{0}	1.72×10^{-5}	6.03×10^{0}	2.31×10^{-5}	4.91×10^{0}	2.15×10^{-5}
5.30×10^{0}	2.05×10^{-5}	3.02×10^{1}	3.13×10^{-5}	2.46×10^{1}	2.47×10^{-5}
2.65×10^{1}	2.55×10^{-5}	1.51×10^{2}	4.19×10^{-5}	1.23×10^{2}	4.01×10^{-5}
1.32×10^{2}	4.17×10^{-5}	7.54×10^{2}	5.27×10^{-5}	6.14×10^{2}	3.73×10^{-5}
6.62×10^{2}	2.55×10^{-5}	3.77×10^{3}	6.26×10^{-5}	3.07×10^{3}	7.18×10^{-5}
3.31×10^{3}	1.06×10^{-4}	-	-	-	-

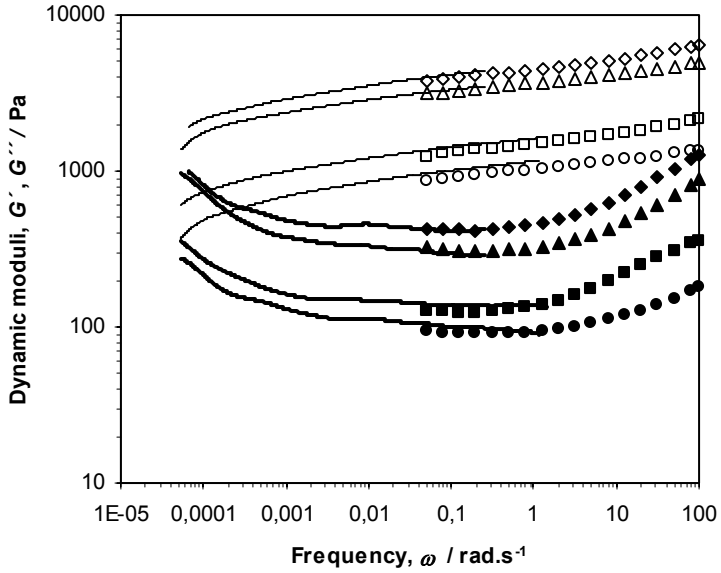

Figure 5.18 Examples of the mechanical spectra of gel systems at 20°C obtained by combining creep recovery data (lines) and dynamic data (symbols): 10%β-Lg (O),10%β-Lg+0.35%LBG (□), 10%β-Lg+0.65%LBG (Δ) and 10%β-Lg+0.78%LBG (◇). Open symbols and thin lines: G'; full symbols and thick lines: G''.

Once the discrete spectrum calculated, $J'(\omega)$, $J''_r(\omega) = J''(\omega)-1/(\eta_0.\omega)$ and $J''(\omega)$, and then $G'(\omega)$ and $G''(\omega)$, were obtained straightforwardly. Figure 5.18 gives examples of composite mechanical spectra plotted in terms of $G'(\omega)$ and $G''(\omega)$ by combining dynamic data and creep converted recoverable data; the data from creep recovery match satisfactorily direct dynamic measurements, a further indication that all rheological measurements were performed within the linear range. The bimodal character of the spectra is clearly visible. The viscoelastic plateau extends down into the 0.001 – 0.0001 rad.s^{-1} range. Its lower frequency limit does not seem to vary much with LBG concentration. Its upper frequency limit is visibly beyond 100 rad.s^{-1}; to encompass it would require dynamic measurements at high frequencies which are not possible with stress controlled rotational rheometers because of moving part inertial problems; in the

case of the present systems, software inertial correction ceased to work effectively above 100 $rad.s^{-1}$.

5.4 Conclusions

The results obtained in this chapter clearly show that the presence of galactomannans influenced the heat-set gelation behaviour of β-lactoglobulin solutions, the linear viscoelasticity, the large amplitude oscillatory shear behaviour and the microstructure of final gels, at pH 4.6 and at pH 7.0. The extent of these changes depended on galactomannan concentration.

From the CLSM images, it was concluded that phase separation occurred for all mixed systems at pH 7.0 and pH 4.6, while for pure β-lactoglobulin gels no phase separation could be detected, within the resolution of the confocal microscope. At pH 4.6, less homogeneous, coarser, particulate gels were observed, differing from the stranded gels obtained at pH 7.0 which means that different aggregation/gelation processes took place at each pH. In both cases, the microstructure coarsened as the polysaccharide concentration increased, which may be due to the formation of denser protein particle aggregates implying that, at a given protein concentration, the volume fraction of the particle aggregates became smaller.

From the low oscillatory shear experiments, no marked differences could be seen between the pure and mixed gels, at each pH, although they presented different microstructures. The shape of the gelation curves and that of the mechanical spectra were little affected. Only an enhancement of the aggregation rate and of the strength of the final gels was observed. The increased protein concentration in the protein-rich phase, due to phase separation, possibly explains the increased aggregation/gelation rate of all the mixed systems studied, as well as the increased strength of the final gels though, in the later case, the network connectivity must also play an important role. The above effects were more pronounced for LBG, the less substituted

of the two galactomannans studied, which points to a possible effect of the chemical structure on the rheology of the mixed systems.

In large oscillatory shear experiments (strain sweeps), gels formed at pH 4.6 were stronger and showed higher sensitivity to strain than gels, of similar concentration, formed at pH 7.0. Differences in the shapes of the curves at pH 7.0 and pH 4.6 were, also, observed in the non-linear region: at pH 7.0, both G' and G'' showed strain hardening behaviour (both moduli increased) followed by strain thinning while, at pH 4.6, no strain hardening was observed; instead, G' and G'' remained almost constant and then suddenly decreased with increasing strain. These different behaviours reflected the very different microstructures of both type of gels.

Applying shear as a pulsing near the gel point, at pH 7.0, did not cause dramatic changes in the viscoelastic properties of shear-treated and unsheared gels. Only small decreases of gel rigidity and gel elasticity were observed for the shear-treated gels; the shape of the G' and G'' curves was the same for all gels. In large deformation measurements, minor differences were, also, observed between shear-treated and unsheared gels, both exhibiting strain hardening. Shear-treated gels fractured at lower strains than unsheared gels. These results may point to changes in the microstructure of the gels, induced by shear. However, other experiments, using different shear rates/time of shear, should be tested to obtain a wider range of data allowing a better characterization of the shear effects on the mixed gels.

Finally, a better characterization of the viscoelasticity of some of the gelled systems, at pH 7.0, was done, in the low frequency direction, by combining the data of the retardation test (creep and creep recovery) with those of dynamic measurements. It was verified that the data from

creep recovery matched satisfactorily direct dynamic measurements, confirming that all rheological measurements were performed within the linear range. Moreover, it was possible to conclude that the viscoelastic plateau extended down into the 0.001 – 0.0001 rad.s^{-1} range, for all the mixed systems analyzed and that its lower frequency limit did not to vary much with galactomannan concentration.

General conclusions and recommendations for future work

General conclusions

In this section, an overview of the results will be presented since, at the end of each chapter of the thesis, the main conclusions have been presented.

It was shown that the thermal gelation and the rheology of the final pure β-lactoglobulin gels depend on the protein concentration, the pH and the processing conditions. At pH 4.6, near the isoelectric point of the protein, gels form at lower temperature and sooner than at pH 7.0 (when the protein bears a net negative charge); the final gels are stronger than those formed at pH 7.0 but show higher sensitivity to strain. These differences are consistent with the microstructures expected for the two types of gels – particulate gels at pH 4.6 and fine-stranded gels, at pH 7.0 – which is a consequence of the balance between repulsive and attractive forces among protein molecules. The rheological analysis proved to be a useful method to analyze the structure of concentrated β-lactoglobulin gels (C > 9 wt%), at pH 7.0. The value of the fractal dimension, evaluated from oscillatory frequency data and strain sweep tests using the scaling relationships of Shin and co-workers and of Wu and Morbidelli, point to reaction-limited cluster-cluster aggregation processes, suggesting that, because of electrostatic repulsions, many collisions must occur before the protein molecules stick together forming aggregates.

Regarding the galactomannans, the results obtained show that locust bean gum and tara gum exhibit quite similar rheological properties, in the range of concentrations and shear rates/frequencies studied. The dependence of the specific viscosity at zero shear rate, η_{sp0}, on the coil overlap parameter, $C[\eta]$, put in evidence a similar behaviour for the two polysaccharides; results support the random coil type behaviour for both galactomannans. Experimental data were correlated with the Cross and Carreau models, in steady shear, and with

the generalized Maxwell model with four elements and the Friedrich-Braun model, in oscillatory shear (mechanical spectra). Also, time-concentration superposition holds for locust bean gum and tara gum solutions, allowing master curves to be found for both the viscous and the linear viscoelastic response in shear flow. The similar profile observed probably reflects the existence of non-specific physical entanglements in these galactomannan solutions.

The subsequent study of β-lactoglobulin / galactomannan mixed aqueous systems focused on investigating the relationship between the rheological properties and the microstructure of the systems, at pH 7.0 and pH 4.6, in the sol and gel states, using a combination of rheology and confocal laser scanning microscopy. Some of our major findings are summarized below:

- For all mixed systems studied, in the sol state, phase separation (thermodynamic incompatibility) occurred at both pH values (7.0 and 4.6), as revealed by CLSM images. The observed microstructure and the rheological response depend on the pH and on the composition of the mixed systems.

At pH 4.6, in the concentration range studied, the microstructure corresponds to systems in the region of the phase diagram where β-lactoglobulin is the enriched continuous phase. The flow curves, like β-lactoglobulin alone, show a Newtonian behaviour.

At pH 7.0, by increasing the galactomannan concentration, phase inversion is detected in the mixed systems: the microstructure evolves from a continuous matrix of β-lactoglobulin enriched phase containing some small inclusions of the galactomannan, to a matrix of galactomannan enriched continuous phase containing aggregates of β-lactoglobulin. The microstructures of the mixed systems with locust bean gum and tara gum are similar when

comparing systems with similar reduced concentration of the two galactomannans. The changes in microstructure correlate with differences observed in the rheology of the systems: in the region where the continuous phase is enriched in β-lactoglobulin, the flow behaviour of the mixtures is Newtonian, like that of the pure protein, though the viscosity is higher. The concentration of the protein in the continuous phase as a result of phase separation, induced by the presence of the polysaccharide, may explain the increase of the viscosity. In the region where the continuous phase is enriched in galactomannan, the flow behaviour is typical of a suspension, probably as a result of the flocculation of the β-lactoglobulin enriched disperse phase. The flow curves, with an apparent yield stress, can be described by the modified Cross model. For all mixtures, the plateau viscosity is lower than the η_0 for the galactomannan solution of the same concentration as in the mixture.

- All mixed gel systems studied are two-phase, at both pH values (7.0 and 4.6). The observed microstructure depends on pH and composition of the gel: stranded gels are obtained at pH 7.0 while less homogeneous, coarser, particulate gels are observed at pH 4.6, meaning that different aggregation/gelation process took place at each pH. In both cases, when the galactomannan concentration increases, the microstructure coarsens. However, the rheological behaviour remains qualitatively similar to that of the pure protein gel and its quantitative modifications remain limited within the experimental window explored. Only an enhancement of the aggregation rate and of the strength of the final gels is observed, in low oscillatory shear experiments. These effects are more pronounced for locust bean gum, the less substituted of the two galactomannans studied, which points to a possible effect of the chemical structure on the rheology of the mixed systems. In large oscillatory shear experiments (strain sweeps), differences between the shapes of the curves at pH 7.0 and pH 4.6 were, however, observed in

the non-linear region which probably reflects the very different microstructures of both type of gels.

- All the results obtained show that it is possible to modify the structural and rheological properties of the mixed β-lactoglobulin / galactomannan aqueous systems, in the sol and gel states, by changing the mixing ratio of the two biopolymers and the pH of the medium.

It is expected that the results obtained in these thesis may contribute to a better understanding of β-lactoglobulin / neutral polysaccharide mixed systems properties. It was shown that, by changing the mixing ratio of the two biopolymers and the pH of the medium, it is possible to manipulate the structure and the rheological properties of the mixed systems, which may find useful applications, for example, in the development of innovative food products.

Recommendations for future work

The study is not complete yet and several other possibilities can be suggested to continue it. The main focus of this work has been directed towards understanding the behaviour of the mixed aqueous systems, in the sol and gel states, in a limited range of protein-to-polysaccharide ratio, due to the experimental constraints. Future work should include design of additional experiments to fill in the gap in our understanding of these systems. The scope of the study can be extended to include characterization of properties in the presence of galactomannans under varying conditions using a combination of rheological properties and microstructural information.

(i) β-lactoglobulin / galactomannan mixed aqueous systems

From the results obtained in the present work, it was found that phase separation occurred at room temperature for all mixtures, at pH 7.0 and pH 4.6. However, the experiments were done in a narrow range of concentrations/mixing ratios, as was mentioned above. Phase diagrams could not be obtained. Thus, it would be interesting to design future experiments for working on other ranges of protein-to-polysaccharide ratio (for instance, fixing the polysaccharide concentration and varying the protein concentration) and temperatures, in order to obtain a wider range of data enabling a more accurate estimation of phase diagrams or, at least, a better characterization of the systems.

(ii) Effect of processing conditions on β-lactoglobulin / galactomannan gels

An investigation into the effect of shear on pure and mixed protein gels, at pH 7.0 and pH 4.6, was initiated in this thesis. The results showed that, for pure protein gels, shear may prevent rapid aggregation into weak networks causing an increase in gel strength, or it may disrupt β-lactoglobulin aggregates causing a decrease in gel strength, depending on shear conditions. In the case of mixed gels, only small decreases of gel rigidity and gel elasticity were observed for the shear-treated gels, under the shear conditions studied. However, only a limited number of experiments were done. Thus, it would be interesting to design new experiments spanning a wider range of shear rates/time of shear, in order to obtain information allowing a better characterization of the shear effects on the mixed gels. In addition, confocal laser scanning microscopy should be used for observing possible changes in microstructure of final gels as compared to unsheared ones.

Besides shear, parameters like time, temperature and rate of heating are known to affect the properties of final β-lactoglobulin gels. These same parameters must also affect the properties of the mixed gels, as was inferred from preliminary experiments done in this thesis. So, a more systematic study of their effect seems relevant too.

References

AOAC, Association of Official Analytical Chemists. (1975). Official methods of analysis. 12th ed. AOAC, Washington, D.C.

Alais, C., & Linden, G. (1991). Food Biochemistry. New York: Ellis Horwood.

Altmann, N., Cooper-White, J. J., Dunstan, D. E., & Stokes, J. R. (2004). Strong through to weak "sheared" gels. *Journal of Non-Newtonian Fluid Mechanics, 124*, 129-136.

Alves, M., Antonov, Y. A., & Gonçalves, M. P. (1999). On the incompatibility of alkaline gelatin and locust bean gum in aqueous solution. *Food Hydrocolloids, 13,* 77-80.

Alves, M., Garnier, C., Lefebvre, J., & Gonçalves, M. P. (2001). Microstructure and flow behaviour of liquid water-gelatin-locust bean gum systems. *Food Hydrocolloids, 15*, 117-125.

Andrade, C. T., Azero, E. G., Luciano, L., & Gonçalves, M.P. (1999). Solution properties of the galactomannans extracted from the seeds of *Caesalpinia pulcherrima* and *Cassia javanica*: comparison with locust bean gum. *International Journal of Biological Macromolecules, 26*, 181-185.

Antonov, Y. A., & Gonçalves, M. P. (1999). Phase separation in aqueous gelatin-κ-carrageenan systems. *Food Hydrocolloids, 13*, 517-524.

Arai, M., Ikura, T., Semisotnov, G. V., Kihara, H., Amemiya, Y., & Kuwajima, K. (1998). Kinetic refolding of β-lactoglobulin. Studies by synchrotron X-ray scattering, and circular dichroism, absorption and fluorescence spectroscopy. *Journal of Molecular Biology, 275*, 149-162.

Aymard, P., Nicolai, T., Durand, D., & Clark, A. (1999). Static and Dynamic Scatting of β-lactoglobulin aggregates formed after hear-induced denaturation at pH 2. *Macromolecules, 32*, 2542-2552.

Batlle, I., & Tous, J. (1997). Carob tree. *Ceratonia siliqua L.*: Promoting the conservation and use of underutilized and neglected crops 17. Rome: Institute of Plant Genetics and Crop Plant Research.

Baussay, K., Le Bon, C., Nicolai, T., Durand, D., & Busnel, J.-P. (2004). Influence of the ionic strength on the heat-induced aggregation of the globular protein β-lactoglobulin at pH 7. *International Journal of Biological Macromolecules, 34*, 21-28.

Blakeney, A. B., Harris, P. J., Henry, R. J., & Stone, B. A. (1983). A simple and rapid preparation of alditol acetates for monosaccharide analysis. *Carbohydrate Research, 113*, 291-299.

BOT, http://www.botgard.ucla.edu/html/botanytextbooks/economicbotany/Ceratonia/a0824tx.html, 2005.

Botelho, M. M., Valente-Mesquita, V. L., Oliveira, K. M. G., Polikarpov, I, & Ferreira, S. T. (2000). Pressure denaturation of β-lactoglobulin different stabilities of isoforms A and B, and an investigation of the Tanford transition. *European Journal of Biochemistry, 267*, 2235-2241.

Bottomley, R. C., Evans, M. T. A., Parkinson, C. J. (1990). Whey proteins. In P. Harris. *Food Gels* (pp. 435-467). UK: Elsevier Applied Science.

Bourriot, S., Garnier, C., & Doublier, J. L. (1999). Phase separation, rheology and structure of micellar casein-galactomannan mixtures. *International Dairy Journal, 9*, 353-357.

Bradford, M. M. (1976). A rapid and sensitive method for quantitation of microgram quantities of protein utilizing the principle of protein-dye-binding. *Analytical Biochemistry, 72*, 248-254.

Bremer, L. G. B., van Vliet, T., & Walstra, P. (1989). Theoretical and experimental study of the fractal nature of the structure of casein gels. *Journal of the Chemical Society, Faraday Transaction 1, 85*, 3359-3372.

Brown, W. D., & Ball, R. C. (1985). Computer simulation of chemically limited aggregation. *Journal of Physics A: Mathematical and General, 18*, L517-L521.

Bryant, C. M., & McClements, D. J. (2000). Optimizing preparation conditions for heat-denatured whey protein solutions to be used as cold-gelling ingredients. *Food Chemistry and Toxicology, 65*, 259-263.

Capron, I., Nicolai, T., & Durand, D. (1999). Heat induced aggregation and gelation of β-lactoglobulin in the presence of κ-carrageenan. *Food Hydrocolloids, 13*, 1-5.

Capron, I., Nicolai, T., & Smith, C. (1999). Effect of addition of κ-carrageenan on the mechanical and structural properties of β-lactoglobulin gels. *Carbohydrate Polymers, 40*, 233-238.

Carreau, P. J. (1972). Rheological equations from molecular network theories. *Transactions of the Society of Rheology, 16*, 99-127.

Castelain, C., Doublier, J. L., & Lefebvre, J. (1987). A study of the viscosity of cellulose derivatives in aqueous solutions. *Carbohydrate Polymers, 7*, 1-16.

Castelain, C., Lefebvre, J., & Doublier, J. L. (1986). Rheological behaviour of BSA-cellulose derivative mixtures in aqueous medium. *Food Hydrocolloids, 1*, 141-151.

CDM, http://www.cdm-impex.de/index.html?entrance.html, 2005.

Clark, A. H., Dea, I. C. M., & Rees, D. A. (1985). The fine structures of carob and guar galactomannans. *Carbohydrate Research, 139*, 237-260.

Clark, A. H., & Ross-Murphy, S. B. (1987). Structural and mechanical properties of biopolymer gels. *Advanced Polymers Science, 83*, 57-192.

Clark, A. H., Kavanagh, G. M., & Ross-Murphy, S. B. (2001). Globular protein gelation-theory and experiment. *Food Hydrocolloids, 15*, 383-400.

CLA, http://class.fst.ohio-state.edu/FST822/lectures/milk2.htm, 2002.

CLA, http://class.fst.ohio-state.edu/FST822/lectures/Funct.htm, 2005.

Coimbra, M. A., Delgadillo, I., Waldron, K. W., & Selvendran, R. R. (1996). Isolation and analysis of cell wall polymers from olive pulp. In H. F. Linskens, & J. F. Jackson, *Modern Methods of Plant Analysis, vol.17-Plant Cell Wall Analysis* (p. 19). Berlin–Heidelberg: Springer-Verlag.

Courtois, J. E., & Le Dizet, P. (1966). Action de l′α-galactosidase du café sur quelques galactomannanes. *Carbohydrate Research, 3*, 141-151.

Croguennec, T., O'Kennedy, B. T., & Mehra, R. (2004). Heat-induced denaturation/aggregation of β-lactoglobulin A and B: kinetics of the first intermediates formed. *International Dairy Journal, 14*, 399-409.

Croguennoc, P., Durand, D., Nicolai, T., & Clark, A. (2001). Phase separation and association of globular protein aggregates in the presence of polysaccharides: 1. mixtures of preheated β-lactoglobulin and κ-carrageenan at room temperature. *Langmuir, 17*, 4372-4379.

Croguennoc, P., Durand, D., Nicolai, T., & Clark, A. (2001). Phase separation and association of globular protein aggregates in the presence of polysaccharides: 2. heated mixtures of native β-lactoglobulin and κ-carrageenan. *Langmuir, 17*, 4380-4385.

Cross, M. M. (1965). Rheology of non Newtonian fluids: a new flow equation for pseudoplastic systems. *Journal of Colloid Science, 20*, 417-437.

Cuvelier, G., & Launay, B. (1986). Concentration regimes in xanthan gum solutions deduced from flow and viscoelastic properties. *Carbohydrate Polymers, 6*, 321-333.

CYB, http://www.cybercolloids.net/library/carob/introduction.php, 2005.

da Silva, J. A. L., & Gonçalves, M. P. (1990). Studies on a purification method for locust bean gum by precipitation with isopropanol. *Food Hydrocolloids, 4*, 277-287.

da Silva, J. A. L., Gonçalves, M. P., & Rao, M. A. (1992). Rheological properties of high-methoxyl pectin and locust bean gum solutions in steady shear. *Journal of Food Science, 57,* 443-448.

da Silva, J. A. L., Gonçalves, M. P., & Rao, M. A. (1993). Viscoelastic behaviour of mixtures of locust bean gum and pectin dispersion. *Journal of Food Engineering, 18,* 211-228.

da Silva, J. A. L., Gonçalves, M. P., & Rao, M. A. (1994). Influence of temperature on the dynamic and steady-shear rheology of pectin dispersions. *Carbohydrate Polymers, 23*, 77-87.

da Silva, J. A. L., & Rao, M. A. (1992). Viscoelastic properties of food hydrocolloid dispersions. In M. A. Rao, & J. F. Steffe, *Viscoelastic Properties of Foods* (pp. 285-315). New York: Elsevier Applied Science.

Dass, P. J. H., Schols, H. A., & de Jongh, H. H. J. (2000). On the galactosyl distribution of commercial galactomannans. *Carbohydrate Research, 329*, 609-619.

Dea, I. C. M., Clark, A. H., & McCleary, B. V. (1986). Effect of galactose substitution patterns on the interaction properties of galactomannans. *Carbohydrate Research, 147*, 275-294.

Dea, I. C. M., & Morrison, A. (1975). Chemistry and interactions of seed galactomannans. *Advances in Carbohydrate Chemistry and Biochemistry, 31*, 241-312.

Dea, I., Morris, E., Rees, D., Welsh, J., Barnes, H., & Price, J. (1977). Associations of like and unlike polysaccharides: mechanism and specificity in galactomannans, interacting bacterial polysaccharides, and related systems, *Carbohydrate Research, 57*, 249-272.

de Bont, P. W., Hendriks, C. L. L., van Kempen, G. M. P., & Vreeker, R. (2004). Time evolution of phase separating milk protein and amylopectin mixtures. *Food Hydrocolloids, 18*, 1023-1031.

de Bont, P. W., van Kempen, G. M. P., & Vreeker, R. (2002). Phase separation in milk protein and amylopectin mixtures. *Food Hydrocolloids, 16*, 127-138.

de Kruif, C. G., & Tuinier, R. (2001). Polysaccharide protein interactions. *Food Hydrocolloids, 15*, 555-563.

DGHS, Directorate General of Health Services. (2005). Manual of methods of analysis of foods (Milk and milk products). Ministry of Health and Family Welfare, New Delhi: Government of India.

Doi, E. (1993). Gels and gelling of globular proteins. *Trends in Food Science & Technology, 4*, 1-5.

Doublier, J. L., Garnier, C., Renard, D., & Sanchez, C. (2000). Protein-polysaccharide interactions. *Current Opinion in Colloid and Interface Science, 5*, 202-214.

Doublier, J. L., & Launay, B. (1981). Rheology of galactomannan solutions: comparative study of guar gum and locust bean gum. *Journal of Texture Studies*, *12*, 151-172.

Doucet, D., Gauthier, S. F., & Foegeding, E. A. (2001). Rheological characterization of a gel formed during extensive enzymatic hydrolysis. Food Engineering and Physical Propretés, 66, 711-715.

Durand, D., Gimel, J. C., & Nicolai, T. (2002). Aggregation, gelation and phase separation of heat denatured globulin proteins. *Physica A, 304*, 253-265.

Durand, D., Le Bon, C., Croguennoc, P., Nicolai, T., & Clark, A. H. (2002). Aggregation and gelation of globular proteins with and without addition of polysaccharides. In P. A. Williams, & G. O. Phillips, *Gum and Stabilisers for the food industry 11* (pp.263-270). Great Britain: Royal Society of Chemistry Published.

Durrani, C. M., Prystupa, D. A., Donald, A. M., & Clark, A. H. (1993). Phase diagram of mixtures of polymers in aqueous solution using FTIR spectroscopy. *Macromolecules, 26*, 981-987.

Dürrenberger, M. B., Handschin, S., Conde-Petit, B., & Escher, F. (2001). Visualization of food structure by confocal laser scanning microsopy (CLSM). *Lebensmittel-Wissenschaft und-Technologie, 34*, 11-17.

EXP, http://www.exportselva.com.pe/en/taraingles.pdf, 2004.

FAO, http://www.fao.org/documents/show_cdr.asp?url_file=/docrep/V9236E/V9236e06.htm, 2003.

FCC III, Food and Nutrition Board-National Research Council. (1981). Food Chemicals Codex. Washington, DC: National Academy Press.

Fernandes, P. B., Gonçalves, M. P., & Doublier, J. L. (1991). A rheological characterization of kappa-carrageenan/galactomannan mixed gels: A comparison of locust bean gum samples. *Carbohydrate Polymers, 16*, 253-274.

Ferry, J. D. (1980). Viscoelastic properties of polymers. New York: John Wiley & Sons.

Flower, D. R. (1996). The lipocalin protein family: structure and function. *Biochemical Journal, 318*, 1-14.

Friedrich, C., & Braun, H. (1992). Generalized Cole-Cole behaviour and its rheological relevance. *Rheologica Acta*, *31*, 309-322.

Gaisford, S. E., Harding, S. E., Mitchell, J. R., & Bradley, T. D. (1986). A comparison between the hot and cold water soluble fractions of two locust bean gum samples. *Carbohydrate Polymers, 6*, 423-442.

Galani, D., & Apenten, R. K. O. (1999). Heat-induced denaturation and aggregation of β-lactoglobulin: kinetics of formation of hydrophobic and disulphide-linked aggregates. *International Journal of Food Science and Technology, 34*, 467-476.

Garnier, C., Schorsch, C., & Doublier, J.-L. (1995). Phase separation in dextran/locust bean gum mixtures. *Carbohydrate Polymers, 28*, 313-317.

Gast, A. P., Russel, W. B., & Hall, C. K. (1986). An experimental and theoretical study of phase transitions in the polystyrene latex and hydroxyethylcellulose system. *Journal of Colloid and Interface Science, 109*, 161-171.

Ghashghaei, K. (2003). Effect of cow phenotype and milk protein structure on biofouling rates in heat exchangers. A Master Thesis, California Polytechnic State: University San Luis Obispo.

Gisler, T., Ball, R. C., & Weitz, D. A. (1999). Strain hardening of fractal colloidal gels. *Physical Review Letter, 82*, 1064-1067.

Gonçalves, M. P. (1984). Coprecipitation des proteines du plasma bovin avec des polyosides anioniques. Etude rheologique des coprecipites et des interactions entre la serumalbumine bovine et le lambda-carraghénane ou l'alginate de sodium. A PhD Thesis, Clermont-Ferrand: University of Clermont-Ferrand II.

Gonçalves, M. P., Torres D., Andrade, C. T., Azero, E. G., & Lefebvre, J. (2004). Rheological study of the effect of *Cassia javanica* galactomannans on the heat-set gelation of a whey protein isolate at pH 7. *Food Hydrocolloids*, *18*, 181-189.

Gosal, W. S., & Ross-Murphy, S. B. (2000). Globular protein gelation. *Current Opinion in Colloid & Interface Science, 5*, 188-194.

Grinberg, V. Ya., & Tolstoguzov, V. B. (1997). Thermodynamic incompatibility of proteins and polysaccharides in solutions. *Food Hydrocolloids, 11*, 145-158.

Hagiwara, T., Kumagai, H., & Matsunaga, T. (1997). Fractal analysis of the elasticity of BSA and β-lactoglobulin gels. *Journal of Agricultural and Food Chemistry, 45*, 3807-3812.

Hagiwara, T., Kumagai, H., & Nakamura, K. (1998). Fractal analysis of aggregates in heat-induced BSA gels. *Food Hydrocolloids, 12*, 29-36.

Havea, P., Carr, A. J., & Creamer, L. K. (2004). The roles of disulphide and non-covalent bonding in the functional properties of heat-induced whey protein gels. *Journal of Dairy Research, 71*, 330-339.

Hegg, P. O. (1980). Thermal stability of β-lactoglobulin as a function of pH and the relative concentration of sodium dodecylsulphate. *Acta Agriculturae Scandinaica, 30*, 401-404.

Hoedemaeker, F. J., Visschers, R. W., Alting, A. C., de Kruif K. G., Kuil, M. E., & Abrahams, J. P. (2002). A novel pH-dependent dimerization motif in beta-lactoglobulin from pig (Sus scrofa). *Acta Crystallographica, D58*, 480-486.

Hoffmann, M. A. M., & van Mill, P. J. J. M. (1997). Heat-induced aggregation of β-Lg: Role of free thiol groups and disulfide bonds. *Journal of Agricultural and Food Chemistry, 45*, 2942-2948.

Huggins, M. L. (1942). The viscosity of dilute solutions of long-chain molecules. IV. Dependence on concentration. *Journal of the American Chemical Society, 64*, 2716-2718.

Hyun, K., Kim, S. H., Ahn, K. H., & Lee, S. J. (2002). Large amplitude oscillatory shear as a way to classify the complex fluids. *Journal of Non-Newtonian Fluid Mechanics, 107*, 51-65.

Ikeda, S., Foegeding, E. A., & Hagiwara, T. (1999). Rheological study on the fractal nature of the protein gel structure. *Langmuir, 15*, 8584-8589.

Jost, R. (1993). Functional characteristics of dairy proteins. *Trends in Food Science & Technology, 4*, 283-288.

Ju, Z. Y., & Kilara, A. (1998). Gelation of pH-aggregated whey protein isolate solution induced by heat, protease, calcium salt, and acidulant. *Journal of Agricultural and Food Chemistry, 46*, 1830-1835.

Kaschta, J., & Schwartzl, F. R. (1994). Calculation of discrete retardation spectra from creep data-I. Method. *Rheologica Acta, 33*, 517-529.

Kontopidis, G., Holt, C., & Sawyer, L. (2004). Invited review: β-lactoglobulin: binding properties, structure, and function. *Journal of Dairy Science, 87*, 785-796.

Langton, M., & Hermansson, A. M. (1992). Fine-stranded and particulate gels of β-lactoglobulin and whey protein at varying pH. *Food Hydrocolloids, 5*, 523-539.

Le Bon, C., Nicolai, T., & Durand, D. (1999). Growth and structure of aggregates of heat-denatured β-lactoglobulin. *International Journal of Food Science and Technology, 34*, 451-465.

Lefebvre, J. (1996). Some examples of the application of rheological methods to the study of macromolecular systems. In seminar at Agricultural Universities of Poznãn and Kraków: Poland.

Lefebvre, J., Doublier, J. L., & Antonov, Y. (1996). Rheology of the aqueous casein-guar gum mixtures. *Composite Mechanics and Design, 2*, 121-132.

Lefèvre, T. & Subirade, M. (1999). Structure and interaction properties of β-lactoglobulin as studied by FTIR spectroscopy. *International Journal of Food Science and Technology, 34*, 419-428.

Lefèvre, T. & Subirade, M. (2000). Molecular differences in the formation and structure of fine-stranded and particulate β-lactoglobulin gels. *Biopolymers, 54*, 578-586.

Lekkerkerker, H. N. W., Poon, W. C. K., Pusey, P. N., Stroobants, A., & Warren, P. B. (1992). Phase behaviour of colloid+polymer mixtures. *Europhysics Letters, 20*, 559-564.

LSB, http://www.lsbu.ac.uk/water/hyloc.html, 2005.

Manca, S., Lapasin, R., Partal, P., & Gallegos, C. (2001). Influence of surfactant addition on the rheological properties of aqueous welan matrices. *Rheologica Acta, 40*, 128-134.

McCleary, B. V., Clark, A. H., Dea, I. M. C., & Rees, D. A. (1985). The fine structure of carob and guar galactomannans. *Carbohydrate Research, 139*, 237-260.

McCleary, B. V., & Neukom, H. (1982). Effect of enzymic modification on the solution and interaction properties of galactomannans. *Progress in Food and Nutrition Science, 6*, 109-118.

McKenzie, H. A., & Sawyer, W. H. (1967). Effect of pH on β-lactoglobulin. *Nature, 214*, 1101-1104.

McSwiney, M., Singh, H., & Campanella, O. H. (1994). Thermal aggregation and gelation of bovine β-lactoglobulin. *Food Hydrocolloids, 8*, 441-453.

Meakin, P. (1987). Fractal aggregates. *Advances in Colloid and Interface Science, 28*, 249-331.

MEM, http://members.frys.com/~bpmosley/Cer_sill.jpg, 2005.

Michon, C., Chapuis, C., Langendorff, V., Boulenger, P., & Cuvelier, G. (2004). Strain-hardening properties of physical gels of biopolymers. *Food Hydrocolloids, 18*, 999-1005.

Mleko, S. (1999). Effect of protein concentration on whey protein gels obtained by a two-stage heating process. *European Food Research Technology, 209*, 389-392.

MLI, http://www.mli.kvl.dk/dairy/special/b-lg/b-lg.htm, 2005.

Monteiro, S. R., Tavares, C., Evtuguin, D. V., Moreno, N., & Lopes da Silva, J. A. (2005). Influence of galactomannans with different molecular weights on the gelation of whey proteins at neutral pH. *Biomacromolecules, 6*, 3291-3299.

Morris, E. R. (1990). Mixed polymer gels. In P. Harris (Ed.), *Food Gels* (pp. 291-359). London: Elsevier.

Morris, E. R. (1995). Polysaccharide rheology and in-mouth perception. In A. M. Stephen, *Food Polysaccharides and their application* (pp. 517-545). New York: Marcel Dekker, Inc.

Morris, E. R., Cutler, A. N., Ross-Murphy, S. B., Rees, D. A., & Price, J. (1981). Concentration and shear rate dependence of viscosity in random coil polysaccharide solutions. *Carbohydrate Polymers, 1*, 5-21.

Morris, E. R., & Ross-Murphy, S. B. (1981). Chain flexibility of polysaccharides and glycoproteins from viscosity measurements. In D. H. Northcote, *Techniques in Carbohydrate Metabolism B310* (p. 1). Amsterdam: Elsevier/North-Holland Scientific Publishers Ltd.

Mota, M. V. T., Ferreira, I. M. P. L. V. O., Oliveira, M. B. P., Rocha, C., Teixeira, J. A., Torres, D., & Gonçalves, M. P. (2004). Enzymatic hydrolysis of whey protein concentrates: peptide HPLC profiles. *Journal of Liquid Chromatography & Related Technologies, 27*, 2625-2639.

Mota, M. V. T., Ferreira, I. M. P. L. V. O., Oliveira, M. B. P., Rocha, C., Teixeira, J. A., Torres, D., & Gonçalves, M. P. (2006). Trypsin hydrolysis of whey protein concentrates: characterization using multivariate data analysis. *Food Chemistry, 94*, 278-286.

Mulvihill, D. M., & Donovan, M. (1987). Whey protein and their thermal denaturation-A review. *Irish Journal of Food Science and Technology, 11*, 43-75.

Oblonsek, M., Sostar-Turk, S., & Lapasin, R. (2003). Rheological studies of concentrated guar gum. *Rheologica Acta, 42*, 491-499.

Olsson, C., Langton, M., & Hermansson, A. M. (2002). Microstructures of β-lactoglobulin/amylopectin gels on different length scales and their significance for rheological properties. *Food Hydrocolloids, 16*, 111-126.

Olsson, C., Stading, M., & Hermansson, A. M. (2000). Rheological influence of non-gelling amylopectins on β-lactoglobulin gel structures. *Food Hydrocolloids*, *14*, 473-483.

Ould Eleya, M. M., Ko, S., & Gunasekaran, K. (2004). Scaling and fractal analysis of viscoelastic properties of heat-induced protein gels. *Food Hydrocolloids, 18*, 315-323.

Ould Eleya, M. M., & Turgeon, S. L. (2000a). The effect of pH on the rheology of β-lactoglobulin / κ-carrageenan mixed gels. *Food Hydrocolloids, 14*, 245-251.

Ould Eleya, M. M., & Turgeon, S. L. (2000b). Rheology of κ-carrageenan and β-lactoglobulin mixed gels. *Food Hydrocolloids, 14*, 29-40.

Pouzot, M., Nicolai, T., Benyahia, L., & Durand, D. (2006). Strain hardening and fracture of heat-set fractal globular protein gels. *Journal of Colloid and Interface Science*, 293, 376-383.

Pouzot, M., Nicolai, T., Durand, D., & Benyahia, L. (2004). Structure factor and elasticity of a heat-set globular protein gel. *Macromolecules, 37*, 614-620.

Rayment, P., Ross-Murphy, S. B., & Ellis, P. R. (1995). Rheological properties of guar galactomannan and rice starch mixture-1. steady shear measurements. *Carbohydrate Polymers, 28*, 121-130.

Renard, D., Lefebvre, J., Griffin, M. C. A., & Griffin, W. G. (1998). Effects of pH and salt environment on the association of β-lactoglobulin revealed by intrinsic fluorescence studies. *International Journal of Biological Macromolecules, 22*, 41-49.

Robinson, G., Ross-Murphy, S. B., & Morris, E. R. (1982). Viscosity-molecular weight relationships, intrinsic chain flexibility, and dynamic solution properties of guar galactomannan. *Carbohydrate Research, 107*, 17-32.

Roefs, P. F. M., & De Kruif, K. G. (1994). A model for the denaturation and aggregation of β-lactoglobulin. *European Journal Biochemistry, 226*, 883-889.

Rol, F. (1973). Locust bean gum. In F. Rol. *Industrial Gums* (pp. 323-337). New York: Academic Press.

Ross-Murphy, S. B. (1995). Structure-property relationships in food biopolymer gels and solutions. *Journal of Rheology, 39*, 1451-1463.

Rueb, C. J., & Zukoski, C. F. (1997). Viscoelastic properties of colloidal gels. *Journal of Rheology*, 41, 197-218.

Ruiz-Ángel, M. J., Simó-Alfonso, E. F., Mongay-Fernández, C., & Ramis-Ramos, G. (2002). Identification of leguminosae gums and evaluation of carob-guar mixtures by capillary zone electrophoresis of protein extracts. *Electrophoresis, 23,* 1709-1715.

Sawyer, L., Brownlow, S., Polikarpov, I., & Wu S. -Y. (1998). β-lactoglobulin: structural studies, biological clues. *International Dairy Journal, 8*, 65-72.

Sawyer, L., & Kontopidis, G. (2000). The core lipocalin, bovine β-lactoglobulin. *Biochimica et Biophysica Acta, 1482*, 136-148.

Schmitt, C., Sanchez, C., Despond, S., Renard, D., Thomas, F., & Hardy, J. (2000). Effect of protein aggregates on the complex coacervation between β-lactoglobulin and acacia gum at pH 4.2. *Food Hydrocolloids, 14*, 403-413.

Schmitt, C., Sanchez, C., Thomas, F., & Hardy, J. (1999). Complex coacervation between β-lactoglobulin and acacia gum in aqueous medium. *Food Hydrocolloids, 13*, 483-496.

Schorsch, C., Jones, M. G., & Norton, I. T. (1999). Thermodynamic incompatibility and microstructure of milk protein/locust bean gum/sucrose systems. *Food Hydrocolloids, 13*, 89-99.

Sedmak, J. J., & Grossberg, S. E. (1977). A rapid, sensitive, and versatile assay for protein using Coomassie brilliant blue G250. *Analytical biochemistry, 79*, 544-552.

Semenova, M. G., Bolotina, V. S., Dmitrochenko, A. P., Leontiev, A. L., Polyakov, V. I., Braudo, E. F., & Tolstoguzov, V. B. (1991). The factors affecting the compatibility of serum albumin and pectinate in aqueous medium, *Carbohydrate Polymers, 15*, 367-385.

Shimada, K., & Cheftel, J. C. (1988). Texture characteristic, protein solubility, and sulfhydryl group/disulfide bond content of heat-induced gels of whey protein isolate. *Journal of Agricultural and Food Chemistry, 36*, 1018-1025.

Shin, W. –H., Shin, W. Y., Kim, S. –I., Liu, J, & Aksay, I. A. (1990). Scaling behavior of the elastic properties of colloidal gels. *Physical Review A, 42*, 4772-4779.

Sim, H. G., Ahn, K. H., & Lee, S. J. (2003). Large amplitude oscillatory shear behavior of complex fluids investigated by a network model: a guideline for classification. *Journal of Non-Newtonian Fluid Mechanics, 112*, 237-250.

Spector, T. (1978). Refinement of the coomassie blue method of protein quantitation. A simple and linear spectrophotometric assay for less than or equal to 0.5 to 50 microgram of protein. *Analytical Biochemistry, 86*, 142-146.

Stading, M., & Hermansson, A. M. (1990). Viscoelastic behaviour of β-lactoglobulin gel structures. *Food Hydrocolloids, 4*, 121-135.

Stading, M., & Hermansson, A. M. (1991). Large deformation properties of β-lactoglobulin gel structures. *Food Hydrocolloids, 5*, 339-352.

Stading, M., Langton, M., & Hermansson, A. M. (1993). Microstructure and rheological behaviour of particulate β-lactoglobulin gels. *Food Hydrocolloids, 7*, 195-212.

Stading, M., Langton, M., & Hermansson, A. M. (1995). Small and large deformation studies of protein gels. *Journal of Rheology, 39*, 1445-1450.

Steffe, J. F. (1996). Rheological methods in food process engineering. USA: Free man Press.

Strzalkowska, N., Krzyzewski, J., Zwierzchowski, L., & Ryniewicz, Z. (2002). Effects of κ-casein and β-lactoglobulin *loci* polymorphism, cows'age, stage of lactation and somatic cell count on daily milk yield and milk composition in Polish Black-and-White cattle. *Animal Science Papers and Reports, 20*, 21-35.

Syrbe, A., Bauer, W. J., & Klostermeyer, H. (1998). Polymer Science concepts in dairy systems- An overview of milk protein and food hydrocolloid interaction. *International Dairy Journal, 8*,179-193.

Syrbe, A., Fernandes, P. B., Dannenberg, F., Bauer, W., & Klostermeyer, H. (1995). Whey protein+polysaccharide mixtures: polymer incompatibility and its application. In E.

Dickinson, & D. Lorient. *Food macromolecules and colloids* (pp. 328-339). London: Royal Society of Chemistry.

Tang, Q., Munro, P. A., & McCarthy, O. J. (1993). Rheology of whey protein concentrate solutions as a function of concentration, temperature, pH and salt concentration. *Journal Dairy Research, 60*, 349-361.

Tavares, C., & da Silva, J. A. L. (2003). Rheology of galactomannan-whey protein mixed systems. *International Dairy Journal, 13*, 699-706.

Tavares, C., Monteiro, S. R., Moreno, N., & Lopes da Silva., J. A. (2005). Does the branching degree of galactomannans influence their effect on whey protein gelation?. *Colloids and Surfaces A: Physicochemical and Engineering Aspects, 270-271*, 213-219.

Taylor, S. M., & Fryer, P. J. (1994). The effect of temperature/shear history on the thermal gelation of whey protein concentrates. *Food Hydrocolloids, 8*, 45-61.

Tolstoguzov, V. B. (1991). Functional properties of food proteins and role of protein-polysaccharide interaction. *Food Hydrocolloids, 4*, 429-468.

Tolstoguzov, V. B. (1992). The functional properties of foods proteins. In G. O. Phillips, P. A. Williams, & D. J. Wedlock. *Gums and stabilizers for the food industry-6*. Oxford: IRL Press.

Totosaus, A., Montejano, J. G., Salazar, J. A., & Guerrero, I. (2002). A review of physical and chemical protein-gel induction. *International Journal of Food Science and Technology, 37*, 589-601.

Tschoegl, N. W. (1989). *The phenomenological theory of linear viscoelastic behavior. An introduction*. New York: Springer.

Tuinier, R., & de Kruif, C. G. (1999). Phase behaviour of casein micelles / exocellular polysaccharide mixtures; experiment and theory, *Journal of Chemical Physics, 110*, 9296-9304.

Tuinier, R., Dhont, J. K. G., & de Kruif, C. G. (2000). Depletion-induced phase separation of aggregated whey protein colloids by an exocellular polysaccharide, *Langmuir, 16*, 1497-1507.

Tuinier, R., Rieger, J., & de Kruif, C. G. (2003). Depletion-induced phase separation in colloid polymer mixtures. *Advances in Colloid and Interface Science, 103*, 1-31.

Tung, C. Y. M., & Dynes, P. J. (1982). Relationship between viscoelastic properties and gelation in thermosetting systems. *Journal of Applied Polymer Science, 27*, 569-574.

Turgeon, S. L., Beaulieu, M., Schmitt, C., & Sanchez, C. (2003). Protein-polysaccharide interactions: Phase-ordering kinetics, thermodynamic and structural aspects. *Current Opinion in Colloid and Interface Science, 8*, 401-414.

Uhrinova, S., Smith M. H., Jameson, G. B., Uhrin, D., Sawyer, L. & Barlow, P. N. (2000). Structural changes accompanying pH-induced dissociation of the beta-lactoglobulin dimer. Biochemistry, 39, 3565-73574.

Verheul, M., Pedersen, J. S., Roefs, P. F. M., & de Kruif, K. G. (1999). Association behavior of native β-lactoglobulin. *Biopolymers, 49*, 11-20.

Verheul, M., & Roefs, S. P. F. M. (1998). Structure of whey protein gels studied by permeability, scanning electron microscopy and rheology. *Food Hydrocolloids, 12*, 17-24.

Verheul, M., Roefs, S. P. F. M., & de Kruif, K. G. (1998). Kinetics of heat-induced aggregation of β-lactoglobulin. *Journal of Agricultural and Food Chemistry, 46*, 896-903.

Walkenström, P., & Hermansson, A. M. (1996). Fine-stranded mixed gels of whey proteins and gelatin. *Food Hydrocolloids, 10*, 51-62.

Walkenström, P., & Hermansson, A. M. (1998). Effects of shear on pure and mixed gels of gelatin and particulate whey protein. *Food Hydrocolloids, 12*, 77-87.

Walkenström, P., Panighetti, N., Windhab, E., & Hermansson, A. M. (1998). Effects of fluid shear and temperature on whey protein gels, pure or mixed with xanthan. *Food Hydrocolloids, 12*, 469-479.

Walkenström, P., Windhab, E., & Hermansson, A. M. (1998). Shear-induced structuring of particulate whey protein gels. *Food Hydrocolloids, 12*, 459-468.

Walters, K. (1975). Rheometry. London: Chapman & Hall Ltd.

Wang, Q., Ellis, P. R., & Ross-Murphy, S. B. (2000). The stability of guar gum in an aqueous system under acidic conditions. *Food Hydrocolloids, 14*, 129-134.

Wang, S., van Dijk, J. A. P. P., Odijk, T., & Smit, J. A. M. (2001). Depletion-induced demixing in aqueous protein-polysaccharide solutions. *Biomacromolecules, 2*, 1080-1088.

Wu, H., & Morbidelli, M. (2001). A model relating structure of colloidal gels to their elastic properties. *Langmuir, 17*, 1030-1036.

Zasypkin, D. V., Dumay, E., & Cheftel, J. C. (1996). Pressure-and heat-induced gelation of mixed β-lactoglobulin/xanthan. *Food Hydrocolloids, 10*, 203-211.

Zhong, Q., Daubert, C. R., & Velev, O. D. (2004). Cooling effects on a model rennet casein gel system: part I. Rheological characterization. *Langmuir, 20*, 7399-7405.

Zor, T., & Selinger, Z. (1996). Linearization of the Bradford protein assay increases its sensitivity: theoretical and experimental studies. *Analytical Biochemistry, 236*, 302-308.

Zupancic, A., & Zumer, M. (2001). Viscoelastic properties of hydrophilic polymers in aqueous dispersions. *Acta Chimica Slovenica, 48,* 469-486.